

Faculty of Science and Technology

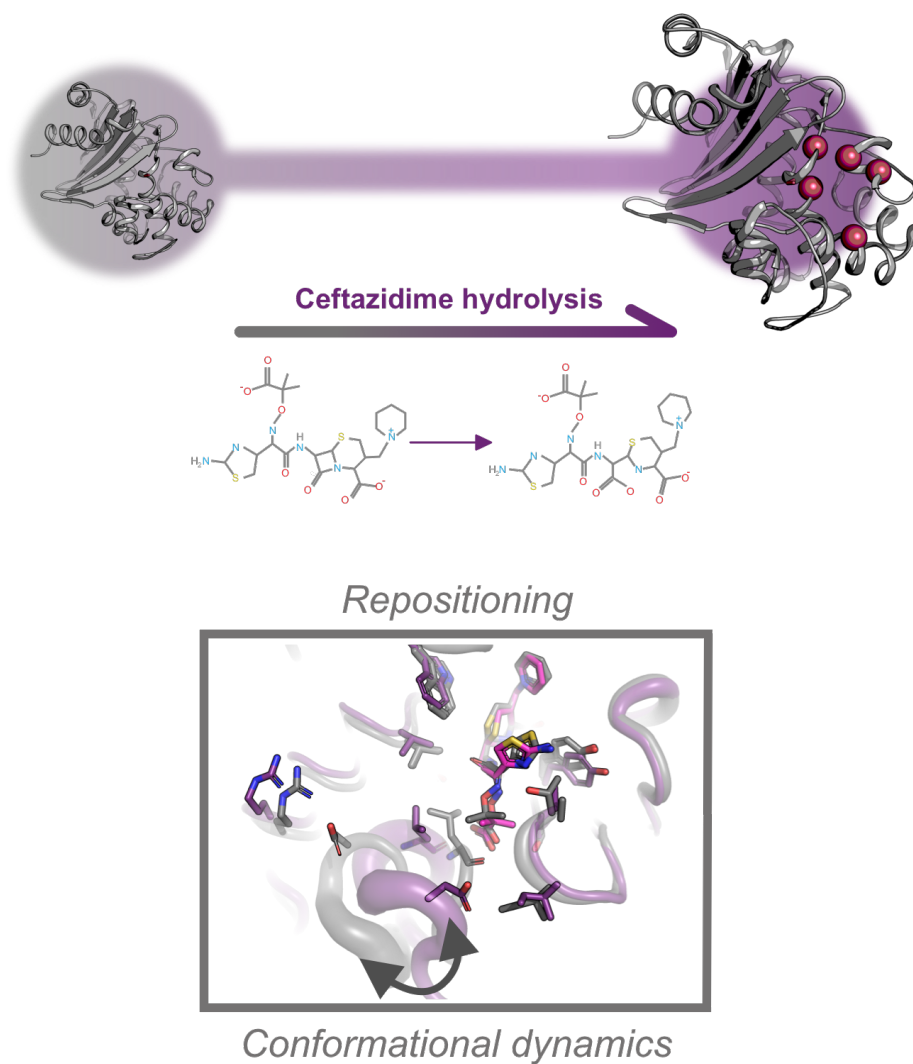
Department of Chemistry

On the Evolvability of OXA-48

A comprehensive study of new functions within the β -lactamase OXA-48

Christopher Fröhlich

A dissertation for the degree of Philosophiae Doctor - June 2021



A dissertation for the degree of Philosophiae Doctor

On the Evolvability of OXA-48

A comprehensive study of new functions within the β -lactamase OXA-48

Christopher Fröhlich



Tromsø – June 2021

Department of Chemistry
Faculty of Science and Technology
UiT The Arctic University of Norway
Norway

Acknowledgement

I was fortunate enough to attend various conferences during my PhD journey, this would have not been possible without the financial support granted by the PhD schools IBA, NFIF and Biocat. The work in this thesis was carried out at the Department of Chemistry in collaboration with the Department of Pharmacy, UiT The Arctic University of Tromsø from 2017 to 2021. Throughout the last four years, I was lucky enough to meet many amazing people who have supported me, and to whom I would like to express my deepest gratitude.

Foremost, I would like to thank my supervisor Prof. Hanna-Kirsti Schrøder Leiros and my co-supervisors Prof. Ørjan Samuelsen, Dr. Vidar Sørum and Prof. Annette Bayer. Hanna-Kirsti, I can't put into words how thankful I am for all the opportunities you have given me, which allowed me to travel, expand my network and ultimately grow as a person and as a scientist. I would certainly not be here without you. Ørjan, it has been a great pleasure working with you. Thank you for all the support professionally and personally. Annette and Vidar, thank you for all the discussions and guidance. I also would like to thank Prof. Pål Jarle Johnsen for giving me the possibility to perform many evolutionary parts in his lab and his invaluable feedback. Thanks for always having an open door and a free lab bench.

I would like to thank the people at Norstruct for their help and support especially Bjarte, Trine and Susann. I am beyond grateful for the hospitality the MicroPop group has shown me. Thank you, Vidar, Julia (Wia gohds?), Elizabeth, Nina, Joao, Klaus, Mikkel, Francois, for the countless coffee breaks, lunches and of course the infamous Valhalla Fridays. Joao, thank you for literally always being there whenever I needed support or only to discuss yet another side project. Klaus, thank you for an uncountable number of project discussions. Vidar, Elizabeth and Julia, thanks for being the social glue keeping everything together. Many thanks also to the hard-working students Alex W. and Leon, it was my pleasure guiding you in the lab.

This work would have not been possible without the contribution of all my co-authors. To that end, I would like to thank my collaborators from Bristol. Thank you, Marc and Viivi, I could not have pulled this off without you. The same accounts for the "Canadian connection". I would very much like to express my deepest gratitude to Prof. Nobuhiko Tokuriki and the whole Tokuriki group for welcoming me so warmly in Canada. It was my pleasure meeting you, Charlotte, Dan, Karol, Janine, John, Morito, Ayse, Sevan. Nobu,

thank you so much for your guidance and your invaluable scientific advice. Charlotte, thank you for being such an amazing person and scientist. You are truly a gem. Dan, please never stop being such an inspiring person. Jaiten, thank you for bearing with my puns. To Dan and Jenni, thank you for making the stay in Canada such an unforgettable experience.

I do not know what I would have done without the support of my great friends who have made this PhD journey an amazing adventure. To my “Tromsø family”, Margherita, Pietro, Antal, Merete, Nina, Joao, Joseph, Gigi, Tena, Jennifer, Selenia, I simply can't find words to express my gratitude for all the great memories together, the dinners, the parties, the hiking trips, and of course your support. Tromsø would have been a different place without you. My journey obviously did not start in Tromsø and I would like to thank Adrian, Kirsten, Patrick, Myriam, Jannik, Felix and of course my mom and brother for all the support throughout the years.

Marge, Vidar and Pietro, thank you for always being there for me and your friendship! Marge, so much has happened since we both came to Tromsø as Erasmus students. We have seen it all - the Good, the Bad and the Ugly. I am forever grateful for the fact that I got to know you, that I could be part of your life and for your friendship. And hey, who would have thought that someone could teach a German how to properly make lasagne? I can't wait to see what the future holds for us.

Finally, Alex. I can't put into words what your unconditional support means to me! Thank you for being my rock, my safe place to land, and my heart. Thanks, for always having my back and keeping up with my little “helicopter“ mind. I treasure every memory we have shared, and I can't wait to see what the future will bring.

There is simply no way that I can express my gratitude to everyone who deserves it. So many people have touched my life and just because their names are not mentioned here, does not in any form diminish the effect those people had on my life.

Tromsø, June 2021

Christopher Pöhlid

Das kölsche Grundgesetz

(The Cologne Constitution)

§05

Et bliev nix wie et wor

(Nothing remains as it was)

Table of Contents

List of papers	II
Authors' contribution	IV
Other publications	VI
Abbreviations	VIII
Abstract.....	X
A. Introduction	1
1 Antibiotic resistance: The storm is here!.....	1
1.1 Antibiotics: molecular targets and resistance mechanisms	2
1.2 Intrinsic and acquired resistance	4
1.3 Drivers of antibiotic resistance.....	5
2 Evolution of new enzymatic functions.....	7
2.1 Mechanistic adaptation of enzymes	10
2.1.1 Reshaping of the active site	10
2.1.2 Substrate interactions and reposition	11
2.1.3 Conformational tinkering by distant mutations	12
2.1.4 Conformational dynamics.....	12
2.2 Epistasis as a driver of divergent evolution	15
2.2.1 Classes of epistatic interactions.....	15
2.2.2 Non-specific and specific epistasis.....	18
2.2.3 Pairwise <i>versus</i> high-order epistasis.....	20
2.3 Trade-offs during adaptation	21
2.3.1 Functional trade-offs: weak <i>versus</i> strong.....	22
2.3.2 Stability-function trade-offs.....	24
3 Evolution and selection of β -lactamases	27
3.1 Penicillin binding proteins and β -lactams	27
3.1.1 Inhibition of penicillin binding proteins by β -lactams	27
3.1.2 Natural pathways of β -lactam synthesis.....	28
3.1.3 Stability of β -lactams	30
3.1.4 β -lactam classes and β -lactam resistance	30
3.2 Evolution of β -lactamases.....	31
3.2.1 PBP-like family and serine β -lactamases	32
3.2.2 Low β -lactam concentrations driving the evolution of β -lactamases?	34
4 Ambler Class D β -lactamases	37

4.1	The OXA-Family	37
4.1.1	Functional diversification	37
4.1.2	Structural conservation and features.....	38
4.1.3	General reaction mechanism	40
4.1.4	Inhibition of serine β -lactamases.....	41
4.2	OXA-48-like β -lactamases	41
4.2.1	Origins, mobilisation and spread	41
4.2.2	Carbapenemase activity.....	42
4.2.3	Cephalosporinase activity	44
4.2.4	Substrate specificity and trade-offs	46
B.	Aims	49
C.	Summary of papers.....	51
	Paper I	51
	Paper II	53
	Paper III (Manuscript, not published).....	55
D.	Methodological considerations.....	57
1	OXA-48 and <i>E. coli</i> and as a model system	57
2	Selection procedures	59
3	Phenotypic characterisation	60
4	Fitness measurements	62
5	Structural evaluation	63
E.	Results and Discussion.....	65
1	Sub-MICs drive the evolution of OXA-48.....	65
1.1	OXA-48 evolves through cryptic phenotypes	65
1.2	Low prevalence of high-level resistant clones	66
2	The evolutionary potential of OXA-48.....	67
2.1	Ceftazidime and ceftazidime-avibactam resistance	67
2.2	Mechanistic view on the evolution of OXA-48	70
2.3	Thermostability related trade-offs	73
2.4	Functional trade-off, cross-resistance, and epistasis	76
F.	Conclusions	79
G.	Perspective	81
H.	References.....	83
	Appendix: Paper I	
	Appendix: Paper II	

Appendix: Paper III

Appendix: Review

List of papers

This thesis is based on the following papers and manuscripts, which are referred to in the text by their Roman numerals.

- I.* **Fröhlich C**, Sørum V, Thomassen AM, Johnsen PJ, Leiros H-KS, Samuelsen Ø. 2019. OXA-48-mediated ceftazidime-avibactam resistance is associated with evolutionary trade-offs. *mSphere* 4:e00024-19. <https://doi.org/10.1128/mSphere.00024-19>.
- II.* **Fröhlich C**, Gama JA, Harms K, Hirvonen VHA, Lund BA, van der Kamp MW, Johnsen PJ, Samuelsen Ø, Leiros H-KS. 2021. Cryptic β -lactamase evolution is driven by low β -lactam concentrations. *mSphere* 6:e00108-21. <https://doi.org/10.1128/mSphere.00108-21>.
- III.* **Fröhlich C**, Buda K, Carlsen TJW, Johnsen PJ, Leiros H-KS, Tokuriki N. OXA-48 evolution is realised by very distinct trajectories leading to similar resistance levels. (**Manuscript, not published**).

Related review:

Fröhlich C, Chen JZ, Gholipour S, Erdogan AN, Tokuriki N, Evolution of β -lactamases and enzyme promiscuity, *Protein Engineering, Design and Selection*, Volume 34, 2021, gzab013, <https://doi.org/10.1093/protein/gzab013>

Authors' contribution

Paper(s)	Conceptual framework	Selection/ Evolution/ Cloning	Susceptibility testing / Microbiology	Protein expression/ Purification	Enzyme kinetics/ characterisation	X-ray Crystallography	Original manuscript preparation	Other
I	CF, VS, PJJ, ØS, HKSL	CF, VS	CF, VS	AMT	CF, AMT	HKSL, CF	CF	NA
II	CF, PJJ, ØS, HKSL	CF, JAG, KH	CF, JAG	CF	CF	HKSL, CF	CF	MD simulations BAL, VHAH, MWVDK
III	CF, NT	CF	CF	CF, TJWC	CF	HKSL, TJWC, CF	CF	Statistical model KB, NT

Authors:

Ane Molden Thomassen (AMT), Bjarte A. Lund (BAL), Christopher Fröhlich (CF), Hanna-Kirsti S. Leiros (HKSL), João A. Gama (JAG), Karol Buda (KB), Klaus Harms (KH), Marc W. van der Kamp (MWVDK), Nobuhiko Tokuriki (NT), Ørjan Samuelsen (ØS), Pål Jarle Johnsen (PJJ), Trine J.W. Carlsen (TJWC), Vidar Sørum (VS), Viivi H. A. Hirvonen (VHAH), NA- not applicable

Other publications

The following work was published during the timeframe of the PhD but is not included in this thesis.

- i. Samuelsen Ø, Åstrand OAH, **Fröhlich C**, Heikal A, Skagseth S, Carlsen TJO, Leiros H-KS, Bayer A, Schnaars C, Kildahl-Andersen G, Lauksund S, Finke S, Huber S, Gjøen T, Andresen AMS, Økstad OA, Rongved P. 2020. ZN148 is a modular synthetic metallo- β -lactamase inhibitor that reverses carbapenem resistance in Gram-negative pathogens *in vivo*. *Antimicrob Agents Chemother* 64:e02415-19. <https://doi.org/10.1128/AAC.02415-19>.
- ii. **Fröhlich C**, Sørnum V, Huber S; Samuelsen Ø, Berglund F; Kristiansson EK, Stathis D, Marathe NP, Larsson J, Leiros H-KS. 2020. Structural and biochemical characterization of the environmental MBLs MYO-1, ECV-1 and SHD-1. *Journal of Antimicrobial Chemotherapy*. doi: doi:10.1093/jac/dkaa175.
- iii. Muhammad Z, Skagseth S, Boomgaren M, Akhter S, **Fröhlich C**, Ismael A, Christopeit T, Bayer A, Leiros H-KS. 2020. Structural studies of triazole inhibitors with promising inhibitor effects against antibiotic resistance metallo- β -lactamases. *Bioorganic & Medicinal Chemistry*. doi: <https://doi.org/10.1016/j.bmc.2020.115598>.
- iv. Kildahl-Andersen G, Schnaars C, Prandina A, Radix S, Le Borgne M, Jordheim LP, Gjøen T, Andresen AMS, Lauksund S, **Fröhlich C**, Samuelsen Ø, Rongved P, Åstrand OAH. 2019. Synthesis and biological evaluation of zinc chelating compounds as metallo- β -lactamase inhibitors. *MedChemComm*. doi: 10.1039/c8md00578h.
- v. Prandina A, Radix S, Le Borgne M, Jordheim LP, Bousfiha Z; **Fröhlich C**, Leiros H-KS, Samuelsen Ø, Frøvdold E, Rongved P, Åstrand OAH. 2019. Synthesis and biological evaluation of new dipicolylamine zinc chelators as metallo- β -lactamase inhibitors. *Tetrahedron*. doi: 10.1016/j.tet.2019.02.004.

- vi. Schnaars C, Kildahl-Andersen G; Prandina A, Popal R, Radix S, Le Borgne M, GjØen T, Andresen AMS, Heikal A, Økstad OAL, **FrØhlich C**, Samuelsen Ø, Lauksund S, Jordheim LP, Rongved P, Åstrand OAH. 2018. Synthesis and preclinical evaluation of TPA-based zinc chelators as metallo-β-lactamase inhibitors. ACS Infectious Diseases. doi: 10.1021/acsinfecdis.8b00137.

Abbreviations

ASKA	A Complete Set of <i>Escherichia coli</i> K-12 Open Reading Frame Archive
AiiA	N-acyl homoserine lactonase of <i>Bacillus thuringiensis</i>
AmpC	Ampicillinase C (class C β -lactamase)
AmpH	Ampicillinase H (AmpC-like, endopeptidase, carboxypeptidase)
β -LS	β -lactam synthetase
CPS	Carbapenem synthetase
CTX-M	Cefotaximase (CTX) from Munich (M) (class A β -lactamases)
DNA	Deoxyribonucleic acid
dGTP	Deoxyguanosine triphosphate (8-oxo: 8-Hydroxy)
dPTP	Deoxy-P-nucleoside triphosphate
ESBL	Extended-spectrum β -lactamase
HMW	High molecular weight
IC ₅₀	Inhibitory concentration 50%
IPNS	Isopenicillin N synthase
KPC	<i>Klebsiella pneumoniae</i> carbapenemase
LB	Lysogeny broth
LMW	Low molecular weight
LovD	Lovastatin biosynthesis cluster protein D
MBLs	Metallo- β -lactamase
MH	Mueller Hinton
MIC	Minimum inhibitory concentration
NDM	New Delhi metallo- β -lactamase (class B)
NRPS	Non ribosomal peptide synthetase
OXA	Oxacillinase
OD ₆₀₀	Optical density at 600 nm
2-NH	2-naphthyl hexanoate
PAS	Aryl sulfatase of <i>Pseudomonas aeruginosa</i>
PBPs	Penicillin binding proteins
PCR	Polymerase chain reaction
PTE	Phosphotriesterase
RNA	Ribonucleic acid
SBLs	serine β -lactamases

SHV	Sulfhydryl reagent variable (class A β -lactamases)
sub-MIC	sub minimum inhibitory concentrations
TEM	Named after the patient (Temoneira) (class A β -lactamases)
TEV	Tobacco etch virus
VIM	Verona integron-encoded metallo- β -lactamase (class B)

Abstract

Antibiotic resistance is ancient and predates the human usage of antibiotic drugs. Yet, our understanding of how enzymes that confer resistance to antibiotic agents evolve and the mechanisms driving resistance development is limited. OXA-48 has become one of the most successfully disseminating β -lactamases with the ability to hydrolyse β -lactam drugs. OXA-48 catalyses the hydrolysis of penicillins with high efficiency, however its activity towards oxyimino cephalosporins is limited. By contrary, OXA-48-like variants conferring increased resistance against oxyimino cephalosporins, such as ceftazidime, have been selected in clinical settings. These variants often exhibit deletions within the active site β 5- β 6 loop. Since ceftazidime is increasingly used in combination with the β -lactamase inhibitor avibactam, the evolutionary consequence of both ceftazidime and ceftazidime-avibactam on OXA-48 was studied in this thesis.

Here, employing different evolutionary protocols such as long-term experimental and directed evolution uncovered that OXA-48 can acquire mutations increasing resistance to both ceftazidime (L67F, P68A/S, F72L, F156C, F156C, L158P and G160C) and ceftazidime-avibactam (P68A/Y211S). Long-term experimental evolution performed at very low ceftazidime concentrations demonstrated that selection takes place below the minimum inhibitory concentration (sub-MIC). Several of these single mutants such as F72L, F156x, and L158P were re-discovered using independent replicates of directed evolution. These mutants acted as steppingstones to increase OXA-48 mediated resistance by up to 40-fold through subsequently acquired mutations. Crystallographic structures on single mutants (L67F and P68A) and a “ceftazidimase” optimised variant (A33V/F72L/S212A/T213A) showed that increased resistance was likely achieved by optimising substrate positioning and the pre-organisation of active site residues. In addition, molecular dynamics simulations revealed that single mutants such as F72L and L158P increased the flexibility of the Ω - and β 5- β 6 loops, likely aiding to an improved accommodation of ceftazidime. As a response to this adaptational process, epistatic and pleiotropic effects of mutations were studied. Mutations initially increasing OXA-48 mediated ceftazidime resistance tended to exhibit strong trade-offs concerning functionality and thermostability. However, while mutational combinations showed strong non-additive effects (epistasis) driving ceftazidime resistance development, they also limited the functional trade-off towards the penicillin piperacillin.

In contrast to variants recovered from clinical isolates, the presented studies show that OXA-48 mediated ceftazidime and ceftazidime-avibactam resistance can also evolve through point mutations *via* distinct mutational pathways. The diversity of these pathways has implications for the genotypic prediction of resistance development as many mutational solutions may exist within an enzyme. In addition, neither resistance nor trade-off development behaved additively demonstrating the presence of intra-molecular epistasis. Such non-additive effects complicate the phenotypic prediction of antibiotic resistance development.

A. Introduction

1 Antibiotic resistance: The storm is here!

If you could succumb to any potential injury, would you do your gardening or even race down a ski slope without a second thought? The easy availability of antibiotics has shaped our daily life in ways that do not immediately come to mind. Since the introduction of penicillin in the 1940s, we often think of antibiotic agents as natural or synthetic drugs able to kill or inhibit bacterial growth, and therefore to fight infections. If we would lose access to these drugs at this very moment, we would obviously lose our possibility to cure life-threatening infections, but it would also increase the risk of countless medical procedures such as cancer treatments and organ transplantations. Now, nearly 80 years after the discovery of penicillin, we have driven ourselves to the brink of a post-antibiotic era, where the constant misuse of antibiotic agents in human medicine, animal husbandry, and agriculture has given rise to bacteria exhibiting resistance to several classes of antibiotics^{1,2}. Multidrug resistant bacteria, strains sometimes resistant to several classes of antibiotics, have already been reported among both Gram-positive and Gram-negative bacteria³. Gram-positives and Gram-negatives can be distinguished by the composition of their cellular envelope shielding the cytoplasm from the environment^{4,5}. For Gram-negatives, this envelope comprises an outer and inner membrane. The periplasmic space between these membranes contains a thin peptidoglycan cell wall. Gram-positives lack the outer membrane, but are surrounded by layers of peptidoglycan that is several times thicker than the one found in the Gram-negatives⁴. The outer membrane of Gram-negatives renders them generally less susceptible to certain drug classes such as β -lactams, and thus limits the selection of antibiotic drugs that can be used as treatment options⁴. Consequently, resistance development in Gram-negative bacteria has become particularly worrisome and resistance to β -lactams has been exposed as a major contributor to the burden of antibiotic resistance⁶. This situation is also reflected in the list of global priority pathogens published by the World Health Organisation in 2017 – a ranking of 12 bacterial species based on their importance for antibiotic resistance⁷. The category where new antibiotics are critically needed is represented by only β -lactam resistant Gram-negatives such as carbapenem-resistant *Acinetobacter baumannii*, carbapenem-resistant *Pseudomonas aeruginosa*, and carbapenem-resistant or

extended-spectrum β -lactamase producing *Enterobacterales*⁷. As a result of the widespread antibiotic resistance, we already face up to ~175,000 deaths on an annual basis in Europe and the USA^{6,8-10}. In addition, the number of deaths caused by antibiotic resistant pathogens is projected to rise up to 10 million world-wide by 2050¹¹.

1.1 Antibiotics: molecular targets and resistance mechanisms

In a simplified scheme, antibiotic resistance can be described by two major factors: an antibiotic agent that kills or inhibits bacterial growth and genetic variation, where the former imposes a selective pressure and the latter allows bacteria to propagate under selective conditions^{12,13}. To date, there are more than 15 classes of antibiotics targeting different physiological and metabolic functions within the bacterial cell (Table 1)¹⁴⁻¹⁶. Generally, they can target:

- i)* protein synthesis
- ii)* bacterial cell wall synthesis and cell wall integrity
- iii)* DNA or RNA synthesis
- iv)* bacterial folate synthesis

None of the antibiotic classes have escaped resistance development¹⁷. Depending on the mode of actions, three main mechanisms involved in resistance development can be distinguished, including¹⁴:

- i)* reduction of the intracellular drug concentrations by either efflux or reduced membrane permeability
- ii)* modifications in the target structure
- iii)* direct changes of the antibiotic drug

A comprehensive overview of drug classes, their mode of actions, main molecular targets, and resistance development is shown in Table 1.

Table 1: Overview of antibiotic drug classes, cellular targets, and resistance mechanisms^{14-16,18}.

Mode of action	Antibiotic class	Main cellular targets	Resistance mechanisms		
			Altered uptake	Target modification	Drug modification
Inhibition of cell wall synthesis or disruption of cell wall integrity	β -lactams	Penicillin binding proteins	x	x	x
	Glycopeptides	Terminal D-Ala-D-Ala		x	
	Lipopeptides	Outer cell wall		x	
	Cationic peptides	Outer cell wall		x	
Inhibition of protein synthesis	Aminoglycosides	30S ribosomal unit	x	x	x
	Tetracyclines	30S ribosomal unit	x	x	
	Macrolides	23S RNA in 50S ribosomal unit	x	x	x
	Lincosamides	50S ribosomal unit		x	
	Streptogramins	23S RNA in 50S ribosomal unit		x	
	Oxazolidinones	23S RNA in 50S ribosomal unit		x	
	Phenicols	50S ribosomal unit	x		x
Inhibition of folic acid synthesis	Sulfonamides	Dihydropteroate synthetase	x	x	
	Trimethoprim	Dihydrofolate reductase	x	x	
Inhibition of DNA synthesis	Fluoroquinolones	DNA gyrase	x	x	
Inhibition of RNA synthesis	Rifampin	RNA polymerase		x	

1.2 Intrinsic and acquired resistance

Bacteria can either exhibit intrinsic resistance or they can acquire resistance. For example, Gram-negative bacteria have been shown to be intrinsically more resistant than Gram-positives to various antibiotic classes such as glycopeptides (e.g., vancomycin)^{4,19}. As mentioned previously, the intrinsic resistance of Gram-negatives is mainly founded in the presence of an outer membrane preventing drugs to enter the bacterial cell and reach their target sites^{4,19}. In addition, screening efforts of genome-wide mutational libraries showed that bacterial species carry genes intrinsically increasing resistance to many clinically important classes of antibiotics including β -lactams, aminoglycosides, and fluoroquinolones^{20,21}.

On the other hand, acquired resistance can be due to genetic changes within already pre-existing loci such as single nucleotide polymorphisms, insertions or deletions. Another way is the acquisition of foreign DNA harbouring antibiotic resistance genes by a process called horizontal gene transfer. Mobile genetic elements are characterized as transferable parts of the genome such as plasmids, transposons and bacteriophages that can be exchanged horizontally between bacteria. To date, there are three main mechanisms by which mobile genetic elements can be transferred^{15,22}:

- i)* transduction, where bacterial DNA can be transferred by bacteriophages and randomly incorporated into the host genome upon infection
- ii)* transformation, where free DNA from the environment can be taken up
- iii)* conjugation, where plasmids can be directly transferred between bacterial cells

1.3 Drivers of antibiotic resistance

In the previous subchapters, general mechanisms, classes, and acquisition of antibiotic resistance were introduced. But what facilitates the emergence and spread of antibiotic resistance? First of all, antibiotic resistance is an ancient natural phenomenon²³. Indeed, antibiotic resistance genes have been estimated to be as old as 2 billion years²³, and have likely co-evolved with antibiotic producing pathways²⁴. This is also supported by studies documenting the presence of resistance genes in pristine and isolated environments such as permafrost^{24,25}. The age of these genes clearly pre-dates the clinical introduction of antibiotics. The functionality of such “ancient” genes was also demonstrated showing that their expression conferred resistance towards different antibiotic classes such as β -lactams, aminoglycosides and tetracyclines²⁶.

The extensive use of antibiotics has likely selected for these resistance mechanisms by providing a selective advantage to bacteria. For example, a relatively large fraction (30 to 90%) of antibiotics used in human medicine²⁷⁻²⁹ or in animals^{30,31} is excreted in their active form. Up to 50% of all antibiotics used in human medicine are either not needed or are not optimal for the desired treatment³². In addition, it is estimated that two-thirds of all globally produced antibiotics are used in animal husbandry³³. Here, these drugs are employed to treat infections and promote growth, which is reflected by the therapeutic and sub-therapeutic concentrations of which these drugs are used, respectively^{33,34}. The misuse of antibiotics is likely one of the leading drivers for the selection of pre-existing resistance genes and for their spread into human pathogens (Figure 1). In addition, various studies have shown that, at least on laboratory scale, the treatment of wastewater accruing during antibiotic production may not be sufficient³⁵. The release of such contaminated wastewater into the environment likely enriches for pre-existing antibiotic resistance³⁶. Other factors influencing and driving the transmission of antibiotic resistance include travel, infection control standards, sanitation and the access to clean water³⁷.

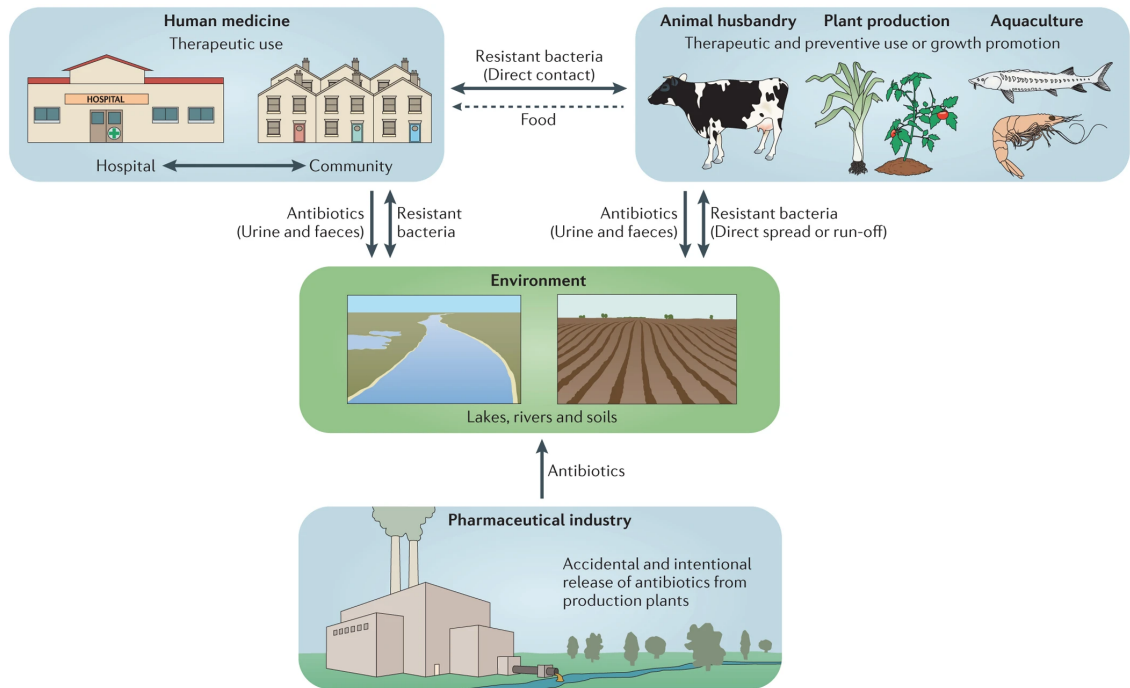


Figure 1: Interplay between antibiotic use in human medicine, agriculture and pharmaceutical industry and the emergence and spread of resistant bacteria (figure reprinted with permission from³⁸)

Although the European Union banned the use of antibiotics as growth promoters and their use is also declining in North-America³⁹, the global usage of these drugs in food production is estimated to grow at least 67% by 2030 (e.g., in countries like China, Brazil, South-Africa)⁴⁰. One-third of this increase is projected to be within the use of sub-therapeutic concentrations⁴⁰. Notably, several laboratory studies have unequivocally shown the importance of very low concentrations in the selection of resistance^{38,41-43}. However, little is known about the selective pressure of e.g., sub-therapeutic concentrations of the most prevalently used drug class, the β -lactams. In the work presented here, long-term experimental evolution was employed to study the effect of low β -lactams concentrations on the evolution of β -lactamases, enzymes conferring resistance to β -lactam drugs.

2 Evolution of new enzymatic functions

Bacterial enzymes are involved in versatile antibiotic resistance mechanisms (Table 1). The presence of such enzymes during a reaction lowers the activation energy barrier of the transition-state and consequently accelerates the rate of a given reaction (Figure 2A). Despite the traditional view of enzymes being highly specific to only one enzymatic reaction, there is an increasing body of literature showing that enzymes possess cross-activities⁴⁴⁻⁴⁹. To date, it is thought that most, if not all, enzymes show promiscuous behaviour, and thus bear the ability to catalyse one or more side reactions³⁷, besides their native or main reaction^{44,46,47,49,50}. These side reactions are commonly performed with catalytic efficiencies (k_{cat}/K_M) many magnitudes lower than the native. Indeed, using the ASKA overexpression library (“A Complete Set of *Escherichia coli* K-12 Open Reading Frame Archive”)⁵¹ against 237 different toxins and antibiotics demonstrated that in 13% of all tested cases, enzyme promiscuity seemed to be the underlying cause of resistance development⁵². Another example of wide-spread promiscuity was presented by Huang *et al.*⁵⁰, where ≥ 200 highly diverse halo alkanolic acid dehalogenases (e.g., dehalogenases, phosphoryltransferases and phosphotransferases) were tested against a substrate library. Their results demonstrate that these enzymes possess cross-activity to usually more than five different substrates. The concept of enzyme promiscuity has been summarized in several reviews over the past years^{46,49,53}. At least three different classes of enzyme promiscuity can be defined (Figure 2B to D)⁵³:

- i) catalytic promiscuity, where one enzyme exhibits the ability to stabilise the transition states of different reaction types and catalyses distinct reactions
- ii) substrate promiscuity, where substrates with different chemical structures but similar or identical transition states are accepted
- iii) product promiscuity, where one substrate is converted into alternative products *via* distinct transition states

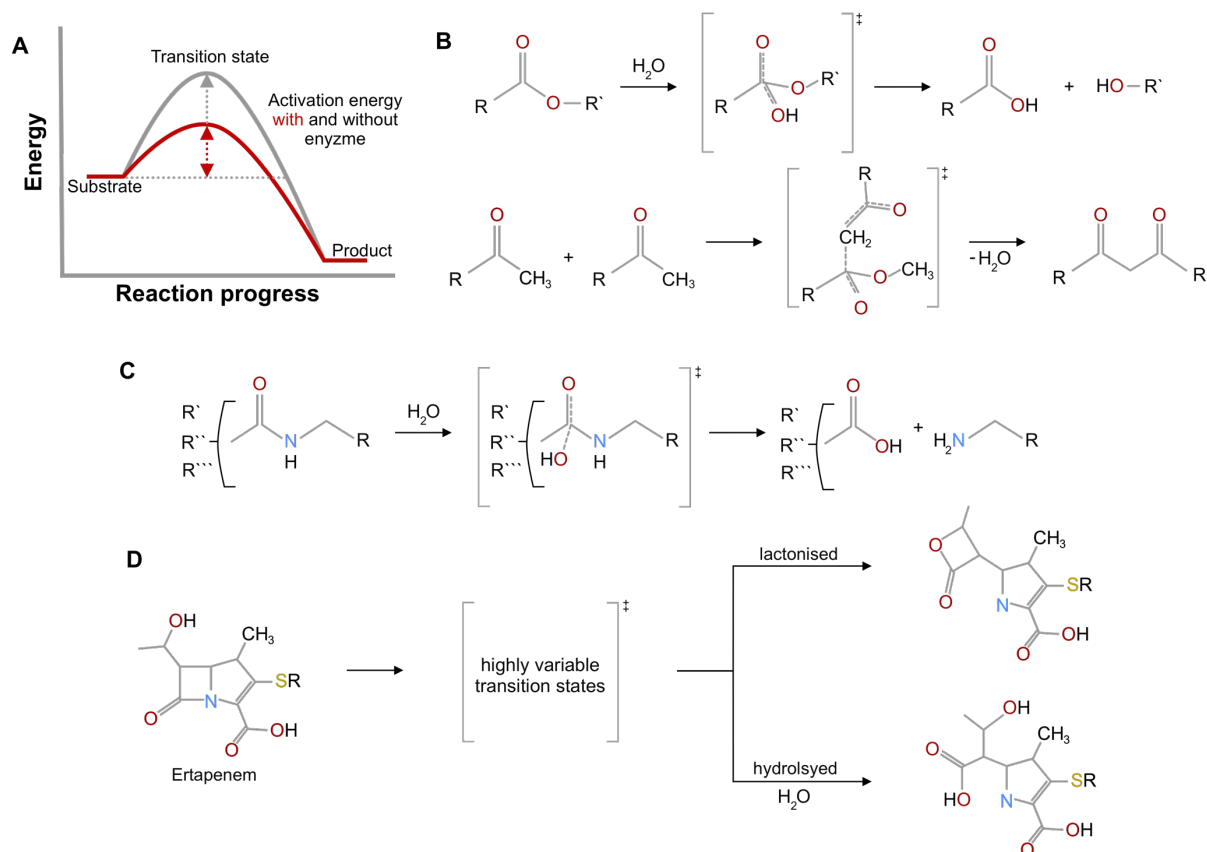


Figure 2: Energetics of catalysis and classes of enzyme promiscuity. A. The energy diagram for a hypothetical catalysed (red line) versus non-catalysed (grey line) reaction from substrate to product via transition state (\ddagger). B. Catalytic promiscuity arises from the stabilisation of structurally different transition states within the same active site as depicted in brackets. For example, lipases natively hydrolyse esters (top reaction) but they have also shown to possess promiscuous activity to catalyse aldol condensations (bottom reaction)⁵⁴. C. Substrate promiscuity involves reactions with similar transition states (brackets) for structurally related substrates (different substituents are indicated with R', R'' and R''')⁵³. D. Product promiscuity results in the conversion of one substrate to different products via distinct transition states. For example, the reaction of the β -lactam drug ertapenem can be catalysed by the β -lactamase OXA-48 to two distinct products - a hydrolysed and lactonised form^{55,56}.

It is thus imaginable that upon changes in environmental conditions, previously non-essential and promiscuous enzymes might confer a selective advantage or become crucial for survival. For example, a study of 104 single-gene knockouts in *E. coli*, affecting central metabolic functions, found that 20% of these auxotroph strains could survive by the overexpression of at least one noncognate promiscuous protein⁵⁷. Similar results were observed for the glycolytic pathway of an auxotroph *E. coli*, where three ambiguous glucokinases were identified complementing its auxotrophy, with catalytic efficiencies 10^4 -fold lower than the endogenous one⁵⁸.

Evolution is therefore thought to recruit these latent enzymatic functions to gradually reshape existing enzymes rather than creating activity *de novo*⁵⁹. While it is still unclear how much enzymatic improvement is necessary to confer a physiological advantage at the cellular level, studies from natural and laboratory evolution have shown that enzymes can follow different strategies to improve these pre-existing functions⁶⁰. However, functional trade-offs between the original and evolved function may hamper the evolution of a new function, as long as selection pressure for the original one persists⁶¹. Consequently, gene duplication events have been discussed as a driving force in the selection of new divergent functions, as an additional gene copy would allow for genetic “drift” and the development of new phenotypic traits^{44,62,63}. To understand the evolution of enzymes involved in antibiotic resistance development, the general mechanisms of how enzymes adapt to new substrates and molecular drivers need to be discussed. For this, I will first present a comprehensive overview of identified molecular mechanisms used by different enzymes to promote and evolve promiscuous functions (Subchapter A-2.1). Second, I will shed light on the non-linearity of mutational effects (epistasis), the classes of epistasis and how intra-molecular epistasis affects enzyme evolution (Subchapter A-2.2). Third, I will introduce how the evolution of promiscuous functions can offset the native function and enzyme stability (Subchapter A-2.3).

2.1 Mechanistic adaptation of enzymes

Enzyme promiscuity can be recruited to improve a pre-existing function through evolution. Yang *et al.*⁶⁰ recently provided a comprehensive review on this process in more than 20 promiscuous enzymes. Before looking into the molecular mechanisms of these adaptive processes, some general questions need to be addressed. For example, how likely is it that a random mutation will improve the enzymatic function? Results from directed evolution as well as deep mutational scanning of large mutational libraries agree and show that the number of beneficial mutations is generally very low⁶⁰. On average ~65% of all mutations are deleterious towards activity, ~30% are neutral and less than 5% improve enzymatic functions⁶⁰. Even though this number seems low, one needs to keep in mind that an enzyme with 250 amino acids can have ~5000 single mutants. Thus, even a fraction of only 1% beneficial mutations would still lead to 50 mutations with the ability to improve a promiscuous function.

Another important question is, how many mutations are needed to enhance a promiscuous function and where are these mutations located? Based on various studies, it has been shown that the number of mutations needed to improve a latent function and the position of these mutations in the three-dimensional structure is highly dependent on the enzyme⁶⁰. This can be exemplified with two different β -lactamases, enzymes hydrolysing β -lactam drugs – VIM-2 (metallo- β -lactamase) and TEM-1 (serine β -lactamase). While in VIM-2 more than 90% of all mutations were within 15 Å of the catalytic site, for TEM-1, half of the acquired mutations were found on the surface^{64,65}. At the same time, mutations closer to the active site (<10 Å) tend to have greater influence on the enzymatic activity than the ones further away (>10 Å)⁶⁰. In addition, directed evolution studies showed that on average a >1,000-fold improvement in catalytic efficiency needs on average ~10 mutations⁶⁰.

2.1.1 Reshaping of the active site

Yang *et al.*⁶⁰ found that active site reshaping was a common molecular mechanism to promote promiscuous activity, as it was observed in 75% of their 20 reviewed cases. Examples of both narrowing and enlarging of active site cavities have been described in the literature⁶⁰. LovD from *Aspergillus terreus* catalyses the production of lovastatin, a derivate of simvastatin which is an important cholesterol-lowering drug. Directed evolution on LovD towards a much smaller substrate showed that, by acquiring 29 mutations, the activity towards a free acyl thioester substrate improved by 1,000-fold⁶⁶.

It also resulted in a reduced size of the active site cavity allowing a better “snug” fit of the new ligand (Figure 3A)⁶⁶. Conversely, expanding the active site has been shown to be necessary to adapt towards bulkier substrates. For example, during the evolution of the metallo- β -lactamase NDM-1 towards phosphonates, steric hindrance within the active site was removed⁶⁷. Also, variants of various other β -lactamases identified in pathogenic bacteria have been shown to expand their active site as a response to the exposure of bulkier β -lactams and β -lactam/ β -lactamase inhibitor combinations⁶⁸⁻⁷³. This observation is not limited to β -lactamases and has been described in different evolutionary studies⁷⁴. For example, the *P. aeruginosa* aryl sulphatase (PAS) catalyses the reaction of sulphate esters, but has also been shown to possess promiscuous activity against phosphodiesteres, phosphonate and phosphate monoesters. The promiscuous function was explored using directed evolution, and PAS was evolved towards hydrolysis of phosphonates resulting in a functional improvement by 100,000-fold⁷⁴. Within five rounds of directed evolution, the accumulation of the amino acid changes T50A and M72T allowed the expansion of the active site cavity enabling the enzyme to harbour the new and bulkier substrate.

2.1.2 Substrate interactions and reposition

Another possibility for enzymes to evolve towards new functions is the creation of new interactions with the substrate. This can often be achieved by recruiting and optimizing pre-existing residues which coordinate substrate specific moieties. The newly acquired interactions can then improve e.g., electrostatic interactions with the substrate and increase its catalysis by e.g., stabilising the transition state⁶⁰.

While this phenomenon has been described, it does not seem to be a very common mechanism during the evolution of promiscuous functions⁶⁰. The phosphotriesterase (PTE) of *Pseudomonas diminuta* catalyses the phosphate ester pesticide paraoxon (P-O bond) with high efficiency, but also exhibits promiscuous activity against aryl esters (C-O bond). Using directed evolution, the repurposing of PTE towards the aryl ester 2-naphthyl hexanoate (2-NH) increased the catalytic efficiency by $\sim 10^9$ -fold⁷⁵. The first round of evolution increased the aryl esterase activity by 2.6-fold due to the amino acid change H254R⁷⁵. The arginine residue was described as a centre piece in the evolutionary trajectory as it directly interacts and stabilises the naphthoxide leaving group of the 2-NH substrate likely *via* cation- π interactions (Figure 3B)⁷⁵. The changes along these trajectories can also influence the

positioning of the substrate within the active site, and thus lead to more productive binding events. Productive binding is important to ensure efficient catalysis. For example, during the above-mentioned evolution of PAS, the substrate was found closer to the catalytic machinery which likely contributed to the overall catalytic improvement⁶⁰.

2.1.3 Conformational tinkering by distant mutations

Not all amino acid changes happen within the active site (1st shell); they often occur distant from the active site cavity affecting 2nd or even 3rd shell residues⁶⁰. Such changes are usually not involved in substrate interactions, and elucidating their role in enzyme adaptation can be challenging. However, they have been described to fine-tune pre-existing active site residues, granting them catalytic competence by mechanism called “conformational tinkering”⁶⁰.

Lactonases are enzymes able to cleave the C-O bond within a lactone ring (cyclic ester). These enzymes, such as the N-acyl homoserine lactonase of *Bacillus thuringiensis* (AiiA), have shown promiscuous PTE activity⁷⁶. Over six rounds of directed evolution, AiiA improved its PTE activity towards paraoxon by 1,000-fold while displaying only a marginal (~3-fold) decrease in its lactonase activity⁷⁶. Structural investigations and molecular dynamics simulations revealed a movement of “loop 3” including the active site residue F68 by ~3 Å. This movement was caused by the two 2nd shell mutations V69G and F64C (Figure 3C). The substituted amino acids were substantially smaller than the wild-type residues, and thus increased conformational space by collapsing the “loop 3” (including F68). This allowed the active site residue F68 to move deeper into the active site where it then engaged into interactions with the p-nitrophenol leaving group of the new paraoxon substrate⁷⁶.

2.1.4 Conformational dynamics

The biochemical properties and conformational dynamics of enzymes are linked. Yet, the extent to which changes in their dynamical character influence catalysis and evolvability is under debate. Nonetheless, the evolution of conformational dynamics has been critical to improve catalysis in a number of enzymes^{60,77}. For example, significant conformational changes can be required to complete an enzymatic reaction mechanism and to host different substrates and intermediates. Such changes can include the sampling of certain loop conformations allowing an either closed or open

state of the active site⁶⁰. The evolution of PTE towards the aryl ester 2-NH was mentioned already several times for other mechanisms, and can also serve as an example here⁷⁸. Kaczmarek *et al.*⁷⁸ found that during PTE evolution, a productive and closed formation of the active site “loop 7” was selected for by “freezing out” the non-productive and open conformation (Figure 3D). On the contrary, the active site “loop 5” increased flexibility during the evolutionary process, likely allowing the loop to adapt to different states⁷⁸.

The serine β -lactamase TEM-1 represents another case where changes in conformational dynamics were studied during resistance development towards the β -lactam cefotaxime⁷⁹. R164S and G238S have been found to be first step mutants during the evolution, opening the path to different evolutionary trajectories⁸⁰. Both mutants enabled, when tested independently, a better accommodation of cefotaxime by either small conformational loop changes (G238S) or local loop disorders (R164S)⁷⁹. Despite their distant location (10 Å) within the structure of TEM-1, the combination of R164S/G238S was not compatible and resulted in non-productive conformations lowering cefotaxime resistance. This demonstrates that several exclusive conformational dynamics may evolve even within one enzyme⁷⁹. Other studies showed that changes in flexibility may affect the active site hydration which may increase enzyme activity^{60,81}.

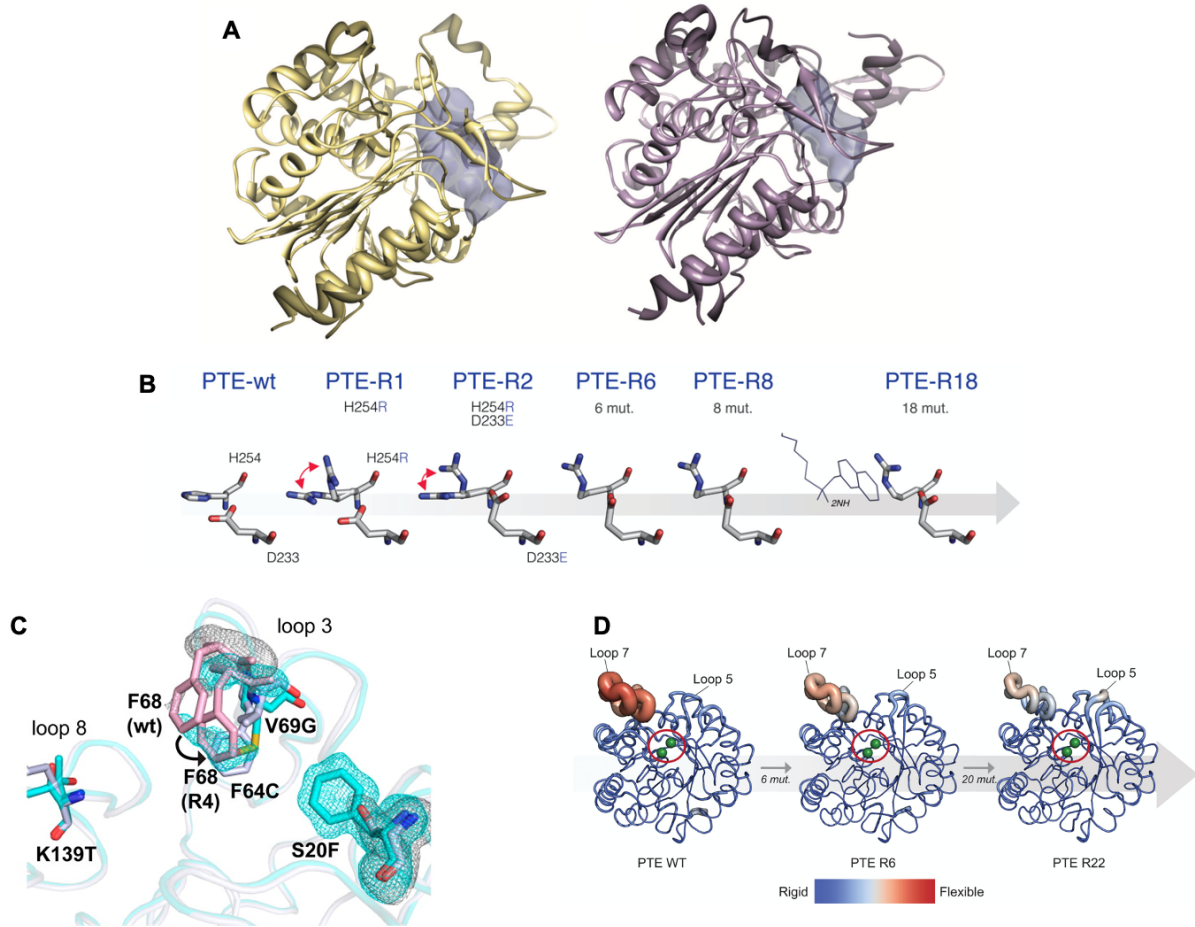


Figure 3: Mechanisms of enzyme adaptation. **A.** Wild-type LovD (left) and LovD after six rounds of evolution (right) demonstrates a significantly reduced size of the active site cavity (grey). **B.** The evolution of the phosphotriesterase (PTE) over 18 rounds of directed evolution towards the aryl ester 2-NH. A corner piece of this adaptation is the acquisition of H254R after the first round of evolution. In H254R, the arginine is interacting directly with the substrate as depicted on the right side. **C.** During the evolution of the lactonase AiiA towards PTE activity, two mutations, V69G and F64C, distant (2nd shell) from the active site were observed. These changes repositioned and enabled F68 to reach deeper into the active site where it then interacts with the substrate. **D.** Changes in conformational dynamics were reported for PTE (mentioned for B) where “loop 7” displayed decreasing levels of flexibility during the adaptive process (adapted with permissions from^{60,66,76}).

2.2 Epistasis as a driver of divergent evolution

The evolution of new enzymatic functions is often a stepwise process and requires the accumulation of several adaptive mutations⁸². This raises the question whether the functional effects of these mutations are dependent on each other? In other words, does the pre-existence of a certain mutation influence the functional effect of subsequently acquired mutations? Various studies have investigated and reviewed the effect of mutants alone and in combinations⁸³⁻⁸⁵. Lessons learned from these studies demonstrate that mutational effects are often non-additive and depend on the genetic context, absence or presence of other mutations, a process known as mutational epistasis. Consequently, epistasis is thought to strongly shape evolutionary trajectories, even yielding in evolutionary dead ends^{70,86}. In addition, epistasis impairs the predictability of enzyme evolution, the engineering of new proteins and the development of new drugs^{82,86,87}. Thus, a deeper understanding of the molecular mechanisms underlying epistasis is needed⁸³⁻⁸⁵. In this subchapter, the classes of epistatic effects (Subchapter A-2.2.1) and a further characterisation of epistasis such as non-specific *versus* specific (Subchapter A-2.2.2) as well as pairwise versus higher-order epistasis (Subchapter A-2.2.3) will be introduced.

2.2.1 Classes of epistatic interactions

To characterise an enzyme's intramolecular epistasis, mutational combinations can be constructed, and their enzymatic "fitness" (W) needs to be determined. For this, mutational landscapes can be analysed representing all mutational combinations such as all single, double, triple, etc. mutants. The "enzyme fitness" can represent phenotypes, such as catalytic efficiency (k_{cat}/K_M), the effect on bacterial growth in presence of antibiotics (e.g., minimum inhibitory concentrations or MIC) or the activity in cell lysate. The "fitness" phenotypes are typically assessed as a fold-change or difference compared to the wild-type or to intermediate variants along the evolutionary trajectory. It is important to note here, that some of these properties may be solely selectable traits which are not necessarily linked to the fitness of the organism. To understand and characterise epistasis, the mutational effects need to be classified. Firstly, mutations themselves can be classified as neutral, if they have no effect on the phenotype in either the wild-type or intermediates within the trajectory, or functional, if they confer a change in a beneficial or selected trait. Secondly, functional mutations

may interact in various ways and can be further classified depending on those interactions (epistasis) according to the following scheme⁸³:

- i)* No epistasis: The functional effects of two or more mutations is additive, and thus are not dependent on the mutational background (additive model, Figure 4A)
- ii)* Positive or negative magnitude epistasis: Mutations that either increase or decrease enzymatic fitness when combined with other mutations. Their effects on the wild-type background are often neutral or only limited, but become strongly beneficial or detrimental along the evolutionary trajectory (Figure 4B)
- iii)* Masking epistasis: Epistatic interactions where the effect of one mutation is masked when combined with another (Figure 4B)
- iv)* Sign epistasis reflects substitutions where the sign (e.g., “+” to “-“) of one mutational effect is changing (Figure 4B)
- v)* Reciprocal sign epistasis describes mutational combinations where the sign of both mutational effects is changed compared to the single mutants (Figure 4B)

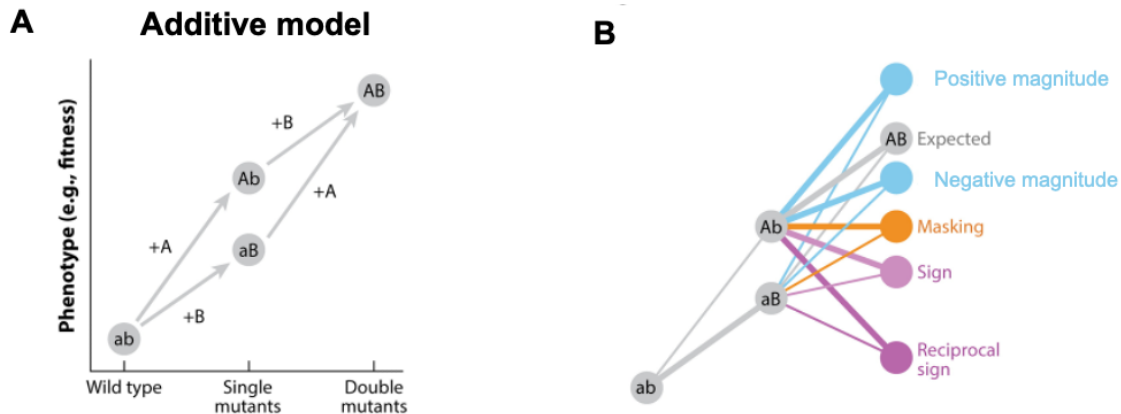


Figure 4: Classes and types of epistasis (adapted with permission from⁸⁵). **A.** The additive effect of non-epistatic mutations according to the additive model. The order how the mutations “A” and “B” are acquired does not matter since “A” and “B” confer an independent phenotypic effect (“enzyme fitness”). **B.** Mutational combinations often do not follow the additive model thus exhibiting epistasis. For example, the genetic background “ab” can acquire two separate mutations, “A” and “B”, resulting in “Ab” and “aB” with different phenotypes. Based on the additive model, the expected phenotypic effect of the two mutations in “AB” should be the sum of single mutants (no epistasis). The phenotypic effect of the double mutant can be higher or lower than expected, reflecting positive or negative magnitude epistasis, respectively. Further, the effect of one mutation can be masked by another. For positive and negative magnitude, the direction of the effect does not change. However, epistasis can even reverse the direction of the phenotypic effect where, for example, the combination of two single mutations, both increasing fitness separately, may lead to phenotype with lower fitness than either or both the single mutants (sign and reciprocal, respectively).

2.2.2 Non-specific and specific epistasis

Epistatic interactions can be either non-specific or specific. Non-specific epistasis is inflicted by the intrinsic non-linear correlation between the biophysical traits of enzymes and phenotypic properties, while specific epistasis is typically caused by one mutation which directly or indirectly interacts with only a few mutational sites, affecting the physical enzymatic properties, and thus shaping a non-additive phenotype⁸⁸.

To understand the underlying principle of non-specific epistasis, first, the effect of mutations on the biophysical properties of enzymes needs to be introduced. A mutation can affect and cause changes in the biophysics of a protein (e.g., folding, enzyme activity). If this effect correlates in a linear fashion with the measured phenotype (e.g., enzyme fitness, stability etc.), the combination of two additively behaving mutations will produce an additive phenotype (Figure 5A). Consequently, in a case where the biophysical effects of these mutations are not linearly correlated, the genotype-phenotype relationship will also be non-linear and lead to non-specific epistasis (Figure 5B)⁸⁵. What is known about the mechanisms causing these non-specific interactions? Protein folding is a spontaneous thermodynamical process and the thermodynamic stability can be described by the Gibbs free energy of folding, ΔG_F , where ΔH_F and ΔS_F represent the enthalpy and entropy of folding, respectively⁸⁹:

$$\Delta G_F = \Delta H_F - T \Delta S_F \text{ or } \Delta G_F = - R T \ln (\text{folded/unfolded})$$

The thermostability of a protein correlates sigmoidally with the fraction of natively folded protein, as indicated in Figure 5B. The most studied proteins tend to be only marginally stable and located on the upper stability plateau^{85,90}. Thus, one mutation weakly destabilising the enzyme will usually affect the folding *versus* unfolding ratio only marginally^{85,90}. However, the accumulation of two destabilizing mutations can significantly alter this ratio leading to non-specific epistasis. This has been shown in several deep mutational scanning studies investigating pairwise combinations of amino acid changes⁸⁵. Other mechanisms include increased cooperative binding due to non-linearity between protein concentration and bound ligands, and the non-linear relationship between protein expression and fitness where high gene expression might lead to reduced fitness⁸⁵. It is important to note that from genotype to phenotype several layers of non-linearities may act in combination and

affect non-specific epistasis. A good example demonstrating the connectivity of at least two non-linear relationships was shown by Li *et al.*⁹¹ for the phage lambda transcription repressor. Their deep mutational scanning revealed that to accurately describe the repressor activity of lambda double mutants, non-linear contributions for both the free folding energy and cooperativity of dimer recruitments needed to be considered.

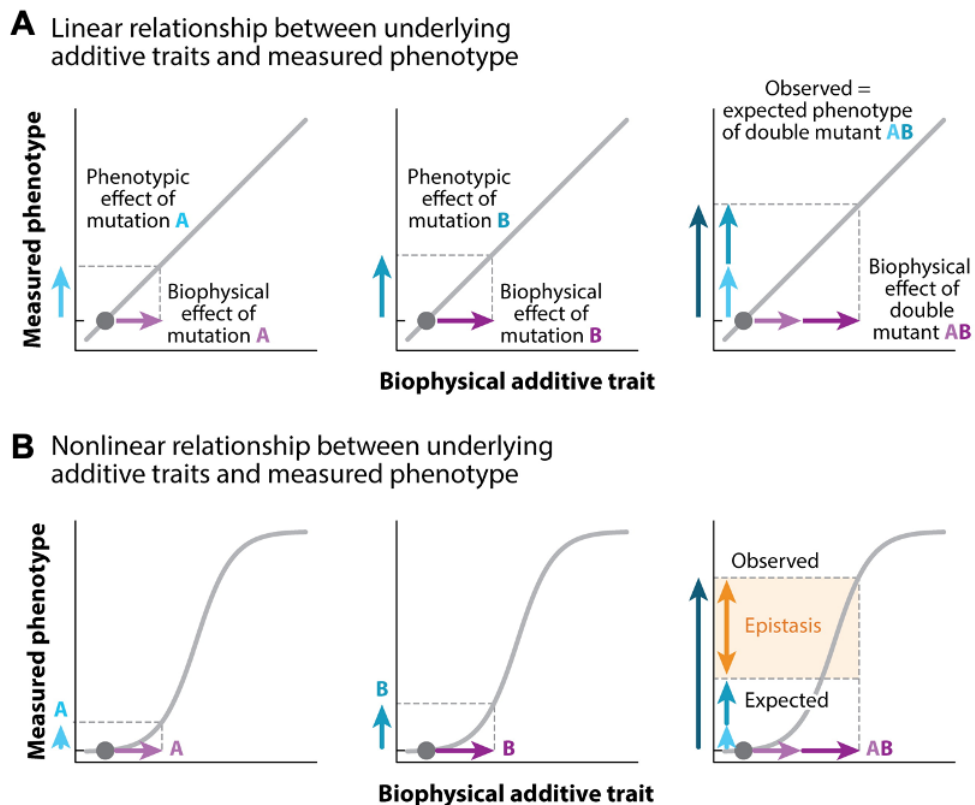


Figure 5: Non-specific epistasis caused by non-linearity between the biophysical traits and the resulting phenotype (adapted with permission from⁸⁵). **A**. No epistasis is caused when the combinational effect of two mutations such as A and B acts additively in both the biophysical and the measured phenotypic properties. **B**. In contrast, a non-linear relationship between the biophysical trait and measured phenotype causes non-specific epistasis.

Besides non-specific epistasis, specific interactions also called structural epistasis have been described in the literature, and are in large parts driven by specifically interacting mutations within the enzymatic structure. The molecular

mechanisms causing specific epistasis are more diverse, and thus more difficult to predict. Miton and Tokuriki⁸³ reviewed nine different proteins and the epistatic effects along their evolutionary trajectories. Based on their observations, four different types of specific epistasis could be characterised:

- i)* mutations interacted directly with each other where at least one of them is involved in substrate binding
- ii)* mutations interacted directly with each other, but without being involved in substrate binding
- iii)* mutations interacted indirectly with each other, and at least one of them is involved in substrate binding
- iv)* mutations were involved in neither direct interactions nor substrate binding

While negative epistasis is often connected to non-specific epistatic interactions, positive epistasis seems to be due to specific interactions⁸⁸. Conversely, mutational pairs in structural proximity (C β atom < 10 Å) of each other are more likely to confer positive epistatic effects and possess the ability to interact⁹².

2.2.3 Pairwise *versus* high-order epistasis

Epistasis events may occur due to specific interaction of only two specific amino acids, as described above⁹³. Indeed, deep mutational scannings have shown that such pairwise interactions substantially contribute to epistasis⁹³. A study on the serine β -lactamase TEM-1, investigating the effect of 12,000 consecutive double mutants, showed that negative epistasis is ~8-times more prevalent than positive epistasis, which accounted for only ~7% of the observed effects⁹³. However, these experiments only reported limited information regarding combinational effects over the whole sequence space. In addition, during long-term evolution, that is the acquisition of several mutations over longer evolutionary timeframes, these negative effects should be purged from the population by purifying selection, and positive permissive mutations should be dominating⁸⁸. Indeed, in their review Miton and Tokuriki⁸³ showed that across different adaptive trajectories positive epistasis such as magnitude and sign epistasis was with 75% the most prevalent.

Since the acquisition of only one permissive mutation can directly influence the type and order of sequentially acquired mutations, this automatically raises the

question of how long this memory effect lasts? In other words, the acquisition of a certain mutation may favour or exclude the accumulation of subsequent mutations, and thus condition the long-term evolution of enzymes. The role of this so called higher-order epistasis and its driving role in the divergent evolution of proteins has only recently been studied⁹⁴⁻⁹⁶. In their review, Sailor and Harms⁸⁶ investigated the prevalence and role of such higher-order epistasis on the long-term adaptive trajectories of six different phenotype-genotype landscapes. All trajectories were affected at least by 3rd order epistasis and four out of the six trajectories even demonstrated epistatic contribution at the 5th order. They also showed that epistasis impairs the predictability of evolutionary outcomes such as resistance development, and thus having implications for human health.

Being able to predict an evolutionary outcome and having the ability to convert a given genotype to the corresponding specific phenotype would revolutionize both molecular evolution and human medicine. This could help to improve treatment strategies and the development of new drugs. However, the prevalence of epistasis limits our ability to do so and, even if partially accounted for, specific pair-wise or higher-order interactions may still impair the predictability of resistance development⁸⁶. Finally, epistasis can drive the evolutionary contingency since the acquisition of only one mutation can limit or constrain the accessibility of subsequently acquired mutations or even whole trajectories^{80,97,98}. Consequently, epistasis may open the path for alternative trajectories which not necessarily reach the global maximum of the fitness landscape (evolutionary dead ends)⁹⁸.

2.3 Trade-offs during adaptation

The effect a mutation causes is usually not unilateral and is highly context dependent. In other words, mutations increasing enzyme activity to catalyse a new substrate likely affect other enzymatic traits such as the activity towards the native reaction or thermostability. This phenomenon, also termed pleiotropy, can be exploited in the context of drug resistance as it results in collateral sensitivity⁹⁹⁻¹⁰⁴. Collateral sensitivity has been proposed to be an exploitable strategy in the clinical setting where resistance development to one drug can cause re-sensitization towards other drugs. Such strategies could, in theory, pave the way for new treatment options during antibiotic and cancer chemotherapy.

2.3.1 Functional trade-offs: weak *versus* strong

Enzymes are often specialised to catalyse one reaction efficiently^{61,82}. However, mutations acquired to evolve a promiscuous function often disturb the pre-existing shape and charge complementation between the active site and the native ligand or substrate. Even small structural changes can result in a trade-off between the newly evolved and the native function (Figure 6)⁶¹.

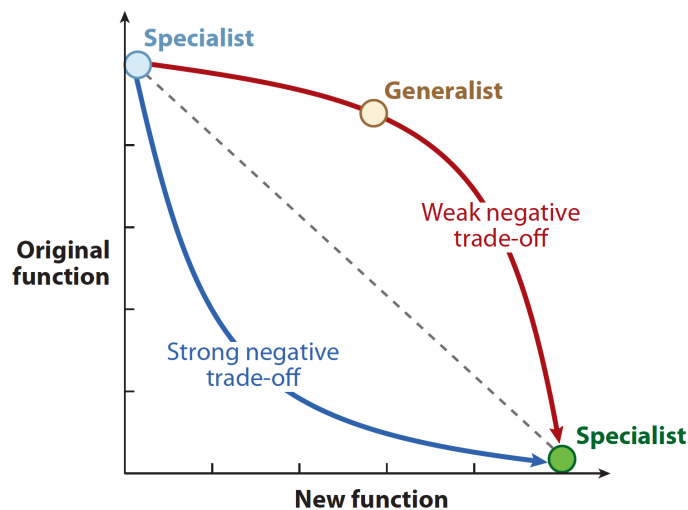


Figure 6: Functional trade-off between the original or native and the newly evolved function. The red line indicates the progression of a weak trade-off where the acquisition of the new function does initially not confer a strong trade-off in their native activity. The blue line indicates the transition through a strong trade-off function where small improvements of a new function result in a sharp reduction of the native function (reprinted with permission from⁴⁹).

Such trade-offs can be strong, where the acquisition of a single amino acid change reduces the ability to catalyse the native substrate by several orders of magnitudes^{61,105,106}. Strong reductions in the native activity have been associated with the structural properties of the substrate or ligand⁶¹. As a rule of thumb, size and charge of the ligand or substrate matters⁴⁹. In studies with strong functional trade-offs, the tested promiscuous substrates tended to be bulkier than the native ones⁴⁹. It is imaginable that adaptation to bulkier substrates may enlarge the active site, which can reduce the ability to catalyse smaller substrates. *Vice versa*, adaptation to smaller

substrate may reduce the active site cavity, and thus limit the accommodation of larger substrates. Yet, exceptions to this rule have also been identified showing that e.g., evolution towards smaller substrates does not always trade-off the native function^{49,107}. As mentioned above, the substrate charge can also be of importance. For example, if the native substrate is neutral and the novel substrate is charged, structural modifications may favour the binding of either substrate¹⁰⁵.

In contrast, by reviewing 11 evolutionary cases, Khersonsky *et al.*⁴⁹ reported that promiscuous activity can be improved by 10 to 10⁶-fold without being highly detrimental to the native function (only 0.8 to 42-fold loss in native activity). This has been shown for the majority of their reviewed cases⁴⁹. It was also proposed that such weak trade-offs arise as a consequence of the inherent evolvability of enzymes⁴⁹. On one hand, enzymes are “plastic” and can improve their promiscuous functions with only some mutations but on the other hand, their native activity is supposed to be “robust” to mutational permutation⁴⁹. However, Kaltenbach *et al.*¹⁰⁸ showed that enzymes are likely less robust to their native activity than initially thought, and that high enzymatic efficiency and mutational robustness might not be compatible. The authors further argue that weak trade-offs may only be a consequence of lacking selective pressure to maintain the native function.

Overall, the presence of strong and weak trade-offs has evolutionary consequences. Strong trade-offs drive the functional divergence of enzymes. In addition, in cases where dual selection pressure requires the presence of the native as well a newly evolved function, either gene duplication or compensatory mutations (e.g., increased copy number when on plasmids or increased protein expression) is needed⁶¹. On the contrary, most of the studied enzymes exhibit only weak trade-offs and their presence results in enzymatic generalists which are able to act bifunctionally⁶¹.

2.3.2 Stability-function trade-offs

The architecture of the active site is thought to be thermodynamically unfavourable as many catalytic residues carry polar or charged side chains which are buried within a hydrophobic core¹⁰⁹. Thus, the replacement of many key catalytic residues has been shown to confer drastic stability improvements while reducing the enzymatic activity¹⁰⁹⁻¹¹¹. For example, the substitution of key residues (e.g., S64, K67 and N152) within the serine β -lactamase AmpC reduced enzyme activity up to 10⁵-fold, but improved steric, electrostatic and polar complementarity, and thus stability¹¹². This has brought up the hypothesis that stability and enzymatic function trade-off. However, based on that perspective, mutations improving the enzymatic function should then be more destabilizing compared to non-functional mutations. Tokuriki *et al.*¹⁰⁹ reviewed the average effect of “new-function” mutations acquired during directed evolution of 22 different enzymes and compared their effects on the stability to all other acquired mutations (e.g., neutral). On average, mutations conferring “new-functions” were just as destabilizing as “all others” exposing that stability and enzymatic activity do not necessarily need to trade-off¹⁰⁹.

Tokuriki *et al.*¹⁰⁹ further showed that only 5% of all amino acid changes behaved in a stabilizing manner⁹⁰. These stability enhancing mutations also included key catalytic residues and their substitution would result in inactive enzymes⁹⁰. Thus, the fraction of mutations that can truly enhance the enzyme stability without inactivating an enzyme is thought to be even lower. The fact that most of the mutations are destabilizing and only a small fraction can improve stability has implications for the evolvability of new functions (Figure 7). In a simple model, the “protein fitness”, W , is dependent on the functional component, f , (e.g., catalytic efficiency) and the concentration of functional protein, $[E]_0$:

$$W = f \times [E]_0$$

The concentration of functional protein is dependent on the stability, and the relationship between thermostability and activity is non-linear (see Subchapter A-2.2.2). To possess a physiological role within the cell, proteins must be maintained above the stability threshold and in a range where folding is unaffected (Figure 7A). While some mutations are predicted to over-stabilize, and thus reduce the enzymatic functionality (e.g., loss of dynamics, and flexibility), most mutations are destabilizing

and are likely to cause aggregation and unfolding^{109,110}. For enzyme adaptation this means that only a limited set of destabilizing and functional improving mutations can be acquired (Figure 7B). Stability must be restored or buffered through mutations which act as followed^{109,110}:

- i) general stabilizers (global suppressors) improving the enzyme stability overall
- ii) compensators which are conditionally beneficial and mask the destabilising effect of certain functional mutation

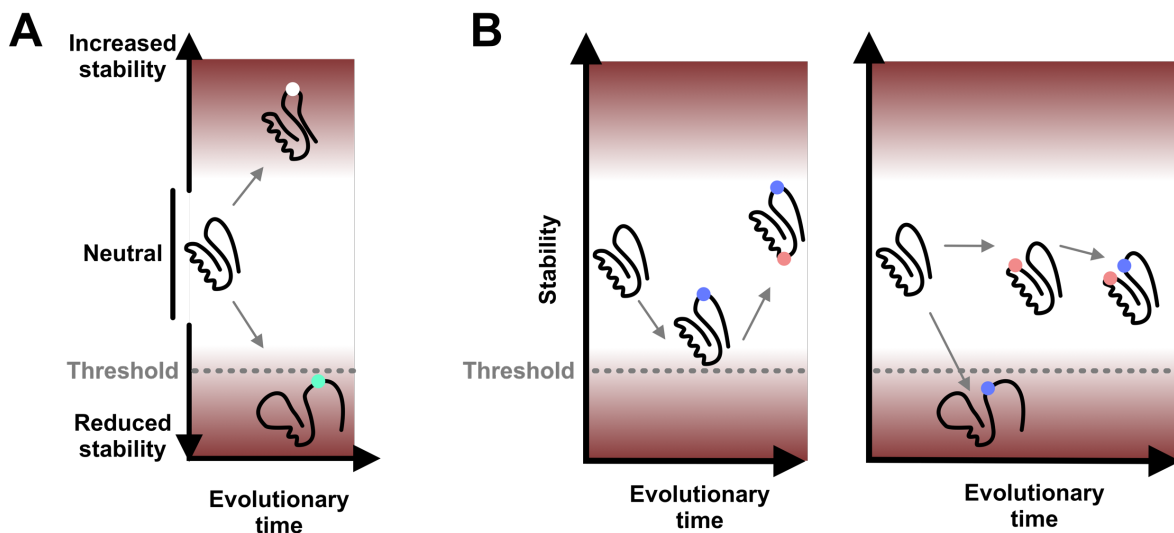


Figure 7: Stability-function trade-off. **A.** Enzymes are often placed on stability optimum, which indicates a “neutral” zone where small changes in stability do not affect folding, and thus activity. The accumulation of mutations may affect the stability (green *versus* white) of proteins. Both can affect the concentration of functional proteins, and thus “enzyme fitness”. The threshold model is a commonly accepted model to describe stability developments during adaptation. The lower cut-off for stability is represented at the lower end of the “neutral” zone. If the protein stability drops below this point its functionality is likely compromised. **B.** During the adaptive processes, functional mutations (blue) are acquired and most of these are destabilising. This limits the number of mutations that can be acquired before crossing the stability threshold. In Considering this, compensatory mutations (salmon) need to be acquired which act

either as global suppressors (left), increasing the general stability, or interact the with destabilising mutation (right) and buffer its effect (Figure based on^{88,89}).

3 Evolution and selection of β -lactamases

The expression of β -lactamases, enzyme hydrolysing β -lactam drugs, contributes to one of the most troublesome antibiotic resistance mechanisms^{6,7}. However, like other antibiotic resistance determinants, β -lactamases are ancient enzymes and have been identified in pristine environments all over the globe^{23-25,113,114}. Their ancestral tales reach back several billion years²³. Since then, they had the opportunity to develop high structural and catalytic diversity. Within this chapter, the evolutionary relationship between β -lactams and β -lactamases will be introduced. First, a brief overview on β -lactams will be provided, concerning their molecular targets, how β -lactams are, presumably, naturally produced at low-concentrations, and their stability. Second, the different mechanisms by which β -lactam resistance can be conferred will be introduced. Lastly, the evolution of serine β -lactamases will be discussed, uncovering the promiscuous β -lactamase functions of non- β -lactamases within the superfamily and how low β -lactam concentrations may select for such low β -lactamase activity.

3.1 Penicillin binding proteins and β -lactams

3.1.1 Inhibition of penicillin binding proteins by β -lactams

The evolutionary story of β -lactamases cannot be written without discussing β -lactam drugs and their molecular target within the bacterial cell – the penicillin binding proteins (PBPs). PBPs represent a diverse enzyme family which is responsible for peptidoglycan synthesis, regulation, and maintenance of the bacterial cell wall¹¹⁵. They can be classified into high molecular weight (HMW) and low molecular weight (LMW) PBPs where HMW-PBPs are multi-domain proteins that incorporate and polymerize peptidoglycan groups into the cell wall, and are functionally subdivided into two classes, class A (transpeptidase and transglycosylase) and class B enzymes (transpeptidase only)¹¹⁵. LMW-PBPs (class C PBPs, subclassified into type-4, -5, -7 and -AmpH) are mainly involved in peptidoglycan maturation and recycling and possess DD-carboxypeptidase and/or DD-endopeptidase activities¹¹⁵. PBPs generally share the same catalytic penicillin-binding domain with a nucleophilic serine in the active site to catalyse their reactions. β -lactam agents and the natural substrate of PBPs, the D-Ala-D-Ala dipeptide exhibit high structural similarity (Figure 8). Consequently, the serine of PBPs active site is able to nucleophilically attack the β -

lactam ring, inhibiting PBPs function by forming a stable acyl-enzyme complex (Figure 8)¹¹⁵.

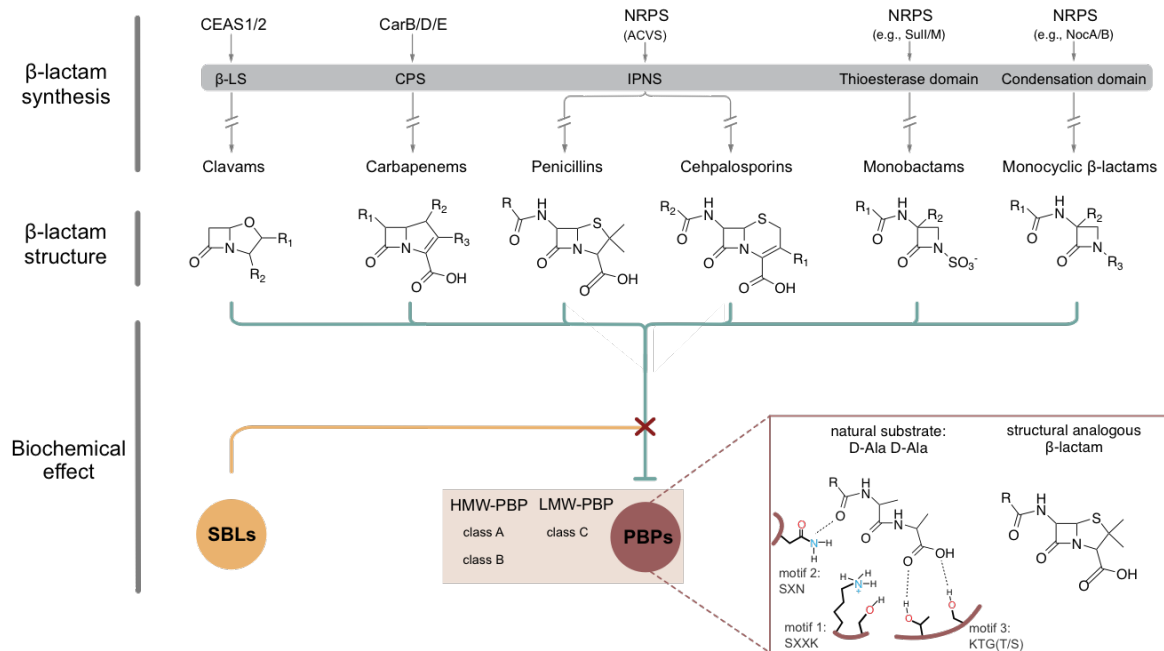


Figure 8: Evolution and diversity of natural β-lactam producing pathways and serine β-lactamases (SBLs) (adapted with permission from¹¹⁶). Biosynthesis pathways of 5 different β-lactam classes, the structural β-lactam backbone where R₁, R₂ and R₃ can represent different substituents (upper part). The inhibitory effect of these agents on the penicillin binding proteins (PBPs) is indicated with the green line, where they act as substrate analogous compounds binding to PBP active site motifs such as SxxK, SxN and KTG(T/S). SBLs have evolved to hydrolyse β-lactams (yellow line).

3.1.2 Natural pathways of β-lactam synthesis

To gain insights into the origins of β-lactam resistance, one first needs to understand that natural pathways for β-lactam synthesis have been found in distinct bacterial (e.g., *Streptomyces*, *Flavobacterium*, *Burkholderia*) and fungal (e.g., *Aspergillus*, *Acremonium*) genera. These pathways have likely co-evolved with β-lactamases for up to a few billion years^{23,117}.

There are at least five independent pathways by which β -lactams are produced biosynthetically in nature, resulting in the following classes: *i*) penicillins and cephalosporins, *ii*) monocyclic β -lactams, *iii*) monobactams, *iv*) carbapenems and *v*) clavams (Figure 8)¹¹⁸⁻¹²⁰. The structural backbone (Figure 8) of penicillins and cephalosporins is synthesised by the same pathway by a non-ribosomal peptide synthetase (NRPS). The β -lactam ring formation is then carried out by an isopenicillin N synthase (IPNS). This initial penicillin compound can be further modified to a cephalosporin^{119,120}. The ring-formation for monobactams and monocyclic β -lactams is catalysed by distantly related NRPS¹²⁰⁻¹²². For carbapenems and clavams, this reaction is performed by carbapenem synthetase (CPS) and β -lactam synthetase (β -LS), respectively¹²⁰. Interestingly, both CPS and β -LS have evolved independently from the asparagine synthetases, enzymes involved in the synthesis of ammonia and amino acids¹²⁰.

β -lactams synthesised through these five pathways are able to inhibit bacterial PBPs^{113,118}. While the natural role of these β -lactam compounds, and their selection pressure in nature is not known, these compounds likely occur at low concentrations in the environment³⁸. However, we do not know if they solely functioned as antibiotics or whether their role is more complex such as the involvement in cell-to-cell communication. To that end, β -lactam biosynthetic pathways have evolved several times in history, resulting in compounds targeting PBPs and inhibiting bacterial cell wall synthesis¹¹⁶. Thus, these compounds have seemingly played an important function within bacterial communities³⁸.

3.1.3 Stability of β -lactams

β -lactams are generally less stable than other classes of antibiotics such as tetracyclines¹²³, and it is thought that the short half-life of these drugs contribute to their lower abundance in environmental samples where hydrolysis could take place biotically and abiotically¹²⁴⁻¹²⁶. But for how long are β -lactam agents stable? For stability in water, laboratory data demonstrated that β -lactam persistence depends strongly on pH and temperature. For example, the half-life of amoxicillin at 30°C and pH 7 was determined to be 12.5 days. However, degradation was accelerated at pH 3 and 10 which was reflected in shorter half-lives of 4.7 days and 0.4 hours, respectively^{127,128}. In addition, a study on the microbial degradation of benzylpenicillin in aqueous solution showed that the drug could be detected up to 8 days at 5°C but was already degraded after 2 days at 20°C¹²⁹. In surface water, the half-life of cefradine, cefuroxime, ceftriaxone, and cefepime ranged from 3 to 19 days without and 2 to 5 days with sunlight exposure, respectively (at room temperature)¹³⁰. Under dry soil conditions, amoxicillin did not degrade within 30 days of incubation¹³¹. In agreement with these findings, comparable results were found for cephalosporins where aerobic degradation of ceftiofur in soil resulted in half-lives of up to 49 days¹³². The stability of cefradine, cefuroxime, ceftriaxone, and cefepime in sediment was determined with half-lives of up to 4 days at room temperature. All these examples show that β -lactam drugs can be stable for up to several days in certain environments where they might play an important role in the selection of β -lactam resistance.

3.1.4 β -lactam classes and β -lactam resistance

First discovered in 1928 by Alexander Fleming, penicillin was the first commercially available β -lactam and β -lactams drugs still comprise the most prescribed antibiotic drug class worldwide¹³³. To date, four different β -lactam classes are in clinical use *i*) penicillins (e.g., piperacillin), *ii*) cephalosporins and oxyimino cephalosporins (e.g., cefotaxime, ceftazidime), *iii*) carbapenems (e.g., meropenem, imipenem, ertapenem) and *iv*) monobactams (aztreonam). As mentioned previously, all classes display different structural backbones as shown in Figure 8, however, all of them carry the four-membered cyclic amide ring which is important for their antibiotic function.

The widespread use of these drugs has selected for various resistance mechanisms including *i*) reduced β -lactam-sensitivity of PBPs, *ii*) changes in cell-wall permeability through active efflux or porin alterations, and *iii*) the expression of β -

lactamases, enzymes able to cleave the β -lactam ring structure. Mechanism *i*) is largely observed among Gram-positives while *iii*) is more common in Gram-negative bacteria where these enzymes are expressed and transported into the periplasmic space¹³⁴.

3.2 Evolution of β -lactamases

β -lactamases are enzymes able to hydrolyse the ring structures of β -lactams and they can be grouped based on their active site properties into metallo- β -lactamases and serine β -lactamases. While metallo- β -lactamases employ zinc in their active site, serine β -lactamases are utilising a catalytic serine residue similar to PBPs to hydrolyse β -lactam drugs^{118,135}. The Ambler classification system groups them according to their sequence identity into class B comprising only metallo- β -lactamases, and the classes A (e.g. KPC-type, SHV-type), C (e.g. AmpC) and D (mostly OXA-type) which are composed of serine β -lactamases¹¹³. In addition, a functional classification system from Bush and Jacoby exists (Figure 9)¹³⁶, grouping these enzymes into the functional groups 1 (class C), 2 (class A), 2d (class D) and 3 (class B). According to their ability to hydrolyse different classes β -lactams they can be further sub-grouped (Figure 9).

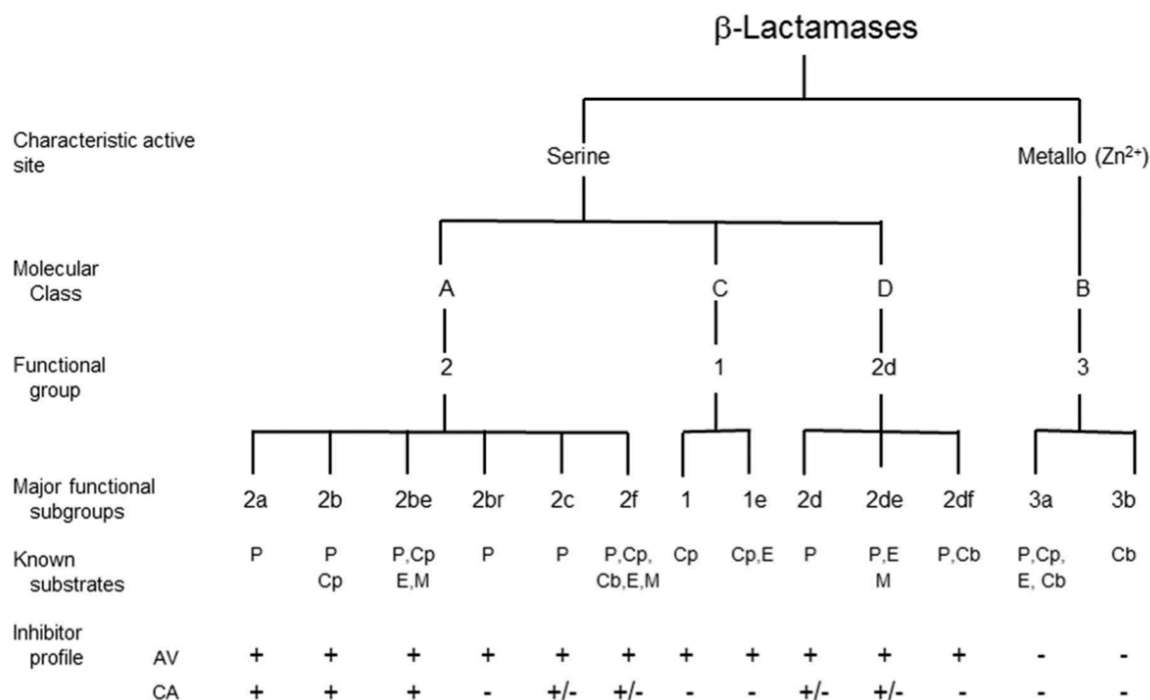


Figure 9: Molecular and functional characterisation of serine and metallo-β-lactamases (reprinted with permission from¹¹³). P, penicillins; Cp, cephalosporins; Cb, carbapenem; M, monobactams; E, extended-spectrum cephalosporins; AV, avibactam; CA, clavulanic acid.

3.2.1 PBP-like family and serine β-lactamases

The exposure to β-lactams, naturally or in anthropological settings, has likely selected and promoted enzymes exhibiting promiscuous β-lactamase activity. It is hypothesised that serine β-lactamases have evolved from the PBPs by acquiring physiological relevant β-lactam hydrolysing mechanisms. The presence of non-β-lactamase enzymes displaying β-lactamase promiscuity within the PBP-like superfamily could strengthen this hypothesis. We recently reviewed the functionality of non-β-lactamases within the PBP-like superfamily to provide a comprehensive overview on this¹¹⁶. Serine β-lactamases belong to the PBP-like superfamily, which is comprised of a large pool of enzymes including over 450,000 sequences (Pfam ID: CL0013). The members of this superfamily share a common αβ structural fold, and conserved (SxxK; serine motif), as well as semi-conserved, (SxN and KTG) active site motifs. A large fraction of these sequences represents HMW- and LMW-PBPs exhibiting transpeptidase,

transglycosylase, DD-carboxypeptidase and DD-endopeptidase activities¹¹⁵. However, the PBP-like superfamily is also host to enzymes catalysing distinct enzymatic reactions such as esterases, acyltransferases, methylbutanoyltransferases, 6-aminohexanoate-dimer hydrolases and β -lactamases^{115,137-139}.

Phylogenetics showed that class A and C β -lactamases have seemingly originated from type-5 and AmpH-type LMW-PBPs, respectively, and class D enzymes were closest related to HMW-PBPs¹¹⁶. The evolutionary relationship was further strengthened as many non- β -lactamase enzymes within the PBP-like superfamily, such as transpeptidases and carboxypeptidases, exhibit promiscuous and selectable β -lactamase activity¹¹⁶. This further indicates that β -lactam concentrations as reported in the environmental samples may be able to select for such promiscuous functions and promote the selection of β -lactam resistance¹⁴⁰.

Ambler class A, C and D serine β -lactamases represent ~10% of all sequences within the PBP-like superfamily. These serine β -lactamases are acylated by β -lactam agents in a similar manner as HMW- and LMW-PBPs, where the serine within the SxxK motif nucleophilically attacks the β -lactam ring and the asparagine in SxN and polar groups in KTG(T/S) assist in stabilising the β -lactam agent within the active site¹¹⁵. While HMW- and LMW-PBPs do not possess sufficient activity to hydrolyse the acyl-enzyme complex, serine β -lactamases have evolved water-assisted deacylation mechanisms¹³⁵. Interestingly, the mechanisms of how class A, C and D enzymes activate this deacylation water is distinct (Figure 10). For class A enzyme such as KPC-2, a conserved glutamic acid at position 166 is responsible for the activation. For class C enzymes such as AmpC, it is thought that this activation is mediated by K67, which polarises the hydroxyl group of the tyrosine at position 150 and enables Y150 to activate the water molecule. Class D β -lactamases, such as OXA-48, employ a posttranslationally carboxylated lysine at position 73 to mediate the water activation (also see Subchapter A-4.1.3).

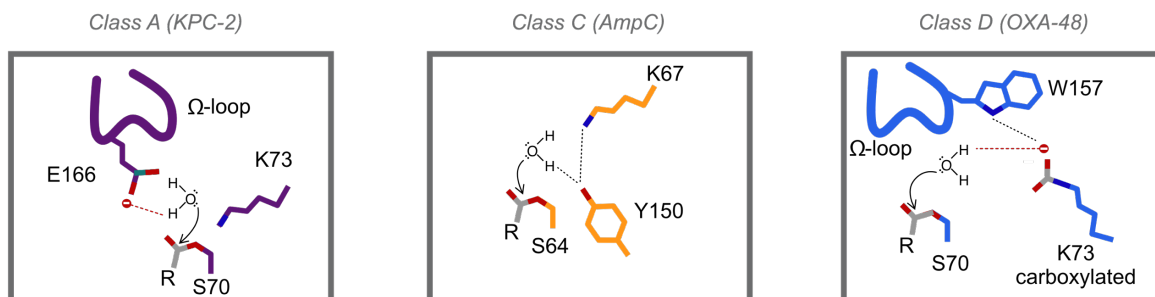


Figure 10: Different water activation mechanisms during the β -lactam deacylation process between Ambler class A, C and D β -lactamases (KPC-2, violet; AmpC, orange; and OXA-48, blue; were used as examples). For class D, the lysine at position 73 is carboxylated (adapted with permission from¹¹⁶).

3.2.2 Low β -lactam concentrations driving the evolution of β -lactamases?

In the previous subchapters, it was shown that *i*) β -lactams are naturally presumably produced at low concentrations³⁸, and *ii*) that they can be environmentally stable (>days) to impose a selective pressure on bacteria. In theory, low β -lactam concentrations as found in the environment might select for such promiscuity and drive the evolution of these enzymes.

Environments with low-level selection pressures were widely neglected for quite some time, mainly because low-level resistance is *i*) rarely identified in the clinical setting and *ii*) it does not impose any immediate threat to patients¹⁴¹. However, over the last 20 years substantial contributions to the field have shown that low selection pressure can lead to low- and high-level resistance^{38,42,43,141-146}. Sub-lethal levels of antibiotics are problematic since they:

- i*) tend to select for fitter variants that can be maintained more stably within a bacterial population¹⁴⁷
- ii*) stimulate horizontal gene transfer and increase the rates of homologous recombination^{144,148-152}
- iii*) favour the occurrence of mutator phenotypes with higher chances to develop multi-drug resistance¹⁵³⁻¹⁵⁵. For example, long-term exposure to

β -lactams has been shown to trigger the bacterial SOS response which is commonly associated with increased mutation frequencies^{152,156,157}

Where can low concentrations of antibiotics be found? Due to pharmacological reasons, the usage of antibiotics creates a wide spanned concentration gradient in the human body¹⁵⁸. Here, high drug concentrations will be found in small, confined compartments, while lower concentration are expected to be present in larger compartments for a much longer time. In addition, low environmental concentrations have been described for various classes of antibiotics because of environmental pollution. A study in Germany found that during the course of one day the ampicillin concentration in hospital effluent reached $\sim 80 \mu\text{g/L}$ and calculated an annual average of $\sim 20 \mu\text{g/L}$ ¹⁵⁹. The same study estimated the annual average concentration of antibiotics, emitted by hospitals and households, to be about 70 mg/L . Here, more than 50% are thought to be represented by β -lactams¹⁵⁹. Further, amoxicillin (up to $1.7 \mu\text{g/L}$) and ampicillin (up to 0.8 ng/L) were reported in river and sea water in Greece, UK, China and Kenya¹⁶⁰. In addition, Ribero *et al.*¹⁴⁰ collected data on cephalosporin pollution from 72 articles published between 2005 and 2018. Accordingly, cephalosporin residues were found in surface and coastal water (up to 16 ng/L), hospital and industrial waste water (up to 5 ng/L) and in influents (up to $64 \mu\text{g/L}$)¹⁶¹ and effluents (up to $2 \mu\text{g/L}$) of waste water treatment plants¹⁴⁰.

While studies have been investigating the role of sub-therapeutic concentrations on resistance development for different antibiotic classes, limited data is available on how β -lactams drive the evolution of β -lactamases¹⁶²⁻¹⁶⁵. Sub-MICs of imipenem have been found to select for mutations in the promotor region of the serine β -lactamase AmpC in *Pseudomonas*, which resulted in increased β -lactam resistance^{165,166}. Another more indirect example has been reported for the serine β -lactamase TEM-1 which does not hydrolyse cephalosporins such as cefotaxime and ceftazidime efficiently. However, after the clinical introduction of these drugs, variants of TEM-1 emerged – first TEM-12 (R164S) and later TEM-10 (R164S/Q240K). While TEM-12 only caused a marginal decrease in cefotaxime susceptibility from 0.03 to 0.06 mg/L (2-fold) in *E. coli*, TEM-10 decreased the susceptibility to 1 mg/L (32-fold). The 2-fold change in susceptibility caused by TEM-12 is, from a clinical microbiology perspective, insignificant. Yet, competing *E. coli* cultures expressing TEM-12 and TEM-1 exhibited

a bacterial fitness benefit for the TEM-12 over the TEM-1 expressing strain at low cefotaxime concentration^{141,167}. Therefore, β -lactams in low concentrations may select for variants with little or no effect on the susceptibility phenotype (cryptic phenotypes), which may act as steppingstones to develop full clinical resistance. While the above-mentioned study showed the selectable potential of β -lactams on pre-existing and cryptic variants, many questions regarding the evolutionary dynamics of very low β -lactam concentrations remained unanswered. For example, can the exposure to sub-therapeutic β -lactam concentrations select for promiscuous β -lactamase activity? Can sub-therapeutic β -lactam concentrations select for variants with expanded or changed substrate profile, and do they select for high or low-level resistance? The here presented work aims to close these gaps within the literature by exposing β -lactamase producing bacteria to sub-lethal β -lactam concentrations using long-term experimental evolution.

4 Ambler Class D β -lactamases

4.1 The OXA-Family

4.1.1 Functional diversification

Enzymes classified as Ambler class D are serine β -lactamases able to catalyse the hydrolysis of β -lactam drugs. The class D consists of 14 different families, however, with more than 900 sequences most of the enzymes within this classification scheme belong to the Oxacillinases or OXA-family¹⁶⁸. Based on their sequence identity, OXA-type enzymes are grouped into ~70 subfamilies with diverse substrate specificity¹⁶⁸. Even though these enzymes can exhibit extremely high sequence similarity within a subfamily, their hydrolysis activity is heterogeneous¹⁶⁹. This clearly creates problems in how to classify those variants regarding their genetic relatedness and substrate specificity. For example, in 2010, Poirel *et al.* introduced groups for the classifications of class D OXA β -lactamases which overlap with the functional classification from Bush and Jacoby^{136,170}:

- i) group I; narrow-spectrum hydrolysing enzymes
- ii) group II; extended-spectrum hydrolysing enzymes
- iii) group III; carbapenem hydrolysing enzymes

While narrow-spectrum enzymes catalyse the hydrolysis of penicillins and early generation cephalosporins, extended-spectrum enzymes possess the ability to hydrolyse later generations of cephalosporins such as ceftazidime, cefotaxime and cefepime. Carbapenemases have the ability to hydrolyse carbapenem drugs such as meropenem and imipenem. Examples for narrow-spectrum enzymes are OXA-1-like, OXA-2-like and OXA-10-like variants. However, not all enzymes within these subfamilies share the same phenotypic traits. For example, OXA-1 and OXA-2 are narrow-spectrum hydrolysers, however, microevolution has selected for variants with an expanded or shifted hydrolytic profile^{168,170,171}. For example, the acquisition of A67P in OXA-31 (OXA-1 variant) expanded the spectrum to extended-spectrum, enabling the hydrolysis of cefepime¹⁷². This shows the fluent transition between e.g., group I and II. Another challenge to classify these enzymes according to their hydrolysis spectrum is the phenotypic characterization which most classification systems are based on. Newly identified variants are often expressed and characterised in *E. coli*

and the effect might be different in another host. For instance, OXA-2 and OXA-10 are classified as narrow-spectrum enzymes, but confer carbapenem resistance comparable to class D carbapenemases when expressed in *A. baumannii*, but not in *E. coli*¹⁷³. The carbapenemase group III is further classified into two sub-groups¹⁷⁴. The first subfamily describes enzymes mainly identified in *Acinetobacter* spp. containing the sub-families of OXA-23-like, OXA-24/40-like, OXA-51-like and OXA-58-like variants, while the second contains the more distantly related OXA-48-like variants which are mainly identified in *Enterobacterales*¹⁷⁵.

4.1.2 Structural conservation and features

Within the OXA family, there are at least four different and conserved structural motifs. The first motif, S⁷⁰xxK, includes the active site serine responsible for the nucleophilic attack of the β -lactam ring. Motif numbers II, III and IV are S¹¹⁸xV, (Y/F)¹⁴⁴GN, and IV, K²¹⁸(T/S)G, respectively, and are close to loop regions such as the P-loop (amino acids D82 to N110), the Ω -loop (amino acids D143 to S165) and the β 5- β 6 loop (amino acids T213 to K218) (Figure 11A and B). These loop regions determine the active site and have been described as important for the substrate specificity within the OXA-family¹⁷⁶⁻¹⁸⁰.

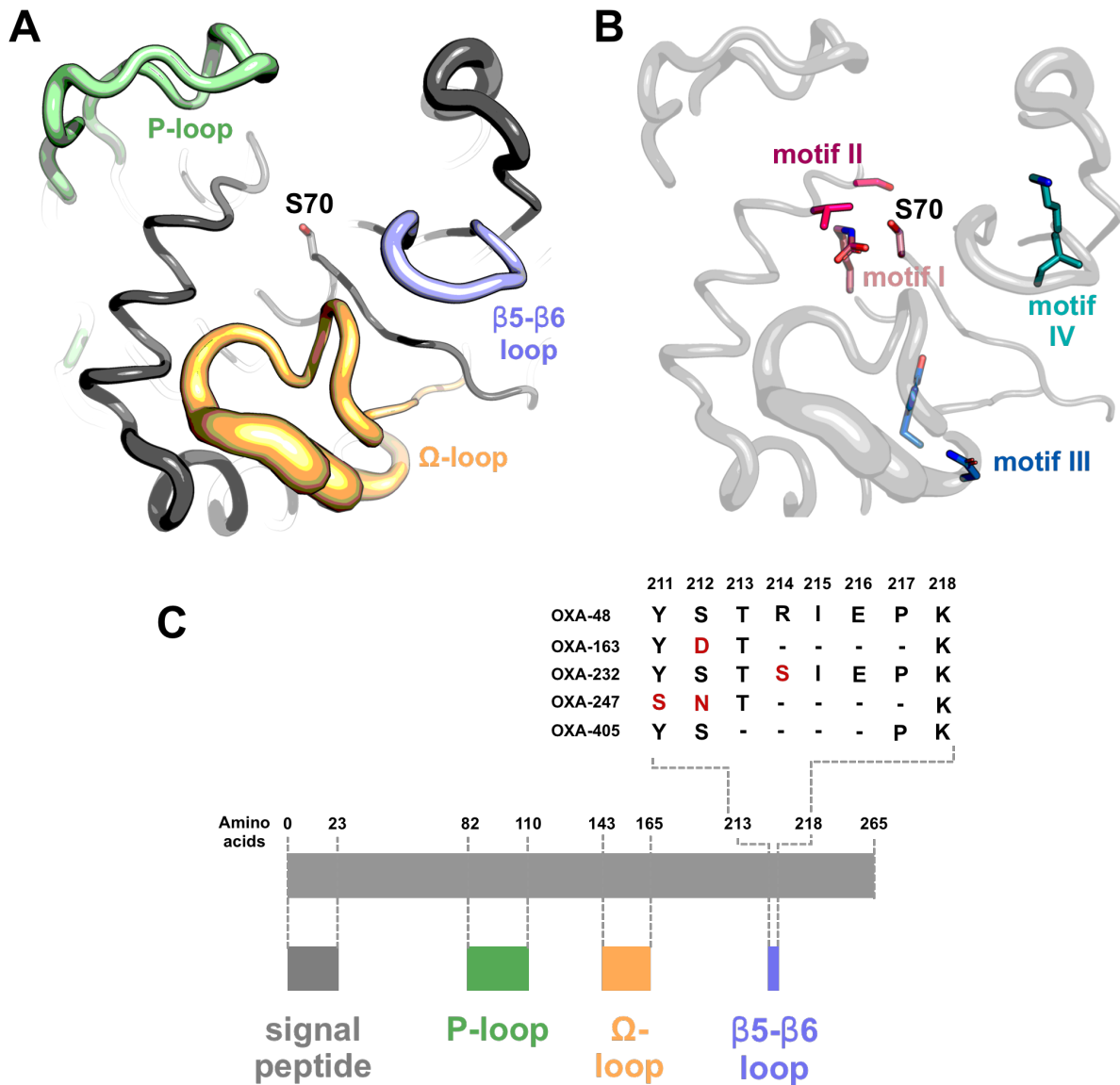


Figure 11: Structural features and conservation. **A.** Structure of OXA-48 based on PDB no. 6P96¹⁸¹ showing the catalytic key residue S70 and the active site loops: P-loop (green), Ω-loop (yellow) and β5-β6 loop (violet). **B.** Residues of the conserved motifs I to IV: S⁷⁰xxK, S¹¹⁸xV, (Y/F)¹⁴⁴GN, and IV, K²¹⁸(T/S)G, respectively. **C.** Sequence of OXA-48 visualising the amino acid positions of the P-loop (green), Ω-loop (yellow) and β5-β6 loop (violet). Amino acid changes around the β5-β6 loop of OXA-48-like variants with extended-spectrum β-lactamase activity including hydrolysis activity for ceftazidime. Amino acid changes are displayed in red letters and deletions with “-”.

4.1.3 General reaction mechanism

β -Lactam hydrolysis by serine β -lactamases such as class D enzymes consists of two steps: acylation and deacylation (Figure 12). First, the β -lactam and β -lactamase form a non-covalent complex. Next, S70 as one of the key active site residues binds to the β -lactam amide bond and forms a covalent acyl-enzyme complex *via* a tetrahedral intermediate¹³⁵.

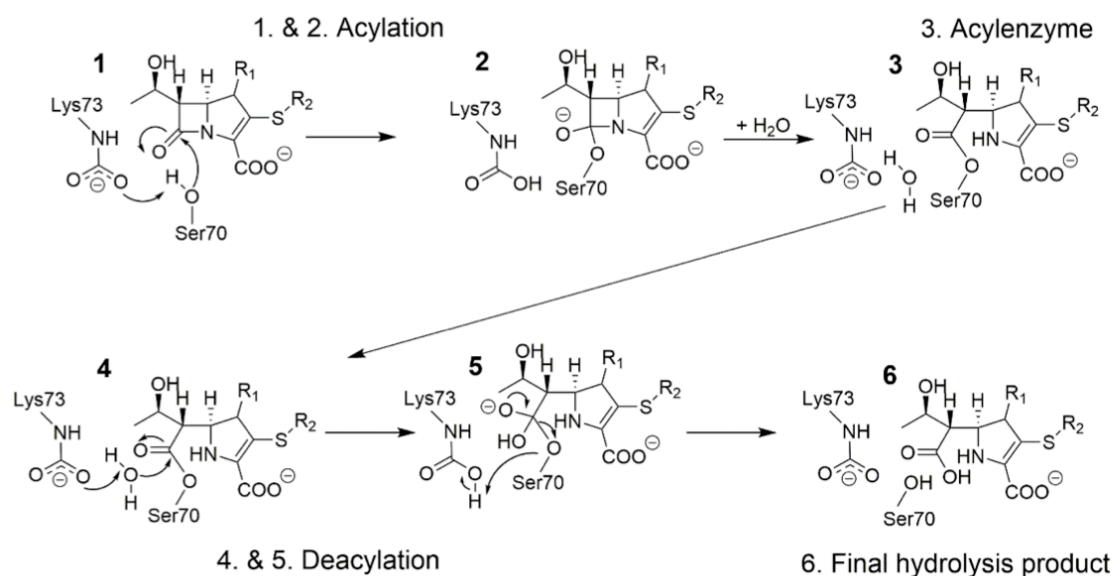


Figure 12: General acylation and deacylation mechanism of serine β -lactamases (reprinted with permission from¹⁸²).

As mentioned in Subchapter A-3, the general deacylation mechanism for Ambler class D enzymes is distinct from those in class A and C (Figure 10). The deacylation step for serine β -lactamases requires the presence of an activated water molecule within the active site which attacks the acyl-enzyme complex and cleaves the product from the enzyme (Figure 12)¹³⁵. For class D serine β -lactamases, the activation of this water molecule is mediated by a posttranslationally carboxylated lysine at position 73¹⁸³⁻¹⁸⁷. Carboxylation likely accelerates both acylation and deacylation¹⁸⁸. Posttranslational carboxylation is a rare phenomenon and supposedly facilitated by the hydrophobic environment surrounding K73, which is shaped by residues such as V120 and W157¹⁸⁹. This hydrophobic pocket is thought to decrease the pK_a value of K73,

stabilising its non-protonated state at physiological pH which favours the reaction with carbon dioxide^{188,190}. In line with this, mutagenesis studies and examples of naturally evolving variants support the importance of V120 and W157 on the stability of this carboxyl group¹⁹⁰⁻¹⁹⁴. In addition, the substitution of K73 to alanine or to negatively charged amino acids such as aspartic acid and glutamic acid strongly reduced catalytic efficiency in OXA-1 demonstrating the general importance of K73 during catalysis¹⁹¹

4.1.4 Inhibition of serine β -lactamases

Combination therapy where β -lactams are co-administered with β -lactamase inhibitors has been proven to be a successful strategy to fight infections caused by β -lactamase producing bacteria^{135,195}. Commonly used clinical inhibitors target serine β -lactamases and comprise different chemical core structures where some are β -lactams (e.g., clavulanic acid, sulbactam, tazobactam), and others are diazabicyclooctanes (e.g., avibactam, relebactam) and boronates (e.g., vaborbactam). Generally, clavulanic acid, sulbactam and tazobactam are not effectively inhibiting OXA-48¹⁶⁸. Also, newer inhibitors such as vaborbactam and relebactam only show limited inhibitory activity against OXA-48^{196,197}. While initially developed to target class A β -lactamases, avibactam has inhibitory activity against class D β -lactamases, and especially OXA-48¹⁹⁸.

4.2 OXA-48-like β -lactamases

4.2.1 Origins, mobilisation and spread

Since its first discovery in 2001, OXA-48 has become one of the most troublesome carbapenemases globally¹⁹⁹. To date, more than 100 enzymes have been reported with amino acid sequence identities ranging from 76.6 to 99.6% compared to OXA-48¹⁶⁸. But what is known about the natural origin of genes encoding for OXA-48-like variants? OXA-48 and OXA-48-like variants have been identified in environmental samples and have been often reported to be encoded on the chromosome of *Shewanella* species¹⁷⁵. For example, OXA-54 with 92% sequence identity to OXA-48 has been identified in *S. oneidensis*¹⁷⁵. Another example is *bla*_{OXA-48b}, which carries four synonymous mutations compared to *bla*_{OXA-48}, and has been identified in *S. xiamenensis* recovered from China¹⁷⁵. The regions flanking *bla*_{OXA-48} in *S. xiamenensis* have high sequence similarity to the transposase of Tn1999, which is found on the clinical *bla*_{OXA-48} harbouring IncL plasmid. It has therefore been

hypothesised that the insertion sequences (IS1999) are responsible for mobilisation of *bla*_{OXA-48} from chromosome into a ~60 kb conjugative IncL plasmid. This pOXA-48 plasmid is highly transmissible and has been described in various species, but rarely in *A. baumannii* and *P. aeruginosa*^{175,200}. Thus, pOXA-48 plasmids seem to possess a host range which is limited to *Enterobacteriales*¹⁷⁵. Similar mobilisation events have also been suggested for other clinically relevant OXA-48-like variants including OXA-162, -181, -204, -232 and -244¹⁷⁵.

4.2.2 Carbapenemase activity

OXA-48 catalyses the hydrolysis of penicillins with high efficiency but possesses only weak hydrolytic activity towards carbapenems^{183,199}. While little is known about the structural aspects for penicillin hydrolysis, substantial progress has been made to structurally understand the carbapenemase activity of OXA-48-like variants¹⁸². The first structure of OXA-48 bound to a carbapenem was only recently (2018) released (PDB no. 5QB4)²⁰¹, and since then, several structures of OXA-48 bound to various carbapenems such as meropenem, imipenem ertapenem, doripenem and OXA-163 complexing imipenem and meropenem have been recently published¹⁸². These studies revealed that common interactions in stabilising the carbapenem acyl-enzyme complex exist¹⁸². For example, the carbonyl group of the cleaved β -lactam ring is often positioned within an oxyanion hole comprising the backbone amides of S70 and Y211¹⁸². The carbapenem molecule was further stabilised by H-bonds to T209, as well as ionic interactions between R250 and the carboxyl group on the carbapenem C3 atom (Figure 13)¹⁸². In addition, the “carbapenem tail” located on the carbapenem C2 atom has been found to not undergo strong interactions, and thus has been observed to be present in multiple conformations (Figure 13)^{181,202,203}. Structural investigation of imipenem and meropenem further exposed that their 6 α -hydroxyethyl group at the C6 atom (Figure 13) reached into the active site, and that the methyl group was placed within a hydrophobic pocket defined by A69, V120 and L158 (Figure 14A)^{181,203,204}.

After the formation of the acyl-enzyme complex, the carbapenem pyrrolidine ring can be present in either the Δ^1 or Δ^2 tautomerized form¹⁸². The Δ^1 tautomerisation of carbapenems produces two isomers (*R*)- Δ^1 and (*S*)- Δ^1 unlikely to possess equivalent deacylation rates^{205,206}. In addition, the 6 α -hydroxyethyl group (Figure 13) has been discussed to reduce the nucleophilicity of the deacylation water by H-bond formation²⁰⁷ or sterically hinder the water from accessing the acyl-enzyme bond²⁰³. However, the

importance of these stereoisomers for the overall catalysis remains elusive, and a recent study showed that this tautomerisation might not explain differences in carbapenemase activity²⁰⁴. Indeed, the majority of class D enzymes such as OXA-2, OXA-10, OXA-23 and OXA-48 possess carbapenemase activity levels which tend to range from 10^4 to 10^5 $M^{-1} s^{-1}$, and their expression in *A. baumannii* confers resistance towards carbapenems¹⁷³.

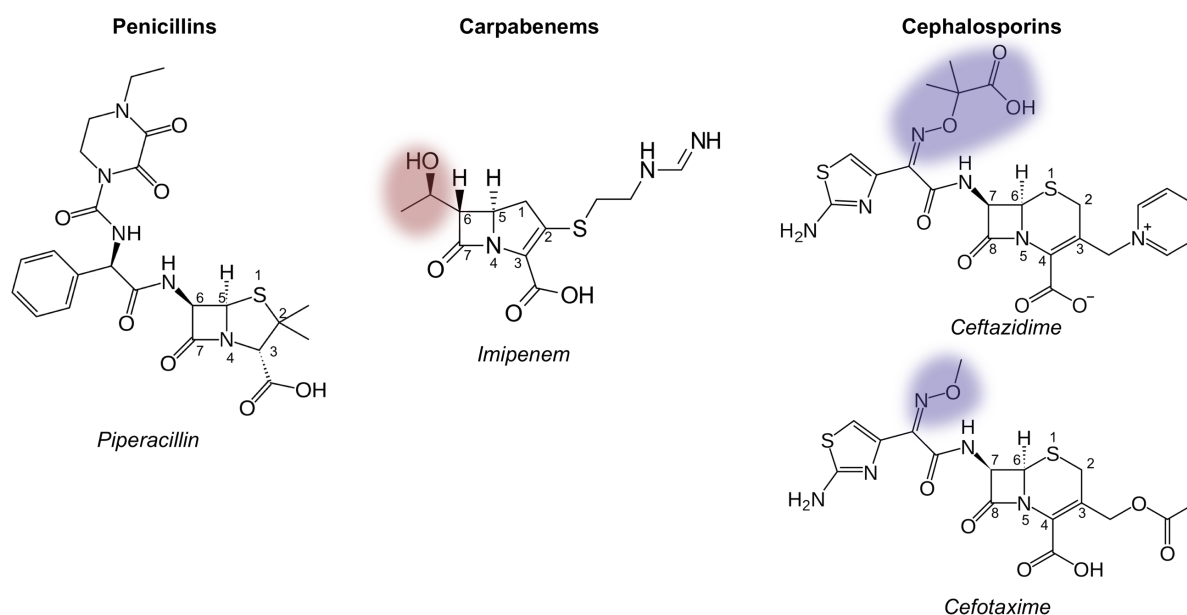


Figure 13: Chemical structure of piperacillin (penicillin), imipenem (carbapenem) and ceftazidime/cefotaxime (cephalosporins) and their corresponding scaffold numbering. In red the 6 α -hydroxyethyl at carbapenem C6 atom is shown (also called R1 side chain). In violet, the oxyimino group of the cephalosporins ceftazidime and cefotaxime is visualised.

4.2.3 Cephalosporinase activity

OXA-48 catalyses the hydrolysis of oxyimino cephalosporins such as ceftazidime (3rd generation cephalosporin) very inefficiently, which seems to be physiological insignificant in *E. coli*^{183,199,208}. Indeed, the catalytic efficiency towards ceftazidime has been reported to be as low as $10^2 \text{ M}^{-1} \text{ s}^{-1}$ and is consequently two to three orders of magnitude lower than the carbapenemase activity of OXA-48²⁰⁸. In addition, the catalytic efficiency of OXA-48 varies slightly towards different cephalosporins. For example, the activity towards cefotaxime (3rd generation cephalosporin) and cefepime (4th generation cephalosporin) has been reported to be 6 and 60-fold higher than for ceftazidime¹⁶⁸ which could be related to differences in the molecular size of these drugs (Figure 13).

Molecular docking showed that ceftazidime binding causes structural clashes with residues within the $\beta 5$ - $\beta 6$ loop such as R214 of OXA-48²⁰⁹. Further, structural investigations using the oxyimino cephalosporin cefotaxime and the cephamycin cefoxitin demonstrated that for both drugs, the dihydrothiazine ring was stabilised within the active site by stacking interaction (W105), H-bonds (S118 and T209) as well as electrostatic static interactions (R250). A pocket consisting out of A69, L158, S212, T213 and R214 was able to host the oxyimino side chain of cefotaxime and the thiophene ring of cefoxitin (Figure 14B and C)²⁰³. L158 is part of the Ω -loop and S212, T213 and R214 are located in the $\beta 5$ - $\beta 6$ loop. Interestingly, the binding of both cefotaxime and cefoxitin caused conformational changes of D101, I102, W105, L158 and T213 within the active site. In addition, the side chain of R214 within the $\beta 5$ - $\beta 6$ loop could no longer be accommodated within the active site upon cefoxitin binding (Figure 14C)²⁰³. Consequently, the active site of OXA-48 seems not optimised to accommodate bulkier substrates such as oxyimino cephalosporins, which may explain the lower catalytic efficiency towards oxyimino cephalosporins compared to carbapenems and penicillins²⁰⁹. On the contrary, OXA-48-like variants with increased ceftazidime activity such as OXA-163, OXA-232, OXA-247, and OXA-405^{177,178,210,211} have evolved and often exhibit four amino acid deletions and/or amino acid substitutions within the $\beta 5$ - $\beta 6$ loop. These structural modifications expand the active site cavity likely aiding the accommodation and catalysis of bulkier substrates such as ceftazidime²⁰⁸.

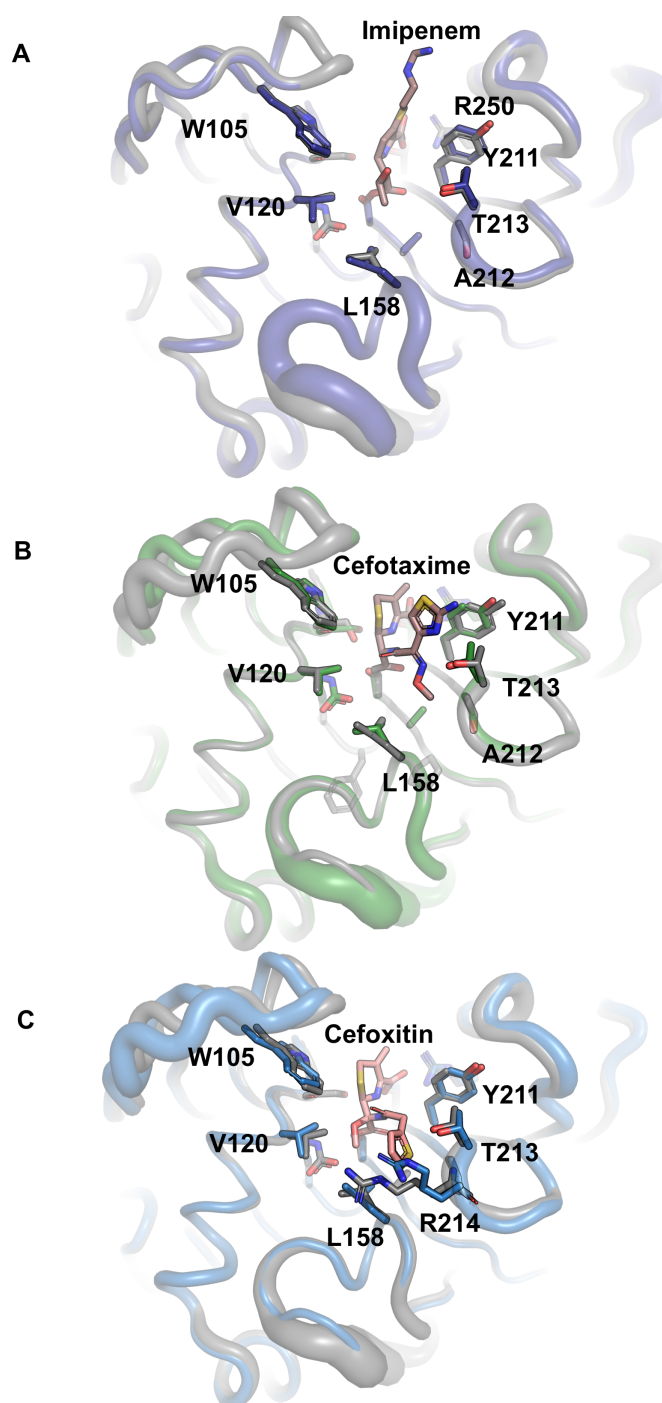


Figure 14: Binding of imipenem, cefotaxime and ceftiofuran within the structure of OXA-48. For comparison, the structure of OXA-48 without bound substrate is shown in grey for all three panel figures (based on PDB no. 4S2P²¹²). The substrates are coloured in salmon. **A.** OXA-48 (violet) bound to imipenem (PDB no. 7KH9²⁰⁴). The 6 α -hydroxyethyl of imipenem points towards L158 and V120. **B.** OXA-48 (green) with bound cefotaxime (PDB no. 6PQI²⁰³). Small conformational changes (e.g., L158 and T213) can be observed upon cefotaxime binding. **C.** OXA-48 (blue) with bound ceftiofuran (PDB no. 6PT5²⁰³). R214 is displaced upon ceftiofuran binding.

4.2.4 Substrate specificity and trade-offs

An increasing number of naturally evolving OXA-48-like variants have recently been reported, including OXA-163, OXA-232, OXA-247 and OXA-405, conferring elevated resistance against ceftazidime^{177,178,210,211}. In these variants, evolution often selected for increased ceftazidime activity by point mutations and/or a shortened β 5- β 6 loop (Figure 11C)^{177,178,210,213,214}. Expansion of their substrate range towards ceftazidime was typically accompanied with a trade-off towards penicillins and carbapenems (Table 2)^{177,178,183,210,213,214}. The trade-off has also been confirmed on the enzymatic level using enzyme kinetics where the catalytic efficiency of OXA-163 for meropenem and imipenem hydrolysis is 5- and 100-fold lower than for OXA-48, respectively²⁰⁴.

Table 2: MIC data in (mg/L) of OXA-48-like variants.

	<i>E. coli</i> TOP10 ^{a,b}	<i>E. coli</i> TOP10 pTOPO- <i>bla</i> _{OXA-48} ^a	<i>E. coli</i> TOP10 pTOPO- <i>bla</i> _{OXA-163} ^a	<i>E. coli</i> TOP10 pTOPO- <i>bla</i> _{OXA-232} ^a	<i>E. coli</i> TOP10 pTOPO- <i>bla</i> _{OXA-405} ^b
Temocillin	4-8	>256	32	32	32
Cefotaxime	0.06-0.12	0.25	16	0.12	0.5
Ceftazidime	0.12	0.25	64	1	3
Imipenem	0.25	2	0.5	1	0.25

^aMIC data from Oueslati *et al*¹⁶⁹

^bMIC data from Dortet *et al*¹⁷⁷

The accumulation of single point mutations in OXA-48 resulted in variants that moderately (4-fold) increase ceftazidime resistance in *E. coli*, such as OXA-232¹⁶⁹. OXA-232 and OXA-181 differ from each other by only one mutation (R214S, where the serine is present in OXA-232). In OXA-181 and OXA-48, R214 interacts with D159 *via* a salt bridge, and thus contributing to the interaction between the Ω - and β 5- β 6 loops. Disturbing that salt bridge by replacing R214 with serine, as in OXA-232, significantly reduced the conferred resistance towards penicillins and carbapenems²¹¹. In OXA-48, the β 5- β 6 loop provides a binding site for the methyl group of the carbapenem R1 side chain (Figure 13)¹⁸³. Previous studies employed molecular dynamics simulations on OXA-48 and OXA-163 in order to gain insights into the carbapenem resistance trade-off. Due to the shortened β 5- β 6 loop in OXA-163, the

methyl group of the carbapenem R1 side chain cannot any longer be stabilised, likely leading to multiple substrate conformations within the active site. Most of these conformations are thought to be incompatible with fast deacylation, which would explain the lower catalytic efficiency of OXA-163 for carbapenems compared to OXA-48²⁰⁴. In addition, the presence of a substrate within the active site is thought to limit the available space, and thus the accessibility of the deacylation water to access and act on the acyl-enzyme bond^{81,203}.

The importance of active site loops on the substrate specificity has been demonstrated by replacing the Ω -loop in OXA-48 with the corresponding loop in OXA-18, an OXA-10-like variant with increased activity against ceftazidime and aztreonam. This resulted in a chimeric enzyme which elevated resistance towards these two drugs¹⁸⁰. In addition, replacing the Ω -loop in OXA-10 with that of OXA-24 and OXA-48 modulated substrate specificity¹⁷⁹. To that end, the significance of the Ω - and β 5- β 6 loops for the substrate profile is not only limited to OXA-48. These loops have been shown to impact substrate profiles for other clinically relevant serine β -lactamases, including TEM and KPC²¹⁵⁻²¹⁷.

Despite numerous variants exhibiting structural variations within active site loops of OXA-48, only a limited set of these variants has been characterised towards various β -lactam substrates (e.g., OXA-245 and OXA-519)^{208,218}. Thus, the substrate specificity of many naturally evolving variants is unknown²¹⁹.

B. Aims

The expression of β -lactamases represents one of the most troublesome antibiotic resistance mechanisms^{6,7}. While substantial progress has been made in understanding the molecular epidemiology and biochemical properties of these enzymes, still little is known about the underlining mechanisms driving the evolution and adaptational process of contemporary β -lactamases^{175,220}. The Ambler class D serine β -lactamase OXA-48 does not catalyse the hydrolysis of ceftazidime efficiently but possesses, with a catalytic efficiency of $10^2 \text{ M}^{-1} \text{ s}^{-1}$, substrate promiscuity²⁰⁸. The β -lactam ceftazidime is of great clinical importance, as it is used in combination with the β -lactamase inhibitor avibactam to treat infections caused by multidrug-resistant *Enterobacterales*. At the same time, OXA-48-like variants such as OXA-163 have been identified from clinical isolates conferring increased ceftazidime hydrolysis. Thus, this thesis aimed to study resistance development and the evolutionary consequences of ceftazidime and ceftazidime-avibactam on OXA-48 (Figure 15A). In detail, the following questions were addressed:

- i) Can the exposure to ceftazidime or ceftazidime in combination with avibactam drive the evolution of OXA-48?
- ii) What is the evolutionary potential of this adaptational process? In other words, how many mutations are needed to develop a potential new “ceftazidimase” function within OXA-48? How does OXA-48 structurally adapt to increase hydrolysis towards ceftazidime?
- iii) Generally, what are drivers of this evolutionary process? Are very low β -lactam concentrations accelerating the evolution? How is intra-molecular epistasis involved in the evolutionary process?
- iv) Does the development of a new “ceftazidimase” activity within OXA-48 impose a trade-off towards other β -lactam substrates? How does the promoting of ceftazidime activity affect the thermostability of OXA-48?

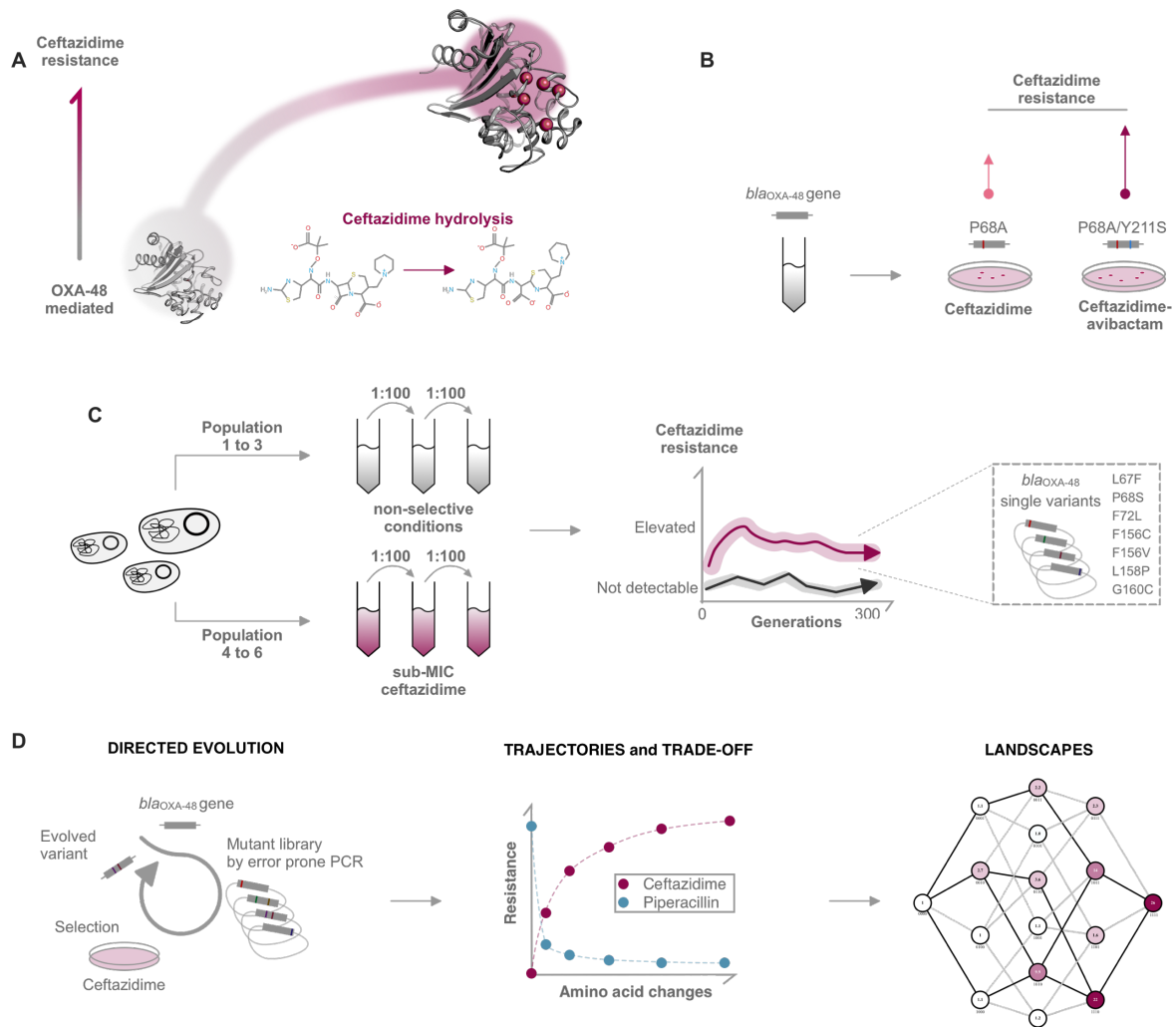


Figure 15: Methodological overview. **A.** Schematic overview on the evolution of OXA-48 towards increased ceftazidime hydrolysis. **B.** Selection of *E. coli* MG1655 expressing OXA-48, from a clinical plasmid, on plates containing either increasing concentrations of ceftazidime or ceftazidime-avibactam (Paper I) resulted in single (P68A) and double (P68A/Y211S) OXA-48 variants, respectively. **C.** Sub-MIC evolution of the same strain at 0.25 mg/L (0.25x ceftazidime MIC) over 300 generations resulted in increased ceftazidime resistance and promoted the evolution of numerous of OXA-48 variants (Paper II). **D.** Iterative cycle of directed evolution (left) were performed and libraries were selected on increasing concentrations of ceftazidime. Variants able to grow on the highest concentrations served as starting points for the next round. Evolution was performed until ceftazidime resistance of the corresponding variants reached a plateau (middle). The trade-off was investigated by measuring the susceptibility towards piperacillin. Fitness landscapes (right) were constructed and characterised to understand epistatic contributions.

C. Summary of papers

Paper I

“OXA-48-mediated ceftazidime-avibactam resistance is associated with evolutionary trade-offs”;

Christopher Fröhlich, Vidar Sørum, Ane Molden Thomassen, Pål Jarle Johnsen, Hanna-Kirsti S. Leiros, Ørjan Samuelsen. *mSphere*. 2019, 4 (2) e00024-19; DOI: 10.1128/mSphere.00024-19

Here, the effect of ceftazidime and ceftazidime-avibactam on *E. coli* MG1655 expressing OXA-48 from a clinical plasmid was studied (Figure 15B). For that, the strain was grown overnight and plated on LB agar plates containing increasing concentrations of either ceftazidime or ceftazidime-avibactam. From these plates clones were recovered and changes within *bla*_{OXA-48} were identified using Sanger sequencing. Upon ceftazidime and ceftazidime-avibactam exposure, variants of OXA-48 exhibiting single (P68A), and double (P68A/Y211S) amino acid changes were identified.

To investigate if these variants affect antibiotic susceptibility, the wild-type and mutant alleles were subcloned into pCR-blunt II expression vectors and expressed in *E. coli* TOP10. The expression of OXA-48 did not significantly (\pm 2-fold change) increase resistance to ceftazidime and ceftazidime-avibactam, compared to *E. coli* TOP10. While the expression of P68A increased ceftazidime resistance by 32-fold without affecting ceftazidime-avibactam resistance, P68A/Y211S lowered the susceptibility to both ceftazidime (16-fold) and ceftazidime-avibactam (4-fold). On the contrary, both variants conferred decreased resistance towards carbapenems (4- to 16-fold) as well as penicillins and penicillin-inhibitor combinations (4- to 8-fold).

Steady-state enzyme kinetics agreed with the changes in susceptibility, where increased k_{cat}/K_M values for ceftazidime and reduced values for penicillins and carbapenems were determined. In addition, P68A and P68A/Y211S demonstrated decreased thermostabilities, 4 to 7°C lower than for wild-type OXA-48. The structure of P68A was solved to 2.5 Å with ceftazidime covalently bound to S70 in two out of four chains. P68A without ceftazidime did not impose large structural changes within OXA-48. Indeed, key active site residues such as S70 and K73 as well as the Ω - and β 5- β 6 loops stayed preserved. Ceftazidime binding was investigated showing that the

residues of the β 5- β 6 loop such as T209, Y211, S212, T213 and R214 contributed to stabilise ceftazidime. In wild-type OXA-48, R214 usually maintains a salt bridge to D159 of the Ω -loop. In the P68A:ceftazidime structure, R214 pointed outwards of the active site and the Ω -loop was found to be disordered.

Paper II

“*Cryptic β -lactamase evolution is driven by low β -lactam concentrations*”;

Christopher Fröhlich, João A. Gama, Klaus Harms, Viivi H. A. Hirvonen, Bjarte A. Lund, Marc W. van der Kamp, Pål J. Johnsen, Ørjan Samuelsen, Hanna-Kirsti S. Leiros. *mSphere*. 2021, 6 (2) e00108-21; DOI: 10.1128/mSphere.00108-21

In this study, the effect of low-level selection on the evolvability of OXA-48 was investigated (Figure 15C). Evolution was performed for ~300 generations without selection pressure (populations 1 to 3) and at one quarter of the ceftazidime MIC (populations 4 to 6). Ceftazidime susceptibilities were determined on the whole evolved populations. Ceftazidime resistance in these population increased by 16-fold already after 50 generations, compared to populations evolved without ceftazidime. Clones exhibiting significantly increased ceftazidime resistance (>2-fold) were isolated by selective plating. The prevalence of these clones was highly dependent on the population. While maintained in population 4 at a frequency of $\sim 10^{-3}$, their frequency declined in populations 5 and 6 by several orders of magnitude.

To understand the contribution of *bla*_{OXA-48} to this resistance development, *bla*_{OXA-48} genes were sequenced for each population. Seven OXA-48 variants were discovered (L67F, P68S, F72L, F156C, F156V, L158P, G160C) and their resistance profile was determined by sub-cloning mutant and wild-type alleles into a high copy number vector pCR-blunt II and expressed in *E. coli* TOP10. The expression of wild-type *bla*_{OXA-48} did not increase ceftazidime resistance but decreased susceptibility towards penicillins and carbapenems. For the mutant *bla*_{OXA-48} alleles, only P68S, F72L and L158P increased ceftazidime resistance by >2-fold. All variants showed drastic antagonistic pleiotropy, strongly reducing their carbapenem and penicillin resistance. All mutant alleles were sub-cloned into a low copy number vector. Using a standard MIC assay and measuring their susceptibility towards ceftazidime showed that only F156V was able to increase the MIC by more than >2-fold. However, increasing the resolution and determining their IC₅₀ values showed that all variants significantly increased resistance (up to 4-fold based on their IC₅₀ values). All variants were recombinantly expressed, purified, and steady-state enzyme kinetics were performed. The steady-state kinetics agreed with the changes in susceptibility. For example, k_{cat}/K_M values towards ceftazidime were by 2- to 31-fold increased and catalytic

efficiencies against penicillins and carbapenems were reduced by up to several orders of magnitude. Thermostability measurements showed that all amino acid changes destabilised the OXA-48 by 4.5 to 7.5°C.

To understand the underlying structural changes leading to increased catalysis of ceftazidime, the crystal structure of L67F was solved. The phenylalanine in the wild-type structure is unlikely to interact with the substrate. However, the crystal structure of L67F showed that several active site residues are slightly repositioned by 1 to 2 Å such as L158 in the Ω -loop and I215 in the β 5- β 6 loop.

In paper I, P68A was hypothesised to increase the flexibility of active loops such as the Ω - and β 5- β 6 loops. Here, several independent molecular dynamics simulations were performed, and the root mean square fluctuations (RMSFs) for amino acids of Ω - and β 5- β 6 loops were calculated on a sub-set of variants (P68S, F72L, L158P). The analysis showed that all of these substitutions increased RMSF values for residues within the β 5- β 6 loop. In addition, F72L and L158P also increased flexibility within the Ω -loop.

Paper III (Manuscript, not published)

“OXA-48 evolution is realised by very distinct trajectories leading to similar resistance levels”;

Christopher Fröhlich, Karol Buda, Trine J.W. Carlsen, Pål J. Johnsen, Hanna-Kirsti S. Leiros, Nobuhiko Tokuriki

To understand the full evolutionary potential of the β -lactamase OXA-48 towards ceftazidime and how long-term evolution is affected by both pleiotropic effects and intra-molecular epistasis, iterative cycles and independent replicates of directed evolution were performed. In addition, fitness landscapes were built with all mutational combinations, and characterised against two drugs: ceftazidime and piperacillin by measuring IC₅₀ values (Figure 15D).

Within five rounds of directed evolution, OXA-48 mediated ceftazidime resistance increased stepwise up to 26- to 40-fold and plateaued in all three replicates. Resistance development was caused by the accumulation of only four to five mutations. Overall, only a fraction of all mutations (four out of 16 tested mutations) was able to increase ceftazidime resistance in the wild-type OXA-48. Mutations initially able to increase ceftazidime resistance tended to cause strong functional (8- to 96-fold loss in piperacillin resistance *versus* ~2- to 3-fold gain in ceftazidime resistance) and thermostability related trade-offs (~6 to 8°C decreased compared to wild type OXA-48). Despite the initially strong piperacillin trade-off, resistance was stably maintained at a low level (~4- to 16-fold above the susceptibility of *E. coli* alone) while ceftazidime resistance could increase further. Similarly, after the initial reduction, the thermostability remained stable and did not decrease further with increasing levels of ceftazidime resistance. Using X-ray crystallography to solve the structure of the optimised variant TI-4 (A33V/F72L/S212A/T213A) uncovered that the active site Ω -loop was turned by 90°, re-shaping the active site, and likely allowing ceftazidime to be better accommodated.

Epistasis was quantified based on a null or additive model, where ceftazidime and piperacillin resistance were predicted based on the IC₅₀ fold-change conferred by only single mutants. The predicted and determined IC₅₀ fold-changes were compared, showing that positive epistasis was predominant in the landscapes, and was driving resistance development, and limiting the overall functional trade-off.

D. Methodological considerations

1 OXA-48 and *E. coli* and as a model system

OXA-48 has become one of the most successfully disseminating β -lactamases¹⁷⁵. The enzyme catalyses the reaction of oxyimino cephalosporins, such as ceftazidime, with low catalytic efficiency, but OXA-48-like variants from clinical isolates have evolved to confer increased resistance towards ceftazidime. In clinical settings, resistance development towards ceftazidime has often been reported due to deletions and amino acid changes within the active site β 5- β 6 loop^{177,178,210,211}. Understanding the factors driving the evolution of OXA-48 mediated ceftazidime resistance is important from a clinical perspective and can shed further light on the evolutionary dynamics of β -lactamases. In addition, while evolutionary examples of class A serine β -lactamases have been studied, the evolutionary dynamics of class D β -lactamases are still poorly understood^{170,87,94,221}. Thus, due to the great clinical importance and limited insights into evolutionary dynamics, OXA-48 was used as a model enzyme within this study.

Genes encoding for β -lactamases are frequently expressed from either the chromosome or plasmids where their copy number is low, and thus their expression is limited²²². To study resistance development within OXA-48 under such conditions, a clinical plasmid (~65 kbp), with presumably low copy number, was used for paper I and II (p50579417_3_OXA-48, see Figure 16)^{222,223}. This plasmid carried *bla*_{OXA-48} as its only resistance gene and was genetically related to other *bla*_{OXA-48} carrying plasmids²²⁴. Compared to standard lab vectors, clinical plasmids often exhibit larger molecular sizes which reduces their transformation efficiency²²⁵. This makes their handling problematic when mutational libraries covering thousands of mutants need to be constructed, as in paper III. Thus, for paper III, the selection was done using a low copy number vector (p15A origin, ~10 copies per cell)²²⁶ instead of the above mentioned clinical plasmid.

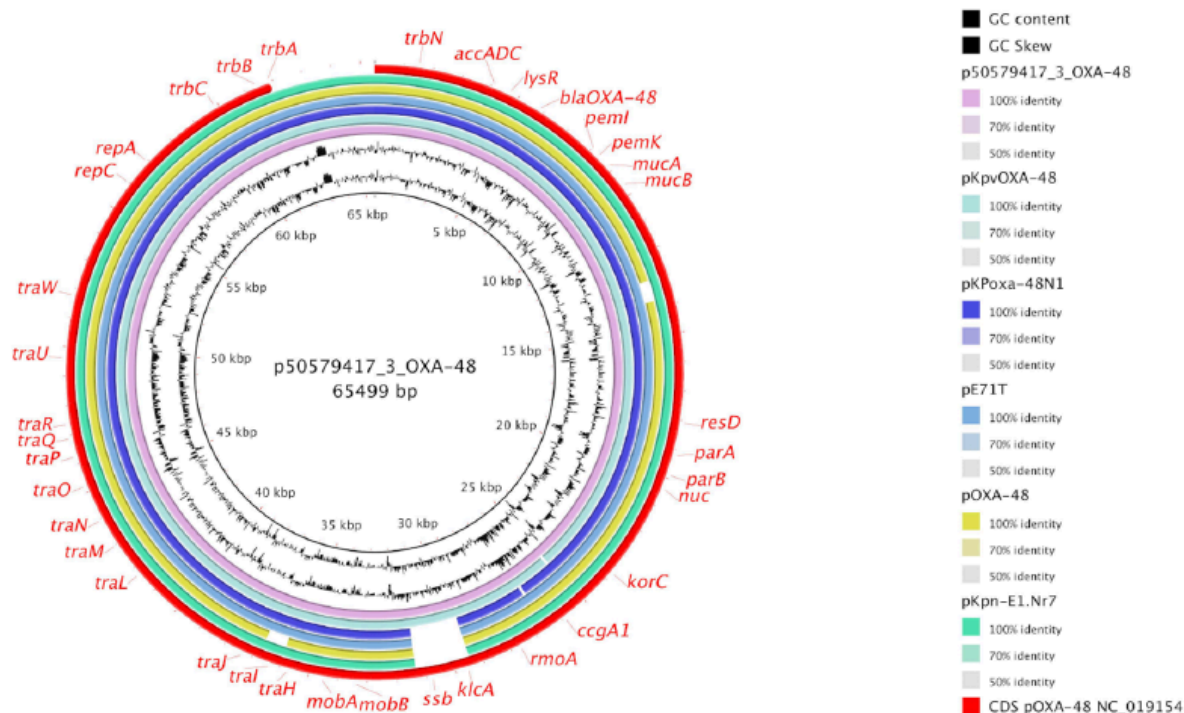


Figure 16: Genetic architecture of the p50579417_3_OXA-48 plasmid compared to other epidemic IncL OXA-48 plasmids such as pOXa-48 (GenBank accession no. NC_019154), pKpvOXA-48 (GenBank accession no. CP031374), pKPoxa-48N1 (GenBank accession no. NC_021488), pE71T (GenBank accession no. KC335143), and pKpn-E1.Nr7 (GenBank accession no. KM406491). The concentric circles represent the sequence identity of p50579417_3_OXA-48 (inner circle) to the other plasmids (see colour code). The red outer ring represents the annotation based on pOXa-48 (reprinted from ²²³).

While first reported in *K. pneumoniae*¹⁹⁹, plasmids harbouring *bla*_{OXA-48} have been transferred and reported in various members of the *Enterobacterales*, including *E. coli*¹⁷⁵. *E. coli* expressing *bla*_{OXA-48} is an important cause of bloodstream infections and community acquired urinary tract infections¹⁷⁵, and thus the development of OXA-48 mediated ceftazidime and ceftazidime-avibactam resistance was studied in *E. coli* strains. This work aimed to understand and provide proof of principle studies on the evolutionary dynamics of OXA-48. Thus, selection was done in laboratory and cloning strains such as *E. coli* MG1655 and *E. coli* E. cloni[®] 10G, respectively, and not in clinical strain backgrounds or other species. I acknowledge the fact that evolution in different strain backgrounds or even species may have resulted in different

evolutionary trajectories of OXA-48. However, the host dependent relationship was not the focus of this study and further work needs to be conducted to explore this.

2 Selection procedures

In this thesis, three different methods of selection and mutagenesis were probed to gain a better understanding of how OXA-48 evolves towards ceftazidime. All studies had one common strategy, namely, to find variants of OXA-48 improving ceftazidime and ceftazidime-avibactam resistance (only paper I). It was hypothesized, that OXA-48 variants may increase resistance to either ceftazidime or ceftazidime-avibactam, and thus can provide a survival or fitness benefit to the bacterial cells. As a consequence, the main selection pressure within this study was cell survival. This is important to keep in mind for the interpretation of biochemical data (e.g., catalytic efficiency) as selection was not performed to obtain the “best” enzyme (highest enzymatic efficiency; for further elaboration see Subchapter A-3). The selection scheme therefore allows for the selection of other mutations affecting e.g., enzyme stability, translocation into the periplasm, translation efficiency which can ultimately lead to increased resistance²²⁷. Thus, the determined catalytic efficiencies and bacterial susceptibilities may not always correlate.

In paper I, stepwise selection from a bacterial overnight culture on LB agar containing increasing concentrations of ceftazidime was performed (Figure 15B). While this approach allows to study genetic changes on the chromosome and the plasmid including *bla*_{OXA-48} target gene, paper I focused on changes on the plasmid and specifically the target *bla*_{OXA-48} gene. Paper I served as a proof of principle study showing that point mutations in OXA-48 can be selected for and the expression of such variants increases resistance towards ceftazidime and ceftazidime-avibactam.

In paper II, the potential of sub-MIC or very low concentrations of ceftazidime on the evolution of OXA-48 was probed (Figure 15C). For that, a long-term experimental evolution was performed, where *E. coli* MG1655 harbouring the above mentioned clinical OXA-48 plasmid was exposed to 0.06 mg/L ceftazidime. This concentration is one of the highest β -lactam concentrations reported in wastewater treatment plants¹⁴⁰ but is still below the MIC of *E. coli* MG1655 (0.25 mg/L). The strain was grown to high density and passaged every 12 hours in fresh MH broth with either no antibiotic or ceftazidime at one quarter of the MIC. The evolution was performed for ~300 generations and the generation time was estimated with 6.6 generations per

growth cycle under a 1:100 dilution/bottleneck²²⁸. Pre-existing mutational variants in the populations with significantly increased resistance towards ceftazidime were then enriched by selective plating on ceftazidime containing agar (2xMIC of *E. coli* MG1655). This again allowed for the selection of mutations not only in the target gene. However, within paper II, only changes within the *bla*_{OXA-48} genes were further analysed and characterised. Indeed, the data from paper II indicated that also other resistance mechanisms were also selected for.

Paper I and II established that single point mutations in OXA-48 can easily occur, and that they can be selected for. However, these studies have the limitation that only a small sequence space of OXA-48 can be sampled. Thus, in paper III, iterative cycles of directed evolution were used as a more targeted approach to study the full *bla*_{OXA-48} sequence space and the whole evolutionary potential of OXA-48 (Figure 15D). In brief, error prone PCR was used to mutagenize *bla*_{OXA-48} by adding mutagenic nucleotides (8-Oxo-dGTP for transversions; dPTP for transitions)²²⁹. In a second PCR, the mutagenic nucleotides were replaced with the corresponding natural ones, resulting in transversion and transition events. The resulting mutant libraries were sub-cloned from the start to stop codon of *bla*_{OXA-48} into an isogenic vector backbone. By doing so, mutations within the promoter region that potentially could increase resistance were actively excluded. Mutant libraries were constructed to have >5000 mutants to ensure that, in theory, the whole sequence space could be sampled. To be able to analyse stepwise adaptations over several rounds of directed evolution, the mutagenesis rate was adjusted to one to two amino acid changes per round and gene. These libraries were then selected on LB agar plates with increasing concentrations of ceftazidime and mutants exhibiting increased ceftazidime resistance served as starting material for the next round of directed evolution.

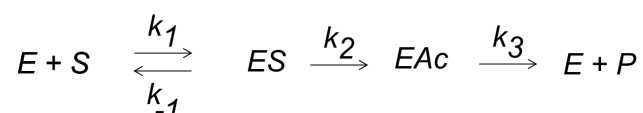
3 Phenotypic characterisation

Throughout paper I to III, different methods were used to analyse and characterise resistance development on various levels. Resistance on the cell-based level was determined based on a broth microdilution test with different read out, where either 100% (MIC) or 50% (IC₅₀) cell growth inhibition was determined. The MIC is traditionally performed along a 2-fold antibiotic gradient (e.g., 0, 2, 4, 8 and 16 mg/L) and since the MIC is defined as the lowest antibiotic concentration where no growth is

visual, the test resolution is rather unprecise and falls within +/- 2-fold changes. This method is important from a clinical microbiology perspective as it provides an international standard that allows to compare MIC values across e.g., different labs. However, the characterisation of genotypes conferring small changes in susceptibility (within +/- 2-fold) is challenging with this method due to the inherent test variability. Yet, small changes in susceptibility have shown to be important from an evolutionary perspective, since they can be selected for¹⁶². Thus, dose response curves were performed by determining and plotting the normalised OD₆₀₀ versus log₂ [antibiotic]. The IC₅₀ values were calculated according to the following equation as a non-linear fit, and allowed for a more precise determination of even small changes in susceptibility:

$$y=100/(1+10^{(x-\log_2 IC_{50})})$$

In addition, in paper I and II, enzyme kinetics on purified enzymes were conducted to understand if changes in susceptibility are also reflected in an increased catalytic efficiency. As mentioned previously, the reaction mechanism for the hydrolysis of β -lactams contains several steps, including the initial formation of non-covalent enzyme (E) substrate (S) complex (ES), followed by the formation of an acyl-enzyme intermediate (EAc) and the hydrolysis of the β -lactam product (P)²²¹:



The reaction is further described by the rate constants for the initial formation of the non-covalent ES (k_1), as well as the acylation (k_2) and deacylation (k_3). The buffer used for all enzyme kinetics was carbonated using H₂CO₃ at a final concentration of 50 mM. The carbonation has been shown to increase enzyme activity in OXA-48 as it promotes the carboxylation of K73²³⁰. Studies showed that the effect of H₂CO₃ depends on the genotype, and performing kinetics also in the absence of H₂CO₃ could give important insight into different mode of actions²³⁰. In paper II, for some variants, saturation of the Michaelis-Menten kinetic could not be achieved. Thus, k_{cat} and K_M could not be calculated independently and only the term of k_{cat}/K_M was reported based on the initial

linear slope of the Michaelis-Menten kinetic. As mentioned previously, in all the experiments OXA-48 variants were selected according to cell survival. Although an improved catalytic efficiency towards one drug can allow bacterial cells to tolerate increased antibiotic concentrations, resistance can be also improved by other mechanisms such as improved enzymatic stability, expression, or translocation into the periplasm^{227,231}. Thus, susceptibility and catalytic efficiency may only demonstrate limited correlation²²⁷.

For purification, constructs were expressed with a 6-H tag followed by TEV cleavage site. For crystallisation, the 6-H tag was cleaved in all three studies. For kinetics and thermostability testing, the 6-H tag was removed for all variants in paper I and II. However, due to the increasing number of purifications in paper III, the thermostability was determined for variants still harbouring the 6-H tag and the TEV cleavage site. Here, corresponding controls (wild-type OXA-48 with and without the 6-H tag) were included, which allowed the quantification of changes in thermostability relative to wild-type OXA-48 and should provide comparability of thermostability results across all three studies.

In addition, in this work the enzyme stability was determined as thermostability, also known as the melting temperature (T_M), which reflects the temperature where 50% of the proteins were unfolded. On the other hand, the thermodynamic stability (ΔG_F) describes the free folding energy at a given temperature (see Subchapter A-2.2.2). Although thermostability and thermodynamic stability can correlate^{232,233}, in the work presented here neither thermodynamic nor the long-term stability of variants was determined⁸⁹.

4 Fitness measurements

In paper II, the majority of the selected OXA-48 mutants displayed only small changes in ceftazidime susceptibility. To understand if these genotypes could have been selected for under sub-MIC conditions, head-to-head competitions were performed between *E. coli* MG1655 expressing *bla*_{OXA-48} from low copy number plasmid (p15A, called pUN in paper II) and *E. coli* MG1655 $\Delta malF$ expressing either *bla*_{OXA-48} (control) or a corresponding mutant of OXA-48. Strains were competed in a 1:1 ratio for 8 h in LB broth without drug and at the same ceftazidime concentration used during long-term experimental evolution (0.06 mg/L). After competition, the cell mixtures were plated on differential maltose tetrazolium agar. Cells were counted and the fitness

cost/benefit was calculated based on the white-red cell ratio ($\Delta malF$ cells exhibit a red colour when plated on maltose tetrazolium agar)²³⁴. Based on that all OXA-48 mutants conferred high fitness benefits (>50%) in the presence of 0.06 mg/L of ceftazidime but behaved neutrally without selection pressure.

Yet, this approach has limitations. The long-term experimental evolution was performed in *E. coli* MG1655 harbouring the clinical plasmid p50579417_3_OXA-48, which is presumably present at very low copy numbers²²². In an effort to simulate fitness effects as close as possible to the experimental evolution, the fitness measurements were performed using the above-mentioned low copy number pUN vector. However, this vector likely has a higher copy number than the clinical plasmid, and increases in copy number have shown to elevate β -lactam resistance²³⁵ which likely affects fitness benefits measured under selective conditions.

A recent study on sub-MIC evolution of *P. aeruginosa* suggest that ceftazidime has selective potential at 1/10 of the MIC²³⁶. In the work presented here, competitions were carried out only at one ceftazidime concentration. To understand the general selective potential of ceftazidime for the here identified OXA-48 mutants, their selective window needs to be determined over a concentration range allowing for the determination of the minimal selective concentration.

5 Structural evaluation

To understand the structural effect of the here identified mutations, X-ray crystallography was employed. The aim of this work was to obtain crystal structures on all mutants identified in the papers I and II as well as on the evolved variants in paper III. However, only a fraction of these mutants was crystallisable or resulted in diffractable crystals, which could be related to their reduced thermostability²³⁷. To improve crystallisation, various strategies were followed such as screening and optimising of commercial crystallisation conditions, co-crystallisation with ligands and inhibitors, and crystallisation at low temperatures (4°C). For the mutants where crystal structures could be solved, it is important to keep in mind, that these structures are based on crystalline protein samples, and that certain regions within the enzyme may adopt different conformations in solution and physiological conditions²³⁸.

Based on the solved crystal structure of P68A (paper I), it was observed that the Ω -loop was disordered upon ceftazidime binding, and thus speculated that P68A

may increase the conformational freedom of the Ω -loop allowing for improved ceftazidime accommodation. To test this, molecular dynamics simulations were performed on a sub-set of mutants (P68S, F72L, and L158P). Since no structural information on these mutants were available, the mutations were introduced *in situ* based on the rotamers with least structural clashes. Although single amino acid changes are generally thought to only have a marginal impact on the protein structure^{239,240}, it cannot be ruled out that the acquisition of these mutations affect the structure, and consequently bias the here performed simulations. In addition, to understand a possible improved accommodation of ceftazidime, all molecular dynamics simulations were performed as acyl-enzyme complexes with ceftazidime covalently bound to the active site S70. Consequently, changes in conformational dynamics during the initial substrate binding, acylation, deacylation and general reaction are not covered by our molecular dynamics simulations.

E. Results and Discussion

OXA-48 has become one of the most successfully disseminating β -lactamases. While not able to catalyse the hydrolysis of ceftazidime efficiently, natural OXA-48-like variants with increased ceftazidime activity (e.g., OXA-163, OXA-232 OXA-247, and OXA-405) have been identified^{177,178,210,211}. While ceftazidime resistance within these variants is frequently associated with deletions around the β 5- β 6 loop region, the contribution of single point mutations during this adaptive process is poorly understood. The β -lactam/ β -lactamase inhibitor combination ceftazidime-avibactam has proven to be effective against extended-spectrum β -lactamase producing pathogens²⁴¹. OXA-48 is frequently co-expressed with extended-spectrum β -lactamase producers²⁴². Thus, the combination of ceftazidime and avibactam is likely used to treat infections caused by OXA-48 producing pathogens and might consequently have played a role in the selection of OXA-48 mediated ceftazidime resistance. This thesis aimed to study the general evolvability of OXA-48 towards ceftazidime and ceftazidime-avibactam by point mutations, and to shed light on factors driving this evolutionary process.

1 Sub-MICs drive the evolution of OXA-48

1.1 OXA-48 evolves through cryptic phenotypes

Antibiotic resistance has been proposed to evolve under low selection pressure through variants with little or no phenotypic changes¹⁵⁸. From a clinical microbiology perspective, these cryptic variants are problematic since they are either not captured within the resolution range of standard MIC determining methods or regarded as only marginal, and thus neglectable changes in resistance¹⁵⁸. For example, the β -lactamase TEM-1 catalyses oxyimino cephalosporins such as cefotaxime poorly. However, shortly after the introduction of cefotaxime, the double mutant TEM-10 with two mutations (R164S/E240K) was identified from clinical isolates, increasing the ceftazidime MIC by 16-fold relatively to TEM-1¹⁶². However, the accumulation of two or more mutations at the same time is very unlikely, based on the assumption that mutation rate in *E. coli* is $\sim 10^{-10}$ per base pair and generation¹⁵⁸. The expression of TEM-12, which carries the R164S, increased cefotaxime resistance by only 2-fold¹⁶². Despite these marginal changes in susceptibility between the two variants, TEM-12 was selectable over TEM-1 and provided a survival benefit at low cefotaxime concentrations¹⁶². As a consequence, despite its cryptic resistance phenotype, R164S

provided bacterial fitness benefits and acted as a gateway to clinical resistance. Furthermore, other studies have also shown that the evolution of new functions evolve through cryptic intermediates towards non-antibiotics^{67,243}. For example, the metallo- β -lactamases VIM-2 and NDM-1 have promiscuous activity against phosphonate monoesters. Directed evolution on these enzymes towards increasing esterase activity happened *via* cryptic intermediates⁶⁷.

In this thesis, OXA-48 and ceftazidime were used as model to study this relationship and showed that the exposure to sub-lethal concentrations can select for OXA-48 mediated resistance. All the here identified single OXA-48 variants displayed, if any, marginal increases in their ceftazidime resistance (judged by their MIC values) but were strongly selectable in head-to-head competitions. This provides further evidence that these enzymes evolve through cryptic variation and that selection takes place in environments with sub-lethal concentrations. Worryingly, β -lactam concentrations as low as those used in this thesis have already been reported in the environment¹⁴⁰. In addition, double mutants conferring increased ceftazidime resistance exhibiting changes in some of the amino acid position identified here, such as F72L and L158P, have already been described in environmental samples²⁴⁴.

These findings are not only important from a clinical point of view but also shed light on the natural evolution of these enzymes and may explain the sheer diversity and low sequence identity of β -lactamases. Cryptic variation and low-level selection pressures likely give rise to less detrimental mutations and allow for much more genetic variation. High selection pressure may act on this standing genetic variation and recruit cryptic variants to further increase resistance. In addition, the genetic diversity caused by low selection levels likely creates multiple evolutionary starting points which may climb to different adaptive peaks, explore otherwise inaccessible regions of an adaptive landscape and drive the divergence of these enzymes²⁴⁵.

1.2 Low prevalence of high-level resistant clones

Evolution at low ceftazidime concentrations resulted only in a small fraction of clones exhibiting significantly increased resistance (paper II). Maximum 0.1% of the whole populations demonstrated an increase in clones exhibiting elevated ceftazidime resistance (paper II). Similar increases of three to four orders of magnitude have been found for *Salmonella enterica* and *Streptomyces coelicolor* in other studies where streptomycin was used at sub-MIC^{43,142}. In contrast to these studies, the data from this

thesis suggests that rather than enriching high level resistance, the populations adapt towards low-level resistance. An aspect that needs to be discussed within this context is the relationship between clones actively detoxifying the environment and cheaters within the population. Several studies have shown that the expression of β -lactamases can protect susceptible cells within a population^{246,247}. Yurtsev *et al.*²⁴⁷ co-cultured *E. coli* strains with and without *bla*_{TEM-1} at β -lactam concentrations 50-fold higher than the wild-type *E. coli* could tolerate. They demonstrated that even with a high starting ratio of 80:20 between TEM-1 *versus* non-TEM-1 expressing cells, the frequency of TEM-1 producers decreased to 25% and was maintained at a stably low equilibrium after several days of culturing. Conversely, when they started the culture with only 10% of the TEM-1 producing strain, the resistant fraction first increased by up to 95% before decaying to an equilibrium afterwards, which is similar to the dynamics observed in paper II. Such evolutionary dynamics depend on multiple variables, such as the frequency of the alleles, population density, habitat structure, and the genomic context of the resistance gene (i.e., plasmid)²⁴⁸. It is likely that a similar effect acts on some populations evolved in paper II, resulting in an apparent adaption towards low-level ceftazidime resistance.

Surprisingly, the beneficial alleles did not take over the populations despite their high fitness benefit (competition assays). This could be simply due the duration of the experimental evolution, such that 300 generations were not enough time to drive beneficial alleles into fixation. Another problem with the co-existence of several beneficial alleles within a population is clonal interference. The data from paper II indicates that the clones selected at low concentrations possess other resistance mechanisms which could be mediated by porin loss, increased efflux activity or plasmid adaptation. In theory, the competition between different alleles or loci has shown to drastically prolong the time until beneficial alleles are fixated²⁴⁹.

2 The evolutionary potential of OXA-48

2.1 Ceftazidime and ceftazidime-avibactam resistance

The results obtained from this work showed OXA-48 can evolve to confer increased resistance against ceftazidime and ceftazidime-avibactam. Further, the here presented work showed that the ability of OXA-48 to catalyse the hydrolysis of ceftazidime can be selected and promoted by sub-MICs of ceftazidime. The selected single OXA-48 variants tended to confer only marginal changes in ceftazidime MICs (paper II). These

cryptic phenotypes may act as a gateway or steppingstones towards clinical resistance, as discussed above for TEM^{141,158}, and multi-step selection may give rise to OXA-48 variants further increasing ceftazidime resistance. To challenge this hypothesis and the whole sequence space, iterative cycles of independent directed evolution experiments were employed to select for variants displaying increasing resistance towards ceftazidime (paper III). Typically, an accumulation of up to five mutations was enough to confer maximum ceftazidime resistance, which was 26- to 40-fold (IC₅₀) higher than the wild-type (paper III). This agrees with findings from other directed evolution studies underlining the limitations of adaptive mutations during the evolution of new enzymatic functions⁶⁰. Comparing resistance development within the trajectory to a null or additive model, where all the mutational effect would behave additively, showed that positive pairwise and higher-order epistasis were mainly driving resistance development. For example, in landscape I of paper III, F72L increased ceftazidime resistance by 2-fold based on the IC₅₀. While S212A did not increase resistance alone, in combination with F72L the IC₅₀ increased up to 11-fold. F72L/S212A represents therefore one of the pairwise interactions exhibiting positive epistasis.

Although, the evolution of the β -lactamase TEM-1 is thought to be predictable^{80,250,251}, other studies have shown that evolutionary landscapes can be more complex where mutational epistasis caused by early beneficial mutations drives enzyme divergence^{94,252,253}. Subsequently, enzyme evolution can take alternative evolutionary trajectories reaching suboptimal fitness maxima^{80,254}. Indeed, mutations acquired early during selection have shown to possess a directing role within evolutionary pathways and are thus thought to drive the divergence of proteins. However, these studies also show the appearance of similar mutations across these independent lineages^{80,254}. Surprisingly, in the work presented here, the three independent replicates of directed evolution resulted in completely distinct mutational trajectories exhibiting similar ceftazidime resistance (paper III). This may indicate that the evolved trajectories are mutationally exclusive to each other, and that a beneficial mutation from one trajectory may show a different effect within another genetic context. To partially probe this, mutations increasing ceftazidime resistance in wild-type OXA-48 (F156D and L158P) from trajectories II and III were constructed onto the optimised quadruple mutant of trajectory I. Determining their susceptibilities showed that F156D and L158P did not further increase ceftazidime resistance when present in the

quadruple mutant, suggesting that the selected trajectories are, at least partially, incompatible. Similarly, the first step mutants R164S and G238S conferred increased cefotaxime resistance in TEM-1⁷⁹. However, those mutations were structurally not compatible, as the cefotaxime resistance conferred by the double mutant R164S/G238S was lower than for the single mutants⁷⁹. It needs to be acknowledged that only a small fraction of mutations were tested to study the exclusivity of the different trajectories in paper III, and further work needs to be done characterising all mutational combinations across the three trajectories. This could be realised by massive gene synthesis and deep sequencing.

Another limitation of paper III is that no direct comparison can be made between the here evolved variants and variants identified from clinical isolates such as OXA-163. The susceptibility profile of clinical variants is frequently characterised by overexpression in high copy number systems¹⁶⁹. Therefore, these susceptibility changes are likely not comparable to the here observed changes using the low-copy number pUN vector. However, to contextualise the susceptibility changes of the here evolved OXA-48 mutants, the class A enzyme KPC-2 was expressed under the same conditions. KPC-2 possesses a catalytic efficiency against ceftazidime one order of magnitude higher than OXA-48²⁵⁵ (paper II) and conferred within the low copy number system an IC₅₀ increase of 10-fold. Since the conferred resistance of KPC-2 is lower than for the fully evolved OXA-48 variants from paper III (up to 40-fold in IC₅₀), it can be speculated that these OXA-48 variants may possess similar or higher catalytic efficiencies towards ceftazidime. Even though other mechanisms, such as improved expression or translocation, could also be responsible for increased resistance which would not be reflected in an overall elevated k_{cat}/K_M ^{227,231}.

Taken together, OXA-48 mediated ceftazidime resistance can evolve and reach local maxima or evolutionary dead-ends through the accumulation of only four to five amino acid changes. In combination, these amino acid changes exhibit positive epistasis driving ceftazidime resistance development. In addition, the data show that several mutationally distinct trajectories within one enzyme exist, leading to a similar overall increase in resistance. However, further investigations, such as the determination of enzyme kinetics, are needed to understand and improve comparability of the findings to other studies.

2.2 Mechanistic view on the evolution of OXA-48

Enzymes have shown the ability to exploit various strategies to promote and evolve promiscuous functions⁶⁰. In this study, X-ray crystallography and molecular dynamics simulations were used to study structural mechanisms of adaptation within OXA-48. Structural information, based on X-ray crystallography, were obtained for single mutants such as P68A and L67F and the quadruple mutant A33V/F72L/S212/T213A (TI-4). In addition, molecular dynamics simulations on wild-type and single mutants such as P68A, F72L and L158P were performed.

X-ray crystallography revealed that the phenylalanine at position 67 is unlikely to interact with the substrate. However, the crystal structure of L67F showed that several active site residues are repositioned by 1 to 2 Å, such as L158P in the Ω -loop and I215 in the β 5- β 6 loop, likely reflecting a fine-tuning process of the active site through “conformational tinkering”⁶⁰. The crystals of P68A and TI-4 were soaked, and crystal structures were refined with ceftazidime bound in the active site of these mutants. Superimposition of P68A and TI-4 with and without ceftazidime showed that upon ceftazidime binding, the Ω -loop was “flipped out” of the active site and disordered (papers I and III). In addition, comparing the quadruple mutant TI-4 (without ceftazidime) to the wild-type structure of OXA-48 revealed that the Ω -loop undergoes a conformational change, expanding and reshaping the active site. This likely allows for a better accommodation of ceftazidime, and especially the oxyimino group (paper III). In addition, ceftazidime was just slightly repositioned and reached \sim 1 Å “deeper” into the active site compared to the single mutant P68A. Reshaping of the active site and repositioning of substrate are commonly described mechanisms during enzyme evolution⁶⁰. In addition, the expansion of the active site by altering the Ω -loop was described for various β -lactamases including TEM and CTX-M^{216,256,257}. To that end, despite the efforts to obtain structures for all mutants, only a fraction of the mutants was crystallisable. More crystallographic data, especially for variants with changes in the Ω -loop, would further our understanding of how OXA-48 mediated ceftazidime resistance can be achieved structurally.

Molecular dynamics simulations on a sub-set of variants (P68S, F72L, and L158P) showed that F72L and L158P increased the flexibility of both the Ω - and β 5- β 6 loops, which may aid ceftazidime accommodation within the active site. For example, F72L, which is located close to the active site S70, disturbs the stacking interactions with F156 and W157 within the Ω -loop, likely leading to increased loop flexibility (paper

II). In other β -lactamases, both increased and decreased flexibility of the Ω -loop have been reported in combination with an increased ability to hydrolyse ceftazidime. For example, in TEM and SHV variants, the amino acid change R164 is thought to increase the conformational dynamics of the Ω -loop, likely aiding improved ceftazidime hydrolysis^{79,221,258,259}. Similar observations have been made for members of the CTX-M family, where point mutations such as P167S expand the active site and likely improve ceftazidime hydrolysis by promoting an open conformation of the active site²⁶⁰. Similarly, ceftazidime binding in KPC-2 imposed structural rearrangements of active site loops including the Ω -loop. However, in the KPC-4 (KPC-2:P104R/V240), a variant with increased catalytic efficiency for ceftazidime, these structural changes were less pronounced, indicating that the mutations acquired from KPC-2 to KPC-4 likely improved the accommodation of ceftazidime²⁶¹. In addition, molecular dynamics simulations showed that the Ω -loop in KPC-4 became less flexible, allowing a more productive position of E166 within the loop structure (E166 activates the deacylation water). This stands in contrast to the molecular dynamics simulations performed on the single OXA-48 mutants. However, it needs to be acknowledged that no simulations are available on the here evolved variants with multiple amino acid changes such as TI-4, and that the loop flexibility in these variants may behave differently.

Compared to other β -lactamase structures, the ceftazidime molecule is positioned differently in P68A and TI-4 (Figure 17). In both OXA-48 structures, the oxyimino side chain reaches into the active site where it would structurally clash with residues of the Ω -loop. It was speculated that because of this clash, the Ω -loop is needed to flip out of the active site in order for ceftazidime to bind (papers I and III). On the contrary, the inspected structures of various β -lactamases from different classes such as KPC-2:E166Q (PDB no. 6Z24²⁶¹), CTX-M-14:E166A (PDB no. 5U53²⁵⁷), AmpC (PDB no. 1IEL²⁶²), OXA-160:V130D (PDB no.4X56²⁶³) and OXA-225:K82D (PDB no. 4X55²⁶³) showed that instead of the oxyimino group, the aminothiazole ring of ceftazidime was positioned close to the Ω -loop (Figure 17). While both groups impose steric hindrance within the active site, the oxyimino group in OXA-48 also brings an additional negative charge within the active site which may have implications for the development of functional trade-offs⁴⁹.

Taken together, the Ω - and β 5- β 6 loops serve as mutational hot-spots not only in OXA-48 and comparable structural hot-spots have been seen for other members of the OXA-family such as the OXA-10-like variants OXA-145 and OXA-147 exhibiting

L158 Δ and W157L, respectively (according to OXA-48 numbering)^{193,230,264}. Increased flexibility and reshaping of the active site through these loop regions may aid the accommodation of bulkier drugs and slightly optimise substrate positioning. Interestingly, while P68A and P68S both increased ceftazidime resistance, no structural changes were evident in P68A (paper I). In addition, no changes in the Ω -loop flexibility and only slight increases the flexibility of the β 5- β 6 were observed for P68S (paper II). Thus, the molecular basis of P68A/S remains elusive.

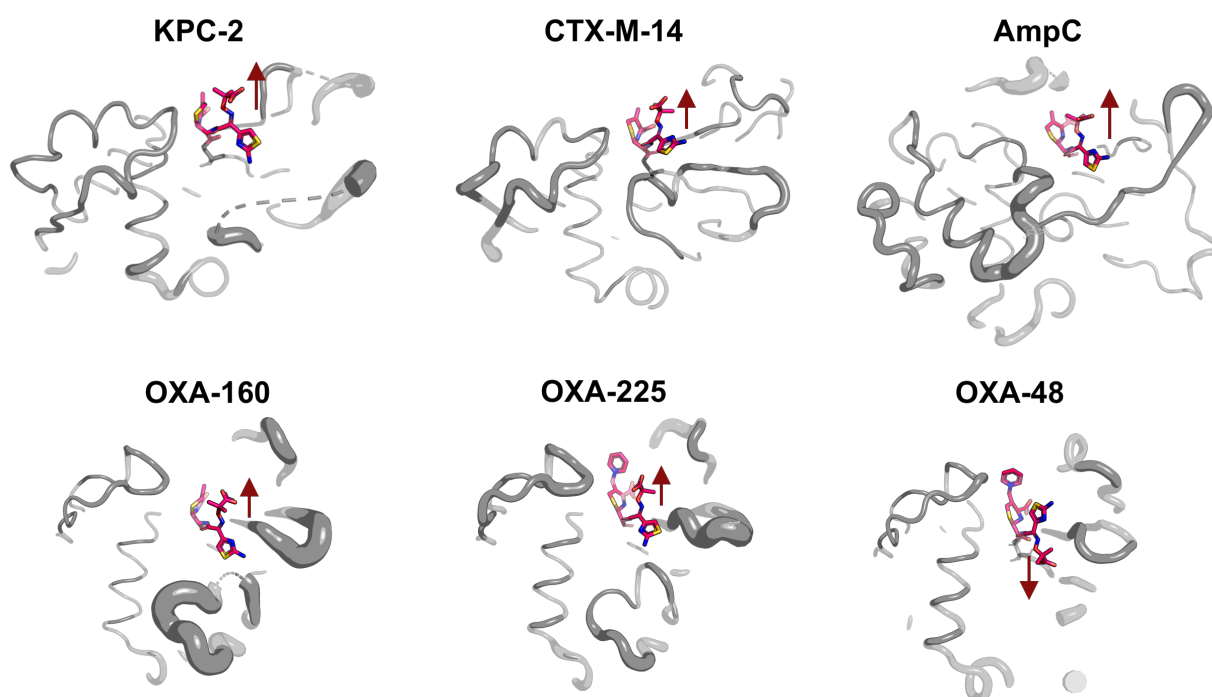


Figure 17: Structure of class A (KPC-2:E166Q, CTX-M-14:E166A and AmpC) as well as class D (OXA-160:V130D, OXA-225:K82D and OXA-48:P68A) β -lactamases bound to ceftazidime (pink). The direction of the oxyimino group of ceftazidime is indicated by a red arrow. While for OXA-48:P68A the oxyimino group of ceftazidime points into the active site, the same group was found to be directed outwards of the active site for all other β -lactamases.

2.3 Thermostability related trade-offs

Thermostability related trade-offs are important from an evolutionary perspective and have consequences for the evolution of new enzymatic functions as many mutations are destabilising^{89,90,109}. The acquisition of too destabilising or several slightly destabilising mutations can lead to unfolding or aggregation, where the protein loses its physiological activity. Thus, the stability may influence how many mutations can be acquired as well as the nature of these mutations and is therefore thought to have implications for the evolvability of enzymes^{89,90,109}.

Throughout papers I to III, both ceftazidime resistance and thermostability of 24 single amino acid changes were determined (paper I: 1, paper II: 7, paper III: 16). This allowed the performance of a comprehensive analysis of how newly acquired mutations arise at the expense of thermostability within OXA-48. Firstly, all single mutations which increased ceftazidime resistance by ≥ 1.5 -fold (based on IC₅₀ values) lowered the thermostability of OXA-48 by ~ 5 to 8°C (Figure 18). P68A (paper I) exhibited the same trend, however, for this mutant only MIC and no IC₅₀ data was available, and thus P68A was not plotted in Figure 18. Secondly, only three mutants (F66V, D154G and T243P) demonstrated decreased thermostability without increasing ceftazidime resistance. Therefore, initial mutations increasing ceftazidime resistance often reduce thermostability in OXA-48. This is in agreement with observation from other β -lactamases such as TEM, CTX-M and KPC, where the evolution towards oxyimino cephalosporins has also been described to result in a thermostability cost²²¹.

In naturally evolving single and double mutants of KPC, a negative correlation between “ceftazidimase” activity and thermostability has been reported²⁶⁵. Thus, this thesis also aimed to understand whether the sequential accumulation of mutations increasing ceftazidime resistance would correlate with steadily decreasing thermostability (paper III). In other words, does a relationship between thermostability and ceftazidime resistance exist? For that, OXA-48 variants within landscape I (A33V, F72L, S212A, T213A; paper III), exhibiting increased ceftazidime resistance, were purified and their thermostability was tested alone (only single mutants) and in combination (single, double, triple mutants, etc.). While the sequential acquisition of F72L \Rightarrow S212A \Rightarrow T213 \Rightarrow A33V increased ceftazidime resistance by 2 \Rightarrow 11 \Rightarrow 31 \Rightarrow 40-fold, only F72L reduced thermostability in wild-type OXA-48 (paper III). All other mutations behaved neutrally ($\leq 0.5^\circ\text{C}$) alone and in combination. This may indicate that the reduction in thermostability is limited due to the presence of a stability

threshold (Figure 7). Below this threshold, unfolding may occur, and the physiological activity of the enzyme is likely to be lost. In addition, compensatory mutations can be acquired such as M182T in TEM-1 or A77V in CTX-M which improve thermostability without comprising the enzymes activity^{256,266,267}.

Taken together, initial mutations allowing for increased ceftazidime resistance tend to cause a strong reduction in the thermostability of OXA-48. However, subsequently acquired mutations did not negatively affect the thermostability, indicating a limitation of a general stability-function relationship. To that end, it needs to be acknowledged that only a few selected variants from one landscape were investigated to understand the relationship between increasing ceftazidime resistance and thermostability (paper III), and that additional investigations are needed to draw a more general conclusion of this relationship.

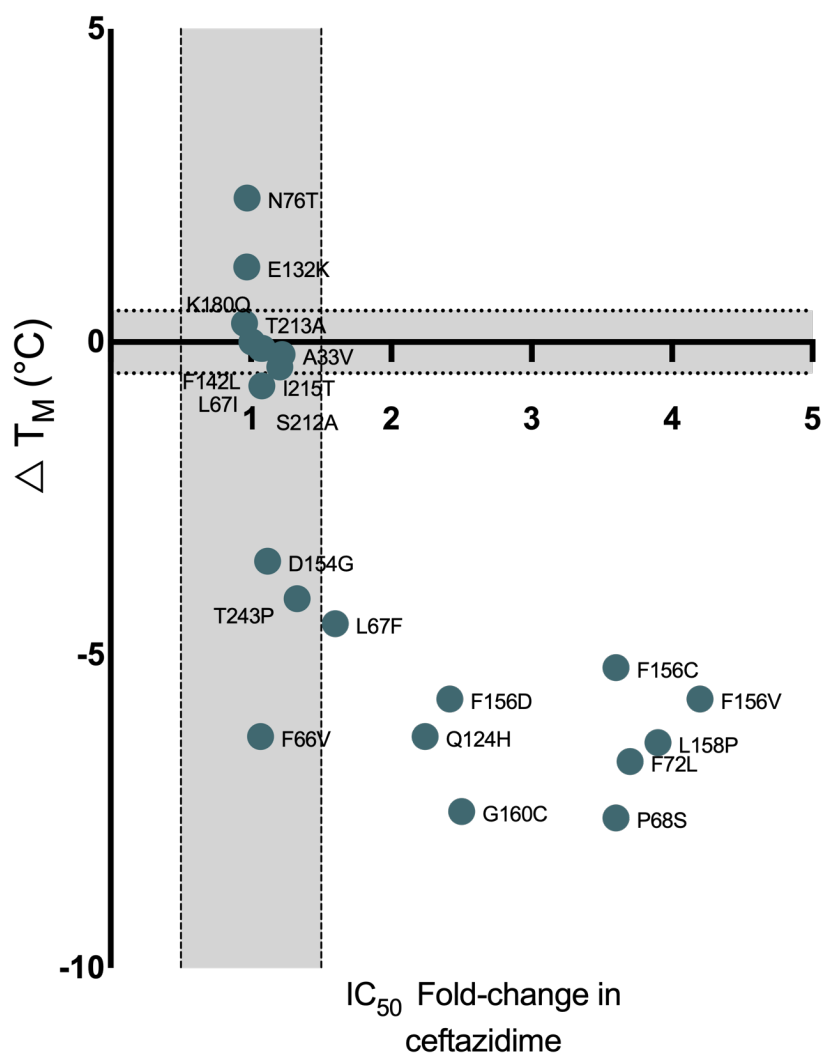


Figure 18: Difference in thermostability (ΔT_M) versus IC_{50} fold-change in ceftazidime resistance. The ΔT_M (°C) was calculated as the difference between the thermostability of wild-type and the corresponding single mutants. For variants carrying a 6-H tag, the difference was calculated based on the 6-H tagged wild-type OXA-48. *Vice versa*, variants without the 6-H tag were compared to wild-type OXA-48 without 6-H tag (L67F, P68S, F156C, F156V and G160C). The IC_{50} fold-changes were calculated based on the ceftazidime IC_{50} fold-change between mutant and wild-type. For L67F, P68S, F156C, F156V and G160C expression was done in *E. coli* MG1655, while all other mutants were expressed in *E. coli* E. cloni[®] 10G. P68A from paper I was not included since no IC_{50} values are available. The grey areas reflect small IC_{50} fold-changes (± 0.5 -fold) and thermostability differences (± 0.5 °C).

2.4 Functional trade-off, cross-resistance, and epistasis

For most of the studied enzymes, it has been shown that there is a weak trade-off between new and native activity during the evolution of a new enzymatic function⁴⁹. In other words, the new promiscuous function can be improved efficiently without compromising the native function to the same extent. This stands in contrast to the commonly seen evolution of β -lactamases towards oxyimino cephalosporins, where strong functional trade-offs against penicillins and carbapenems have been reported for variants of TEM, SHV and CTX-M²²¹. Interestingly, while enzymes from the KPC-family have shown to acquire point mutations conferring increased resistance against oxyimino cephalosporins without exhibiting significantly reduced resistance to penicillins and carbapenems²⁶⁵, the exposure to the β -lactam/ β -lactamase inhibitor combination ceftazidime-avibactam has given rise to KPC variants exhibiting functional trade-offs against penicillins and carbapenems^{68,73}.

The work presented here focused on the evolutionary trade-offs associated with the development of OXA-48 mediated ceftazidime (papers I to III) and ceftazidime-avibactam resistance (paper I). All single mutants (papers I and II) as well the double mutant P68A/Y211S (paper I) increased ceftazidime and ceftazidime-avibactam resistance, respectively, and demonstrated strong functional trade-offs against penicillins and carbapenems. For example, the ability of these mutants to catalyse the hydrolysis of piperacillin dropped usually by two to three orders of magnitude while ceftazidime activity improved by 2- to 31-fold. Similarly, activity against the carbapenems imipenem and meropenem dropped by one to four orders of magnitude. In addition, there was no cross-resistance to other oxyimino cephalosporins, such as cefepime or cefotaxime. Some mutants such as F72L and L158P even demonstrated functional trade-offs against cefepime.

In paper III, the development of the piperacillin trade-off was systematically explored by building fitness landscapes for all mutational combinations. In agreement with susceptibilities from paper I and II, the trade-off against piperacillin was strong after the acquisition of mutations initially increasing ceftazidime resistance (e.g., F72L, Q124H, F156D, L158P). However, the accumulation of subsequent mutations such as S212A and T213A, which enabled increased ceftazidime resistance, did not further reduce piperacillin resistance.

To understand whether epistasis could be involved in shaping this trade-off, determined and predicted (based on the additive model) IC₅₀ fold-changes were

compared. Assuming a non-additive behaviour of mutations (additive model), the piperacillin resistance was predicted to be completely abolished in the ceftazidime optimised variants. Surprisingly, for all three trajectories, piperacillin resistance was maintained at low levels likely due to presence of positive epistasis. Taken together, mutations initially increasing ceftazidime resistance tend to cause a strong functional trade-off against penicillins and carbapenems. For the penicillin, piperacillin, this trade-off was limited, and epistatic investigations showed that positive epistasis was majorly responsible for retaining piperacillin resistance, and thus limiting the trade-off. However, to generalise this observation, the landscapes need to be characterised towards the spectrum of different β -lactam drugs.

The structural work in this thesis has shown that mutations increasing ceftazidime resistance can increase the flexibility of loop regions and reshape or fine-tune the active site of OXA-48. For example, L158 is located within the Ω -loop and L158P exhibits increased flexibility of both the Ω -loop and β 5- β 6 loop. Previous structural studies have shown that L158, A69 and V120 form a hydrophobic pocket which accommodates the 6α -hydroxyethyl side chain of carbapenems such as imipenem and meropenem (Figure 13 and Figure 14A)^{181,203,204}. Similarly, the pocket comprising A69, L158, S212, T213 and R214 was able to host the oxyimino side chain of cefotaxime and the thiophene ring of cefoxitin (Figure 14B and C)²⁰³. Reshaping and fine-tuning mechanisms during the evolution of OXA-48 may disturb the interaction of carbapenems, cephalosporins and potentially penicillins with these pockets, causing functional trade-offs and limiting the emergence of cross-resistance. Similarly, for the β -lactamase OXA-163, a variant displaying increased activity against ceftazidime but reduced activity against penicillins and carbapenems, kinetic measurements exposed that variation within the β 5- β 6 loop affects the deacylation rate while the acylation rate was unaffected²⁰⁴. The authors concluded that this may be due to “non-productive” binding. Thus, I speculate that the trade-off mechanism of the here evolved variants may be comparable to OXA-163. However, to further understand the molecular mechanism of how this trade-off is caused, further studies are needed.

F. Conclusions

What drives the evolution of β -lactamases such as OXA-48? Is their evolution predictable? And to that end, how many genetic solutions may evolve to increase resistance? To answer these questions, the globally circulating β -lactamase OXA-48 with promiscuous activity against the oxyimino cephalosporin ceftazidime was evolved using different selection schemes such as long-term experimental evolution under sub-MIC conditions and directed evolution.

The data from this study exposed that the very low “ceftazidimase” activity of OXA-48 can be selected for, even at low β -lactam concentrations, and further improved stepwise, by the accumulation of point mutations. In addition, OXA-48 mediated ceftazidime resistance was driven by positive epistasis among mutations and was structurally achieved by reshaping and expanding the active site, as well as by increasing the flexibility of active site loops.

In terms of pleiotropy, mutations initially increasing ceftazidime resistance caused strong functional and thermostability related trade-offs. However, while ceftazidime resistance increased by the accumulation of subsequential mutations, the functional and stability related trade-off was limited likely due to positive epistasis and selection along the stability threshold, respectively. Surprisingly, under laboratory conditions, three distinct mutational trajectories arose increasing ceftazidime resistance to similar extent. These insights in combination with knowledge on naturally evolving OXA-48 variants exposes the diversity of possible genetic solutions leading to similar phenotypic outcomes even within one enzyme. To that end, the presence of intramolecular epistasis and the heterogeneity of mutational paths likely complicates our ability to predict the phenotypic outcomes during resistance development.

Finally, ~half of the amino acid positions identified in this work have been described to be under selective pressure in naturally evolving OXA-48-like variants²¹⁹, indicating that ceftazidime likely has a selective role and drives the evolution of OXA-48 in clinical and environmental settings.

G. Perspective

The approaches utilised within this study enabled the discovery of how new enzymatic functions within OXA-48 can be promoted in different selective environments. However, the methods and approaches chosen within this thesis impose many limitations on the interpretation of the acquired data, and additional studies are needed to fill these knowledge gaps. For example, the selection of OXA-48 mediated resistance resulted in three distinct trajectories. Initial mutations may have played an important role in driving the divergence of these trajectories. However, to fully understand the compatibility of these trajectories, a landscape comprising all possible mutational combinations is needed. This could be achieved by massive gene synthesis where each mutation is genetically barcoded, and deep sequencing is used during susceptibility testing. To that end, understanding how many different evolutionary starting points and distinct trajectories exist would be important to further elucidate the role of molecular epistasis on enzyme evolution. This work has shown that there are at least 10 different amino acid changes conferring increased ceftazidime resistance. However, there might be many more, and performing deep mutational scanning on OXA-48, where all amino acid positions will be mutated to all possible amino acids, can further shed light on the availability of initial mutations and mutational hot-spots within the structure.

While strong functional trade-offs have been frequently reported for naturally evolving β -lactamases towards oxyimino cephalosporins, it cannot be excluded that dual or alternating selection may give rise to variants overcoming the trade-off. After all, the here evolved variants such as TI-4 still exhibited substantial piperacillin resistance where penicillin selection in the environment or under clinical settings could likely act on. Therefore, additional investigations are required to understand the evolutionary dynamics of strong trade-offs.

H. References

- 1 Laxminarayan, R., Duse, A., Wattal, C., Zaidi, A. K., Wertheim, H. F., Sumpradit, N., Vlieghe, E., Hara, G. L., Gould, I. M., Goossens, H., Greko, C., So, A. D., Bigdeli, M., Tomson, G., Woodhouse, W., Ombaka, E., Peralta, A. Q., Qamar, F. N., Mir, F., Kariuki, S., Bhutta, Z. A., Coates, A., Bergstrom, R., Wright, G. D., Brown, E. D. & Cars, O. Antibiotic resistance-the need for global solutions. *Lancet Infect Dis* **13**, 1057-1098, doi:10.1016/S1473-3099(13)70318-9 (2013).
- 2 CDC. Antibiotic resistance threats in the United States, 2019. (doi:10.15620/cdc:82532, Atlanta, GA, 2019).
- 3 Rossolini, G. M., Arena, F., Pecile, P. & Pollini, S. Update on the antibiotic resistance crisis. *Curr Opin Pharmacol* **18**, 56-60, doi:10.1016/j.coph.2014.09.006 (2014).
- 4 Silhavy, T. J., Kahne, D. & Walker, S. The bacterial cell envelope. *Cold Spring Harb Perspect Biol* **2**, a000414, doi:10.1101/cshperspect.a000414 (2010).
- 5 Wang, T. Z., Kodiyanplakkal, R. P. L. & Calfee, D. P. Antimicrobial resistance in nephrology. *Nat Rev Nephrol* **15**, 463-481, doi:10.1038/s41581-019-0150-7 (2019).
- 6 Cassini, A., Hogberg, L. D., Plachouras, D., Quattrocchi, A., Hoxha, A., Simonsen, G. S., Colomb-Cotinat, M., Kretzschmar, M. E., Devleeschauwer, B., Cecchini, M., Ouakrim, D. A., Oliveira, T. C., Struelens, M. J., Suetens, C. & Monnet, D. L. Attributable deaths and disability-adjusted life-years caused by infections with antibiotic-resistant bacteria in the EU and the European Economic Area in 2015: a population-level modelling analysis. *Lancet Infect Dis* **19**, 56-66, doi:10.1016/S1473-3099(18)30605-4 (2019).
- 7 WHO. Global priority list of antibiotic-resistant bacteria to guide research, discovery, and development of new antibiotics, Access:<http://www.who.int/mediacentre/news/releases/2017/bacteria-antibiotics-needed/en/>, Access date:01.05.2021 (2017).
- 8 Hampton, T. Report reveals scope of US antibiotic resistance threat. *JAMA* **310**, 1661-1663, doi:10.1001/jama.2013.280695 (2013).
- 9 WHO. Antimicrobial resistance: global report on surveillance. xxii, 232 p., Summary report published as technical document with reference number: WHO/HSE/PED/AIP/2014.2 (World Health Organization, 2014).
- 10 Burnham, J. P., Olsen, M. A. & Kollef, M. H. Re-estimating annual deaths due to multidrug-resistant organism infections. *Infect Control Hosp Epidemiol* **40**, 112-113, doi:10.1017/ice.2018.304 (2019).

- 11 O'Neill, J. Antimicrobial resistance: tackling a crisis for the health and wealth of nations, Access:<http://amr-review.org/Publications>., Access date:15.05.2021 (2014).
- 12 Levy, S. B. The 2000 Garrod lecture. Factors impacting on the problem of antibiotic resistance. *J Antimicrob Chemother* **49**, 25-30, doi:10.1093/jac/49.1.25 (2002).
- 13 Levy, S. B. Balancing the drug-resistance equation. *Trends Microbiol* **2**, 341-342, doi:10.1016/0966-842x(94)90607-6 (1994).
- 14 Blair, J. M., Webber, M. A., Baylay, A. J., Ogbolu, D. O. & Piddock, L. J. Molecular mechanisms of antibiotic resistance. *Nat Rev Microbiol* **13**, 42-51, doi:10.1038/nrmicro3380 (2015).
- 15 van Hoek, A. H., Mevius, D., Guerra, B., Mullany, P., Roberts, A. P. & Aarts, H. J. Acquired antibiotic resistance genes: an overview. *Front Microbiol* **2**, 203, doi:10.3389/fmicb.2011.00203 (2011).
- 16 Vikesland, P., Garner, E., Gupta, S., Kang, S., Maile-Moskowitz, A. & Zhu, N. Differential Drivers of Antimicrobial Resistance across the World. *Acc Chem Res* **52**, 916-924, doi:10.1021/acs.accounts.8b00643 (2019).
- 17 Levy, S. B. *Antibiotic Paradox: How Misuse of Antibiotics Destroys their Curative*. (Perseus Cambridge, 2002).
- 18 Goering, V., Dockrell, M., Zuckerman, M., Roitt, I. & LP, C. *Mims' medical microbiology*. 5th edn, (Edinburgh Elsevier, 2013).
- 19 Tsuchido, T. & Takano, M. Sensitization by heat treatment of *Escherichia coli* K-12 cells to hydrophobic antibacterial compounds. *Antimicrob Agents Chemother* **32**, 1680-1683, doi:10.1128/aac.32.11.1680 (1988).
- 20 Liu, A., Tran, L., Becket, E., Lee, K., Chinn, L., Park, E., Tran, K. & Miller, J. H. Antibiotic sensitivity profiles determined with an *Escherichia coli* gene knockout collection: generating an antibiotic bar code. *Antimicrob Agents Chemother* **54**, 1393-1403, doi:10.1128/AAC.00906-09 (2010).
- 21 Blake, K. L. & O'Neill, A. J. Transposon library screening for identification of genetic loci participating in intrinsic susceptibility and acquired resistance to antistaphylococcal agents. *J Antimicrob Chemother* **68**, 12-16, doi:10.1093/jac/dks373 (2013).
- 22 Vikesland, P. J., Pruden, A., Alvarez, P. J. J., Aga, D., Burgmann, H., Li, X. D., Manaia, C. M., Nambi, I., Wigginton, K., Zhang, T. & Zhu, Y. G. Toward a Comprehensive Strategy to Mitigate Dissemination of Environmental Sources

- of Antibiotic Resistance. *Environ Sci Technol* **51**, 13061-13069, doi:10.1021/acs.est.7b03623 (2017).
- 23 Hall, B. G. & Barlow, M. Evolution of the serine β -lactamases: past, present and future. *Drug Resist Updat* **7**, 111-123, doi:10.1016/j.drup.2004.02.003 (2004).
- 24 D'Costa, V. M., King, C. E., Kalan, L., Morar, M., Sung, W. W., Schwarz, C., Froese, D., Zazula, G., Calmels, F., Debruyne, R., Golding, G. B., Poinar, H. N. & Wright, G. D. Antibiotic resistance is ancient. *Nature* **477**, 457-461, doi:10.1038/nature10388 (2011).
- 25 Perry, J., Waglechner, N. & Wright, G. The Prehistory of Antibiotic Resistance. *Cold Spring Harb Perspect Med* **6**, doi:10.1101/cshperspect.a025197 (2016).
- 26 Perron, G. G., Whyte, L., Turnbaugh, P. J., Goordial, J., Hanage, W. P., Dantas, G. & Desai, M. M. Functional characterization of bacteria isolated from ancient arctic soil exposes diverse resistance mechanisms to modern antibiotics. *PLoS One* **10**, e0069533, doi:10.1371/journal.pone.0069533 (2015).
- 27 Singer, A. C., Colizza, V., Schmitt, H., Andrews, J., Balcan, D., Huang, W. E., Keller, V. D., Vespignani, A. & Williams, R. J. Assessing the ecotoxicologic hazards of a pandemic influenza medical response. *Environ Health Perspect* **119**, 1084-1090, doi:10.1289/ehp.1002757 (2011).
- 28 Zhang, Q. Q., Ying, G. G., Pan, C. G., Liu, Y. S. & Zhao, J. L. Comprehensive evaluation of antibiotics emission and fate in the river basins of China: source analysis, multimedia modeling, and linkage to bacterial resistance. *Environ Sci Technol* **49**, 6772-6782, doi:10.1021/acs.est.5b00729 (2015).
- 29 Verlicchi, P. & Zambello, E. Predicted and measured concentrations of pharmaceuticals in hospital effluents. Examination of the strengths and weaknesses of the two approaches through the analysis of a case study. *Sci Total Environ* **565**, 82-94, doi:10.1016/j.scitotenv.2016.04.165 (2016).
- 30 Sarmah, A. K., Meyer, M. T. & Boxall, A. B. A global perspective on the use, sales, exposure pathways, occurrence, fate and effects of veterinary antibiotics (VAs) in the environment. *Chemosphere* **65**, 725-759, doi:10.1016/j.chemosphere.2006.03.026 (2006).
- 31 Berendsen, B. J., Wegh, R. S., Memelink, J., Zuidema, T. & Stolker, L. A. The analysis of animal faeces as a tool to monitor antibiotic usage. *Talanta* **132**, 258-268, doi:10.1016/j.talanta.2014.09.022 (2015).

- 32 CDC. Antibiotic Resistance Threats in the United States, 2013, Access:<https://www.cdc.gov/drugresistance/pdf/ar-threats-2013-508.pdf>, Access date:08.06.2021 (2013).
- 33 Gelband, H., Miller-Petrie, M., Pant, S., Gandra, S., Levinson, J., Barter, D. & al., e. The State of the World's Antibiotics. (Center of Disease Dynamics, 2015).
- 34 McEwen, S. A. & Fedorka-Cray, P. J. Antimicrobial Use and Resistance in Animals. *Clinical Infectious Diseases* **34**, S93–S106, doi:10.1086/340246 (2002).
- 35 Collado, S., Quero, D., Laca, A. & Díaz, M. Efficiency and sensitivity of the wet oxidation/biological steps in coupled pharmaceutical wastewater treatment. *Chemical Engineering Journal* **234**, 484-490, doi:10.1016/j.cej.2013.07.075 (2013).
- 36 Wang, J., Mao, D., Mu, Q. & Luo, Y. Fate and proliferation of typical antibiotic resistance genes in five full-scale pharmaceutical wastewater treatment plants. *Sci Total Environ* **526**, 366-373, doi:10.1016/j.scitotenv.2015.05.046 (2015).
- 37 Holmes, A. H., Moore, L. S., Sundsfjord, A., Steinbakk, M., Regmi, S., Karkey, A., Guerin, P. J. & Piddock, L. J. Understanding the mechanisms and drivers of antimicrobial resistance. *Lancet* **387**, 176-187, doi:10.1016/S0140-6736(15)00473-0 (2016).
- 38 Andersson, D. I. & Hughes, D. Microbiological effects of sublethal levels of antibiotics. *Nat Rev Microbiol* **12**, 465-478, doi:10.1038/nrmicro3270 (2014).
- 39 Singer, A. C., Shaw, H., Rhodes, V. & Hart, A. Review of Antimicrobial Resistance in the Environment and Its Relevance to Environmental Regulators. *Front Microbiol* **7**, 1728, doi:10.3389/fmicb.2016.01728 (2016).
- 40 Van Boeckel, T. P., Brower, C., Gilbert, M., Grenfell, B. T., Levin, S. A., Robinson, T. P., Teillant, A. & Laxminarayan, R. Global trends in antimicrobial use in food animals. *Proc Natl Acad Sci U S A* **112**, 5649-5654, doi:10.1073/pnas.1503141112 (2015).
- 41 Baquero, F. & Coque, T. M. Widening the spaces of selection: evolution along sublethal antimicrobial gradients. *mBio* **5**, e02270, doi:10.1128/mBio.02270-14 (2014).
- 42 Gullberg, E., Albrecht, L. M., Karlsson, C., Sandegren, L. & Andersson, D. I. Selection of a multidrug resistance plasmid by sublethal levels of antibiotics and heavy metals. *mBio* **5**, e01918-01914, doi:10.1128/mBio.01918-14 (2014).

- 43 Westhoff, S., van Leeuwe, T. M., Qachach, O., Zhang, Z., van Wezel, G. P. & Rozen, D. E. The evolution of no-cost resistance at sub-MIC concentrations of streptomycin in *Streptomyces coelicolor*. *ISME J* **11**, 1168-1178, doi:10.1038/ismej.2016.194 (2017).
- 44 O'Brien, P. J. & Herschlag, D. Catalytic promiscuity and the evolution of new enzymatic activities. *Chem Biol* **6**, R91-R105, doi:10.1016/S1074-5521(99)80033-7 (1999).
- 45 Kazlauskas, R. J. Enhancing catalytic promiscuity for biocatalysis. *Curr Opin Chem Biol* **9**, 195-201, doi:10.1016/j.cbpa.2005.02.008 (2005).
- 46 Hult, K. & Berglund, P. Enzyme promiscuity: mechanism and applications. *Trends Biotechnol* **25**, 231-238, doi:10.1016/j.tibtech.2007.03.002 (2007).
- 47 Nobeli, I., Favia, A. D. & Thornton, J. M. Protein promiscuity and its implications for biotechnology. *Nat Biotechnol* **27**, 157-167, doi:10.1038/nbt1519 (2009).
- 48 Tokuriki, N. & Tawfik, D. S. Protein dynamism and evolvability. *Science* **324**, 203-207, doi:10.1126/science.1169375 (2009).
- 49 Khersonsky, O. & Tawfik, D. S. Enzyme promiscuity: a mechanistic and evolutionary perspective. *Annu Rev Biochem* **79**, 471-505, doi:10.1146/annurev-biochem-030409-143718 (2010).
- 50 Huang, H., Pandya, C., Liu, C., Al-Obaidi, N. F., Wang, M., Zheng, L., Toews Keating, S., Aono, M., Love, J. D., Evans, B., Seidel, R. D., Hillerich, B. S., Garforth, S. J., Almo, S. C., Mariano, P. S., Dunaway-Mariano, D., Allen, K. N. & Farelli, J. D. Panoramic view of a superfamily of phosphatases through substrate profiling. *Proc Natl Acad Sci U S A* **112**, E1974-1983, doi:10.1073/pnas.1423570112 (2015).
- 51 Kitagawa, M., Ara, T., Arifuzzaman, M., Ioka-Nakamichi, T., Inamoto, E., Toyonaga, H. & Mori, H. Complete set of ORF clones of *Escherichia coli* ASKA library (a complete set of *E. coli* K-12 ORF archive): unique resources for biological research. *DNA Res* **12**, 291-299, doi:10.1093/dnares/dsi012 (2005).
- 52 Soo, V. W., Hanson-Manful, P. & Patrick, W. M. Artificial gene amplification reveals an abundance of promiscuous resistance determinants in *Escherichia coli*. *Proc Natl Acad Sci U S A* **108**, 1484-1489, doi:10.1073/pnas.1012108108 (2011).
- 53 Atkins, W. M. Biological messiness vs. biological genius: Mechanistic aspects and roles of protein promiscuity. *J Steroid Biochem Mol Biol* **151**, 3-11, doi:10.1016/j.jsbmb.2014.09.010 (2015).

- 54 Manco, G., Merone, L., Porzio, E., Feng, Y. & Mandrich, L. Enzyme Promiscuity in the Hormone-sensitive Lipase Family of Proteins. *Protein & Peptide Letters* **19**, 144-154, doi:doi: 10.2174/092986612799080400. (2012).
- 55 Aertker, K. M. J., Chan, H. T. H., Lohans, C. T. & Schofield, C. J. Analysis of β -lactone formation by clinically observed carbapenemases informs on a novel antibiotic resistance mechanism. *J Biol Chem* **295**, 16604-16613, doi:10.1074/jbc.RA120.014607 (2020).
- 56 Lohans, C. T., van Groesen, E., Kumar, K., Tooke, C. L., Spencer, J., Paton, R. S., Brem, J. & Schofield, C. J. A New Mechanism for β -Lactamases: Class D Enzymes Degrade 1 β -Methyl Carbapenems through Lactone Formation. *Angew Chem Int Ed Engl* **57**, 1282-1285, doi:10.1002/anie.201711308 (2018).
- 57 Patrick, W. M., Quandt, E. M., Swartzlander, D. B. & Matsumura, I. Multicopy suppression underpins metabolic evolvability. *Mol Biol Evol* **24**, 2716-2722, doi:10.1093/molbev/msm204 (2007).
- 58 Miller, B. G. & Raines, R. T. Identifying latent enzyme activities: substrate ambiguity within modern bacterial sugar kinases. *Biochemistry* **43**, 6387-6392, doi:10.1021/bi049424m (2004).
- 59 Tracewell, C. A. & Arnold, F. H. Directed enzyme evolution: climbing fitness peaks one amino acid at a time. *Curr Opin Chem Biol* **13**, 3-9, doi:10.1016/j.cbpa.2009.01.017 (2009).
- 60 Yang, G., Miton, C. M. & Tokuriki, N. A mechanistic view of enzyme evolution. *Protein Sci* **29**, 1724-1747, doi:10.1002/pro.3901 (2020).
- 61 Soskine, M. & Tawfik, D. S. Mutational effects and the evolution of new protein functions. *Nat Rev Genet* **11**, 572-582, doi:10.1038/nrg2808 (2010).
- 62 Kimura, M. & Ohta, T. On Some Principles Governing Molecular Evolution. *Proceedings of the National Academy of Sciences* **71**, 2848-2852, doi:10.1073/pnas.71.7.2848 (1974).
- 63 Lynch, M. & Katju, V. The altered evolutionary trajectories of gene duplicates. *Trends Genet* **20**, 544-549, doi:10.1016/j.tig.2004.09.001 (2004).
- 64 Stiffler, M. A., Hekstra, D. R. & Ranganathan, R. Evolvability as a function of purifying selection in TEM-1 β -lactamase. *Cell* **160**, 882-892, doi:10.1016/j.cell.2015.01.035 (2015).
- 65 Chen, J. Z., Fowler, D. M. & Tokuriki, N. Comprehensive exploration of the translocation, stability and substrate recognition requirements in VIM-2 lactamase. *Elife* **9**, doi:10.7554/eLife.56707 (2020).

- 66 Jimenez-Oses, G., Osuna, S., Gao, X., Sawaya, M. R., Gilson, L., Collier, S. J., Huisman, G. W., Yeates, T. O., Tang, Y. & Houk, K. N. The role of distant mutations and allosteric regulation on LovD active site dynamics. *Nat Chem Biol* **10**, 431-436, doi:10.1038/nchembio.1503 (2014).
- 67 Baier, F., Hong, N., Yang, G., Pabis, A., Miton, C. M., Barrozo, A., Carr, P. D., Kamerlin, S. C., Jackson, C. J. & Tokuriki, N. Cryptic genetic variation shapes the adaptive evolutionary potential of enzymes. *Elife* **8**, doi:10.7554/eLife.40789 (2019).
- 68 Livermore, D. M., Warner, M., Jamrozy, D., Mushtaq, S., Nichols, W. W., Mustafa, N. & Woodford, N. *In vitro* selection of ceftazidime-avibactam resistance in *Enterobacteriaceae* with KPC-3 carbapenemase. *Antimicrob Agents Chemother* **59**, 5324-5330, doi:10.1128/AAC.00678-15 (2015).
- 69 Giddins, M. J., Macesic, N., Annavaiahala, M. K., Stump, S., Khan, S., McConville, T. H., Mehta, M., Gomez-Simmonds, A. & Uhlemann, A. C. Successive Emergence of Ceftazidime-Avibactam Resistance through Distinct Genomic Adaptations in *bla*_{KPC-2}-Harboring *Klebsiella pneumoniae* Sequence Type 307 Isolates. *Antimicrob Agents Chemother* **62**, doi:10.1128/AAC.02101-17 (2018).
- 70 Novais, A., Comas, I., Baquero, F., Canton, R., Coque, T. M., Moya, A., Gonzalez-Candelas, F. & Galan, J. C. Evolutionary trajectories of β -lactamase CTX-M-1 cluster enzymes: predicting antibiotic resistance. *PLoS Pathog* **6**, e1000735, doi:10.1371/journal.ppat.1000735 (2010).
- 71 Shields, R. K., Chen, L., Cheng, S., Chavda, K. D., Press, E. G., Snyder, A., Pandey, R., Doi, Y., Kreiswirth, B. N., Nguyen, M. H. & Clancy, C. J. The Emergence of Ceftazidime-Avibactam Resistance Due to Plasmid-Borne *bla*_{KPC-3} Mutations during Treatment of Carbapenem-Resistant *Klebsiella pneumoniae* Infections. *Antimicrob Agents Chemother* **61**, doi:10.1128/AAC.02097-16 (2017).
- 72 Shields, R. K., Nguyen, M. H., Press, E. G., Chen, L., Kreiswirth, B. N. & Clancy, C. J. Emergence of Ceftazidime-Avibactam Resistance and Restoration of Carbapenem Susceptibility in *Klebsiella pneumoniae* Carbapenemase-Producing *K pneumoniae*: A Case Report and Review of Literature. *Open Forum Infect Dis* **4**, ofx101, doi:10.1093/ofid/ofx101 (2017).
- 73 Haidar, G., Clancy, C. J., Shields, R. K., Hao, B., Cheng, S. & Nguyen, M. H. Mutations in *bla*_{KPC-3} That Confer Ceftazidime-Avibactam Resistance Encode Novel KPC-3 Variants That Function as Extended-Spectrum β -Lactamases. *Antimicrob Agents Chemother* **61**, doi:10.1128/AAC.02534-16 (2017).
- 74 Miton, C. M., Jonas, S., Fischer, G., Duarte, F., Mohamed, M. F., van Loo, B., Kintsjes, B., Kamerlin, S. C. L., Tokuriki, N., Hyvonen, M. & Hollfelder, F. Evolutionary repurposing of a sulfatase: A new Michaelis complex leads to

- efficient transition state charge offset. *Proc Natl Acad Sci U S A* **115**, E7293-E7302, doi:10.1073/pnas.1607817115 (2018).
- 75 Tokuriki, N., Jackson, C. J., Afriat-Jurnou, L., Wyganowski, K. T., Tang, R. & Tawfik, D. S. Diminishing returns and tradeoffs constrain the laboratory optimization of an enzyme. *Nat Commun* **3**, 1257, doi:10.1038/ncomms2246 (2012).
- 76 Yang, G., Hong, N., Baier, F., Jackson, C. J. & Tokuriki, N. Conformational Tinkering Drives Evolution of a Promiscuous Activity through Indirect Mutational Effects. *Biochemistry* **55**, 4583-4593, doi:10.1021/acs.biochem.6b00561 (2016).
- 77 Dusan, P. & Shina Caroline Lynn, K. Molecular modeling of conformational dynamics and its role in enzyme evolution. *Curr Opin Struct Biol* **52**, 50-57, doi:10.1016/j.sbi.2018.08.004 (2018).
- 78 Campbell, E., Kaltenbach, M., Correy, G. J., Carr, P. D., Porebski, B. T., Livingstone, E. K., Afriat-Jurnou, L., Buckle, A. M., Weik, M., Hoffelder, F., Tokuriki, N. & Jackson, C. J. The role of protein dynamics in the evolution of new enzyme function. *Nat Chem Biol* **12**, 944-950, doi:10.1038/nchembio.2175 (2016).
- 79 Dellus-Gur, E., Elias, M., Caselli, E., Prati, F., Salverda, M. L., de Visser, J. A., Fraser, J. S. & Tawfik, D. S. Negative Epistasis and Evolvability in TEM-1 β -Lactamase-The Thin Line between an Enzyme's Conformational Freedom and Disorder. *J Mol Biol* **427**, 2396-2409, doi:10.1016/j.jmb.2015.05.011 (2015).
- 80 Salverda, M. L., Dellus, E., Gorter, F. A., Debets, A. J., van der Oost, J., Hoekstra, R. F., Tawfik, D. S. & de Visser, J. A. Initial mutations direct alternative pathways of protein evolution. *PLoS Genet* **7**, e1001321, doi:10.1371/journal.pgen.1001321 (2011).
- 81 Hirvonen, V. H. A., Mulholland, A. J., Spencer, J. & van der Kamp, M. W. Small Changes in Hydration Determine Cephalosporinase Activity of OXA-48 β -Lactamases. *ACS Catalysis* **10**, 6188-6196, doi:10.1021/acscatal.0c00596 (2020).
- 82 Goldsmith, M. & Tawfik, D. S. Enzyme engineering: reaching the maximal catalytic efficiency peak. *Curr Opin Struct Biol* **47**, 140-150, doi:10.1016/j.sbi.2017.09.002 (2017).
- 83 Miton, C. M. & Tokuriki, N. How mutational epistasis impairs predictability in protein evolution and design. *Protein Sci* **25**, 1260-1272, doi:10.1002/pro.2876 (2016).

- 84 Storz, J. F. Compensatory mutations and epistasis for protein function. *Curr Opin Struct Biol* **50**, 18-25, doi:10.1016/j.sbi.2017.10.009 (2018).
- 85 Domingo, J., Baeza-Centurion, P. & Lehner, B. The Causes and Consequences of Genetic Interactions (Epistasis). *Annu Rev Genomics Hum Genet* **20**, 433-460, doi:10.1146/annurev-genom-083118-014857 (2019).
- 86 Sailer, Z. R. & Harms, M. J. High-order epistasis shapes evolutionary trajectories. *PLoS Comput Biol* **13**, e1005541, doi:10.1371/journal.pcbi.1005541 (2017).
- 87 Bontron, S., Poirel, L. & Nordmann, P. *In vitro* prediction of the evolution of GES-1 β -lactamase hydrolytic activity. *Antimicrob Agents Chemother* **59**, 1664-1670, doi:10.1128/AAC.04450-14 (2015).
- 88 Starr, T. N. & Thornton, J. W. Epistasis in protein evolution. *Protein Sci* **25**, 1204-1218, doi:10.1002/pro.2897 (2016).
- 89 Socha, R. D. & Tokuriki, N. Modulating protein stability - directed evolution strategies for improved protein function. *FEBS J* **280**, 5582-5595, doi:10.1111/febs.12354 (2013).
- 90 Tokuriki, N. & Tawfik, D. S. Stability effects of mutations and protein evolvability. *Curr Opin Struct Biol* **19**, 596-604, doi:10.1016/j.sbi.2009.08.003 (2009).
- 91 Li, X., Lalic, J., Baeza-Centurion, P., Dhar, R. & Lehner, B. Changes in gene expression predictably shift and switch genetic interactions. *Nat Commun* **10**, 3886, doi:10.1038/s41467-019-11735-3 (2019).
- 92 Olson, C. A., Wu, N. C. & Sun, R. A comprehensive biophysical description of pairwise epistasis throughout an entire protein domain. *Curr Biol* **24**, 2643-2651, doi:10.1016/j.cub.2014.09.072 (2014).
- 93 Gonzalez, C. E. & Ostermeier, M. Pervasive Pairwise Intragenic Epistasis among Sequential Mutations in TEM-1 β -Lactamase. *J Mol Biol* **431**, 1981-1992, doi:10.1016/j.jmb.2019.03.020 (2019).
- 94 Weinreich, D. M., Delaney, N. F., Depristo, M. A. & Hartl, D. L. Darwinian evolution can follow only very few mutational paths to fitter proteins. *Science* **312**, 111-114, doi:10.1126/science.1123539 (2006).
- 95 Palmer, A. C., Toprak, E., Baym, M., Kim, S., Veres, A., Bershtein, S. & Kishony, R. Delayed commitment to evolutionary fate in antibiotic resistance fitness landscapes. *Nat Commun* **6**, 7385, doi:10.1038/ncomms8385 (2015).

- 96 Yang, G., Anderson, D. W., Baier, F., Dohmen, E., Hong, N., Carr, P. D., Kamerlin, S. C. L., Jackson, C. J., Bornberg-Bauer, E. & Tokuriki, N. Author Correction: Higher-order epistasis shapes the fitness landscape of a xenobiotic-degrading enzyme. *Nat Chem Biol* **16**, 930, doi:10.1038/s41589-020-0588-8 (2020).
- 97 Shah, P., McCandlish, D. M. & Plotkin, J. B. Contingency and entrenchment in protein evolution under purifying selection. *Proc Natl Acad Sci U S A* **112**, E3226-3235, doi:10.1073/pnas.1412933112 (2015).
- 98 Wu, N. C., Dai, L., Olson, C. A., Lloyd-Smith, J. O. & Sun, R. Adaptation in protein fitness landscapes is facilitated by indirect paths. *Elife* **5**, doi:10.7554/eLife.16965 (2016).
- 99 Imamovic, L. & Sommer, M. O. A. Use of Collateral Sensitivity Networks to Design Drug Cycling Protocols That Avoid Resistance Development. *Science Translational Medicine* **5**, 204ra132-204ra132, doi:10.1126/scitranslmed.3006609 (2013).
- 100 Pal, C., Papp, B. & Lazar, V. Collateral sensitivity of antibiotic-resistant microbes. *Trends Microbiol* **23**, 401-407, doi:10.1016/j.tim.2015.02.009 (2015).
- 101 Podnecky, N. L., Fredheim, E. G. A., Kloos, J., Sorum, V., Primicerio, R., Roberts, A. P., Rozen, D. E., Samuelsen, O. & Johnsen, P. J. Conserved collateral antibiotic susceptibility networks in diverse clinical strains of *Escherichia coli*. *Nat Commun* **9**, 3673, doi:10.1038/s41467-018-06143-y (2018).
- 102 Munck, C., Gumpert, H. K., Wallin, A. I., Wang, H. H. & Sommer, M. O. Prediction of resistance development against drug combinations by collateral responses to component drugs. *Sci Transl Med* **6**, 262ra156, doi:10.1126/scitranslmed.3009940 (2014).
- 103 Rosenkilde, C. E. H., Munck, C., Porse, A., Linkevicius, M., Andersson, D. I. & Sommer, M. O. A. Collateral sensitivity constrains resistance evolution of the CTX-M-15 β -lactamase. *Nat Commun* **10**, 618, doi:10.1038/s41467-019-08529-y (2019).
- 104 Baym, M., Stone, L. K. & Kishony, R. Multidrug evolutionary strategies to reverse antibiotic resistance. *Science* **351**, aad3292, doi:10.1126/science.aad3292 (2016).
- 105 McLoughlin, S. Y. & Copley, S. D. A compromise required by gene sharing enables survival: Implications for evolution of new enzyme activities. *Proc Natl Acad Sci U S A* **105**, 13497-13502, doi:10.1073/pnas.0804804105 (2008).

- 106 Watts, K. T., Mijts, B. N., Lee, P. C., Manning, A. J. & Schmidt-Dannert, C. Discovery of a substrate selectivity switch in tyrosine ammonia-lyase, a member of the aromatic amino acid lyase family. *Chem Biol* **13**, 1317-1326, doi:10.1016/j.chembiol.2006.10.008 (2006).
- 107 Gould, S. M. & Tawfik, D. S. Directed evolution of the promiscuous esterase activity of carbonic anhydrase II. *Biochemistry* **44**, 5444-5452, doi:10.1021/bi0475471 (2005).
- 108 Kaltenbach, M., Emond, S., Hollfelder, F. & Tokuriki, N. Functional Trade-Offs in Promiscuous Enzymes Cannot Be Explained by Intrinsic Mutational Robustness of the Native Activity. *PLoS Genet* **12**, e1006305, doi:10.1371/journal.pgen.1006305 (2016).
- 109 Tokuriki, N., Stricher, F., Serrano, L. & Tawfik, D. S. How protein stability and new functions trade off. *PLoS Comput Biol* **4**, e1000002, doi:10.1371/journal.pcbi.1000002 (2008).
- 110 DePristo, M. A., Weinreich, D. M. & Hartl, D. L. Missense meanderings in sequence space: a biophysical view of protein evolution. *Nat Rev Genet* **6**, 678-687, doi:10.1038/nrg1672 (2005).
- 111 Stojanoski, V., Adamski, C. J., Hu, L., Mehta, S. C., Sankaran, B., Zwart, P., Prasad, B. V. & Palzkill, T. Removal of the side chain at the active site serine by a glycine substitution increases the Stability of a wide range of serine β -Lactamases by relieving steric strain. *Biochemistry* **55**, 2479-2490, doi:10.1021/acs.biochem.6b00056 (2016).
- 112 Beadle, B. M. & Shoichet, B. K. Structural bases of stability-function tradeoffs in enzymes. *J Mol Biol* **321**, 285-296, doi:10.1016/s0022-2836(02)00599-5 (2002).
- 113 Bush, K. Past and Present Perspectives on β -Lactamases. *Antimicrob Agents Chemother* **62**, doi:10.1128/AAC.01076-18 (2018).
- 114 Shatilovich, A., Stoupin, D. & Rivkina, E. Ciliates from ancient permafrost: Assessment of cold resistance of the resting cysts. *Eur J Protistol* **51**, 230-240, doi:10.1016/j.ejop.2015.04.001 (2015).
- 115 Sauvage, E., Kerff, F., Terrak, M., Ayala, J. A. & Charlier, P. The penicillin-binding proteins: structure and role in peptidoglycan biosynthesis. *FEMS Microbiol Rev* **32**, 234-258, doi:10.1111/j.1574-6976.2008.00105.x (2008).
- 116 Fröhlich, C., Chen, J. Z., Gholipour, S., Erdogan, A. N. & Tokuriki, N. Evolution of β -lactamases and enzyme promiscuity. *Protein Engineering, Design and Selection* **34**, doi:10.1093/protein/gzab013 (2021).

- 117 Tahlan, K. & Jensen, S. E. Origins of the β -lactam rings in natural products. *J Antibiot (Tokyo)* **66**, 401-410, doi:10.1038/ja.2013.24 (2013).
- 118 Bush, K. & Bradford, P. A. β -Lactams and β -Lactamase Inhibitors: An Overview. *Cold Spring Harb Perspect Med* **6**, doi:10.1101/cshperspect.a025247 (2016).
- 119 Hamed, R. B., Gomez-Castellanos, J. R., Henry, L., Ducho, C., McDonough, M. A. & Schofield, C. J. The enzymes of β -lactam biosynthesis. *Nat Prod Rep* **30**, 21-107, doi:10.1039/c2np20065a (2013).
- 120 Townsend, C. A. Convergent biosynthetic pathways to β -lactam antibiotics. *Curr Opin Chem Biol* **35**, 97-108, doi:10.1016/j.cbpa.2016.09.013 (2016).
- 121 Long, D. H. & Townsend, C. A. Mechanism of Integrated β -Lactam Formation by a Nonribosomal Peptide Synthetase during Antibiotic Synthesis. *Biochemistry* **57**, 3353-3358, doi:10.1021/acs.biochem.8b00411 (2018).
- 122 Oliver, R. A., Li, R. & Townsend, C. A. Monobactam formation in sulfazecin by a nonribosomal peptide synthetase thioesterase. *Nat Chem Biol* **14**, 5-7, doi:10.1038/nchembio.2526 (2018).
- 123 Cycon, M., Mroziak, A. & Piotrowska-Seget, Z. Antibiotics in the Soil Environment-Degradation and Their Impact on Microbial Activity and Diversity. *Front Microbiol* **10**, 338, doi:10.3389/fmicb.2019.00338 (2019).
- 124 Alexy, R., Kumpel, T. & Kummerer, K. Assessment of degradation of 18 antibiotics in the Closed Bottle Test. *Chemosphere* **57**, 505-512, doi:10.1016/j.chemosphere.2004.06.024 (2004).
- 125 Al-Ahmad, A., Daschner, F. D. & Kummerer, K. Biodegradability of cefotiam, ciprofloxacin, meropenem, penicillin G, and sulfamethoxazole and inhibition of waste water bacteria. *Arch Environ Contam Toxicol* **37**, 158-163, doi:10.1007/s002449900501 (1999).
- 126 Junker, T., Alexy, R., Knacker, T. & Kummerer, K. Biodegradability of ^{14}C -labeled antibiotics in a modified laboratory scale sewage treatment plant at environmentally relevant concentrations. *Environ Sci Technol* **40**, 318-324, doi:10.1021/es051321j (2006).
- 127 Hirte, K., Seiwert, B., Schuurmann, G. & Reemtsma, T. New hydrolysis products of the β -lactam antibiotic amoxicillin, their pH-dependent formation and search in municipal wastewater. *Water Res* **88**, 880-888, doi:10.1016/j.watres.2015.11.028 (2016).
- 128 Chadha, R., Kashid, N. & Jain, D. V. Kinetic studies of the degradation of an aminopenicillin antibiotic (amoxicillin trihydrate) in aqueous solution using heat

- conduction microcalorimetry. *J Pharm Pharmacol* **55**, 1495-1503, doi:10.1211/0022357022179 (2003).
- 129 Bergheim, M., Helland, T., Kallenborn, R. & Kummerer, K. Benzyl-penicillin (Penicillin G) transformation in aqueous solution at low temperature under controlled laboratory conditions. *Chemosphere* **81**, 1477-1485, doi:10.1016/j.chemosphere.2010.08.052 (2010).
- 130 Jiang, M., Wang, L. & Ji, R. Biotic and abiotic degradation of four cephalosporin antibiotics in a lake surface water and sediment. *Chemosphere* **80**, 1399-1405, doi:10.1016/j.chemosphere.2010.05.048 (2010).
- 131 Braschi, I., Blasioli, S., Fellet, C., Lorenzini, R., Garelli, A., Pori, M. & Giacomini, D. Persistence and degradation of new β -lactam antibiotics in the soil and water environment. *Chemosphere* **93**, 152-159, doi:10.1016/j.chemosphere.2013.05.016 (2013).
- 132 Gilbertson, T., Hornish, R., Jaglan PS, K., Koshy, K., Nappier, J., Stahl, G., Cazars AR, Nappier, J., Kubicek, M., Hoffman, G. & Hamlow, P. Environmental Fate of Ceftiofur Sodium, a Cephalosporin Antibiotic. Role of Animal Excreta in Its Decomposition. *J. Agríc. Food Chem.* **38**, 894-898 (1990).
- 133 Meletis, G. Carbapenem resistance: overview of the problem and future perspectives. *Ther Adv Infect Dis* **3**, 15-21, doi:10.1177/2049936115621709 (2016).
- 134 Worthington, R. J. & Melander, C. Overcoming resistance to β -lactam antibiotics. *J Org Chem* **78**, 4207-4213, doi:10.1021/jo400236f (2013).
- 135 Tooke, C. L., Hinchliffe, P., Bragginton, E. C., Colenso, C. K., Hirvonen, V. H. A., Takebayashi, Y. & Spencer, J. β -Lactamases and β -Lactamase Inhibitors in the 21st Century. *J Mol Biol* **431**, 3472-3500, doi:10.1016/j.jmb.2019.04.002 (2019).
- 136 Bush, K. & Jacoby, G. A. Updated functional classification of β -lactamases. *Antimicrob Agents Chemother* **54**, 969-976, doi:10.1128/AAC.01009-09 (2010).
- 137 Grijseels, S., Pohl, C., Nielsen, J. C., Wasil, Z., Nygard, Y., Nielsen, J., Frisvad, J. C., Nielsen, K. F., Workman, M., Larsen, T. O., Driessen, A. J. M. & Frandsen, R. J. N. Identification of the decumbenone biosynthetic gene cluster in *Penicillium decumbens* and the importance for production of calbistrin. *Fungal Biol Biotechnol* **5**, 18, doi:10.1186/s40694-018-0063-4 (2018).
- 138 Abe, Y., Suzuki, T., Ono, C., Iwamoto, K., Hosobuchi, M. & Yoshikawa, H. Molecular cloning and characterization of an ML-236B (compactin)

- biosynthetic gene cluster in *Penicillium citrinum*. *Mol Genet Genomics* **267**, 636-646, doi:10.1007/s00438-002-0697-y (2002).
- 139 Ohki, T., Shibata, N., Higuchi, Y., Kawashima, Y., Takeo, M., Kato, D. & Negoro, S. Two alternative modes for optimizing nylon-6 byproduct hydrolytic activity from a carboxylesterase with a β -lactamase fold: X-ray crystallographic analysis of directly evolved 6-aminohexanoate-dimer hydrolase. *Protein Sci* **18**, 1662-1673, doi:10.1002/pro.185 (2009).
- 140 Ribeiro, A. R., Sures, B. & Schmidt, T. C. Cephalosporin antibiotics in the aquatic environment: A critical review of occurrence, fate, ecotoxicity and removal technologies. *Environ Pollut* **241**, 1153-1166, doi:10.1016/j.envpol.2018.06.040 (2018).
- 141 Baquero, F. Low-level antibacterial resistance: a gateway to clinical resistance. *Drug Resist Updat* **4**, 93-105, doi:10.1054/drup.2001.0196 (2001).
- 142 Gullberg, E., Cao, S., Berg, O. G., Ilback, C., Sandegren, L., Hughes, D. & Andersson, D. I. Selection of resistant bacteria at very low antibiotic concentrations. *PLoS Pathog* **7**, e1002158, doi:10.1371/journal.ppat.1002158 (2011).
- 143 Davies, J., Spiegelman, G. B. & Yim, G. The world of subinhibitory antibiotic concentrations. *Curr Opin Microbiol* **9**, 445-453, doi:10.1016/j.mib.2006.08.006 (2006).
- 144 Lopez, E., Elez, M., Matic, I. & Blazquez, J. Antibiotic-mediated recombination: ciprofloxacin stimulates SOS-independent recombination of divergent sequences in *Escherichia coli*. *Mol Microbiol* **64**, 83-93, doi:10.1111/j.1365-2958.2007.05642.x (2007).
- 145 Liu, A., Fong, A., Becket, E., Yuan, J., Tamae, C., Medrano, L., Maiz, M., Wahba, C., Lee, C., Lee, K., Tran, K. P., Yang, H., Hoffman, R. M., Salih, A. & Miller, J. H. Selective advantage of resistant strains at trace levels of antibiotics: a simple and ultrasensitive color test for detection of antibiotics and genotoxic agents. *Antimicrob Agents Chemother* **55**, 1204-1210, doi:10.1128/AAC.01182-10 (2011).
- 146 Baquero, F. & Negri, M. C. Selective compartments for resistant microorganisms in antibiotic gradients. *Bioessays* **19**, 731-736, doi:10.1002/bies.950190814 (1997).
- 147 Andersson, D. I. & Hughes, D. Antibiotic resistance and its cost: is it possible to reverse resistance? *Nat Rev Microbiol* **8**, 260-271, doi:10.1038/nrmicro2319 (2010).

- 148 Barr, V., Barr, K., Millar, M. R. & Lacey, R. W. β -lactam antibiotics increase the frequency of plasmid transfer in *Staphylococcus aureus*. *J Antimicrob Chemother* **17**, 409-413, doi:10.1093/jac/17.4.409 (1986).
- 149 Bahl, M. I., Sorensen, S. J., Hansen, L. H. & Licht, T. R. Effect of tetracycline on transfer and establishment of the tetracycline-inducible conjugative transposon Tn916 in the guts of gnotobiotic rats. *Appl Environ Microbiol* **70**, 758-764, doi:10.1128/aem.70.2.758-764.2004 (2004).
- 150 Couce, A. & Blazquez, J. Side effects of antibiotics on genetic variability. *FEMS Microbiol Rev* **33**, 531-538, doi:10.1111/j.1574-6976.2009.00165.x (2009).
- 151 Canton, R. & Morosini, M. I. Emergence and spread of antibiotic resistance following exposure to antibiotics. *FEMS Microbiol Rev* **35**, 977-991, doi:10.1111/j.1574-6976.2011.00295.x (2011).
- 152 Maiques, E., Ubeda, C., Campoy, S., Salvador, N., Lasa, I., Novick, R. P., Barbe, J. & Penades, J. R. β -lactam antibiotics induce the SOS response and horizontal transfer of virulence factors in *Staphylococcus aureus*. *J Bacteriol* **188**, 2726-2729, doi:10.1128/JB.188.7.2726-2729.2006 (2006).
- 153 Mao, E. F., Lane, L., Lee, J. & Miller, J. H. Proliferation of mutators in A cell population. *J Bacteriol* **179**, 417-422, doi:10.1128/jb.179.2.417-422.1997 (1997).
- 154 Taddei, F., Radman, M., Maynard-Smith, J., Toupance, B., Gouyon, P. H. & Godelle, B. Role of mutator alleles in adaptive evolution. *Nature* **387**, 700-702, doi:10.1038/42696 (1997).
- 155 Shaver, A. C., Dombrowski, P. G., Sweeney, J. Y., Treis, T., Zappala, R. M. & Sniegowski, P. D. Fitness evolution and the rise of mutator alleles in experimental *Escherichia coli* populations. *Genetics* **162**, 557-566 (2002).
- 156 Miller, C., Thomsen, L. E., Gaggero, C., Mosseri, R., Ingmer, H. & Cohen, S. N. SOS response induction by β -lactams and bacterial defense against antibiotic lethality. *Science* **305**, 1629-1631, doi:10.1126/science.1101630 (2004).
- 157 Perez-Capilla, T., Baquero, M. R., Gomez-Gomez, J. M., Ionel, A., Martin, S. & Blazquez, J. SOS-independent induction of *dinB* transcription by β -lactam-mediated inhibition of cell wall synthesis in *Escherichia coli*. *J Bacteriol* **187**, 1515-1518, doi:10.1128/JB.187.4.1515-1518.2005 (2005).
- 158 Baquero, F., Negri, M. C., Morosini, M. I. & Blazquez, J. Selection of very small differences in bacterial evolution. *Int Microbiol* **1**, 295-300 (1998).

- 159 Kummerer, K. & Henninger, A. Promoting resistance by the emission of antibiotics from hospitals and households into effluent. *Clin Microbiol Infect* **9**, 1203-1214, doi:10.1111/j.1469-0691.2003.00739.x (2003).
- 160 Valitalo, P., Kruglova, A., Mikola, A. & Vahala, R. Toxicological impacts of antibiotics on aquatic micro-organisms: A mini-review. *Int J Hyg Environ Health* **220**, 558-569, doi:10.1016/j.ijheh.2017.02.003 (2017).
- 161 Watkinson, A. J., Murby, E. J., Kolpin, D. W. & Costanzo, S. D. The occurrence of antibiotics in an urban watershed: from wastewater to drinking water. *Sci Total Environ* **407**, 2711-2723, doi:10.1016/j.scitotenv.2008.11.059 (2009).
- 162 Negri, M. C., Lipsitch, M., Blazquez, J., Levin, B. R. & Baquero, F. Concentration-dependent selection of small phenotypic differences in TEM β -lactamase-mediated antibiotic resistance. *Antimicrob Agents Chemother* **44**, 2485-2491, doi:10.1128/aac.44.9.2485-2491.2000 (2000).
- 163 Bagge, N., Hentzer, M., Andersen, J. B., Ciofu, O., Givskov, M. & Hoiby, N. Dynamics and spatial distribution of β -lactamase expression in *Pseudomonas aeruginosa* biofilms. *Antimicrob Agents Chemother* **48**, 1168-1174, doi:10.1128/aac.48.4.1168-1174.2004 (2004).
- 164 Murray, A. K., Zhang, L., Yin, X., Zhang, T., Buckling, A., Snape, J. & Gaze, W. H. Novel Insights into Selection for Antibiotic Resistance in Complex Microbial Communities. *mBio* **9**, doi:10.1128/mBio.00969-18 (2018).
- 165 Li, Y., Xia, L., Chen, J., Lian, Y., Dandekar, A. A., Xu, F. & Wang, M. Resistance elicited by sub-lethal concentrations of ampicillin is partially mediated by quorum sensing in *Pseudomonas aeruginosa*. *Environ Int* **156**, 106619, doi:10.1016/j.envint.2021.106619 (2021).
- 166 Bagge, N., Schuster, M., Hentzer, M., Ciofu, O., Givskov, M., Greenberg, E. P. & Hoiby, N. *Pseudomonas aeruginosa* biofilms exposed to imipenem exhibit changes in global gene expression and β -lactamase and alginate production. *Antimicrob Agents Chemother* **48**, 1175-1187, doi:10.1128/aac.48.4.1175-1187.2004 (2004).
- 167 Blazquez, J., Morosini, M. I., Negri, M. C., Gonzalez-Leiza, M. & Baquero, F. Single amino acid replacements at positions altered in naturally occurring extended-spectrum TEM β -lactamases. *Antimicrob Agents Chemother* **39**, 145-149, doi:10.1128/aac.39.1.145 (1995).
- 168 Yoon, E. J. & Jeong, S. H. Class D β -lactamases. *J Antimicrob Chemother*, doi:10.1093/jac/dkaa513 (2020).

- 169 Oueslati, S., Nordmann, P. & Poirel, L. Heterogeneous hydrolytic features for OXA-48-like β -lactamases. *J Antimicrob Chemother* **70**, 1059-1063, doi:10.1093/jac/dku524 (2015).
- 170 Poirel, L., Naas, T. & Nordmann, P. Diversity, epidemiology, and genetics of class D β -lactamases. *Antimicrob Agents Chemother* **54**, 24-38, doi:10.1128/AAC.01512-08 (2010).
- 171 Danel, F., Hall, L. M. & Livermore, D. M. Laboratory mutants of OXA-10 β -lactamase giving ceftazidime resistance in *Pseudomonas aeruginosa*. *J Antimicrob Chemother* **43**, 339-344, doi:10.1093/jac/43.3.339 (1999).
- 172 Aubert, D., Poirel, L., Chevalier, J., Leotard, S., Pages, J. M. & Nordmann, P. Oxacillinase-mediated resistance to cefepime and susceptibility to ceftazidime in *Pseudomonas aeruginosa*. *Antimicrob Agents Chemother* **45**, 1615-1620, doi:10.1128/AAC.45.6.1615-1620.2001 (2001).
- 173 Antunes, N. T., Lamoureaux, T. L., Toth, M., Stewart, N. K., Frase, H. & Vakulenko, S. B. Class D β -lactamases: are they all carbapenemases? *Antimicrob Agents Chemother* **58**, 2119-2125, doi:10.1128/AAC.02522-13 (2014).
- 174 Docquier, J. D. & Mangani, S. Structure-Function Relationships of Class D Carbapenemases. *Current Drug Targets* **17**, 1061 - 1071, doi:10.2174/1389450116666150825115824 (2015).
- 175 Pitout, J. D. D., Peirano, G., Kock, M. M., Strydom, K. A. & Matsumura, Y. The Global Ascendency of OXA-48-Type Carbapenemases. *Clin Microbiol Rev* **33**, doi:10.1128/CMR.00102-19 (2019).
- 176 Szarecka, A., Lesnock, K. R., Ramirez-Mondragon, C. A., Nicholas, H. B., Jr. & Wymore, T. The Class D β -lactamase family: residues governing the maintenance and diversity of function. *Protein Eng Des Sel* **24**, 801-809, doi:10.1093/protein/gzr041 (2011).
- 177 Dortet, L., Oueslati, S., Jeannot, K., Tande, D., Naas, T. & Nordmann, P. Genetic and biochemical characterization of OXA-405, an OXA-48-type extended-spectrum β -lactamase without significant carbapenemase activity. *Antimicrob Agents Chemother* **59**, 3823-3828, doi:10.1128/AAC.05058-14 (2015).
- 178 Poirel, L., Castanheira, M., Carrer, A., Rodriguez, C. P., Jones, R. N., Smayevsky, J. & Nordmann, P. OXA-163, an OXA-48-related class D β -lactamase with extended activity toward expanded-spectrum cephalosporins. *Antimicrob Agents Chemother* **55**, 2546-2551, doi:10.1128/AAC.00022-11 (2011).

- 179 De Luca, F., Benvenuti, M., Carboni, F., Pozzi, C., Rossolini, G. M., Mangani, S. & Docquier, J. D. Evolution to carbapenem-hydrolyzing activity in noncarbapenemase class D β -lactamase OXA-10 by rational protein design. *Proc Natl Acad Sci U S A* **108**, 18424-18429, doi:10.1073/pnas.1110530108 (2011).
- 180 Dabos, L., Zavala, A., Bonnin, R. A., Beckstein, O., Retailleau, P., Iorga, B. I. & Naas, T. Substrate Specificity of OXA-48 after β 5- β 6 Loop Replacement. *ACS Infect Dis* **6**, 1032-1043, doi:10.1021/acsinfecdis.9b00452 (2020).
- 181 Smith, C. A., Stewart, N. K., Toth, M. & Vakulenko, S. B. Structural Insights into the Mechanism of Carbapenemase Activity of the OXA-48 β -Lactamase. *Antimicrob Agents Chemother* **63**, doi:10.1128/AAC.01202-19 (2019).
- 182 Hirvonen, V. H. A., Spencer, J. & van der Kamp, M. W. Antimicrobial resistance conferred by OXA-48 β -lactamases: towards a detailed mechanistic understanding. *Antimicrob Agents Chemother*, doi:10.1128/AAC.00184-21 (2021).
- 183 Docquier, J. D., Calderone, V., De Luca, F., Benvenuti, M., Giuliani, F., Bellucci, L., Tafi, A., Nordmann, P., Botta, M., Rossolini, G. M. & Mangani, S. Crystal structure of the OXA-48 β -lactamase reveals mechanistic diversity among class D carbapenemases. *Chem Biol* **16**, 540-547, doi:10.1016/j.chembiol.2009.04.010 (2009).
- 184 Paetzel, M., Danel, F., de Castro, L., Mosimann, S. C., Page, M. G. & Strynadka, N. C. Crystal structure of the class D β -lactamase OXA-10. *Nat Struct Biol* **7**, 918-925, doi:10.1038/79688 (2000).
- 185 Sun, T., Nukaga, M., Mayama, K., Crichlow, G. V., Kuzin, A. P. & Knox, J. R. Crystallization and preliminary X-ray study of OXA-1, a class D β -lactamase. *Acta Crystallogr D Biol Crystallogr* **57**, 1912-1914, doi:10.1107/s0907444901016274 (2001).
- 186 Docquier, J. D., Benvenuti, M., Calderone, V., Giuliani, F., Kapetis, D., De Luca, F., Rossolini, G. M. & Mangani, S. Crystal structure of the narrow-spectrum OXA-46 class D β -lactamase: relationship between active-site lysine carbamylation and inhibition by polycarboxylates. *Antimicrob Agents Chemother* **54**, 2167-2174, doi:10.1128/AAC.01517-09 (2010).
- 187 Smith, C. A., Antunes, N. T., Stewart, N. K., Toth, M., Kumarasiri, M., Chang, M., Mobashery, S. & Vakulenko, S. B. Structural basis for carbapenemase activity of the OXA-23 β -lactamase from *Acinetobacter baumannii*. *Chem Biol* **20**, 1107-1115, doi:10.1016/j.chembiol.2013.07.015 (2013).
- 188 Golemi, D., Maveyraud, L., Vakulenko, S., Samama, J. P. & Mobashery, S. Critical involvement of a carbamylated lysine in catalytic function of class D β -

- lactamases. *Proc Natl Acad Sci U S A* **98**, 14280-14285, doi:10.1073/pnas.241442898 (2001).
- 189 Maveyraud, L., Golemi, D., Kotra, L. P., Tranier, S., Vakulenko, S., Mobashery, S. & Samama, J. P. Insights into class D β -lactamases are revealed by the crystal structure of the OXA-10 enzyme from *Pseudomonas aeruginosa*. *Structure* **8**, 1289-1298, doi:10.1016/s0969-2126(00)00534-7 (2000).
- 190 Vercheval, L., Bauvois, C., di Paolo, A., Borel, F., Ferrer, J.-L., Sauvage, E., Matagne, A., Frère, J.-M., Charlier, P., Galleni, M. & Kerff, F. Three factors that modulate the activity of class D β -lactamases and interfere with the post-translational carboxylation of Lys70. *Biochemical Journal* **432**, 495-506, doi:10.1042/bj20101122 (2010).
- 191 Schneider, K. D., Bethel, C. R., Distler, A. M., Hujer, A. M., Bonomo, R. A. & Leonard, D. A. Mutation of the active site carboxy-lysine (K70) of OXA-1 β -lactamase results in a deacylation-deficient enzyme. *Biochemistry* **48**, 6136-6145, doi:10.1021/bi900448u (2009).
- 192 Hocquet, D., Colomb, M., Dehecq, B., Belmonte, O., Courvalin, P., Plesiat, P. & Meziane-Cherif, D. Ceftazidime-hydrolysing β -lactamase OXA-145 with impaired hydrolysis of penicillins in *Pseudomonas aeruginosa*. *J Antimicrob Chemother* **66**, 1745-1750, doi:10.1093/jac/dkr187 (2011).
- 193 Baurin, S., Vercheval, L., Bouillenne, F., Falzone, C., Brans, A., Jacquamet, L., Ferrer, J. L., Sauvage, E., Dehareng, D., Frere, J. M., Charlier, P., Galleni, M. & Kerff, F. Critical role of tryptophan 154 for the activity and stability of class D β -lactamases. *Biochemistry* **48**, 11252-11263, doi:10.1021/bi901548c (2009).
- 194 Che, T., Bethel, C. R., Pusztai-Carey, M., Bonomo, R. A. & Carey, P. R. The different inhibition mechanisms of OXA-1 and OXA-24 β -lactamases are determined by the stability of active site carboxylated lysine. *J Biol Chem* **289**, 6152-6164, doi:10.1074/jbc.M113.533562 (2014).
- 195 Yahav, D., Giske, C. G., Gramatniece, A., Abodakpi, H., Tam, V. H. & Leibovici, L. New β -Lactam- β -Lactamase Inhibitor Combinations. *Clin Microbiol Rev* **34**, doi:10.1128/CMR.00115-20 (2020).
- 196 Lomovskaya, O., Sun, D., Rubio-Aparicio, D., Nelson, K., Tsivkovski, R., Griffith, D. C. & Dudley, M. N. Vaborbactam: Spectrum of β -Lactamase Inhibition and Impact of Resistance Mechanisms on Activity in *Enterobacteriaceae*. *Antimicrob Agents Chemother* **61**, doi:10.1128/AAC.01443-17 (2017).
- 197 Lob, S. H., Hackel, M. A., Kazmierczak, K. M., Young, K., Motyl, M. R., Karlowsky, J. A. & Sahm, D. F. In Vitro Activity of Imipenem-Relebactam

- against Gram-Negative ESKAPE Pathogens Isolated by Clinical Laboratories in the United States in 2015 (Results from the SMART Global Surveillance Program). *Antimicrob Agents Chemother* **61**, doi:10.1128/AAC.02209-16 (2017).
- 198 Aktas, Z., Kayacan, C. & Oncul, O. *In vitro* activity of avibactam (NXL104) in combination with β -lactams against Gram-negative bacteria, including OXA-48 β -lactamase-producing *Klebsiella pneumoniae*. *Int J Antimicrob Agents* **39**, 86-89, doi:10.1016/j.ijantimicag.2011.09.012 (2012).
- 199 Poirel, L., Heritier, C., Tolun, V. & Nordmann, P. Emergence of oxacillinase-mediated resistance to imipenem in *Klebsiella pneumoniae*. *Antimicrob Agents Chemother* **48**, 15-22, doi:10.1128/aac.48.1.15-22.2004 (2004).
- 200 Meunier, D., Doumith, M., Findlay, J., Mustafa, N., Mallard, K., Anson, J., Panagea, S., Pike, R., Wright, L., Woodford, N. & Hopkins, K. L. Carbapenem resistance mediated by *bla*_{OXA-181} in *Pseudomonas aeruginosa*. *J Antimicrob Chemother* **71**, 2056-2057, doi:10.1093/jac/dkw087 (2016).
- 201 Akhter, S., Lund, B. A., Ismael, A., Langer, M., Isaksson, J., Christopeit, T., Leiros, H. S. & Bayer, A. A focused fragment library targeting the antibiotic resistance enzyme - Oxacillinase-48: Synthesis, structural evaluation and inhibitor design. *Eur J Med Chem* **145**, 634-648, doi:10.1016/j.ejmech.2017.12.085 (2018).
- 202 Papp-Wallace, K. M., Kumar, V., Zeiser, E. T., Becka, S. A. & van den Akker, F. Structural Analysis of The OXA-48 Carbapenemase Bound to A "Poor" Carbapenem Substrate, Doripenem. *Antibiotics (Basel)* **8**, doi:10.3390/antibiotics8030145 (2019).
- 203 Akhtar, A., Pemberton, O. A. & Chen, Y. Structural Basis for Substrate Specificity and Carbapenemase Activity of OXA-48 Class D β -Lactamase. *ACS Infect Dis* **6**, 261-271, doi:10.1021/acsinfecdis.9b00304 (2020).
- 204 Stojanoski, V., Hu, L., Sankaran, B., Wang, F., Tao, P., Prasad, B. V. V. & Palzkill, T. Mechanistic Basis of OXA-48-like β -Lactamases' Hydrolysis of Carbapenems. *ACS Infect Dis* **7**, 445-460, doi:10.1021/acsinfecdis.0c00798 (2021).
- 205 Kalp, M. & Carey, P. R. Carbapenems and SHV-1 β -lactamase form different acyl-enzyme populations in crystals and solution. *Biochemistry* **47**, 11830-11837, doi:10.1021/bi800833u (2008).
- 206 Tremblay, L. W., Fan, F. & Blanchard, J. S. Biochemical and structural characterization of *Mycobacterium tuberculosis* β -lactamase with the carbapenems ertapenem and doripenem. *Biochemistry* **49**, 3766-3773, doi:10.1021/bi100232q (2010).

- 207 Fonseca, F., Chudyk, E. I., van der Kamp, M. W., Correia, A., Mulholland, A. J. & Spencer, J. The basis for carbapenem hydrolysis by class A β -lactamases: a combined investigation using crystallography and simulations. *J Am Chem Soc* **134**, 18275-18285, doi:10.1021/ja304460j (2012).
- 208 Lund, B. A., Thomassen, A. M., Carlsen, T. J. O. & Leiros, H. K. S. Structure, activity and thermostability investigations of OXA-163, OXA-181 and OXA-245 using biochemical analysis, crystal structures and differential scanning calorimetry analysis. *Acta Crystallogr F Struct Biol Commun* **73**, 579-587, doi:10.1107/S2053230X17013838 (2017).
- 209 Stojanoski, V., Chow, D. C., Fryszczyn, B., Hu, L., Nordmann, P., Poirel, L., Sankaran, B., Prasad, B. V. & Palzkill, T. Structural basis for different substrate profiles of two closely related class D β -lactamases and their inhibition by halogens. *Biochemistry* **54**, 3370-3380, doi:10.1021/acs.biochem.5b00298 (2015).
- 210 Gomez, S., Pasteran, F., Faccone, D., Bettiol, M., Veliz, O., De Belder, D., Rapoport, M., Gatti, B., Petroni, A. & Corso, A. Inpatient emergence of OXA-247: a novel carbapenemase found in a patient previously infected with OXA-163-producing *Klebsiella pneumoniae*. *Clin Microbiol Infect* **19**, E233-235, doi:10.1111/1469-0691.12142 (2013).
- 211 Oueslati, S., Retailleau, P., Marchini, L., Berthault, C., Dortet, L., Bonnin, R. A., Iorga, B. I. & Naas, T. Role of Arginine 214 in the Substrate Specificity of OXA-48. *Antimicrob Agents Chemother* **64**, doi:10.1128/AAC.02329-19 (2020).
- 212 King, D. T., King, A. M., Lal, S. M., Wright, G. D. & Strynadka, N. C. Molecular Mechanism of Avibactam-Mediated β -Lactamase Inhibition. *ACS Infect Dis* **1**, 175-184, doi:10.1021/acsinfecdis.5b00007 (2015).
- 213 Mairi, A., Pantel, A., Sotto, A., Lavigne, J. P. & Touati, A. OXA-48-like carbapenemases producing *Enterobacteriaceae* in different niches. *Eur J Clin Microbiol Infect Dis* **37**, 587-604, doi:10.1007/s10096-017-3112-7 (2018).
- 214 Poirel, L., Potron, A. & Nordmann, P. OXA-48-like carbapenemases: the phantom menace. *J Antimicrob Chemother* **67**, 1597-1606, doi:10.1093/jac/dks121 (2012).
- 215 Venditti, C., Nisii, C., Ballardini, M., Meledandri, M. & Di Caro, A. Identification of L169P mutation in the Ω loop of KPC-3 after a short course of ceftazidime/avibactam. *J Antimicrob Chemother* **74**, 2466-2467, doi:10.1093/jac/dkz201 (2019).
- 216 Stojanoski, V., Chow, D. C., Hu, L., Sankaran, B., Gilbert, H. F., Prasad, B. V. & Palzkill, T. A triple mutant in the Ω -loop of TEM-1 β -lactamase changes the substrate profile via a large conformational change and an altered general

- base for catalysis. *J Biol Chem* **290**, 10382-10394, doi:10.1074/jbc.M114.633438 (2015).
- 217 Levitt, P. S., Papp-Wallace, K. M., Taracila, M. A., Hujer, A. M., Winkler, M. L., Smith, K. M., Xu, Y., Harris, M. E. & Bonomo, R. A. Exploring the role of a conserved class A residue in the Ω -Loop of KPC-2 β -lactamase: a mechanism for ceftazidime hydrolysis. *J Biol Chem* **287**, 31783-31793, doi:10.1074/jbc.M112.348540 (2012).
- 218 Dabos, L., Bogaerts, P., Bonnin, R. A., Zavala, A., Sacre, P., Iorga, B. I., Huang, D. T., Glupczynski, Y. & Naas, T. Genetic and Biochemical Characterization of OXA-519, a Novel OXA-48-Like β -Lactamase. *Antimicrob Agents Chemother* **62**, doi:10.1128/AAC.00469-18 (2018).
- 219 Naas, T., Oueslati, S., Bonnin, R. A., Dabos, M. L., Zavala, A., Dortet, L., Retailleau, P. & Iorga, B. I. β -lactamase database (BLDB) - structure and function. *J Enzyme Inhib Med Chem* **32**, 917-919, doi:10.1080/14756366.2017.1344235 (2017).
- 220 Bonomo, R. A. β -Lactamases: A Focus on Current Challenges. *Cold Spring Harb Perspect Med* **7**, doi:10.1101/cshperspect.a025239 (2017).
- 221 Palzkill, T. Structural and Mechanistic Basis for Extended-Spectrum Drug-Resistance Mutations in Altering the Specificity of TEM, CTX-M, and KPC β -lactamases. *Front Mol Biosci* **5**, 16, doi:10.3389/fmolb.2018.00016 (2018).
- 222 Preston, K. E., Hitchcock, S. A., Aziz, A. Y. & Tine, J. A. The complete nucleotide sequence of the multi-drug resistance-encoding IncL/M plasmid pACM1. *Plasmid* **76**, 54-65, doi:10.1016/j.plasmid.2014.08.005 (2014).
- 223 Fröhlich, C., Sorum, V., Thomassen, A. M., Johnsen, P. J., Leiros, H. S. & Samuelsen, O. OXA-48-Mediated Ceftazidime-Avibactam Resistance Is Associated with Evolutionary Trade-Offs. *mSphere* **4**, doi:10.1128/mSphere.00024-19 (2019).
- 224 Poirel, L., Bonnin, R. A. & Nordmann, P. Genetic features of the widespread plasmid coding for the carbapenemase OXA-48. *Antimicrob Agents Chemother* **56**, 559-562, doi:10.1128/AAC.05289-11 (2012).
- 225 Tu, Q., Yin, J., Fu, J., Herrmann, J., Li, Y., Yin, Y., Stewart, A. F., Muller, R. & Zhang, Y. Room temperature electrocompetent bacterial cells improve DNA transformation and recombineering efficiency. *Sci Rep* **6**, 24648, doi:10.1038/srep24648 (2016).
- 226 Chang, A. C. & Cohen, S. N. Construction and characterization of amplifiable multicopy DNA cloning vehicles derived from the P15A cryptic miniplasmid. *J Bacteriol* **134**, 1141-1156, doi:10.1128/JB.134.3.1141-1156.1978 (1978).

- 227 Socha, R. D., Chen, J. & Tokuriki, N. The Molecular Mechanisms Underlying Hidden Phenotypic Variation among Metallo- β -Lactamases. *J Mol Biol* **431**, 1172-1185, doi:10.1016/j.jmb.2019.01.041 (2019).
- 228 Chevin, L. M. On measuring selection in experimental evolution. *Biol Lett* **7**, 210-213, doi:10.1098/rsbl.2010.0580 (2011).
- 229 Zacco, M., Williams, D. M., Brown, D. M. & Gherardi, E. An approach to random mutagenesis of DNA using mixtures of triphosphate derivatives of nucleoside analogues. *J Mol Biol* **255**, 589-603, doi:10.1006/jmbi.1996.0049 (1996).
- 230 Meziane-Cherif, D., Bonnet, R., Haouz, A. & Courvalin, P. Structural insights into the loss of penicillinase and the gain of ceftazidimase activities by OXA-145 β -lactamase in *Pseudomonas aeruginosa*. *J Antimicrob Chemother* **71**, 395-402, doi:10.1093/jac/dkv375 (2016).
- 231 Lopez, C., Ayala, J. A., Bonomo, R. A., Gonzalez, L. J. & Vila, A. J. Protein determinants of dissemination and host specificity of metallo- β -lactamases. *Nat Commun* **10**, 3617, doi:10.1038/s41467-019-11615-w (2019).
- 232 Pucci, F. & Rooman, M. Towards an accurate prediction of the thermal stability of homologous proteins. *J Biomol Struct Dyn* **34**, 1132-1142, doi:10.1080/07391102.2015.1073631 (2016).
- 233 Rees, D. C. & Robertson, A. D. Some thermodynamic implications for the thermostability of proteins. *Protein Sci* **10**, 1187-1194, doi:10.1110/ps.180101 (2001).
- 234 Shuman, H. A. & Silhavy, T. J. The art and design of genetic screens: *Escherichia coli*. *Nat Rev Genet* **4**, 419-431, doi:10.1038/nrg1087 (2003).
- 235 Sun, S., Berg, O. G., Roth, J. R. & Andersson, D. I. Contribution of gene amplification to evolution of increased antibiotic resistance in *Salmonella typhimurium*. *Genetics* **182**, 1183-1195, doi:10.1534/genetics.109.103028 (2009).
- 236 Sanz-García, F., Hernando-Amado, S. & Martínez, J. L. Evolution under low antibiotic concentrations: a risk for the selection of *Pseudomonas aeruginosa* multidrug resistant mutants in nature. *bioRxiv*, 2021.2004.2021.440750, doi:10.1101/2021.04.21.440750 (2021).
- 237 Deller, M. C., Kong, L. & Rupp, B. Protein stability: a crystallographer's perspective. *Acta Crystallogr F Struct Biol Commun* **72**, 72-95, doi:10.1107/S2053230X15024619 (2016).

- 238 Acharya, K. R. & Lloyd, M. D. The advantages and limitations of protein crystal structures. *Trends Pharmacol Sci* **26**, 10-14, doi:10.1016/j.tips.2004.10.011 (2005).
- 239 Schaefer, C. & Rost, B. Predict impact of single amino acid change upon protein structure. *BMC Genomics* **13 Suppl 4**, S4, doi:10.1186/1471-2164-13-S4-S4 (2012).
- 240 Shakhnovich, E. I. & Gutin, A. M. Influence of point mutations on protein structure: probability of a neutral mutation. *J Theor Biol* **149**, 537-546, doi:10.1016/s0022-5193(05)80097-9 (1991).
- 241 Isler, B., Ezure, Y., Romero, J. L. G.-F., Harris, P., Stewart, A. G. & Paterson, D. L. Is Ceftazidime/Avibactam an Option for Serious Infections Due to Extended-Spectrum- β -Lactamase- and AmpC-Producing *Enterobacterales*?: a Systematic Review and Meta-analysis. *Antimicrobial Agents and Chemotherapy* **65**, e01052-01020, doi:10.1128/aac.01052-20 (2020).
- 242 Potron, A., Poirel, L., Rondinaud, E. & Nordmann, P. Intercontinental spread of OXA-48 β -lactamase-producing *Enterobacteriaceae* over a 11-year period, 2001 to 2011. *Euro Surveill* **18**, doi:10.2807/1560-7917.es2013.18.31.20549 (2013).
- 243 Selleck, C., Pedroso, M. M., Wilson, L., Krco, S., Knaven, E. G., Miraula, M., Mitic, N., Larrabee, J. A., Bruck, T., Clark, A., Guddat, L. W. & Schenk, G. Structure and mechanism of potent bifunctional β -lactam- and homoserine lactone-degrading enzymes from marine microorganisms. *Sci Rep* **10**, 12882, doi:10.1038/s41598-020-68612-z (2020).
- 244 Tacao, M., Silva, I. & Henriques, I. Culture-independent methods reveal high diversity of OXA-48-like genes in water environments. *J Water Health* **15**, 519-525, doi:10.2166/wh.2017.260 (2017).
- 245 Zheng, J., Payne, J. L. & Wagner, A. Cryptic genetic variation accelerates evolution by opening access to diverse adaptive peaks. *Science* **365**, 347-353, doi:10.1126/science.aax1837 (2019).
- 246 Dugatkin, L. A., Perlin, M., Lucas, J. S. & Atlas, R. Group-beneficial traits, frequency-dependent selection and genotypic diversity: an antibiotic resistance paradigm. *Proc Biol Sci* **272**, 79-83, doi:10.1098/rspb.2004.2916 (2005).
- 247 Yurtsev, E. A., Chao, H. X., Datta, M. S., Artemova, T. & Gore, J. Bacterial cheating drives the population dynamics of cooperative antibiotic resistance plasmids. *Mol Syst Biol* **9**, 683, doi:10.1038/msb.2013.39 (2013).

- 248 Domingues, I. L., Gama, J. A., Carvalho, L. M. & Dionisio, F. Social behaviour involving drug resistance: the role of initial density, initial frequency and population structure in shaping the effect of antibiotic resistance as a public good. *Heredity (Edinb)* **119**, 295-301, doi:10.1038/hdy.2017.33 (2017).
- 249 de Visser, J. A. & Rozen, D. E. Clonal interference and the periodic selection of new beneficial mutations in *Escherichia coli*. *Genetics* **172**, 2093-2100, doi:10.1534/genetics.105.052373 (2006).
- 250 van Dijk, T., Hwang, S., Krug, J., de Visser, J. & Zwart, M. P. Mutation supply and the repeatability of selection for antibiotic resistance. *Phys Biol* **14**, 055005, doi:10.1088/1478-3975/aa7f36 (2017).
- 251 Barlow, M. & Hall, B. G. Predicting evolutionary potential: in vitro evolution accurately reproduces natural evolution of the TEM β -lactamase. *Genetics* **160**, 823-832 (2002).
- 252 Ravikumar, A., Arzumanyan, G. A., Obadi, M. K. A., Javanpour, A. A. & Liu, C. C. Scalable, Continuous Evolution of Genes at Mutation Rates above Genomic Error Thresholds. *Cell* **175**, 1946-1957 e1913, doi:10.1016/j.cell.2018.10.021 (2018).
- 253 Xie, V. C., Pu, J., Metzger, B. P., Thornton, J. W. & Dickinson, B. C. Contingency and chance erase necessity in the experimental evolution of ancestral proteins. *Elife* **10**, doi:10.7554/eLife.67336 (2021).
- 254 Novais, A., Canton, R., Coque, T. M., Moya, A., Baquero, F. & Galan, J. C. Mutational events in cefotaximase extended-spectrum β -lactamases of the CTX-M-1 cluster involved in ceftazidime resistance. *Antimicrob Agents Chemother* **52**, 2377-2382, doi:10.1128/AAC.01658-07 (2008).
- 255 Yigit, H., Queenan, A. M., Anderson, G. J., Domenech-Sanchez, A., Biddle, J. W., Steward, C. D., Alberti, S., Bush, K. & Tenover, F. C. Novel carbapenem-hydrolyzing β -lactamase, KPC-1, from a carbapenem-resistant strain of *Klebsiella pneumoniae*. *Antimicrob Agents Chemother* **45**, 1151-1161, doi:10.1128/AAC.45.4.1151-1161.2001 (2001).
- 256 Wang, X., Minasov, G. & Shoichet, B. K. Evolution of an antibiotic resistance enzyme constrained by stability and activity trade-offs. *J Mol Biol* **320**, 85-95, doi:10.1016/S0022-2836(02)00400-X (2002).
- 257 Patel, M. P., Hu, L., Stojanoski, V., Sankaran, B., Prasad, B. V. V. & Palzkill, T. The Drug-Resistant Variant P167S Expands the Substrate Profile of CTX-M β -Lactamases for Oxyimino-Cephalosporin Antibiotics by Enlarging the Active Site upon Acylation. *Biochemistry* **56**, 3443-3453, doi:10.1021/acs.biochem.7b00176 (2017).

- 258 Liakopoulos, A., Mevius, D. & Ceccarelli, D. A Review of SHV Extended-Spectrum β -Lactamases: Neglected Yet Ubiquitous. *Front Microbiol* **7**, 1374, doi:10.3389/fmicb.2016.01374 (2016).
- 259 Soweik, J. A., Singer, S. B., Ohringer, S., Malley, M. F., Dougherty, T. J., Gougoutas, J. Z. & Bush, K. Substitution of lysine at position 104 or 240 of TEM-1pTZ18R β -lactamase enhances the effect of serine-164 substitution on hydrolysis or affinity for cephalosporins and the monobactam aztreonam. *Biochemistry* **30**, 3179-3188, doi:10.1021/bi00227a004 (1991).
- 260 Brown, C. A., Hu, L., Sun, Z., Patel, M. P., Singh, S., Porter, J. R., Sankaran, B., Prasad, B. V. V., Bowman, G. R. & Palzkill, T. Antagonism between substitutions in β -lactamase explains a path not taken in the evolution of bacterial drug resistance. *J Biol Chem* **295**, 7376-7390, doi:10.1074/jbc.RA119.012489 (2020).
- 261 Tooke, C. L., Hinchliffe, P., Bonomo, R. A., Schofield, C. J., Mulholland, A. J. & Spencer, J. Natural variants modify *Klebsiella pneumoniae* carbapenemase (KPC) acyl-enzyme conformational dynamics to extend antibiotic resistance. *J Biol Chem*, doi:10.1074/jbc.RA120.016461 (2020).
- 262 Powers, R. A., Caselli, E., Focia, P. J., Prati, F. & Shoichet, B. K. Structures of ceftazidime and its transition-state analogue in complex with AmpC β -lactamase: implications for resistance mutations and inhibitor design. *Biochemistry* **40**, 9207-9214, doi:10.1021/bi0109358 (2001).
- 263 Mitchell, J. M., Clasman, J. R., June, C. M., Kaitany, K. C., LaFleur, J. R., Taracila, M. A., Klinger, N. V., Bonomo, R. A., Wymore, T., Szarecka, A., Powers, R. A. & Leonard, D. A. Structural basis of activity against aztreonam and extended spectrum cephalosporins for two carbapenem-hydrolyzing class D β -lactamases from *Acinetobacter baumannii*. *Biochemistry* **54**, 1976-1987, doi:10.1021/bi501547k (2015).
- 264 Fournier, D., Hocquet, D., Dehecq, B., Cholley, P. & Plesiat, P. Detection of a new extended-spectrum oxacillinase in *Pseudomonas aeruginosa*. *J Antimicrob Chemother* **65**, 364-365, doi:10.1093/jac/dkp438 (2010).
- 265 Mehta, S. C., Rice, K. & Palzkill, T. Natural Variants of the KPC-2 Carbapenemase have Evolved Increased Catalytic Efficiency for Ceftazidime Hydrolysis at the Cost of Enzyme Stability. *PLoS Pathog* **11**, e1004949, doi:10.1371/journal.ppat.1004949 (2015).
- 266 Huang, W. & Palzkill, T. A natural polymorphism in β -lactamase is a global suppressor. *Proc Natl Acad Sci U S A* **94**, 8801-8806, doi:10.1073/pnas.94.16.8801 (1997).
- 267 Patel, M. P., Frysyczyn, B. G. & Palzkill, T. Characterization of the global stabilizing substitution A77V and its role in the evolution of CTX-M β -

lactamases. *Antimicrob Agents Chemother* **59**, 6741-6748, doi:10.1128/AAC.00618-15 (2015).

Appendix: Paper I



OXA-48-Mediated Ceftazidime-Avibactam Resistance Is Associated with Evolutionary Trade-Offs

 Christopher Fröhlich,^a Vidar Sørum,^b Ane Molden Thomassen,^a Pål Jarle Johnsen,^b Hanna-Kirsti S. Leiros,^a
 Ørjan Samuelsen^{b,c}

^aThe Norwegian Structural Biology Centre (NorStruct), Department of Chemistry, UiT—The Arctic University of Norway, Tromsø, Norway

^bDepartment of Pharmacy, UiT—The Arctic University of Norway, Tromsø, Norway

^cNorwegian National Advisory Unit on Detection of Antimicrobial Resistance, Department of Microbiology and Infection Control, University Hospital of North Norway, Tromsø, Norway

ABSTRACT Infections due to carbapenemase-producing Gram-negative pathogens are associated with limited treatment options and consequently lead to increased mortality and morbidity. In response, combinations of existing β -lactams and novel β -lactamase inhibitors, such as ceftazidime-avibactam (CAZ-AVI), have been developed as alternative treatment options. To understand the development of resistance and evolutionary trajectories under CAZ-AVI exposure, we studied the effects of ceftazidime (CAZ) and CAZ-AVI on the carbapenemase OXA-48 and the epidemic OXA-48 plasmid in *Escherichia coli*. Exposure of CAZ and CAZ-AVI resulted in single (P68A) and double (P68A,Y211S) amino acid substitutions in OXA-48, respectively. The antimicrobial susceptibility data and enzyme kinetics showed that the P68A substitution was responsible for an increased activity toward CAZ, whereas P68A,Y211S led to a decrease in the inhibitory activity of AVI. X-ray crystallography and molecular modeling of the mutants demonstrated increased flexibility within the active site, which could explain the elevated CAZ hydrolysis and reduced inhibitory activity of AVI. Interestingly, these substitutions resulted in collateral effects compromising the activity of OXA-48 toward carbapenems and penicillins. Moreover, exposure to CAZ-AVI selected for mutations within the OXA-48-encoding plasmid that severely reduced fitness in the absence of antimicrobial selection. These evolutionary trade-offs may contribute to limit the evolution of OXA-48-mediated CAZ and CAZ-AVI resistance, as well as potentially resensitize isolates toward other therapeutic alternatives.


IMPORTANCE The recent introduction of novel β -lactam/ β -lactamase inhibitor combinations like ceftazidime-avibactam has increased our ability to treat infections caused by multidrug-resistant Gram-negative bacteria, including carbapenemase-producing *Enterobacteriales*. However, the increasing number of cases of reported resistance to ceftazidime-avibactam is a concern. OXA-48 is a carbapenemase that has no significant effect on ceftazidime, but is inhibited by avibactam. Since isolates with OXA-48 frequently harbor extended-spectrum β -lactamases that are inhibited by avibactam, it is likely that ceftazidime-avibactam will be used to treat infections caused by OXA-48-producing *Enterobacteriales*. Our data show that exposure to ceftazidime-avibactam can lead to changes in OXA-48, resulting in increased ability to hydrolyze ceftazidime and withstand the inhibitory effect of avibactam. Thus, resistance toward ceftazidime-avibactam among OXA-48-producing *Enterobacteriales* should be monitored. Interestingly, the compromising effect of the amino acid substitutions in OXA-48 on other β -lactams and the effect of ceftazidime-avibactam exposure on the epidemic OXA-48 plasmid indicate that the evolution of ceftazidime-avibactam resistance comes with collateral effects.

Citation Fröhlich C, Sørum V, Thomassen AM, Johnsen PJ, Leiros H-KS, Samuelsen Ø. 2019. OXA-48-mediated ceftazidime-avibactam resistance is associated with evolutionary trade-offs. *mSphere* 4:e00024-19. <https://doi.org/10.1128/mSphere.00024-19>.

Editor Ana Cristina Gales, Escola Paulista de Medicina/Universidade Federal de São Paulo

Copyright © 2019 Fröhlich et al. This is an open-access article distributed under the terms of the [Creative Commons Attribution 4.0 International license](https://creativecommons.org/licenses/by/4.0/).

Address correspondence to Christopher Fröhlich, christopher.frohlich@uit.no, or Ørjan Samuelsen, orjan.samuelsen@unn.no.

 Ceftazidime-avibactam triggers the evolution of OXA-48. @chrfrohlich

Received 10 January 2019

Accepted 2 March 2019

Published 27 March 2019

KEYWORDS *Escherichia coli*, *Klebsiella pneumoniae*, OXA-48, carbapenem, carbapenemase, ceftazidime, ceftazidime-avibactam, collateral sensitivity, evolution, resistance development

The increasing rates of carbapenem resistance among Gram-negative pathogens is considered a critical public health threat and is associated with significant morbidity and mortality (1, 2). Recent estimates indicate that carbapenem-resistant *Escherichia coli* and *Klebsiella pneumoniae* caused 0.5 million bloodstream infections and 3.1 million serious infections worldwide in 2014 (3). A major contributor to carbapenem resistance is the acquisition of plasmid-mediated β -lactamases (carbapenemases), enabling the inactivation of carbapenems (4, 5). A wide range of carbapenemases have been identified among carbapenemase-producing *Enterobacteriales* (CPE), including the serine β -lactamases KPC (Ambler class A) and OXA-48-like (Ambler class D), as well as the metallo- β -lactamases NDM, VIM, and IMP (Ambler class B) (6, 7). Since CPE are commonly multidrug-resistant, treatment options are limited (8).

Combination therapy with preexisting β -lactams and β -lactamase inhibitors has been a successful strategy to overcome the impact of β -lactamases, such as extended-spectrum β -lactamases (ESBLs) (9). In line with this approach, the combination of the third-generation cephalosporin ceftazidime (CAZ) with the novel diazabicyclooctane non- β -lactam β -lactamase inhibitor avibactam (AVI) (10–12) has recently been developed and approved for clinical use (13–15). The CAZ-AVI combination has shown potent activity against CPE isolates since AVI has inhibitory activity toward several carbapenemases, including KPC and OXA-48 (16). Moreover, AVI also inhibits ESBLs and class C cephalosporinases, offering a potential treatment option for infections caused by multidrug-resistant Gram-negative pathogens (16–18). Unfortunately, several reports have now described the emergence of CAZ-AVI resistance in the clinical setting (19, 20). In a retrospective study at a U.S. medical center, CAZ-AVI resistance emerged in 8% of the investigated cases (21). A variety of resistance mechanisms causing CAZ-AVI resistance have been described, including specific amino acid substitutions in β -lactamases such as KPC-2, KPC-3, and CTX-M-14 (22–24) and duplications in OXA-2 (20), as well as deletions of the Ω -loop in AmpC (25). Moreover, CAZ-AVI resistance has been associated with porin mutations (e.g., OmpK36) (23, 26, 27), efflux activity (23), and increased β -lactamase expression (27). Interestingly, specific amino acid substitutions in KPC and OXA-2 are associated with a collateral effect decreasing the enzymatic activity toward carbapenems, reversing resistance to these antibiotics (20, 22, 23, 26, 28–31).

In contrast to the majority of carbapenemases, OXA-48-like carbapenemases have low activity toward carbapenems and show no significant hydrolysis of extended-spectrum cephalosporins, including CAZ (32, 33). However, some OXA-48-like variants (e.g., OXA-163, OXA-247, and OXA-405), possess increased hydrolytic activity against CAZ due to a 4-amino-acid deletion and different single nucleotide polymorphisms around the β 5- β 6 loop (34–38). Interestingly, these regions have been described as important for the carbapenemase activity of OXA-48 (32), and increased cephalosporinase activity came with reduced activity toward carbapenems (34–38). In terms of the epidemiology, OXA-48-producing isolates are increasingly identified in many parts of the world and are dominating in certain regions, such as North Africa, the Middle East, and many European countries (1, 34). A major factor for the dissemination of OXA-48 is the strong association with a self-transferable IncL plasmid (39, 40).

To investigate the evolutionary implication of CAZ and CAZ-AVI treatment on OXA-48-producing isolates, we have studied the effects on both the *bla*_{OXA-48} gene and the epidemic plasmid associated with dissemination of OXA-48. Here, we report the occurrence of single (OXA-48:P68A) and double (OXA-48:P68A,Y211S) amino acid substitutions within OXA-48 as a response to CAZ and CAZ-AVI exposure, respectively. OXA-48:P68A demonstrated increased MICs toward CAZ, and OXA-48:P68A,Y211S showed increased MICs against both CAZ and CAZ-AVI. X-ray crystallography structures

TABLE 1 *E. coli* strains used and constructed in this study

Strain	Description	Reference or source
50579417	Host strain of p50579417_3_OXA-48	61, 62
MP100	DA4201 <i>E. coli</i> K-12 MG1655	Uppsala University
MP101	MP100 transformed with p50579417_3_OXA-48	This study
MP102	MP101 subjected to CAZ and host of p50579417_3_OXA-48-CAZ	This study
MP103	MP101 subjected to CAZ-AVI and host of p50579417_3_OXA-48-CAZ-AVI	This study
TOP10	Recipient strain for pCR-blunt II-TOPO	Invitrogen
MP104	<i>E. coli</i> TOP10 transformed with pCR-blunt II- <i>bla</i> _{OXA-48}	This study
MP105	<i>E. coli</i> TOP10 transformed with pCR-blunt II- <i>bla</i> _{OXA-48} -P68A	This study
MP106	<i>E. coli</i> TOP10 transformed with pCR-blunt II- <i>bla</i> _{OXA-48} -48-P68A,Y211S	This study
MP107	MP100 transformed with p50579417_3_OXA-48-CAZ	This study
MP108	MP100 transformed with p50579417_3_OXA-48-CAZ-AVI	This study

revealed that OXA-48:P68A leads to increased flexibility within the OXA-48 structure, likely contributing to elevated CAZ hydrolysis. Molecular modeling of OXA-48:P68A,Y211S showed an altered H-bond network due to Y211S. The alteration of this network is likely to affect the enzyme stability and confer higher CAZ resistance. In addition, Y211 in OXA-48 stabilizes AVI binding by aromatic stacking. In OXA-48:P68A,Y211S, the loss of this interaction might contribute to the reduced inhibitory activity of AVI. However, development of resistance toward CAZ and CAZ-AVI led to evolutionary trade-offs where (i) amino acid substitutions in OXA-48 compromised its carbapenemase and penicillinase activities and (ii) plasmid adaptation to CAZ and CAZ-AVI conferred a significant fitness cost as well as loss of stability.

RESULTS

Selection of mutants with decreased susceptibility toward CAZ and CAZ-AVI.

To investigate how the clinical use of CAZ and CAZ-AVI influences the evolution of OXA-48, as well as the plasmid carrying OXA-48, we initially subjected a clinical *E. coli* strain previously known to carry *bla*_{OXA-48} on a conjugative IncL plasmid (34, 35) to PacBio sequencing. The genomic data revealed that the clinical strain harbored *bla*_{OXA-48} on a 65,499-bp IncL plasmid (p50579417_3_OXA-48; GenBank accession no. [CP033880](https://doi.org/10.1101/2020.03.03.33880)) with no other resistance genes (see Fig. S1 and reference 73). The plasmid was closely related to the epidemic IncL OXA-48 plasmid (40) and other OXA-48 plasmids (Fig. S1). We subsequently transferred the plasmid by conjugation into rifampin-resistant *E. coli* TOP10, isolated the plasmid, and transformed it into *E. coli* MG1655 (MP100 [Table 1]). Due to the lack of cephalosporinase activity of OXA-48, the introduction of p50579417_3_OXA-48 in *E. coli* MG1655 (MP101) did not result in any change in the MICs toward CAZ and CAZ-AVI (Table 2). MP101 was subsequently subjected to a two-step mutant selection regimen, using increasing concentrations of CAZ and CAZ-AVI up to 64× the MIC of MP101. Analysis of selected mutants after CAZ (MP102) and CAZ-AVI (MP103) exposure showed that the MICs toward both CAZ and CAZ-AVI increased irrespectively of selection regimen (Table 2). With CAZ selection, the CAZ MIC increased 128-fold and the CAZ-AVI MIC increased 16-fold. Selection with CAZ-AVI resulted in a 128-fold increase in the MICs for both CAZ and CAZ-AVI (Table 2).

TABLE 2 MIC after mutant selection of *E. coli* MG1655 (MP100) expressing OXA-48 (MP101) toward CAZ (MP102) and CAZ-AVI (MP103)^a

Strain	MIC (mg/liter) ^b	
	CAZ	CAZ-AVI
MP100	0.25	0.12
MP101	0.25	0.12
MP102	32	2
MP103	32	16

^aMutants were selected by a two-step selection procedure on plates. Tests were performed in duplicates.

^bCAZ, ceftazidime; CAZ-AVI, ceftazidime-avibactam with avibactam fixed at 4 μg/ml.

TABLE 3 MIC of *E. coli* TOP10 strains expressing native OXA-48, OXA-48:P68A, and OXA-48:P68A,Y211S

Antimicrobial agent ^a	MIC (mg/liter) ^b			
	TOP10	MP104	MP105	MP106
Penicillins and inhibitor combinations				
TRM	16	256	64	32
TZP	2	64	2	2
AMC	4	128	128	64
Cephalosporins				
CAZ	1	0.5	16	8
CAZ-AVI	0.25	0.25	0.25	1
CXM	16	16	16	16
FEP	0.06	0.12	0.25	0.12
FOT	0.12	0.25	0.25	0.12
Carbapenems				
MEM	0.03	0.25	0.03	0.03
IMI	0.25	1	0.25	0.25
ETP	0.015	1	0.06	0.06
DOR	0.03	0.03	0.03	0.03

^aTRM, temocillin; TZP, piperacillin-tazobactam with tazobactam fixed at 4 μ g/ml; AMC, amoxicillin-clavulanic acid with clavulanic acid fixed at 2 μ g/ml; CAZ, ceftazidime; CAZ-AVI, ceftazidime-avibactam, with avibactam fixed at 4 μ g/ml; CXM, cefuroxime; FEP, cefepime; FOT, cefotaxime; MEM, meropenem; IMI, imipenem; ETP, ertapenem; DOR, doripenem.

^bShown are the MICs of *E. coli* TOP10 and corresponding strains expressing native OXA-48, OXA-48:P68A, and OXA-48:P68A,Y211S (MP104, MP105 and MP106, respectively). For expression, genes were subcloned into the pCR-blunt II TOPO vector. Tests were performed in duplicates.

Amino acid substitutions in OXA-48 cause resistance and collateral effects.

Sequencing of *bla*_{OXA-48} after CAZ selection revealed a single mutation, resulting in the amino acid substitution P68A (OXA-48:P68A). Under CAZ-AVI selection, a double mutant sharing the same amino acid change (P68A) and an additional substitution, Y211S, was observed (OXA-48:P68A,Y211S). To determine the effect of both the single (P68A) and double (P68A,Y211S) amino acid substitutions in OXA-48, we cloned the native *bla*_{OXA-48} gene (MP104) and mutated versions into an expression vector in *E. coli* TOP10. Subsequent MIC determination revealed that the P68A substitution (MP105) increased the MIC toward CAZ by 32-fold (Table 3). No change in the MIC toward CAZ-AVI was observed. For the P68A,Y211S (MP106), the MIC toward CAZ was increased by 32-fold and that toward CAZ-AVI was increased by 4-fold.

Changes in OXA-2 and KPC-2/3, leading to CAZ or CAZ-AVI resistance, respectively, have been shown to come along with functional constraints (20, 26, 29, 31). Therefore, we performed MIC testing against a panel of β -lactams. Both the OXA-48:P68A and P68A,Y211S substitutions caused altered effects toward other β -lactams compared to the native OXA-48 (Table 3). The effect against carbapenems was equal for both the single and double amino acid substitution, with a 4- to 16-fold decrease in the MIC against meropenem, imipenem, and ertapenem (Table 3). No change in MIC toward doripenem was observed. Moreover, expression of both mutants of OXA-48 resulted in reduced activity against piperacillin-tazobactam (32-fold MIC decrease) and temocillin (4- to 8-fold MIC decrease). For other β -lactams, including other cephalosporins such as cefepime and cefotaxime, the changes were within a 2-fold dilution step (nonsignificant).

Thermostability and enzyme kinetics of OXA-48:P68A and OXA-48:P68A,Y211S. OXA-48, OXA-48:P68A, and OXA-48:P68A,Y211S were expressed and purified (>95% purity). From an initial starting culture of 1 liter, yields of 23.9, 9.9, and 16.7 mg, respectively, were obtained. P68A and P68A,Y211S caused a reduction in the thermostability of OXA-48, with melting temperatures of $49.5 \pm 0.1^\circ\text{C}$ and $46.7 \pm 0.2^\circ\text{C}$, respectively, compared to $53.5 \pm 0.1^\circ\text{C}$ for the native OXA-48. We further determined the effect of the amino acid changes, with respect to both the hydrolytic activity

TABLE 4 Kinetic values of recombinantly expressed and purified OXA-48, OXA-48:P68A, and OXA-48:P68A,Y211S^a

Substrate ^b	OXA-48			OXA-48:P68A			OXA-48:P68A,Y211S		
	K_m (μM)	k_{cat} (s^{-1})	k_{cat}/K_m ($\text{s}^{-1} \text{mM}^{-1}$)	K_m (μM)	k_{cat} (s^{-1})	k_{cat}/K_m ($\text{s}^{-1} \text{mM}^{-1}$)	K_m (μM)	k_{cat} (s^{-1})	k_{cat}/K_m ($\text{s}^{-1} \text{mM}^{-1}$)
AMP	370 ± 70	608 ± 53	1,643 ± 455	77 ± 12	25 ± 1	331 ± 66	211 ± 26	18 ± 1	86 ± 14
PIP	898 ± 155	3.9 ± 0.5	4 ± 1	290 ± 67	0.15 ± 0.02	0.5 ± 0.2	155 ± 38	0.06 ± 0.01	0.4 ± 0.2
NIT	226 ± 34	141 ± 12	624 ± 148	53 ± 8	37 ± 2	703 ± 149	63 ± 9	12 ± 1	193 ± 40
CAZ	300 ± 150	3.0 ± 0.8	10 ± 8	220 ± 50	26 ± 3	117 ± 41	190 ± 40	42 ± 5	220 ± 72
FEP	1,678 ± 686	1.7 ± 0.6	1.0 ± 0.8	462 ± 126	0.5 ± 0.1	1.2 ± 0.5	1,459 ± 635	1.1 ± 0.4	0.8 ± 0.6
IMI	13 ± 2	4.8 ± 0.2	365 ± 71	4.2 ± 0.9	0.80 ± 0.04	190 ± 50	14 ± 3	0.57 ± 0.04	41 ± 11
MEM	4 ± 1	0.71 ± 0.02	177 ± 50	3 ± 1	(8 ± 0.8) × 10 ⁻⁴	0.3 ± 0.1	2 ± 1	(2 ± 0.2) × 10 ⁻³	1.2 ± 0.7

^aErrors are displayed as 95% confidence intervals based on a minimum of triplicates.

^bAMP, ampicillin; PIP, piperacillin; NIT, nitrocefin; CAZ, ceftazidime; FEP, cefepime; IMI, imipenem; MEM, meropenem.

against β -lactams as well as the inhibitory effect (50% inhibitory concentration [IC_{50}]) of AVI and tazobactam. Compared to native OXA-48, P68A and P68A,Y211S caused >10-fold and >20-fold increased catalytic efficiency (k_{cat}/K_m) toward CAZ, respectively (Table 4). In addition, both substitutions conferred reduced hydrolytic activity toward penicillins (ampicillin and piperacillin) and carbapenems (imipenem and meropenem [Table 4]). The reduced catalytic efficiency varied from 2- to ~600-fold compared to the native OXA-48. No change was observed for the cephalosporin cefepime.

For OXA-48:P68A, we observed no change in the inhibitory activity of AVI (Table 5). However, the double substitution P68A,Y211S resulted in a >5-fold decrease in inhibitory activity of AVI. Moreover, both the P68A and P68A,Y211S substitutions led to an increased inhibitory activity of tazobactam with >20-fold and >3-fold reductions in the IC_{50} compared to the native OXA-48 (Table 5).

P68A and P68A,Y211S increase flexibility of the active site. Two new crystal structures of OXA-48:P68A were obtained after soaking (see Table S1 in the supplemental material). Both structures displayed four molecules in the asymmetric unit arranged in two dimers (chains A to D). In the first OXA-48:P68A structure (resolved to 2.50 Å), we found CAZ bound to chain A/C (OXA-48:P68A-CAZ), as well as two empty active sites (chain B/D, OXA-48:P68A)—thus, one CAZ molecule per dimer. The second OXA-48:P68A structure was in complex with AVI (OXA-48:P68A-AVI) and resolved to 2.22 Å. The effect of the amino acid change P68A was studied by superimposing the unbound chains B and D (OXA-48:P68A) onto native OXA-48 (PDB no. 4S2P) (10) which demonstrated similar conformations (Fig. 1A) and an insignificant root mean square deviation (RMSD) of 0.3 Å. In chains A and C of OXA-48:P68A-CAZ, CAZ was found covalently bound to the active-site residue S70 and stabilized by H-bonds involving residues S70, T209, Y211, S212, T213, R214, and R250 (Fig. 1B). Comparing the CAZ unbound and bound chains of OXA-48:P68A, several conformational changes were evident.

CAZ binding forces R214 in the β 5- β 6 loop to move out of the active site. As a result, R214 would then clash with parts of the Ω -loop (D143 to S165) in the native OXA-48 (Fig. 1B). Indeed, we found residues 149 to 161 (for both chains A and C) in the Ω -loop of OXA-48:P68A to be disordered (Fig. 1B) and thus not visible in the electron density maps. Therefore, P68A seems to impose increased flexibility within OXA-48, and this enables both the β 5- β 6 loop and Ω -loop to occupy alternative conformations and

TABLE 5 IC_{50} s of tazobactam and avibactam against OXA-48, OXA-48:P68A, and OXA-48:P68A,Y211S

Antimicrobial agent	IC_{50} (μM) for ^a :		
	OXA-48	OXA-48:P68A	OXA-48:P68A,Y211S
Tazobactam	95 ± 9	4 ± 1	31 ± 5
Avibactam	2.2 ± 0.6	1.3 ± 0.3	13 ± 3

^a IC_{50} s (50% inhibitory concentrations) were determined using nitrocefin as a reporter substrate. Enzymes and inhibitor were incubated together for 5 min. Errors are displayed as 95% confidence intervals.

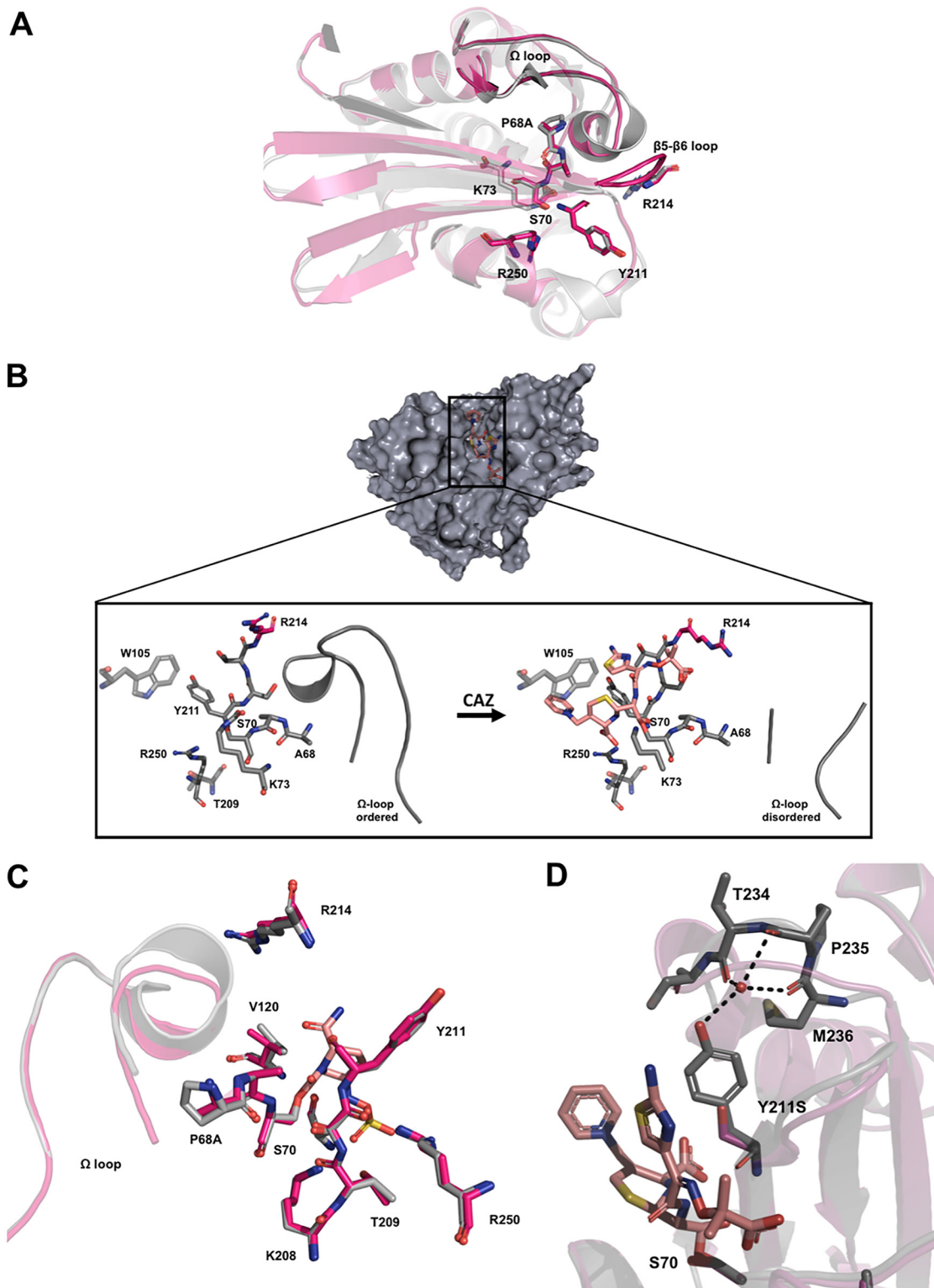


FIG 1 Crystal structure of OXA-48:P68A and molecular modeling of OXA-48:P68A,Y211S. (A) Structure in the absence of CAZ (red) superimposed onto native OXA-48 (gray; PDB no. 4S2P) (10). (B) Structure of OXA-48:P68A (gray) in the absence of CAZ (left) and with CAZ covalently bound (right [CAZ is displayed in orange]). CAZ binding causes a displacement of R214 (red) as well as a disorder of the Ω -loop. (C) Superimposition of OXA-48:P68A-AVI (red) with native OXA-48 binding AVI (gray; PDB no. 4S2P) (10). In both native OXA-48 and OXA-48:P68A, we found AVI interacting and binding to the same residues. (D) Superimposition of OXA-48:P68A (gray) binding CAZ (orange) with the modeled structure of OXA-48:P68A,Y211S (red). Here Y211 and T234, P235, and M236 form H-bonds with a central coordinated water molecule. Formation of the same H-bonds in the presence of S211 in OXA-48:P68A,Y211S is unlikely.

TABLE 6 MIC after transformation of *E. coli* MG1655 with the native and adapted plasmids

Antimicrobial agent ^a	MIC (mg/liter) ^b			
	MP100	MP101	MP107	MP108
Penicillins and inhibitor combinations				
TRM	8	256	128	32
TZP	8	128	128	128
AMC	2	64	4	4
Cephalosporins				
CAZ	0.25	0.25	16	32
CAZ-AVI	0.12	0.12	0.25	4
CXM	8	16	16	8
FEP	0.06	0.25	0.5	0.25
FOT	0.12	0.5	1	0.25
Carbapenems				
MEM	0.03	0.25	0.06	0.06
IMI	0.12	1	0.25	0.25
ETP	0.015	1	0.25	0.12
DOR	0.015	0.03	0.03	0.03

^aTRM, temocillin; TZP, piperacillin-tazobactam with tazobactam fixed at 4 μ g/ml; AMC, amoxicillin-clavulanic acid with clavulanic acid fixed at 2 μ g/ml; CAZ, ceftazidime; CAZ-AVI, ceftazidime-avibactam with avibactam fixed at 4 μ g/ml; CXM, cefuroxime; FEP, cefepime; FOT, cefotaxime; MEM, meropenem; IMI, imipenem; ETP, ertapenem; DOR, doripenem.

^bShown are the MICs after transformation of *E. coli* MG1655 (MP100) with the native plasmid (MP101) and adapted plasmids p50579417-OXA-48-CAZ (MP107) and p50579417-OXA-48-CAZ-AVI (MP108). Tests were performed in duplicates.

consequently favors CAZ binding. Interestingly, the β 5- β 6-loop region has been shown to be relevant for the carbapenemase versus ceftazidimase activity of OXA-48 (32, 41). Furthermore, we found AVI covalently bound to S70 in all OXA-48:P68A-AVI chains. Superimposition of OXA-48:P68A-AVI with the structure of native OXA-48 in a complex with AVI (PDB no. 4S2K) (11) showed no difference in interaction with AVI (Fig. 1C). R214 and the Ω -loop were in the same conformation as in the native OXA-48.

Crystallization of OXA-48:P68A,Y211S was unsuccessful; therefore, we used molecular modeling and superimposed the obtained structure onto the structure of OXA-48:P68A-CAZ. In native OXA-48 (PDB no. 4S2P) and OXA-48:P68A, the Y211 side chain is part of a water-mediated H-bond network, including T234, P235, and M236, where the water molecule is centrally coordinated (Fig. 1D). In contrast, the formation of this H-bond network seems not feasible with serine at position 211. In principle, this could lead to a higher flexibility within the structure of OXA-48:P68A,Y211S and could be related to the \sim 4°C reduced thermostability, as well as to elevated CAZ hydrolysis, compared to OXA-48:P68A.

Effect of plasmid adaptations on resistance and host fitness. In order to investigate the effect of selection on the plasmid backbone, we isolated and transformed the plasmids after CAZ (p50579417_3_OXA-48-CAZ) and CAZ/AVI (p50579417_3_OXA-48-CAZ-AVI) selection into MP100. MIC determination of the resulting strains MP107 and MP108 mirrored the fold changes observed in the cloned expression vector system (Table 6; see Fig. S2 in the supplemental material). This indicates that the P68A and P68A,Y211S in OXA-48 are the main contributors to the altered susceptibility profiles. To further investigate the role of the plasmid during resistance development, we measured the fitness costs of MP101, MP107, and MP108 in head-to-head competition assays. The native OXA-48 plasmid did not significantly reduce fitness (relative fitness [w] = 1.01, P = 0.509, df = 6) in MP101 relative to the plasmid-free strain MP100. However, after CAZ-AVI adaptation, MP103 showed severely reduced fitness, by 18% (w = 0.82, P = 0.008, df = 3) relative to the plasmid-free strain MP100 (Fig. 2).

In an attempt to isolate the fitness effects conferred by the plasmids after adaptation alone, we competed MP107 and MP108 with the native OXA-48 plasmid-

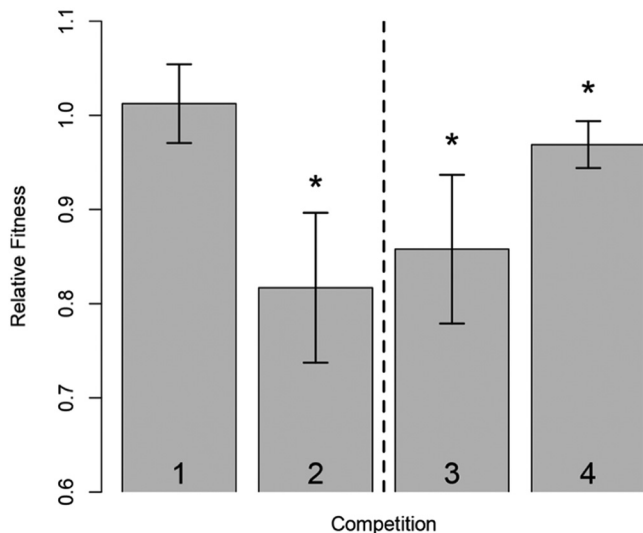


FIG 2 Mixed head-to-head competitions. Strains were mixed in a 1:1 ratio and grown together overnight. Ratios before and after incubation were determined by selective plating. For bar 1, MP100 (*E. coli* MG1655) competed with MP101 (*E. coli* MG1655 carrying p50579417_3_OXA-48) demonstrated no initial cost of the native OXA-48 plasmid. For bar 2, competitions of MP100 (*E. coli* MG1655) with MP103 (MP101 subjected to CAZ-AVI) resulted in a high fitness cost of 18% for the strain subjected to CAZ-AVI. For bars 3 and 4, comparisons of MP101 versus MP107 (*E. coli* MG1655 transformed with p50579417_3_OXA-48-CAZ) and MP108 (*E. coli* MG1655 transformed with p50579417_3_OXA-48-CAZ-AVI) demonstrated significant costs of 14% and 3%, respectively. All measurements were done at least in triplicates. Statistically significant results are marked with asterisks. Strain abbreviations are listed in Table 1.

carrying strain MP101. Both adapted plasmids significantly reduced fitness, by 14% (p50579417_3_OXA-48-CAZ; $P = 0.003$, $df = 9$) and 3% (p50579417_3_OXA-48-CAZ-AVI; $P = 0.026$, $df = 6$), respectively. Sequencing of the plasmids after selection revealed mutational differences on the plasmid backbone. Different point mutations in *repA*, 79G→T (p50579417_3_OXA-48-CAZ) and 79G→T (p50579417_3_OXA-48-CAZ-AVI) (42), as well as a 62-bp deletion in the DNA binding side of a xenobiotic response element (transcriptional regulator) in the p50579417_3_OXA-48-CAZ plasmid were observed. To investigate the effect of CAZ-AVI exposure on OXA-48 plasmid stability, we serially passaged MP101 harboring the native OXA-48 plasmid and the CAZ-AVI-exposed strain MP103 for 350 generations under nonselective conditions. Consistent with the fitness data, the native OXA-48 plasmid was stably maintained throughout the experiment, whereas loss of p50579417_3_OXA-48-CAZ-AVI was observed after ~100 generations. The plasmid was completely lost from the population after ~250 generations (Fig. 3).

DISCUSSION

Treatment options for infections caused by carbapenemase-producing Gram-negative bacteria are limited, and the increased spread of these multidrug-resistant bacteria is considered a public health threat (1, 2). Several novel β -lactamase inhibitors, including inhibitors of carbapenemases, have recently been introduced to resurrect the activity of existing β -lactams (43, 44). This includes AVI, a novel diazabicyclooctane β -lactamase inhibitor able to inhibit class A and class D carbapenemases, such as KPC and OXA-48, respectively. Thus, the introduction of the combination CAZ-AVI offers a possible treatment option for class A and class D carbapenemase-producing *Enterobacteriales* (16). Unfortunately, several reports are now describing the emergence of CAZ-AVI-resistant *Enterobacteriales*, particularly KPC-producing *K. pneumoniae* (22, 23, 30). In contrast to carbapenemases such as KPC, the OXA-48 carbapenemase has an insignificant hydrolysis activity toward third-generation cephalosporins, including CAZ. However, the CAZ-AVI combination is a promising treatment option since OXA-48-

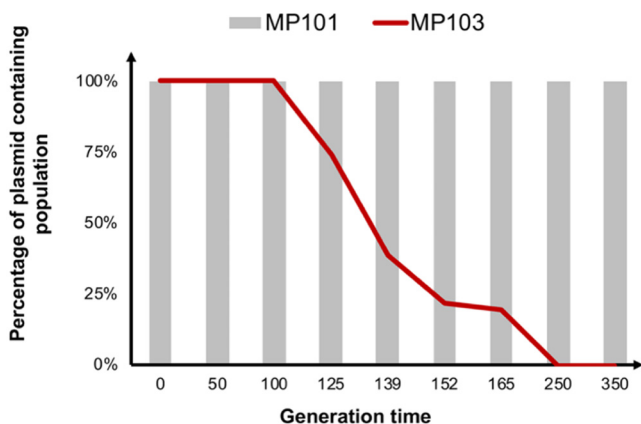


FIG 3 Plasmid stability of MP101 and MP103 in nonselective MH broth over 350 generations (Table 1). The native plasmid (p50579417_3_OXA-48) was stably maintained in MP101 over 350 generations without selection pressure. In the strain subjected to CAZ-AVI, MP103, the adapted plasmid (p50579417_3_OXA-48-CAZ-AVI) was purged out of the population within 350 generations.

producing isolates frequently also carry an ESBL (12, 45, 46). Thus, we investigated the effect of CAZ and CAZ-AVI on the evolution of OXA-48 and an OXA-48 plasmid closely related to the epidemic IncL plasmid frequently associated with *bla*_{OXA-48} (39, 40).

Our results show that both CAZ and CAZ-AVI exposure resulted in mutations in *bla*_{OXA-48} that increased the ability of OXA-48 to hydrolyze CAZ. After CAZ-AVI exposure, we also identified a reduced inhibitory effect of AVI. Moreover, development of OXA-48 resistance toward CAZ/CAZ-AVI conferred collateral sensitivity where the carbapenem and penicillin activities of the enzyme were reduced. Several studies have reported OXA-48-like variants (OXA-163, OXA-247, and OXA-405) with increased activity toward extended-spectrum cephalosporins (36–38). These variants carry amino acid deletions/substitutions within and around the β 5- β 6 loop also leading to reduced carbapenemase activity. OXA-247 carries the identified Y211S substitution in addition to a 4-amino-acid deletion (36). From these studies, it was unclear, however, whether this evolutionary trajectory could have been triggered by the exposure to extended-spectrum cephalosporins. We show that CAZ and CAZ-AVI have the potential to affect the evolution of OXA-48 and that the substitutions P68A and P68A,Y211S re-evolve the function of OXA-48 and specialize the enzyme toward ceftazidime hydrolysis. These results agree with other studies in which the adaptive changes in enzymes caused collateral effects, compromising or reversing the original function (20, 29, 31, 47, 48). While Y211 in OXA-48 is located at the β 5- β 6 loop and is involved in AVI binding by the formation of an oxyanion hole (11, 32), as well as in aromatic stacking with the side chain (~4.3 Å), the role of P68 in the beginning of the α 3 helix is poorly understood. *In silico* modeling of OXA variants identified loops flanking the α 3 helix to play an important role for the carbapenemase or CAZ hydrolysis activity in those variants. In general, increased stability in these loop regions was also correlated with higher affinity to carbapenems, whereby more flexible loops revealed their catalytic proficiency toward CAZ (41).

The X-ray structure of OXA-48:P68A with four chains in the asymmetric unit revealed that CAZ binding requires higher structural flexibility. Generally, CAZ binding resulted in a displacement of the β 5- β 6 loop carrying R214, as well as a disordered Ω -loop (Fig. 1B). Docking experiments in OXA-48 have shown that CAZ hydrolysis is mechanically unfeasible. This is mainly due to the high rigidity and the small active-site cavity confined by R214, as well as the length of the β 5- β 6 loop (41, 49). In contrast, a strongly shortened β 5- β 6 loop and the absence of R214, as observed in OXA-163, expand the active-site cavity and allow OXA-163 to hydrolyze CAZ more efficiently (49). This supports the hypothesis that P68A increases the flexibility and changes the plasticity of the substrate binding site in OXA-48, allowing the hydrolysis of bulkier

drugs such as CAZ. Decreased rigidity is also supported by a reduction in thermostability of $\sim 4^{\circ}\text{C}$, compared to native OXA-48. Interestingly, OXA-163 (as well as OXA-247 and OXA-405) displayed collateral sensitivity toward carbapenems (36–38, 50) but also cross-resistance toward some cephalosporins (e.g., cefotaxime). Molecular docking of OXA-163 suggests that cefotaxime is more embedded within the active site (49). However, cross-resistance toward other cephalosporins than CAZ was not observed for the OXA-48:P68A variant. Depending on their R2 side chain, cephalosporins display different binding behavior in metallo- β -lactamases (51). While OXA-48:P68A allows CAZ binding by a displacement of the $\beta 5$ - $\beta 6$ and Ω -loops, we hypothesize that for other cephalosporins, the active site of OXA-48:P68A might still be too narrow and rigid to achieve significant hydrolysis.

The double mutant carrying P68A,Y211S conferred a high level of resistance toward CAZ and elevated MIC levels against CAZ-AVI. Furthermore, P68A,Y211S caused a 20-fold increase in CAZ hydrolysis and a 5-fold reduction in the inhibitory activity of AVI, compared to native OXA-48. Therefore, our data suggest that OXA-48-mediated development of resistance toward CAZ-AVI is due to both increased enzymatic hydrolysis toward CAZ and reduced inhibitory activity of AVI. Molecular modeling of OXA-48:P68A,Y211S suggested the alteration of a water-mediated H-bond network between Y211 OH and T234 O and P235 O and M236 O (Fig. 1D). In OXA-48:P68A,Y211S, S211 is unlikely to be part of the same H-bond network due to its less-space-filling properties. The loss of H-bonds can increase enzyme flexibility; however, this is usually accompanied by decreased enzyme stability (52). Indeed, we found OXA-48:P68A,Y211S to be $\sim 7^{\circ}\text{C}$ and $\sim 4^{\circ}\text{C}$ less thermostable compared to native OXA-48 and OXA-48:P68A. We therefore believe that P68A,Y211S in OXA-48 further increases the flexibility of the active site, resulting in increased CAZ hydrolysis. In addition, S211 contributes to the reduced inhibitory activity of AVI by the loss of aromatic stacking, which stabilizes AVI in OXA-48 and OXA-48:P68A.

In addition, clinically relevant reversion of piperacillin-tazobactam resistance was shown for both the single and double OXA-48 mutants. Enzyme kinetics also revealed a double effect where the OXA-48 variants demonstrate reduced piperacillin hydrolysis activity and stronger inhibition by tazobactam. Similar effects were shown for CAZ-AVI-mediated mutations within KPC-2 and KPC-3 (29–31). Resensitization through exploitation of such evolutionary trade-offs could in principle provide the basis for alternative treatment strategies that potentiate the activities of earlier-generation β -lactams, and several strategies have recently been proposed (53–56).

Since the dissemination of *bla*_{OXA-48} is partially linked to closely related IncI plasmids (39, 40), we wanted to investigate the effect of CAZ and CAZ-AVI exposure on p50579417_3_OXA-48. Interestingly, the adapted plasmids showed a significant fitness cost compared to the native plasmid (Fig. 2), as well as reduced plasmid stability (p50579417_3_OXA-48-CAZ-AVI) in the absence of β -lactam selection (Fig. 3). Sequencing of the CAZ- and CAZ-AVI-exposed plasmids displayed mutations in a regulatory region (*repA*) known to be involved in plasmid copy number control (42, 57). Upregulation of plasmid copy number has been shown previously to correlate with both decreased bacterial fitness and increased drug resistance (58). These data suggest that P68A and P68A,Y211S mutations, alone or in combination with putative copy number changes, might negatively impact the fitness of the adapted plasmids.

Mutations in *bla*_{KPC-2/3} conferring CAZ-AVI resistance have been observed in the clinical setting (19, 22, 28, 30, 59). However, to the best of our knowledge, OXA-48-mediated reduced susceptibility to CAZ-AVI has not yet been reported in clinical settings (60). This might be due to the evolutionary trade-offs and reduced fitness reported here, which in principle may limit the occurrence and spread of resistance. Taken together, our data suggest that CAZ and CAZ-AVI conferred collateral sensitivity effects where the enzyme compromised its original carbapenemase and penicillinase activity. In principle, these evolutionary constraints and resensitizations can be exploited in order to improve future treatment protocols.

MATERIALS AND METHODS

Media, antibiotics, and strains. Mueller-Hinton (MH) agar and broth were purchased from Thermo Fisher Scientific (East Grinstead, United Kingdom). Luria-Bertani (LB) broth, LB agar, ampicillin, amoxicillin, cefepime, CAZ, imipenem, meropenem, piperacillin, and tazobactam were obtained from Sigma-Aldrich (St. Louis, MO). Nitrocefin was purchased from Merck (Darmstadt, Germany). All strains used and constructed within this study are listed in Table 1. The characteristics of the clinical *E. coli* strain 50579417 harboring the OXA-48 plasmid (p50579417_3_OXA-48) have been described previously (61, 62). The plasmid p50579417_3_OXA-48 was conjugated into rifampin-resistant *E. coli* TOP10 and subsequently isolated using a plasmid mini-purification kit (Qiagen, Germany). *E. coli* MG1655 (DA4201) was electroporated with p50579417_3_OXA-48 as published previously (63). Transformants positive for *bla*_{OXA-48} were checked by PCR using REDTaq ready mix (Sigma-Aldrich, St. Louis, MO) and preOXA-48 primers (61).

PacBio sequencing of *E. coli* 50579417. Genomic DNA of *E. coli* 50579417 was prepared from an overnight culture using the GenElute bacterial genomic DNA kit (Sigma-Aldrich, St. Louis, MO) according to the manufacturer's instructions. The DNA library was prepared using the Pacific Biosciences 20-kb library preparation protocol and size selection with a 9-kb cutoff using BluePippin (Sage Sciences, Beverly, MA). Sequencing was performed using the Pacific Biosciences RSII instrument using P6-C4 chemistry with a 360-min movie time and one single-molecule real-time sequencing (SMRT) cell. The sequences were assembled and polished at The Norwegian Sequencing Centre (<https://www.sequencing.uio.no/>) using HGAP v3 (Pacific Biosciences, SMRT Analysis Software v.2.3.0). Minimus2 from AMOS was used to circularize contigs, and RS_Resequencing.1 software (Pacific Biosciences, SMRT Analysis Software v.2.3.0) was used for correction of bases after circularization.

Selection of mutants with increased CAZ and CAZ-AVI MIC. Ten milliliters of an MP101 culture was grown in MH broth at 37°C overnight and then centrifuged for 10 min at 4,000 × *g*, and the pellet was suspended in 1 ml MH broth. One hundred microliters was plated on MH agar containing increasing concentrations of either CAZ alone or in combination with AVI up to 2 mg/liter. For CAZ-AVI, we utilized the clinical ratio of 4:1, respectively. Colonies growing on the highest concentration were recovered and grown in a fresh overnight culture (MH broth) and subsequently plated on concentrations of CAZ or CAZ-AVI up to 32 mg/liter.

Antibiotic susceptibility testing. For MIC determination, single colonies were suspended in 0.9% saline buffer to a 0.5 McFarland standard and further diluted 1:100 in MH broth. Fifty microliters of the bacterial suspension was loaded onto in-house-designed and premade Sensititre microtiter plates (TREK Diagnostic Systems/Thermo Fisher Scientific, East Grinstead, United Kingdom). The plates were incubated for 20 h at 37°C. Antibiotic susceptibility testing was performed in duplicates.

***bla*_{OXA-48} sequencing and subcloning.** After CAZ and CAZ-AVI exposure, plasmids were isolated using a plasmid mini-purification kit (Qiagen, Germany), and mutations within *bla*_{OXA-48} were identified by Sanger sequencing (BigDye 3.1 technology; Applied Biosystems, CA) using preOXA-48 primers (61).

For a functional resistance profile, the native and mutated *bla*_{OXA-48} genes were cloned in the pCR-blunt II-TOPO vector (Invitrogen, CA) and expressed in *E. coli* TOP10 (Invitrogen, CA). The PCR product was obtained by Phusion High Fidelity PCR mastermix with High Fidelity buffer (New England Biolabs, MA) and preOXA-48 primers (61). Transformants were selected on LB agar plates containing 50 or 100 mg/liter ampicillin. Insertion size was verified by Sanger sequencing using M13 forward (5'-GTA AAACGACGGCCAG-3') and reverse (5'-CAGGAAACAGCTATGAC-3') primers.

Recombinant enzyme construction, expression, and purification. In order to construct OXA-48:P68A and OXA-48:P68A,Y211S, site-directed mutagenesis of *bla*_{OXA-48} in a pDEST17 vector was performed using the QuikChange II site-directed mutagenesis kit (Agilent Biosciences, Santa Clara, CA) (64, 65). XL1-Blue competent cells were heat shock transformed with the constructed DNA. Point mutations were verified by Sanger sequencing using T7 primers, as described above. OXA-48 expression and purification were done as described previously (51, 52). For the mutants, expression was performed in Rosetta 2(DE3)/pLysS. In general, cultures were grown to log phase in Terrific broth supplemented with ampicillin (100 mg/liter) at 37°C and 180 rpm. Enzyme expression was induced with 0.1 mM IPTG (isopropyl-β-D-thiogalactopyranoside) and performed at 15°C and 180 rpm overnight. Harvested cells were sonicated, and recombinant proteins were purified as described previously (64).

Thermostability. Fluorescence-based protein thermostability was determined for OXA-48, OXA-48:P68A, and OXA-48:P68A,Y211S in an MJ minicycler (Bio-Rad) across a temperature gradient of 25 to 60°C (at a heating rate of 1°C per min). Thermostability was determined in 50 mM HEPES (VWR, PA) at pH 7.5 supplemented with 50 mM potassium sulfate (Honeywell, NC) using 0.2 mg/ml protein and 5× SYPRO orange (Sigma-Aldrich, St. Louis, MO). The excitation and emission wavelengths of SYPRO orange are 470 and 570 nm, respectively. The melting temperatures were determined as the inflection point of the melting transition found from the first derivative. All experiments were performed in triplicates.

Steady-state enzyme kinetics. The K_m and k_{cat} for recombinantly expressed OXA-48, OXA-48:P68A, and OXA-48:P68A,Y211S were determined under steady-state conditions for ampicillin ($\Delta\xi = -820 \text{ M}^{-1} \text{ cm}^{-1}$, 232 nm, 1 nM), piperacillin ($\Delta\xi = -820 \text{ M}^{-1} \text{ cm}^{-1}$, 235 nm, 1, 10, and 100 nM for OXA-48, OXA-48:P68A, and OXA-48:P68A,Y211S, respectively), nitrocefin ($\Delta\xi = 17,400 \text{ M}^{-1} \text{ cm}^{-1}$, 482 nm, 0.75 nM), CAZ ($\Delta\xi = -9,000 \text{ M}^{-1} \text{ cm}^{-1}$, 260 nm, 150 nM), cefepime ($\Delta\xi = -10,000 \text{ M}^{-1} \text{ cm}^{-1}$, 260 nm, 1 nM), imipenem ($\Delta\xi = -9,000 \text{ M}^{-1} \text{ cm}^{-1}$, 300 nm, 150 nM), and meropenem ($\Delta\xi = -6,500 \text{ M}^{-1} \text{ cm}^{-1}$, 300 nm, 150 nM) by measuring the initial enzymatic reaction rate. The half-maximal inhibitory concentrations (IC_{50}) for AVI and tazobactam were obtained after incubation of recombinant enzymes (0.75 nM) with inhibitors for 5 min at 25°C. Nitrocefin (20 μM) was utilized as the reporter substrate, and the initial enzymatic reaction rate was measured at 482 nm. All determinations were performed at least in duplicates at a final assay volume of 100 μl. For nitrocefin-dependent reactions, 96-well plates (Thermo

Fisher Scientific, Roskilde, Denmark) were utilized. For all the substances, UV-transparent 96-well plates (Corning, Kennebunk, ME) were used. All test results were obtained at 25°C and in 0.1 M phosphate buffer (pH 7.0) supplemented with 50 mM NaHCO₃ (Sigma-Aldrich, St. Louis, MO). Calculations were performed by using GraphPad Prism 7.0 (GraphPad Software, Inc.).

Crystallization, structure determination, and molecular modeling. OXA-48:P68A was crystallized by the sitting-drop method in 22% to 26% polyethylene glycol monomethyl ether 5000 (Sigma-Aldrich, St. Louis, MO) and 0.1 M BIS-Tris-propane buffer (Sigma-Aldrich, St. Louis, MO) at pH 6.5 to 7.5 at 4°C. Crystals were soaked for some seconds in CAZ (saturated) or AVI (saturated) in cryoprotector, which was in mother lipid and 10% ethylene glycol (Sigma-Aldrich, St. Louis, MO, USA), followed by being flash-cooled in liquid nitrogen. Diffraction data were collected on BL14.1 and BL14.2 BESSY II, Berlin, Germany, at 100 K at a wavelength of 0.9184 Å, and the diffraction images were indexed and integrated using XDS (66). AIMLESS was used for scaling (67). During scaling, the final data sets were carefully inspected (Table S1), where we aimed for high completeness: a $CC_{1/2}$ of >0.5 in the outer resolution shell and a mean above 1.0. Both structures were solved by molecular replacement with chain A of PDB no. 5QB4 (68) and the program Phenix 1.12 (69). Parts of the models were rebuilt using Coot (70). Figures were prepared using PyMOL version 1.8 (Schrödinger). For OXA-48:P68A,Y211S, molecular modeling was performed using Swiss-Model (71) and OXA-46:P68A as a template (PDB no. 6Q5F).

Fitness experiments. Two-milliliter overnight cultures were inoculated by picking single colonies from LB agar plates and incubated for 24 h at 37°C and 700 rpm. Competitors were then mixed and diluted 1:100 in a volumetric 1:1 ratio by passaging 5 μ l of each overnight culture into 990 μ l LB broth in a 96-deep-well plate (VWR, PA). Initial (time 0 [T_0]) and endpoint (time 24 h [T_{24}]) CFU values for each competitor were determined by selective plating on LB agar and LB agar containing 50 mg/liter amoxicillin. Competitions were carried out at 37°C in at least triplicates. Relative fitness (w) was calculated by determining the ratio between each pair of competitors using a Malthusian parameter and the equation $w = \ln(A_{T_{24}}/A_{T_0})/\ln(B_{T_{24}}/B_{T_0})$ (72), where A and B are the competing strains.

Plasmid sequencing. Plasmid DNA after CAZ and CAZ-AVI exposure was isolated as described above, and fragment libraries were constructed by using the Nextera kit (Illumina, Little Chesterford, United Kingdom) followed by 251-bp paired-end sequencing (MiSeq, Illumina). This was done according to the manufacturer's instructions. Paired-end sequence data were assembled using CLCbio's Genomics Workbench 8.0 (Qiagen, Aarhus, Denmark). Sequences were aligned against the native OXA-48 plasmid, and mutations were identified using DNASTAR (DNASTAR, Madison, WI).

Plasmid stability. MP101 and MP103 were evolved under nonselective conditions in MH broth for 350 generations. Initially, 990 μ l MH broth was inoculated with 10 μ l of an overnight culture and incubated for 12 h at 37°C and 700 rpm. Every 12 h, 10 μ l of the culture was transferred into 990 μ l MH broth. Plasmid stability was tested after 0, 50, 100, 125, 140, 155, 165, 250, and 350 generations. For each time point, an overnight culture was diluted 10^{-4} to 10^{-6} in 0.9% saline. One hundred microliters of each concentration was plated on MH agar and incubated overnight at 37°C. Subsequently, 100 single colonies were picked and streaked on MH agar containing 100 mg/liter ampicillin.

Data availability. Atom coordinates and structure factors for OXA-48:P68A and OXA-48:P68A-AVI have been deposited in the Protein Data Bank (PDB no. 6Q5F and 6Q5B, respectively). The plasmid sequence data (p50579417_3_OXA-48) are available in GenBank under accession no. CP033880. All other relevant data are available within this article, the supplemental material, or from the corresponding author upon request.

SUPPLEMENTAL MATERIAL

Supplemental material for this article may be found at <https://doi.org/10.1128/mSphere.00024-19>.

FIG S1, PDF file, 1.9 MB.

FIG S2, PDF file, 0.2 MB.

TABLE S1, PDF file, 0.03 MB.

ACKNOWLEDGMENTS

We are very grateful to Jürgen Brem, Department of Chemistry, University of Oxford, United Kingdom, for providing the avibactam used in this study, as well as Linus Sandegren, Uppsala University, Sweden, for providing *E. coli* MG1655 (DA4201). Provision of beam time at BL14.1 and BL14.2 at Bessy II, Berlin, Germany, is highly valued. We thank Maria Chiara di Luca for sequencing *E. coli* 50579417, as well as Nicole Podnecky and Joao Pedro Alves Gama for their support in the analysis of the next-generation sequencing data. The PacBio sequencing was performed at the Norwegian Sequencing Centre.

Pål Jarle Johnsen was supported by Northern Norway Regional Health Authority, UiT—The Arctic University of Norway (project SFP1292-16), and JPI-EC-AMR (project 271176/H10).

C.F., H.-K.S.L., and Ø.S. conceived the study. C.F., V.S., P.J.J., Ø.S., and H.-K.S.L. designed experiments. C.F. performed mutant selection. C.F. sequenced and cloned

*bla*_{OXA-48}-C.F. and V.S. performed antibiotic susceptibility testing. C.F. and V.S. performed serial transfers. C.F. measured plasmid stability. V.S. performed fitness cost analysis. A.M.T. inserted point mutations and purified enzymes. C.F. and A.M.T. performed enzyme kinetics. C.F. and H.-K.S.L. crystallized, solved, and refined crystal structures. C.F., V.S., and Ø.S. wrote the manuscript with input from all authors.

The authors declare no competing financial interest.

REFERENCES

- van Duin D, Doi Y. 2017. The global epidemiology of carbapenemase-producing *Enterobacteriaceae*. *Virulence* 8:460–469. <https://doi.org/10.1080/21505594.2016.1222343>.
- Cassini A, Högberg LD, Plachouras D, Quattrocchi A, Hoxha A, Simonsen GS, Colomb-Cotinat M, Kretzschmar ME, Devleeschauwer B, Cecchini M, Ouakrim DA, Oliveira TC, Struelens MJ, Suetens C, Monnet DL, Strauss R, Mertens K, Struyf T, Catry B, Latour K, Ivanov IN, Dobrova EG, Tambic Andrašević A, Soprek S, Budimir A, Paphitou N, Žemlicková H, Schytte Olsen S, Wolff Sönksen U, Märtin P, Ivanova M, Lyytikäinen O, Jalava J, Coignard B, Eckmanns T, Abu Sin M, Haller S, Daikos GL, Gikas A, Tsiodras S, Kontopidou F, Tóth Á, Hajdu Á, Guólaugsson Ó, Kristinsson KG, Murchan S, Burns K, Pezzotti P, Gagliotti C, Dumpis U, et al. 2019. Attributable deaths and disability-adjusted life-years caused by infections with antibiotic-resistant bacteria in the EU and the European Economic Area in 2015: a population-level modelling analysis. *Lancet Infect Dis* 19:56–66. [https://doi.org/10.1016/S1473-3099\(18\)30605-4](https://doi.org/10.1016/S1473-3099(18)30605-4).
- Temkin E, Fallach N, Almagor J, Gladstone BP, Tacconelli E, Carmeli Y, DRIVE-AB Consortium. 2018. Estimating the number of infections caused by antibiotic-resistant *Escherichia coli* and *Klebsiella pneumoniae* in 2014: a modelling study. *Lancet Glob Health* 6:e969–e979. [https://doi.org/10.1016/S2214-109X\(18\)30278-X](https://doi.org/10.1016/S2214-109X(18)30278-X).
- Walsh TR. 2010. Emerging carbapenemases: a global perspective. *Int J Antimicrob Agents* 36(Suppl 3):S8–14. [https://doi.org/10.1016/S0924-8579\(10\)70004-2](https://doi.org/10.1016/S0924-8579(10)70004-2).
- Nordmann P, Dortet L, Poirel L. 2012. Carbapenem resistance in *Enterobacteriaceae*: here is the storm! *Trends Mol Med* 18:263–272. <https://doi.org/10.1016/j.molmed.2012.03.003>.
- Jacoby GA, Munoz-Price LS. 2005. The new β -lactamases. *N Engl J Med* 352:380–391. <https://doi.org/10.1056/NEJMr041359>.
- Queenan AM, Bush K. 2007. Carbapenemases: the versatile β -lactamases. *Clin Microbiol Rev* 20:440–458. <https://doi.org/10.1128/CMR.00001-07>.
- Patel G, Bonomo RA. 2013. “Stormy waters ahead”: global emergence of carbapenemases. *Front Microbiol* 4:48. <https://doi.org/10.3389/fmicb.2013.00048>.
- Endimiani A, Choudhary Y, Bonomo RA. 2009. *In vitro* activity of NXL104 in combination with β -lactams against *Klebsiella pneumoniae* isolates producing KPC carbapenemases. *Antimicrob Agents Chemother* 53:3599–3601. <https://doi.org/10.1128/AAC.00641-09>.
- Ehmann DE, Jahic H, Ross PL, Gu RF, Hu J, Kern G, Walkup GK, Fisher SL. 2012. Avibactam is a covalent, reversible, non- β -lactam β -lactamase inhibitor. *Proc Natl Acad Sci U S A* 109:11663–11668. <https://doi.org/10.1073/pnas.1205073109>.
- King DT, King AM, Lal SM, Wright GD, Strynadka NC. 2015. Molecular mechanism of avibactam-mediated β -lactamase inhibition. *ACS Infect Dis* 1:175–184. <https://doi.org/10.1021/acsinfecdis.5b00007>.
- Zasowski EJ, Rybak JM, Rybak MJ. 2015. The β -lactams strike back: ceftazidime-avibactam. *Pharmacotherapy* 35:755–770. <https://doi.org/10.1002/phar.1622>.
- Lagace-Wiens P, Walky A, Karlowsky JA. 2014. Ceftazidime-avibactam: an evidence-based review of its pharmacology and potential use in the treatment of Gram-negative bacterial infections. *Core Evid* 9:13–25. <https://doi.org/10.2147/CE.S40698>.
- Zhanell GG, Lawson CD, Adam H, Schweizer F, Zelenitsky S, Lagace-Wiens PR, Denisuk A, Rubinstein E, Gin AS, Hoban DJ, Lynch JP, III, Karlowsky JA. 2013. Ceftazidime-avibactam: a novel cephalosporin/ β -lactamase inhibitor combination. *Drugs* 73:159–177. <https://doi.org/10.1007/s40265-013-0013-7>.
- Sharma R, Park TE, Moy S. 2016. Ceftazidime-avibactam: a novel cephalosporin/ β -lactamase inhibitor combination for the treatment of resistant Gram-negative organisms. *Clin Ther* 38:431–444. <https://doi.org/10.1016/j.clinthera.2016.01.018>.
- Ehmann DE, Jahic H, Ross PL, Gu RF, Hu J, Durand-Reville TF, Lahiri S, Thresher J, Livchak S, Gao N, Palmer T, Walkup GK, Fisher SL. 2013. Kinetics of avibactam inhibition against class A, C, and D β -lactamases. *J Biol Chem* 288:27960–27971. <https://doi.org/10.1074/jbc.M113.485979>.
- Aktaş Z, Kayacan C, Oncul O. 2012. *In vitro* activity of avibactam (NXL104) in combination with β -lactams against Gram-negative bacteria, including OXA-48 β -lactamase-producing *Klebsiella pneumoniae*. *Int J Antimicrob Agents* 39:86–89. <https://doi.org/10.1016/j.ijantimicag.2011.09.012>.
- Bonnefoy A, Dupuis-Hamelin C, Steier V, Delachaux C, Seys C, Stachyra T, Fairley M, Guitton M, Lampilas M. 2004. *In vitro* activity of AVE1330A, an innovative broad-spectrum non- β -lactam β -lactamase inhibitor. *J Antimicrob Chemother* 54:410–417. <https://doi.org/10.1093/jac/dkh358>.
- Gaibani P, Campoli C, Lewis RE, Volpe SL, Scaltriti E, Giannella M, Pongolini S, Berlinger A, Cristini F, Bartoletti M, Tedeschi S, Ambretti S. 2018. *In vivo* evolution of resistant subpopulations of KPC-producing *Klebsiella pneumoniae* during ceftazidime/avibactam treatment. *J Antimicrob Chemother* 73:1525–1529. <https://doi.org/10.1093/jac/dky082>.
- Fraile-Ribot PA, Mulet X, Cabot G, Del Barrio-Tofino E, Juan C, Perez JL, Oliver A. 2017. *In vivo* emergence of resistance to novel cephalosporin- β -lactamase inhibitor combinations through the duplication of amino acid D149 from OXA-2 β -lactamase (OXA-539) in sequence type 235 *Pseudomonas aeruginosa*. *Antimicrob Agents Chemother* 61:e01117-17. <https://doi.org/10.1128/AAC.01117-17>.
- Shields RK, Potoski BA, Haidar G, Hao B, Doi Y, Chen L, Press EG, Kreiswirth BN, Clancy CJ, Nguyen MH. 2016. Clinical outcomes, drug toxicity, and emergence of ceftazidime-avibactam resistance among patients treated for carbapenem-resistant *Enterobacteriaceae* infections. *Clin Infect Dis* 63:1615–1618. <https://doi.org/10.1093/cid/ciw636>.
- Giddins MJ, Macesic N, Annavajhala MK, Stump S, Khan S, McConville TH, Mehta M, Gomez-Simmonds A, Uhlemann AC. 2018. Successive emergence of ceftazidime-avibactam resistance through distinct genomic adaptations in *bla*_{KPC-2}-harboring *Klebsiella pneumoniae* sequence type 307 isolates. *Antimicrob Agents Chemother* 62:e02101-17. <https://doi.org/10.1128/AAC.02101-17>.
- Nelson K, Hemarajata P, Sun D, Rubio-Aparicio D, Tsivkovski R, Yang S, Sebra R, Kasarskis A, Nguyen H, Hanson BM, Leopold S, Weinstock G, Lomovskaya O, Humphries RM. 2017. Resistance to ceftazidime-avibactam is due to transposition of KPC in a porin-deficient strain of *Klebsiella pneumoniae* with increased efflux activity. *Antimicrob Agents Chemother* 61:e00989-17. <https://doi.org/10.1128/AAC.00989-17>.
- Both A, Buttner H, Huang J, Perbandt M, Belmar Campos C, Christner M, Maurer FP, Kluge S, König C, Aepfelbacher M, Wichmann D, Rohde H. 2017. Emergence of ceftazidime/avibactam non-susceptibility in an MDR *Klebsiella pneumoniae* isolate. *J Antimicrob Chemother* 72:2483–2488. <https://doi.org/10.1093/jac/dkx179>.
- Lahiri SD, Walkup GK, Whiteaker JD, Palmer T, McCormack K, Tanudra MA, Nash TJ, Thresher J, Johnstone MR, Hajec L, Livchak S, McLaughlin RE, Alm RA. 2015. Selection and molecular characterization of ceftazidime/avibactam-resistant mutants in *Pseudomonas aeruginosa* strains containing derepressed AmpC. *J Antimicrob Chemother* 70:1650–1658. <https://doi.org/10.1093/jac/dkv004>.
- Shields RK, Nguyen MH, Press EG, Chen L, Kreiswirth BN, Clancy CJ. 2017. *In vitro* selection of meropenem resistance among ceftazidime-avibactam-resistant, meropenem-susceptible *Klebsiella pneumoniae* isolates with variant KPC-3 carbapenemases. *Antimicrob Agents Chemother* 61:e00079-17. <https://doi.org/10.1128/AAC.00079-17>.
- Humphries RM, Yang S, Hemarajata P, Ward KW, Hindler JA, Miller SA, Gregson A. 2015. First report of ceftazidime-avibactam resistance in a KPC-3-expressing *Klebsiella pneumoniae* isolate. *Antimicrob Agents Chemother* 59:6605–6607. <https://doi.org/10.1128/AAC.01165-15>.
- Shields RK, Nguyen MH, Press EG, Chen L, Kreiswirth BN, Clancy CJ. 2017. Emergence of ceftazidime-avibactam resistance and restoration of carbapenem susceptibility in *Klebsiella pneumoniae* carbapenemase-

- producing *K pneumoniae*: a case report and review of literature. *Open Forum Infect Dis* 4:ofx101. <https://doi.org/10.1093/ofid/ofx101>.
29. Livermore DM, Warner M, Jamroz D, Mushtaq S, Nichols WW, Mustafa N, Woodford N. 2015. *In vitro* selection of ceftazidime-avibactam resistance in *Enterobacteriaceae* with KPC-3 carbapenemase. *Antimicrob Agents Chemother* 59:5324–5330. <https://doi.org/10.1128/AAC.00678-15>.
 30. Haidar G, Clancy CJ, Shields RK, Hao B, Cheng S, Nguyen MH. 2017. Mutations in *bla*_{KPC-3} that confer ceftazidime-avibactam resistance encode novel KPC-3 variants that function as extended-spectrum β -lactamases. *Antimicrob Agents Chemother* 61:e02534-16. <https://doi.org/10.1128/AAC.02534-16>.
 31. Compain F, Arthur M. 2017. Impaired inhibition by avibactam and resistance to the ceftazidime-avibactam combination due to the D(179)Y substitution in the KPC-2 β -lactamase. *Antimicrob Agents Chemother* 61:e00451-17. <https://doi.org/10.1128/AAC.00451-17>.
 32. Docquier JD, Calderone V, De Luca F, Benvenuti M, Giuliani F, Bellucci L, Tafi A, Nordmann P, Botta M, Rossolini GM, Mangani S. 2009. Crystal structure of the OXA-48 β -lactamase reveals mechanistic diversity among class D carbapenemases. *Chem Biol* 16:540–547. <https://doi.org/10.1016/j.chembiol.2009.04.010>.
 33. Poirel L, Heritier C, Tolun V, Nordmann P. 2004. Emergence of oxacillinase-mediated resistance to imipenem in *Klebsiella pneumoniae*. *Antimicrob Agents Chemother* 48:15–22. <https://doi.org/10.1128/AAC.48.1.15-22.2004>.
 34. Mairi A, Pantel A, Sotto A, Lavigne JP, Touati A. 2018. OXA-48-like carbapenemases producing *Enterobacteriaceae* in different niches. *Eur J Clin Microbiol Infect Dis* 37:587–604. <https://doi.org/10.1007/s10096-017-3112-7>.
 35. Poirel L, Potron A, Nordmann P. 2012. OXA-48-like carbapenemases: the phantom menace. *J Antimicrob Chemother* 67:1597–1606. <https://doi.org/10.1093/jac/dks121>.
 36. Gomez S, Pasteran F, Faccione D, Bettiol M, Veliz O, De Belder D, Rapoport M, Gatti B, Petroni A, Corso A. 2013. Inpatient emergence of OXA-247: a novel carbapenemase found in a patient previously infected with OXA-163-producing *Klebsiella pneumoniae*. *Clin Microbiol Infect* 19:E233–E235. <https://doi.org/10.1111/1469-0691.12142>.
 37. Poirel L, Castanheira M, Carrer A, Rodriguez CP, Jones RN, Smayevsky J, Nordmann P. 2011. OXA-163, an OXA-48-related class D β -lactamase with extended activity toward expanded-spectrum cephalosporins. *Antimicrob Agents Chemother* 55:2546–2551. <https://doi.org/10.1128/AAC.00022-11>.
 38. Dortet L, Oueslati S, Jeannot K, Tande D, Naas T, Nordmann P. 2015. Genetic and biochemical characterization of OXA-405, an OXA-48-type extended-spectrum β -lactamase without significant carbapenemase activity. *Antimicrob Agents Chemother* 59:3823–3828. <https://doi.org/10.1128/AAC.05058-14>.
 39. Potron A, Kalpoe J, Poirel L, Nordmann P. 2011. European dissemination of a single OXA-48-producing *Klebsiella pneumoniae* clone. *Clin Microbiol Infect* 17:E24–E26. <https://doi.org/10.1111/j.1469-0691.2011.03669.x>.
 40. Poirel L, Bonnin RA, Nordmann P. 2012. Genetic features of the widespread plasmid coding for the carbapenemase OXA-48. *Antimicrob Agents Chemother* 56:559–562. <https://doi.org/10.1128/AAC.05289-11>.
 41. Pal A, Tripathi A. 2016. An *in silico* approach to elucidate structure based functional evolution of oxacillinase. *Comput Biol Chem* 64:145–153. <https://doi.org/10.1016/j.compbiolchem.2016.06.001>.
 42. Athanasopoulos V, Praszkiar J, Pittard AJ. 1999. Analysis of elements involved in pseudoknot-dependent expression and regulation of the *repA* gene of an IncL/M plasmid. *J Bacteriol* 181:1811–1819.
 43. Papp-Wallace KM, Bonomo RA. 2016. New β -lactamase inhibitors in the clinic. *Infect Dis Clin North Am* 30:441–464. <https://doi.org/10.1016/j.idc.2016.02.007>.
 44. King DT, Sobhanifar S, Strynadka NC. 2016. One ring to rule them all: current trends in combating bacterial resistance to the β -lactams. *Protein Sci* 25:787–803. <https://doi.org/10.1002/pro.2889>.
 45. Karlowsky JA, Biedenbach DJ, Kazmierczak KM, Stone GG, Sahn DF. 2016. Activity of ceftazidime-avibactam against extended-spectrum- and AmpC β -lactamase-producing *Enterobacteriaceae* collected in the IN-FORM Global Surveillance Study from 2012 to 2014. *Antimicrob Agents Chemother* 60:2849–2857. <https://doi.org/10.1128/AAC.02286-15>.
 46. Castanheira M, Mendes RE, Sader HS. 2017. Low frequency of ceftazidime-avibactam resistance among *Enterobacteriaceae* isolates carrying *bla*_{KPC} collected in U.S. hospitals from 2012 to 2015. *Antimicrob Agents Chemother* 61:e02369-16. <https://doi.org/10.1128/AAC.02369-16>.
 47. Linkevicius M, Sandegren L, Andersson DI. 2016. Potential of tetracycline resistance proteins to evolve tigecycline resistance. *Antimicrob Agents Chemother* 60:789–796. <https://doi.org/10.1128/AAC.02465-15>.
 48. Kaltenbach M, Emond S, Hollfelder F, Tokuriki N. 2016. Functional trade-offs in promiscuous enzymes cannot be explained by intrinsic mutational robustness of the native activity. *PLoS Genet* 12:e1006305. <https://doi.org/10.1371/journal.pgen.1006305>.
 49. Stojanovski V, Chow DC, Fryszyzyn B, Hu L, Nordmann P, Poirel L, Sankaran B, Prasad BV, Palzkill T. 2015. Structural basis for different substrate profiles of two closely related class D β -lactamases and their inhibition by halogens. *Biochemistry* 54:3370–3380. <https://doi.org/10.1021/acs.biochem.5b00298>.
 50. Lund BA, Thomassen AM, Carlsen TJO, Leiros H-KS. 2017. Structure, activity and thermostability investigations of OXA-163, OXA-181 and OXA-245 using biochemical analysis, crystal structures and differential scanning calorimetry analysis. *Acta Crystallogr F Struct Biol Commun* 73:579–587. <https://doi.org/10.1107/S2053230X17013838>.
 51. Borra PS, Leiros HK, Ahmad R, Spencer J, Leiros I, Walsh TR, Sundsfjord A, Samuelsen O. 2011. Structural and computational investigations of VIM-7: insights into the substrate specificity of VIM metallo- β -lactamases. *J Mol Biol* 411:174–189. <https://doi.org/10.1016/j.jmb.2011.05.035>.
 52. Leiros HK, Skagseth S, Edvardsen KS, Lorentzen MS, Bjerga GE, Leiros I, Samuelsen O. 2014. His224 alters the R2 drug binding site and Phe218 influences the catalytic efficiency of the metallo- β -lactamase VIM-7. *Antimicrob Agents Chemother* 58:4826–4836. <https://doi.org/10.1128/AAC.02735-13>.
 53. Imamovic L, Sommer MO. 2013. Use of collateral sensitivity networks to design drug cycling protocols that avoid resistance development. *Sci Transl Med* 5:204ra132. <https://doi.org/10.1126/scitranslmed.3006609>.
 54. Podnecky NL, Fredheim EGA, Kloos J, Sorum V, Primicerio R, Roberts AP, Rozen DE, Samuelsen O, Johnsen PJ. 2018. Conserved collateral antibiotic susceptibility networks in diverse clinical strains of *Escherichia coli*. *Nat Commun* 9:3673. <https://doi.org/10.1038/s41467-018-06143-y>.
 55. Roemhild R, Barbosa C, Beardmore RE, Jansen G, Schulenburg H. 2015. Temporal variation in antibiotic environments slows down resistance evolution in pathogenic *Pseudomonas aeruginosa*. *Evol Appl* 8:945–955. <https://doi.org/10.1111/eva.12330>.
 56. Gonzales PR, Pesesky MW, Bouley R, Ballard A, Bidy BA, Suckow MA, Wolter WR, Schroeder VA, Burnham CA, Mobashery S, Chang M, Dantas G. 2015. Synergistic, collaterally sensitive β -lactam combinations suppress resistance in MRSA. *Nat Chem Biol* 11:855–861. <https://doi.org/10.1038/nchembio.1911>.
 57. del Solar G, Espinosa M. 2000. Plasmid copy number control: an ever-growing story. *Mol Microbiol* 37:492–500.
 58. San Millan A, Escudero JA, Gifford DR, Mazel D, MacLean RC. 2016. Multicopy plasmids potentiate the evolution of antibiotic resistance in bacteria. *Nat Ecol Evol* 1:10. <https://doi.org/10.1038/s41559-016-0010>.
 59. Shields RK, Chen L, Cheng S, Chavda KD, Press EG, Snyder A, Pandey R, Doi Y, Kreiswirth BN, Nguyen MH, Clancy CJ. 2017. Emergence of ceftazidime-avibactam resistance due to plasmid-borne *bla*_{KPC-3} mutations during treatment of carbapenem-resistant *Klebsiella pneumoniae* infections. *Antimicrob Agents Chemother* 61:e02097-16. <https://doi.org/10.1128/AAC.02097-16>.
 60. Stewart A, Harris P, Henderson A, Paterson D. 2018. Treatment of infections by OXA-48-producing *Enterobacteriaceae*. *Antimicrob Agents Chemother* 62:e01195-18. <https://doi.org/10.1128/AAC.01195-18>.
 61. Samuelsen O, Naseer U, Karah N, Lindemann PC, Kanestrom A, Leegaard TM, Sundsfjord A. 2013. Identification of *Enterobacteriaceae* isolates with OXA-48 and coproduction of OXA-181 and NDM-1 in Norway. *J Antimicrob Chemother* 68:1682–1685. <https://doi.org/10.1093/jac/dkt058>.
 62. Samuelsen O, Overballe-Petersen S, Bjørnholt JV, Brisse S, Doumith M, Woodford N, Hopkins KL, Aasnaes B, Haldorsen B, Sundsfjord A, Norwegian Study Group on CPE. 2017. Molecular and epidemiological characterization of carbapenemase-producing *Enterobacteriaceae* in Norway, 2007 to 2014. *PLoS One* 12:e0187832. <https://doi.org/10.1371/journal.pone.0187832>.
 63. Tu Q, Yin J, Fu J, Herrmann J, Li Y, Yin Y, Stewart AF, Muller R, Zhang Y. 2016. Room temperature electrocompetent bacterial cells improve DNA transformation and recombineering efficiency. *Sci Rep* 6:24648. <https://doi.org/10.1038/srep24648>.
 64. Lund BA, Christopheit T, Guttormsen Y, Bayer A, Leiros HK. 2016. Screen-

- ing and design of inhibitor scaffolds for the antibiotic resistance oxacillinase-48 (OXA-48) through surface plasmon resonance screening. *J Med Chem* 59:5542–5554. <https://doi.org/10.1021/acs.jmedchem.6b00660>.
65. Lund BA, Leiros HK, Bjerga GE. 2014. A high-throughput, restriction-free cloning and screening strategy based on *ccdB*-gene replacement. *Microb Cell Fact* 13:38. <https://doi.org/10.1186/1475-2859-13-38>.
66. Kabsch W. 2010. XDS. *Acta Crystallogr D Biol Crystallogr* 66:125–132. <https://doi.org/10.1107/S09074449100047337>.
67. Evans PR, Murshudov GN. 2013. How good are my data and what is the resolution? *Acta Crystallogr D Biol Crystallogr* 69:1204–1214. <https://doi.org/10.1107/S0907444913000061>.
68. Akhter S, Lund BA, Ismael A, Langer M, Isaksson J, Christopheit T, Leiros H-KS, Bayer A. 2018. A focused fragment library targeting the antibiotic resistance enzyme—oxacillinase-48: synthesis, structural evaluation and inhibitor design. *Eur J Med Chem* 145:634–648. <https://doi.org/10.1016/j.ejmech.2017.12.085>.
69. Adams PD, Afonine PV, Bunkoczi G, Chen VB, Davis IW, Echols N, Headd JJ, Hung LW, Kapral GJ, Grosse-Kunstleve RW, McCoy AJ, Moriarty NW, Oeffner R, Read RJ, Richardson DC, Richardson JS, Terwilliger TC, Zwart PH. 2010. PHENIX: a comprehensive Python-based system for macromolecular structure solution. *Acta Crystallogr D Biol Crystallogr* 66:213–221. <https://doi.org/10.1107/S0907444909052925>.
70. Emsley P, Lohkamp B, Scott WG, Cowtan K. 2010. Features and development of Coot. *Acta Crystallogr D Biol Crystallogr* 66:486–501. <https://doi.org/10.1107/S0907444910007493>.
71. Waterhouse A, Bertoni M, Bienert S, Studer G, Tauriello G, Gumienny R, Heer FT, de Beer TAP, Rempfer C, Bordoli L, Lepore R, Schwede T. 2018. SWISS-MODEL: homology modelling of protein structures and complexes. *Nucleic Acids Res* 46:W296–W303. <https://doi.org/10.1093/nar/gky427>.
72. Lenski RE. 2017. Convergence and divergence in a long-term experiment with bacteria. *Am Nat* 190:S57–S68. <https://doi.org/10.1086/691209>.
73. Alikhan NF, Petty NK, Ben Zakour NL, Beatson SA. 2011. BLAST Ring Image Generator (BRIG): simple prokaryote genome comparisons. *BMC Genomics* 12:402. <https://doi.org/10.1186/1471-2164-12-402>.

Appendix: Paper II



Cryptic β -Lactamase Evolution Is Driven by Low β -Lactam Concentrations

 Christopher Fröhlich,^a  João A. Gama,^b  Klaus Harms,^b  Viivi H. A. Hirvonen,^c  Bjarte A. Lund,^d  Marc W. van der Kamp,^c
 Pål J. Johnsen,^b  Ørjan Samuelsen,^{b,e}  Hanna-Kirsti S. Leiros^a

^aThe Norwegian Structural Biology Centre (NorStruct), Department of Chemistry, UiT The Arctic University of Norway, Tromsø, Norway

^bDepartment of Pharmacy, UiT The Arctic University of Norway, Tromsø, Norway

^cSchool of Biochemistry, University of Bristol, Bristol, United Kingdom

^dHylleraas Centre for Quantum Molecular Sciences, Department of Chemistry, UiT The Arctic University of Norway, Tromsø, Norway

^eNorwegian National Advisory Unit on Detection of Antimicrobial Resistance, Department of Microbiology and Infection Control, University Hospital of North Norway, Tromsø, Norway

Ørjan Samuelsen and Hanna-Kirsti S. Leiros contributed equally.

ABSTRACT Our current understanding of how low antibiotic concentrations shape the evolution of contemporary β -lactamases is limited. Using the widespread carbapenemase OXA-48, we tested the long-standing hypothesis that selective compartments with low antibiotic concentrations cause standing genetic diversity that could act as a gateway to developing clinical resistance. Here, we subjected *Escherichia coli* expressing *bla*_{OXA-48} on a clinical plasmid, to experimental evolution at sub-MICs of ceftazidime. We identified and characterized seven single variants of OXA-48. Susceptibility profiles and dose-response curves showed that they increased resistance only marginally. However, in competition experiments at sub-MICs of ceftazidime, they demonstrated strong selectable fitness benefits. Increased resistance was also reflected in elevated catalytic efficiencies toward ceftazidime. These changes are likely caused by enhanced flexibility of the Ω - and β 5- β 6 loops and fine-tuning of preexisting active site residues. In conclusion, low-level concentrations of β -lactams can drive the evolution of β -lactamases through cryptic phenotypes which may act as stepping-stones toward clinical resistance.

IMPORTANCE Very low antibiotic concentrations have been shown to drive the evolution of antimicrobial resistance. While substantial progress has been made to understand the driving role of low concentrations during resistance development for different antimicrobial classes, the importance of β -lactams, the most commonly used antibiotics, is still poorly studied. Here, we shed light on the evolutionary impact of low β -lactam concentrations on the widespread β -lactamase OXA-48. Our data indicate that the exposure to β -lactams at very low concentrations enhances β -lactamase diversity and drives the evolution of β -lactamases by significantly influencing their substrate specificity. Thus, in contrast to high concentrations, low levels of these drugs may substantially contribute to the diversification and divergent evolution of these enzymes, providing a standing genetic diversity that can be selected and mobilized when antibiotic pressure increases.

KEYWORDS OXA-48, ceftazidime, resistance development, cryptic evolution, *Escherichia coli*, carbapenemase, carbapenem, sub-MIC, structural flexibility, catalytic efficiency


Since the discovery of the first β -lactam, penicillin, this antimicrobial class has diversified into a broad range of agents, and it remains the most widely used class of antimicrobials worldwide (1). The extensive use of these agents has inevitably led to the selection of

Citation Fröhlich C, Gama JA, Harms K, Hirvonen VHA, Lund BA, van der Kamp MW, Johnsen PJ, Samuelsen Ø, Leiros H-KS. 2021. Cryptic β -lactamase evolution is driven by low β -lactam concentrations. *mSphere* 6:e00108-21. <https://doi.org/10.1128/mSphere.00108-21>.

Editor Patricia A. Bradford, Antimicrobial Development Specialists, LLC

Copyright © 2021 Fröhlich et al. This is an open-access article distributed under the terms of the [Creative Commons Attribution 4.0 International license](https://creativecommons.org/licenses/by/4.0/).

Address correspondence to Christopher Fröhlich, christofrohlich@gmail.com, or Hanna-Kirsti S. Leiros, hanna-kirsti.leiros@uit.no.

 How do very low β -lactam concentrations shape the evolution of β -lactamases? Check out the newest paper of @chrfrohlich et al. exposing OXA-48 to sub-MIC of ceftazidime to understand the underlying evolutionary and structural consequences of adaptation.

Received 3 February 2021

Accepted 2 April 2021

Published 28 April 2021

multiple resistance mechanisms where the expression of β -lactamase enzymes plays a major role, particularly in Gram-negative bacteria (2). Consequently, β -lactamases are arguably among the most-studied enzymes worldwide. Considerable progress has been made in understanding their molecular epidemiology and biochemical properties (3, 4). The evolutionary forces driving the diversification of these enzymes are, however, poorly understood. Already, more than 20 years ago, it was proposed that suboptimal antibiotic concentrations within the host fuel the evolution of β -lactamases, altering their substrate profiles (5–8). This “compartment hypothesis” was later supported by a series of studies unequivocally demonstrating that selection for antibiotic resistance determinants can occur at very low antibiotic concentrations (9–11). These low concentrations are thus widening the window in which selection can take place (12). Despite their clinical significance, few studies have investigated the effects of sub-MICs of β -lactams on the evolution and selection of contemporary, globally circulating β -lactamases (5, 13, 14).

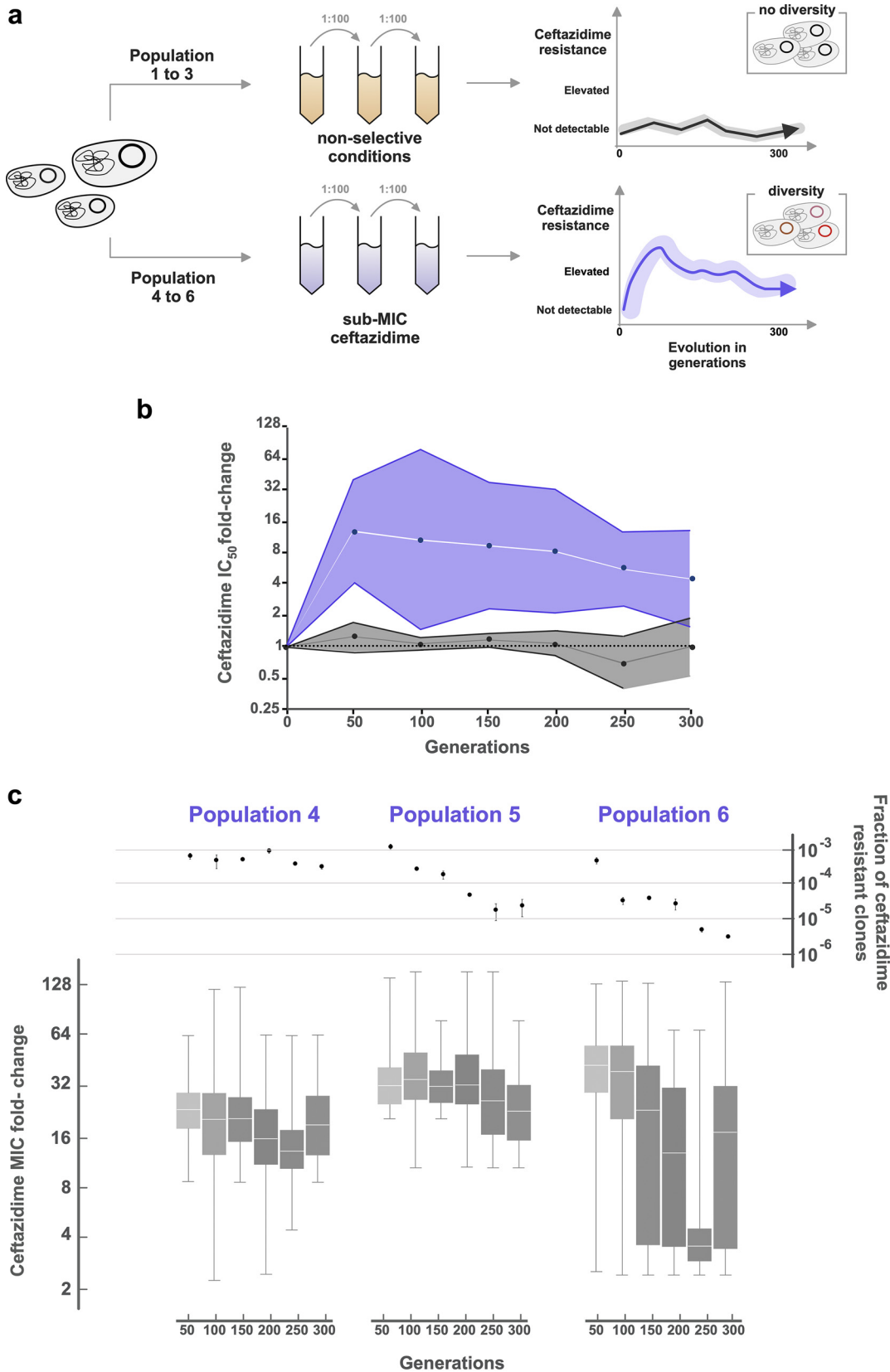
Within the last decade, OXA-48 has become one of the most widespread serine β -lactamases. This Ambler class D β -lactamase confers resistance toward penicillins and decreases susceptibility to our last-resort drugs, the carbapenems. However, it is a poor hydrolyzer of extended-spectrum cephalosporins, including ceftazidime (15–17). Despite that, naturally occurring OXA-48-like variants have been identified exhibiting increased ceftazidime activity but antagonistic pleiotropy toward penicillins and carbapenems (e.g., OXA-163, OXA-247, and OXA-405) (18–20). Ceftazidime resistance development in these variants was mostly due to single amino acid changes and a shortened β 5- β 6 loop (4, 18–21). We previously showed that exposure to increasing concentrations of ceftazidime can select for this latent ceftazidimase function of OXA-48 in the laboratory (17).

To test the long-standing hypothesis, that β -lactams at sub-MICs can drive the evolution of these enzymes, we subjected *Escherichia coli* MG1655 expressing OXA-48 to concentrations of ceftazidime below the MIC ($0.25 \times$ MIC). Over the course of 300 generations, we identified seven single variants of OXA-48 (L67F, P68S, F72L, F156C/V, L158P, and G160C). Their ceftazidime MICs were indistinguishable or only marginally increased compared to wild-type OXA-48. However, when expressed at sub-MICs of ceftazidime, all allele variants conferred strong fitness benefits. Measuring dose-response curves (50% inhibitory concentration [IC_{50}]) and enzyme kinetics revealed further that (i) all genotypes decreased ceftazidime susceptibility significantly and (ii) all enzyme variants exhibited increased catalytic efficiencies against ceftazidime. Molecular dynamics (MD) simulations of P68S, F72L, and L158P showed elevated flexibility of both the Ω (D143 to I164) and β 5- β 6 (T213 to K218) loops likely to aid hydrolysis of the bulkier ceftazidime by increasing active site accessibility. Structural investigations of L67F also revealed a novel binding pocket outside of the active site where the β 5- β 6 loop was involved in stabilizing the binding of the hydrolyzed ceftazidime molecule. Worryingly, double mutants, such as F72I/G131S (OXA-D320, GenBank accession no. [KJ620465](https://www.ncbi.nlm.nih.gov/nuccore/KJ620465)) and N146S/L158P (OXA-D319, GenBank accession no. [KJ620462](https://www.ncbi.nlm.nih.gov/nuccore/KJ620462)), were recently identified in environmental samples (22, 23), underlining the importance and evolutionary power of environments with low selective pressure.

RESULTS

Sub-MICs of ceftazidime select for high-level resistance. Here, we wanted to study the evolvability of the carbapenemase OXA-48 under sub-MICs of the cephalosporin ceftazidime. OXA-48 does not hydrolyze ceftazidime efficiently (19). However, we recently showed that the exposure to increasing concentrations of ceftazidime can select for OXA-48 variants with elevated activity toward ceftazidime (17). We used the previously constructed *E. coli* MG1655 (Table S1, MP13-06) (17) carrying a globally disseminated IncI plasmid with *bla*_{OXA-48} as the only antibiotic resistance gene. MP13-06 was evolved without selection pressure and at one quarter of the ceftazidime MIC (0.06 mg/liter), resulting in the populations 1 to 3 (Pop1 to 3) and 4 to 6 (Pop4 to 6), respectively (Fig. 1a).

To elucidate the effect of ceftazidime, we measured dose-response curves of the whole evolved populations and calculated the ceftazidime concentrations inhibiting



50% of cell growth (IC_{50}). In Pop1 to 3, evolution without selection pressure did not result in altered ceftazidime susceptibility (Fig. 1b). In contrast, under ceftazidime selection (Pop4 to 6), susceptibility decreased on average 16-fold already after 50 generations (Fig. 1b). We observed that, during the course of experimental evolution, the susceptibilities of Pop4 to 6 shifted toward lower ceftazidime resistance (Fig. 1b).

From the evolved populations, we measured the fraction of clones exhibiting a clinically significant MIC change (>2-fold) by nonselective and selective plating on 1 mg/liter ceftazidime. No clones were identified during selection-free evolution above the detection limit (10^{-7} of the population). Under sub-MIC conditions, we found a significant fraction of the populations to be able to grow on ceftazidime containing plates (Fig. 1c). While this fraction was stably maintained in Pop4, we found that Pop5 and Pop6 showed a significant reduction over time (Pearson correlation, $P=0.54$, $P=0.01$, $P=0.03$).

To determine the MIC distribution of clones with increased MICs, we selected approximately 50 colonies every 50th generation from the selective plates and tested their susceptibility to ceftazidime (Fig. 1c). All preselected clones displayed a MIC increase ranging from 2- to 128-fold. For Pop 4 to 6, we found that on average, 11%, 28%, and 34% of the tested colonies exhibited MIC values above the clinical resistance breakpoint of 4 mg/liter, respectively (EUCAST breakpoint table v. 10.0). These results are consistent with recent reports demonstrating that low-level concentrations of antibiotics facilitate the selection of high-level resistance (9, 11).

Sub-MIC evolution selects for beneficial single point mutations in *bla*_{OXA-48}. To understand the effect of sub-MIC exposure on OXA-48, we sequenced the *bla*_{OXA-48} gene of approximately 50 clones after 50 and 300 generations, which were preselected on agar plates containing 1 mg/liter ceftazidime. In total, seven single variants of OXA-48 were identified: L67F, P68S, F72L, F156C, F156V, L158P, and G160C. The relative frequency of these variants varied among populations and generations (Fig. 2a). Interestingly, double mutants with similar (F72L/G131S) or identical (N146S/L158P) amino acid changes have been already reported in environmental samples (23). To elucidate the effect of these second mutations, we constructed the OXA-48 double mutants F72L/G131S (instead of F72L) and N146S/L158P and included them in the following characterization.

To isolate the effects of OXA-48 on antimicrobial susceptibility, we subcloned all allele variants into a high copy number vector (pCR-Blunt II-TOPO) and expressed them in *E. coli* TOP10 (Table 1). As previously shown (17), the expression of OXA-48 resulted in up to 32- and 64-fold increased MIC toward penicillins and carbapenems (except for doripenem), respectively. While wild-type OXA-48 expression did not increase the MIC against cephalosporins (<2-fold), we found that P68S, F72L, L158P, and N146S/L158P resulted in 4- to 16-fold increased MIC against ceftazidime. Interestingly, the expression of all other alleles (L67F, F156C/V, G160C, F72L/G131S) did not increase the ceftazidime MIC significantly (i.e., not more than 2-fold compared to wild-type OXA-48). In addition, none of the alleles showed a significant effect on cephalosporins other than ceftazidime (Table 1). In contrast, the susceptibility to carbapenems and penicillins was increased by 2- to ≥ 64 -fold for all the variants. The expression of F156C and G160C did not increase the MIC to any β -lactam. In clinical strains, *bla*_{OXA-48} is frequently located on IncL plasmids, which are typically present in low copy numbers (24). To mimic this situation, we subcloned all OXA-48 alleles into a low copy number vector (p15A origin, here called pUN), expressed these in *E. coli* MG1655, and repeated the ceftazidime MIC measurements. Within this more realistic genetic architecture, only F156V increased the ceftazidime MIC by more than 2-fold (Table 2).

Clinically insignificant or marginal changes in MICs have been reported to still confer high fitness benefits in the presence of low-level selection (5). To address this, we first increased the resolution of the susceptibility testing by measuring the dose-response curves in the low copy number vector. Calculating their corresponding IC_{50} values, we found that all variants conferred marginal but significant decreases in

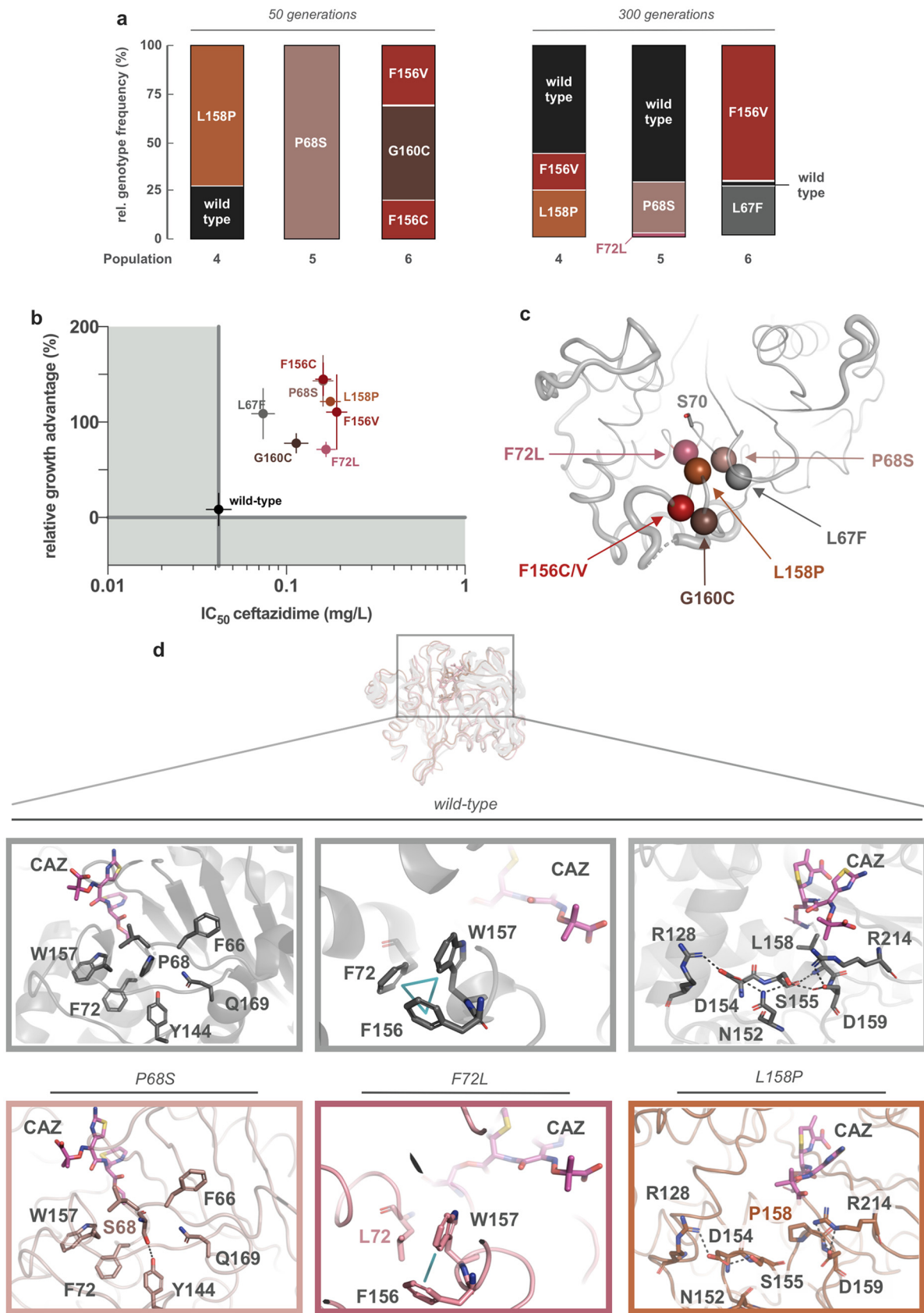


FIG 2 Phenotypic and structural investigation of OXA-48 allele variants. (a) Relative genotype frequencies of *bla*_{OXA-48} variants within Pop4 to 6, at 50 and 300 generations. (b) Relative growth advantage of OXA-48 variants expressed at sub-MICs of ceftazidime versus their (Continued on next page)

TABLE 1 MIC of OXA-48 and allele variants expressed in the high copy number vector pCR-Blunt II-TOPO in *E. coli* TOP10

Antimicrobial agent(s) ^a	MICs (mg/liter) for:											
	MP13-11										MP13-33	MP13-20
	MP13-04	wild-type OXA-48	MP13-21 L67F	MP13-16 P68S	MP13-14 F72L	MP13-17 F156C	MP13-18 F156V	MP13-15 L158P	MP13-19 G160C	MP13-33 F72L/G131S	MP13-20 N146S/L158P	
Temocillin	16	256	64	64	64	16	16	64	16	16	32	
Piperacillin-tazobactam	2	64	2	2	2	2	2	2	2	2	2	
Amoxicillin-clavulanic acid	4	128	128	64	64	16	64	16	8	8	8	
Ceftazidime	0.5	0.5	1	8	4	0.5	0.5	8	0.5	0.5	2	
Ceftazidime-avibactam	0.25	0.25	0.5	0.25	0.5	0.5	0.5	0.5	0.5	0.25	0.5	
Cefuroxime	16	16	8	16	8	8	8	8	8	16	8	
Cefepime	0.06	0.12	0.06	0.12	0.12	0.06	0.06	0.25	0.06	0.06	0.12	
Cefotaxime	0.12	0.25	0.12	0.12	0.12	0.12	0.12	0.25	0.12	0.25	0.12	
Meropenem	0.03	0.25	0.12	0.03	0.03	0.03	0.03	0.03	0.03	0.03	0.03	
Imipenem	0.25	1	0.25	0.25	0.25	0.25	0.25	0.25	0.25	0.25	0.5	
Ertapenem	0.015	1	0.12	0.03	0.03	0.015	0.015	0.06	0.015	0.015	0.015	
Doripenem	0.03	0.03	0.03	0.03	0.06	0.03	0.03	0.06	0.03	0.06	0.06	

^aTazobactam fixed at 4 μg/ml; clavulanic acid fixed at 2 μg/ml; avibactam fixed at 4 μg/ml.

ceftazidime susceptibility (Fig. 2b and Table 2; analysis of variance [ANOVA], $df = 10$, $P < 0.0001$, followed by a Dunnett *post hoc* test with OXA-48 as the control group).

Second, we performed head-to-head competitions between isogenic *E. coli* MG1655 strains (only differing in $\Delta malF$) to test the fitness effect of OXA-48 variants in the absence and presence of sub-MIC ceftazidime. To exclude an effect of the *malF* deletion on the bacterial fitness, we initially competed the strains both carrying the pUN vector encoding wild-type *bla*_{OXA-48} (MP08-61 and MP14-24). No significant change in bacterial fitness was observed in either condition (Welch *t*-test, $P = 0.24$ and $P = 0.48$), ruling out a detectable effect of the *malF* deletion. Next, we expressed all OXA-48 variants in MP14-23 and subjected those to competitions against MP08-61. Without ceftazidime, no difference in fitness was observed between variants and wild type (Fig. 3a; ANOVA, not assuming equal variances, $df = 7$, $P = 0.33$). However, at sub-MIC ceftazidime, all allele variants showed strong significant growth benefits (Fig. 2b and 3a; ANOVA, not assuming equal variances, $df = 7$, $P = 0.0003$, followed by a Dunnett *post hoc* test with OXA-48 as the control group).

Two mutational targets identified in our study (F72L and L158P) were recently isolated from the environment, in combination with a second amino acid substitution (23). We aimed to elucidate the effect of G131S and N146S in combination with F72L and L158P, respectively. To do so, we competed F72L and L158P against the double mutants F72L/G131S and N146S/L158P, respectively. No significant change in fitness was detectable in the absence of selection pressure (Fig. 3b; Welch *t*-test, $P = 0.24$ and 0.62 for F72L/G131S and N146S/L158P, respectively). At sub-MIC ceftazidime, our data suggest no positive selection for the double mutants (Fig. 3b; paired Welch *t*-test between conditions, $P = 0.038$ and 0.59 for F72L/G131S and N146S/L158P, respectively). Thus, the role of these second mutations remains unclear.

Mutations within *bla*_{OXA-48} alter enzymatic properties. In this study, sub-MIC levels of ceftazidime were shown to select for OXA-48 variants conferring high bacterial fitness advantages despite only cryptic resistance phenotypes, suggesting that, in the clinical setting, these genetic changes are likely to remain undetected. To further our understanding of how these cryptic changes influence the enzymatic properties of OXA-48, we expressed the enzymes without their leader sequence in *E. coli* BL21 AI (Table S1). After enzyme purification,

FIG 2 Legend (Continued)

ceftazidime IC₅₀. Despite marginal changes in their ceftazidime susceptibility (IC₅₀ increased by 2- to 4-fold), the expression of these alleles displays large fitness benefits at sub-MIC ceftazidime. Error bars represent the standard deviation. (c) Ribbon structure of OXA-48 including the amino acid changes close to the active site. (d) Representative structures from molecular dynamics simulations of wild type, P68S, F72L, and L158P performed with ceftazidime covalently bound to the active site S70. In short, S68 in P68S displays an H-bond with the tyrosine in the conserved Y¹⁴⁴GN motif of OXA-48. F72L lacks the aromatic stacking interaction between F72 and F156/W157. L158P disrupts the H-bond network within the Ω-loop.

TABLE 2 Ceftazidime susceptibility (MIC and IC₅₀) measurements of OXA-48 and variants expressed from the low copy number vector pUN in *E. coli* MG1655 Δ*malF* (MP14-23)^a

		Data for:										
		MP14-24 wild-type										
Measurement	MP14-23	MP14-29 L67F	MP14-26 P68S	MP14-27 F72L	MP14-30 F156C	MP14-31 F156V	MP14-25 L158P	MP14-28 G160C	MP14-32 F72L/ G131S	MP14-33 N146S/ L158P		
MIC (mg/liter)	0.5	0.5	1	1	1	2	1	0.5	0.5	1		
IC ₅₀ (mg/liter)	0.045	0.074	0.160	0.167	0.161	0.191	0.176	0.114	0.078	0.220		
CI95%	0.033–0.061	0.057–0.096	0.128–0.201	0.136–0.205	0.135–0.192	0.153–0.239	0.142–0.219	0.087–0.148	0.062–0.097	0.164–0.295		

^aSusceptibility was determined based on a minimum of 2 biological replicates. The 95% confidence intervals (CI95%) were calculated for the IC₅₀ values.

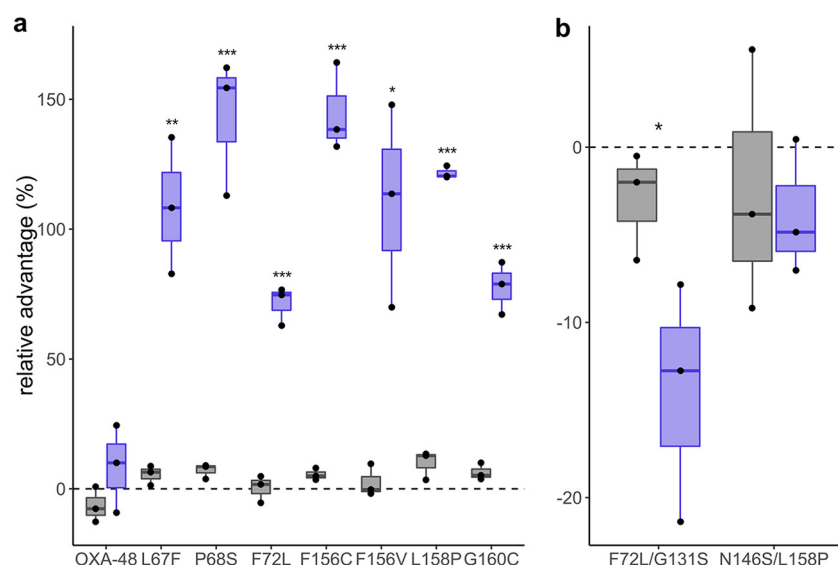


FIG 3 Head-to-head competitions. (a) *E. coli* MG1655 *mal*⁺ competed with MG1655 Δ *malF* expressing wild-type and allele variants of OXA-48, respectively, without (gray) and at sub-MICs (violet) of ceftazidime. While expression without selection pressure was neutral for all alleles, at sub-MICs, all allele variants showed fitness benefits over the wild-type allele. (b) *E. coli* MG1655 *mal*⁺ expressing F72L versus Δ *malF* F72L/G131S and *mal*⁺ L158P versus Δ *malF* N146S/L158P. G131S and N146S did not improve bacterial fitness at sub-MIC ceftazidime. The dots represent biological replicates, and significantly different averages compared to OXA-48 in the presence of ceftazidime (0.06 mg/liter) are marked with * ($P < 0.05$), ** ($P < 0.01$), and *** ($P < 0.001$).

protein masses were verified using electrospray ionization mass spectrometry (ESI-MS). The molecular weight of five out of seven variants corresponded to their calculated monoisotopic masses (Table 3). For F156C and G160C, we observed an increase in molecular weight by 76 Da, likely caused by the β -mercaptoethanol used during the purification process to minimize aggregation.

We determined their catalytic efficiencies (k_{cat}/K_m) toward a panel of β -lactams and found that they were in line with the antimicrobial susceptibility data. Toward ceftazidime, k_{cat}/K_m values were increased by 2- to 31-fold (Table 3) for all variants compared to wild-type OXA-48. Moreover, all variants exhibited strongly reduced activity (up to several magnitudes) against penicillins (ampicillin and piperacillin) as well as toward carbapenems (meropenem and imipenem). To test for cross-activity against 4th-generation cephalosporins, we determined

TABLE 3 Overview of enzyme kinetic values, molecular weight, and thermal stability of OXA-48 and variants

OXA-48 variant	Calculated mol wt (Da) ^a	Measured mol wt (Da) ^a	Thermostability (°C) ^b	k_{cat}/K_m (mM ⁻¹ s ⁻¹) for: ^c					
				Ampicillin	Piperacillin	Ceftazidime	Cefepime ^f	Imipenem	Meropenem
Wild type	28,186.3	28,186.5	55.9	5.56×10^3	2.26×10^3	3.4×10^{-1}	1.20×10^{-1}	1.05×10^2	4.58×10^1
L67F	28,220.3	28,220.4	51.4	4.66×10^2	7.80×10^0	9.4×10^{-1}	1.68×10^{-2}	6.38×10^0	7.81×10^{-1}
P68S	28,176.3	28,176.3	48.3	1.80×10^2	1.48×10^1	1.6×10^0	9.12×10^{-2}	3.56×10^0	3.20×10^0
F72L	28,152.3	28,151.5	49.2	1.44×10^2	1.35×10^1	1.1×10^1	8.81×10^{-3}	3.38×10^0	4.47×10^0
F156C ^d	28,142.3	28,218.3	50.7	2.24×10^2	9.39×10^0	1.5×10^0	2.42×10^{-2}	8.17×10^{-2}	6.54×10^{-2}
F156V	28,138.3	28,138.5	50.2	1.18×10^2	9.03×10^0	1.5×10^0	3.35×10^{-2}	2.85×10^0	6.10×10^{-1}
L158P	28,170.3	28,170.5	50.3	2.37×10^2	2.69×10^1	6.7×10^{-1}	ND	1.38×10^0	4.56×10^{-1}
G160C ^d	28,232.3	28,308.3	48.4	2.24×10^2	1.40×10^1	3.6×10^0	1.27×10^{-1}	4.36×10^0	6.52×10^0
F72L/G131S ^e	28,182.3	28,182.0	45.2	1.46×10^2	3.07×10^1	5.9×10^{-1}	1.27×10^{-1}	2.03×10^0	8.94×10^0
N146S/ L158P ^e	28,143.3	28,142.0	50.7	2.05×10^2	2.87×10^1	6.9×10^1	ND	3.02×10^{-1}	5.76×10^{-1}

^aMonoisotopic mass after TEV cleavage.

^bMeasured as thermostability.

^cMichaelis-Menten kinetics could not be saturated for most of the variants; therefore, only k_{cat}/K_m values were reported.

^dPurified in the presence of β -mercaptoethanol to minimize aggregation.

^eSecond mutations (G131S and N146S) described in environmental samples.

^fND, no activity detected.

the catalytic efficiencies against ceftapime. Also, here, we found that the OXA-48 variants tended to display k_{cat}/K_m values several magnitudes lower than the wild-type OXA-48 (Table 3).

Functional mutations within serine β -lactamases have frequently been described to decrease the thermostability (17, 25, 26). Indeed, compared to wild-type OXA-48, all single amino acid changes were deleterious with respect to thermostability, which decreased by 4.5 to 7.6°C (Table 3). F72L/G131S exhibited the lowest melting temperature, with a decrease of 10.7°C. Generally, we found the following order for the thermal stability OXA-48 > L67F > F156C = N146S/L158P > L158P = F156V > F72L > G160C = P68S > F72L/G131S.

P68S, F72L, and L158P increase the loop flexibility within OXA-48. Single amino acid changes in OXA-48 were responsible for increased catalytic activity against ceftazidime. To understand the underlying structural changes allowing these OXA-48 variants to hydrolyze ceftazidime more efficiently, we first mapped all amino acid changes onto the structure of OXA-48, showing that they clustered around the α 3-helix (L67F, P68S, and F72L) and the Ω -loop (F156C, F156V, L158P, and G160C) (Fig. 2c). Second, multiple independent MD simulations were performed on a subset of variants (P68S, F72L, and L158P) with covalently bound ceftazidime in their active site. Our previous study showed that an amino acid change at position 68 (P68A) decreases ceftazidime susceptibility in OXA-48 (17). Additionally, positions 72 and 158 were selected due to amino acid changes recently identified in environmental samples (F72I and L158P). Changes in enzyme flexibility were analyzed by calculating root mean square fluctuations (RMSF) for the backbone atoms in the Ω - and β 5- β 6 loops and compared to wild-type OXA-48 and the ceftazidimase OXA-163 (only Ω -loop, due to the shortened β 5- β 6 loop).

For the Ω -loop, P68S displayed very similar RMSF values relative to OXA-48; however, F72L and L158P showed increased flexibility in this region, displaying even higher RMSF values than OXA-163 (Fig. 4a). Notably, the L158P substitution increased fluctuations specifically for residues N152 to S155. V153 demonstrated the largest overall shift in RMSF values, with an increase of 0.7 Å compared to OXA-48. For the β 5- β 6 loop, all variants exhibited an increase in fluctuations, especially for the residues T213 to E216 (Fig. 4b).

Possible changes in intramolecular interactions due to the amino acid changes P68S, F72L, and L158P were also studied from MD simulations. For P68S, an H-bond was observed between the hydroxyl groups of S68 and Y144 (Fig. 2d). However, no other apparent structural changes near the active site were directly observed, and therefore, the effect of P68S on the dynamic nature remains elusive.

In wild-type OXA-48, W157 in the Ω -loop stacks with both F72 and F156 (Fig. 2d). Consequently, the lack of this interaction in F72L likely increases the flexibility of W157, which is reflected by a 0.2-Å increase in calculated RMSF (Fig. 4a). Furthermore, the wild-type Ω -loop displays an organized H-bond network, which extends to R128 and R214 on either side (Fig. 2d). We found that L158P is likely affecting this network by disrupting the interactions with S155 and D159 (Fig. 2d). Consequently, the salt bridge between R128 and D154 was found to be weakened, as its presence was reduced from 87% to 43% of the simulation time. The loss of the backbone H-bond between L158 and S155, in the proline variant (L158P), has a knock-on effect on the rest of the loop, making it more flexible and likely to better accommodate bulkier β -lactam substrates such as ceftazidime.

Aside from flexibility and changes in amino acid interactions, possible further effects on the overall enzyme dynamics were inspected by performing principal component (PC) analysis on the combined MD trajectories (using the $C\alpha$ -atom positions). The overall sampling of conformational space is highly similar for OXA-48 and the three variants. There are no specific large conformational changes or coordinated loop movements induced by the mutations. Some differences between variants and wild-type OXA-48 were observed particularly for PCs that primarily involve movement of

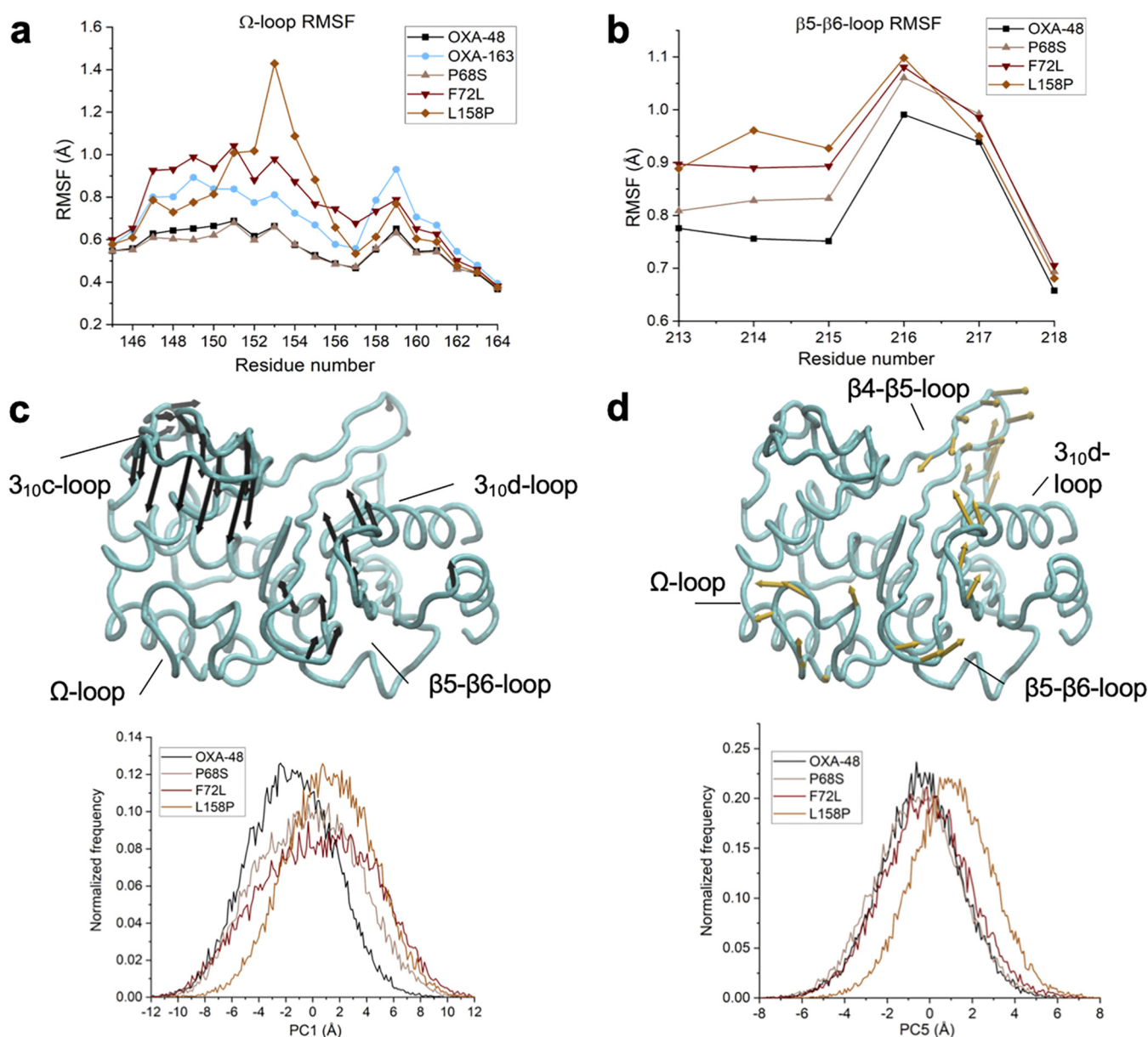


FIG 4 Differences in dynamics between wild-type OXA-48 and variants P68S, F72L, and L158P (as well as OXA-163). Loop flexibility as measured by backbone root mean square fluctuations (RMSFs) from molecular dynamics simulations for residues in the Ω -loop (a) and in the β 5- β 6 loop (b). Principal component (PC) analysis of the C_{α} atoms from molecular dynamics simulations of OXA-48 and the P68S, F72L, and L158P variants, with PC1 (c, top) and PC5 (d, top) illustrated on ribbon structures using arrows indicating the direction of the eigenvectors and the magnitude of the corresponding eigenvalue (for clarity, arrows are only shown for atoms with eigenvalues of >2.5 Å). Normalized histograms (using 200 bins per enzyme) for PC1 (c, bottom) and PC5 (d, bottom) indicate differences of the range of the PC sampled in different variants.

loops, including those surrounding the active site, further indicating that the mutations introduce small changes in loop dynamics (Fig. 4c and d).

Cryptic binding pocket for ceftazidime in OXA-48. To investigate substrate binding, all OXA-48 variants were crystallized and soaked with ceftazidime. We were able to solve the crystal structure of L67F to 1.9 Å with four chains (A to D) in the asymmetric unit (space group $P2_12_12_1$), which were arranged into two dimers (chains A/C and B/D). Chain C and D carried a hydrolyzed ceftazidime molecule approximately 9 Å away from the active site S70. The R1-group of ceftazidime including the dihydrothiazine ring demonstrated clear electron density (2Fo-Fc); however, no electron density was observed for the R2-ring (Fig. 5, top).

We first investigated the binding of ceftazidime to the L67F variant. Here, we found that Q98, R100, D101, W105, V120, P121, Q124, L158, T213, and R214 formed a cryptic

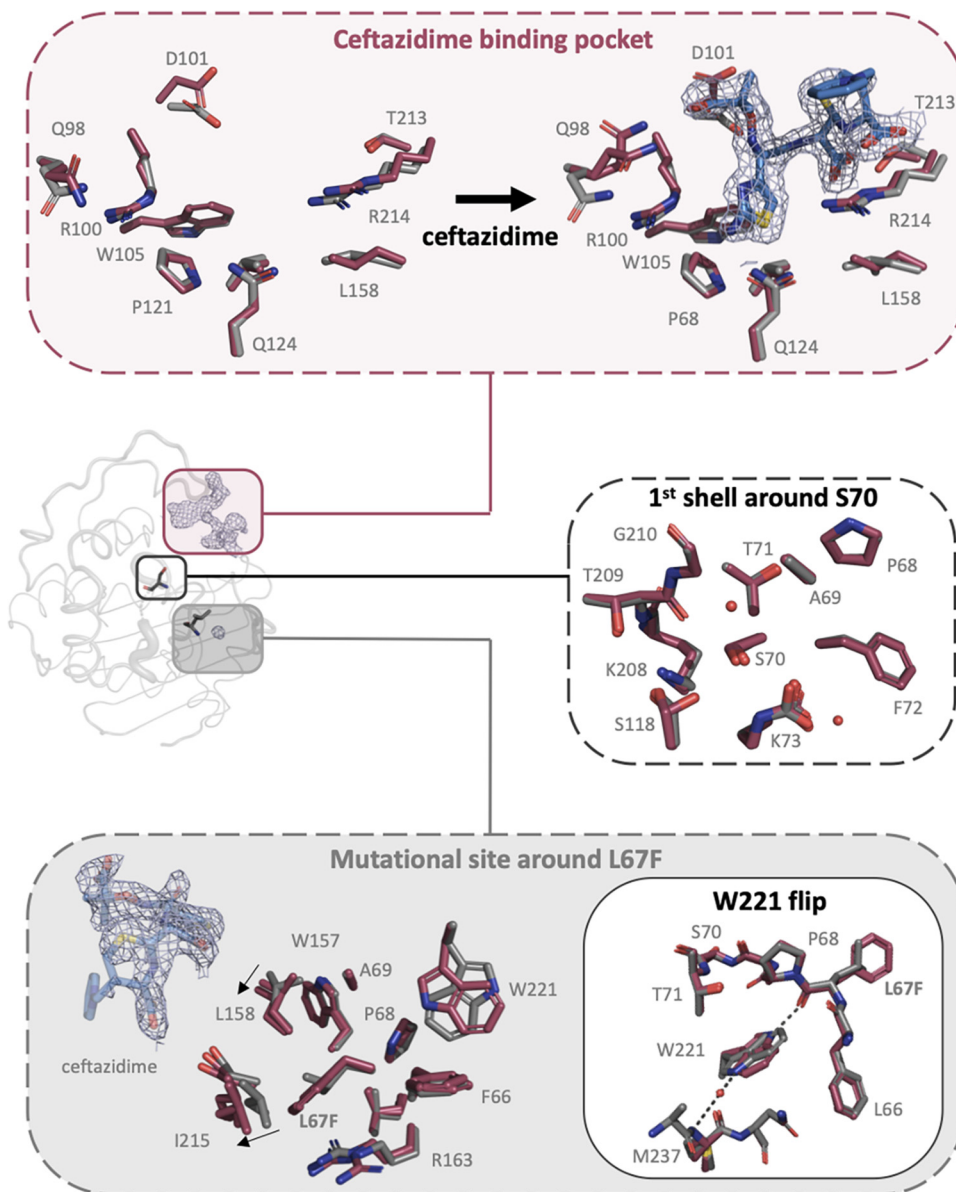


FIG 5 Ceftazidime binding pocket (top panel), the 1st shell residues interacting with S70 (middle) and the mutational site (bottom panel) of L67F (red) compared to the wild-type structure of OXA-48, shown in gray (PDB no. 3HBR) (15). The crystal structure of L67F was solved to 1.9 Å and displayed hydrolyzed ceftazidime ~9 Å away from the active site S70. (Top) Binding pocket of L67F without (left, chain C) and with (right, chain A) ceftazidime compared to wild-type OXA-48. For ceftazidime, no 2Fo-Fc electron density was detected for the R2 group. (Middle) Superimposition of the first shell residues of L67F (chain A) around the active site S70 compared the wild-type structure. (Bottom) Investigation of the mutational site, shown as the first shell residues around L67F (both chain A and C), compared to wild-type OXA-48. Displacements of L158 (1 Å) and I215 (2 Å) in the L67F structure are indicated with arrows. W221 was flipped 180° in the L67F structure.

pocket outside the active side and that these residues were involved in stabilizing the hydrolyzed ceftazidime molecule (Fig. 5, top). D101, Q124, T213, and R214 were found to interact with ceftazidime via H-bonds. R214 was further involved in ionic interactions with two of the carboxylic acid groups of hydrolyzed ceftazidime (Fig. 6).

Second, we investigated the active site architecture, including the first shell residues around S70. Chain A was therefore superimposed onto a wild-type structure of OXA-48 (PDB no. 3HBR) (15). As expected, superimposition resulted in low root mean square deviations of 0.21 Å. We found that K73 was carboxylated and that all first shell residues nicely aligned with the wild-type structure (Fig. 5, middle).

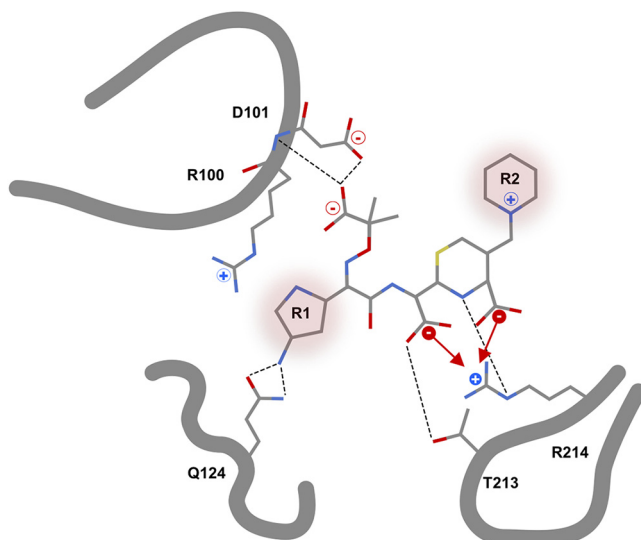


FIG 6 Schematic representation of hydrolyzed ceftazidime in front of the active site of the OXA-48 variant L67F (based on PDB no. 7ASS). The ceftazidime side chains R1 and R2 are labeled and marked. For R2, no electron density was observed and therefore no interactions were detected. Hydrogen bonds from ceftazidime to D101, Q124, T213, and R214 are represented with dashed lines. The ionic interactions with R214 are indicated with arrows.

Third, we investigated the mutational site around L67F that is located “below” the active site (Fig. 5, bottom). We found F66, P68, A69, W157, L158, R163, I215, and W221 to be directly interacting with amino acid position 67. In the L67F variant, both with and without ceftazidime, L158 and I215 were shifted by 1 to 2 Å, respectively. In addition, we found W221 to be flipped by 180°. While in the wild-type structure, the W221 side chain forms a water-mediated H-bond to the backbone nitrogen of M237, in L67F, W221 formed a H-bond to the main chain of F67 (Fig. 5).

DISCUSSION

Here, we asked if sub-MICs of the clinically relevant β -lactam ceftazidime could affect the evolution of the contemporary, globally circulating carbapenemase OXA-48. To test this, we evolved an OXA-48 producing *E. coli* strain in the presence of one-quarter of its ceftazidime MIC. The identification of seven single variants of OXA-48, conferring only marginal changes in susceptibility (Fig. 2b, Table 2), demonstrates that the exposure to sub-MICs of ceftazidime drives the emergence of cryptic *bla*_{OXA-48} genetic diversity. Thus, our data provide further support for the proposed compartment hypothesis (6, 8, 27, 28), where low-grade selection promotes cryptic genetic variation that could act as stepping-stones toward full clinical antibiotic resistance (29, 30). Notably, even though all seven single OXA-48 variants largely displayed, from a clinical microbiology perspective, negligible changes in ceftazidime susceptibility, competition experiments revealed strong beneficial fitness effects (Fig. 2b). Taken together with earlier work, using reconstructed TEM-1 variants from clinical samples (5), our data underscore the significance of divergent evolution and selection of genetic variation imposed by sub-MICs of β -lactams.

To further our understanding of how the detected single amino changes affect the structure-activity relationship of OXA-48, we first measured enzyme kinetics (Table 3). The catalytic efficiency mirrored the observed changes in susceptibility toward β -lactams at the cellular level and confirmed our previous findings that mutational changes increasing ceftazidime activity come with a functional trade-off against penicillins and carbapenems (17). However, decreased susceptibility might not only be reflected by differences in the catalytic efficiency, as protein stability and translocation also affect resistance levels toward β -lactams (31). Structurally, all amino acid changes clustered

either around the active site S70 (L67F, P68S, F72L) or within the Ω -loop (F156C, F156V, L158P, G160C; Fig. 2c).

In wild-type OXA-48, the Ω -loop interacts with the $\beta 5$ - $\beta 6$ loop via a salt bridge mediated by D159-R214 maintaining a closed conformation of the active site (15). MD simulations performed on a subset of variants revealed that F72L and L158P weaken the interaction between these loops, resulting in increased structural flexibility (Fig. 4). We postulate that these changes aid the hydrolysis of bulkier substrates such as ceftazidime but result in decreased activity toward penicillins and carbapenems. Indeed, mutations affecting the salt bridge are associated with reduced carbapenemase activity presumably due to increased loop flexibility (32).

In clinical OXA-48-like variants (e.g., OXA-163, OXA-247, and OXA-405) with increased ceftazidime activity, larger structural variations (deletions in combination with single point mutations) within and around the $\beta 5$ - $\beta 6$ loop have been reported (18–20). However, also, single amino acid changes structurally close to the Ω - and $\beta 5$ - $\beta 6$ loops have been shown to slightly elevate the catalytic efficiency toward ceftazidime (E125Y in OXA-245 and V120L in OXA-519) (33, 34). The significance of the Ω - and $\beta 5$ - $\beta 6$ loops for the substrate profile is not limited to OXA-48 (35, 36). These loops have been shown to impact substrate profiles for other clinically relevant β -lactamases, including TEM and KPC (37–39). In addition, comparable modes of action have been hypothesized for the OXA-10-like variants OXA-145 and OXA-147, exhibiting L158 Δ and W157L, respectively (according to OXA-48 numbering) (40–42).

We were able to solve the structure of the OXA-48 variant L67F, which showed the reorientation of several active site residues such as L158 and I215 (Fig. 5, bottom). Fine-tuning of active site residue conformations through more distal amino acid changes is a common strategy in enzyme evolution (43) and may enable L67F to increase activity toward ceftazidime. In addition, our structure revealed the presence of a new cryptic binding site for ceftazidime, approximately 9 Å away from the active site residue S70, involving interaction with the above-described $\beta 5$ - $\beta 6$ loop (Fig. 5, bottom) and R214, in particular. However, the mechanistic importance of this binding and the pocket remains elusive, and more structural investigations are necessary.

Taken together, combining experimental evolution and structure-activity relationships allowed us to identify and characterize single step mutations with cryptic resistance that yet demonstrated significant fitness effects and structural changes. Our data show that to understand the evolutionary potential of standing genetic diversity, susceptibilities characterized solely by traditional MIC measurements provide too low resolution.

We acknowledge that our study is not without limitations, as despite strong fitness effects, none of the variants went to fixation in any of the populations (Fig. 1c). We argue that there can be at least two reasons for this. First, we have focused solely on changes within OXA-48 and on a single drug. It is clear from our data that the evolution at sub-MICs also selected for other potential resistance mechanisms (e.g., efflux, porins). These mechanisms could lead to potential widespread epistatic interactions that would slow down any fixation process (9, 11, 44–46) and warrant further investigations, e.g., whole-genome sequencing. Second, it has been shown that β -lactamase producers can detoxify their environment, allowing coexistence of genotypes with different susceptibilities, resulting in a stable equilibrium between resistant and susceptible clones (47).

Our work sheds light on the evolution of β -lactamases and their selection dynamics toward altered substrate profiles. This is supported by recent studies reporting environmental contamination of cephalosporins at concentrations similar to those applied here (48, 49). Moreover, OXA-48 variants, with the same or similar amino acid changes as identified and characterized here, have been reported in environmental samples (22, 50). We speculate that the identified mutations are only first step mutations toward full clinical ceftazidime resistance mediated by OXA-48. However, more studies are needed to fully understand the complete fitness landscape of OXA-48 and other carbapenemases.

MATERIALS AND METHODS

Media, chemicals, and strains. Mueller-Hinton (MH) agar and broth were purchased from Thermo Fisher Scientific (East Grinstead, UK). Luria-Bertani (LB) broth, LB agar, yeast extract, agar, terrific broth, ampicillin, amoxicillin, cefepime, ceftazidime, chloramphenicol, imipenem, meropenem, piperacillin, 2,3,5 tri-phenyl tetrazolium, sodium chloride, and maltose were obtained from Sigma-Aldrich (St. Louis, MO, USA). Tryptone was obtained from Oxoid (Hampshire, UK). All strains used and constructed within this study are listed in Table S1.

Sub-MIC evolution. MP13-06, previously constructed and tested (17), was evolved by serial passaging without selection pressure and at $0.25 \times$ MIC (0.06 mg/liter) of ceftazidime for 300 generations. In short, bacterial suspensions were grown at 37°C and 700 rpm on a plate shaker (Edmund Bühler, Bodelshausen, Germany) in 1 ml MH broth to full density and passaged every 12 h with a bottleneck of 1:100. The evolution was performed in triplicates.

Dose-response curves and susceptibility testing. Dose-response curves were obtained initially and after every 50 generations for the whole evolved populations. Cultures were grown to full density and diluted in 0.9% saline to 10^5 CFU/ml. Then, 384-well plates (VWR, Radnor, PA, USA) were inoculated with 10^5 CFU and increasing concentrations of ceftazidime ranging from 0 to 32 mg/liter. Plates were statically incubated for 20 h at 37°C. The optical density at 600 nm (OD_{600}) was measured with a microtiter plate reader (BioTek Instruments, Winooski, VT, USA), and dose-response curves including IC_{50} values were calculated using Prism 9.0 (GraphPad Software, San Diego, CA, USA). In this setup, the ceftazidime MIC was determined by measuring the OD_{600} as the first well with an optical density comparable to the negative control.

For MIC measurements against β -lactams other than ceftazidime, in-house-designed and premade Sensititre microtiter plates (TREK Diagnostic Systems/Thermo Fisher Scientific, East Grinstead, UK) were loaded with 10^5 CFU. The plates were incubated statically for 20 h at 37°C. All susceptibility tests were performed in at least two biological replicates.

Determination of clones with altered ceftazidime susceptibility. To determine clones exhibiting decreased ceftazidime susceptibility, we plated 10^7 cells from every 50th generation on MH agar without and with 1 mg/liter ceftazidime. The plates were incubated for 24 h at 37°C. Clone frequencies were determined as the ratio between colonies found on selective versus nonselective plates. About 50 preselected colonies were subjected to susceptibility testing, as described above. For creating the boxplots, a probability function was calculated based on the MIC per replicate. Since the MICs were determined in 2-fold steps, we generated smoother boxplots by creating 1,000 random measurements per generation. We did so by drawing a random number between the \log_2 (MIC values) and \log_2 (MIC values) + 1 a $1,000 \times f_{mic}$, where f_{mic} is the fraction of the population. All calculations were done in Mathematica 11.0 (Wolfram Research, Champaign, IL, USA).

Strain construction. For functional resistance profiles, wild-type bla_{OXA-48} and allele variants were subcloned into the high copy number vector pCR-blunt II-TOPO vector (Invitrogen, Carlsbad, CA, USA) and expressed in *E. coli* TOP10 (Invitrogen). For wild-type TOPO- bla_{OXA-48} , the construction has been described previously (17). Point mutations were inserted by using the QuikChange II kit for site-directed mutagenesis (Agilent Biosciences, Santa Clara, CA, USA), TOPO- bla_{OXA-48} as a template, and the respective primers (Table S2). The double mutants TOPO- bla_{OXA-48} -F72L/G131S and TOPO- bla_{OXA-48} -N146S/L158P were created by inverse PCR using Phusion polymerase (New England Biolabs, Ipswich, MA, USA) and TOPO- bla_{OXA-48} -F72L or TOPO- bla_{OXA-48} -L158P as a template, respectively. PCR products were 5'-phosphorylated with polynucleotide kinase (Thermo Fisher Scientific, Waltham, MA, USA) and circularized using T4 DNA ligase (Thermo Fisher Scientific). Transformants were selected on LB agar plates containing 50 or 100 mg/liter ampicillin. bla_{OXA-48} was Sanger sequenced (BigDye 3.1 technology; Applied Biosystems, Foster City, CA, USA) using M13 primers (Thermo Fisher Scientific) (Table S2).

For expression in a low copy number vector (pUN), we PCR-amplified a segment containing the p15A origin of replication and the *cat* chloramphenicol resistance gene of the pACYC184 vector using the primers cat-r and p15A46 (Table S2). To obtain the bla_{OXA-48} inserts, the pCR-blunt II-TOPO constructs (see above) were used as templates. We amplified the bla_{OXA-48} genes by using the primers OXA-48-prof, containing the constitutive artificial CP6 promoter (51), and preOXA-48B (Table S2) (52). These PCR products were 5'-phosphorylated with polynucleotide kinase (Thermo Fisher Scientific) and then blunt ligated with the amplified vector backbone. The pUN- bla_{OXA-48} vector and the corresponding variants were transformed into *E. coli* DH5 α and plated on LB agar containing chloramphenicol (25 mg/liter). Genotypes of selected clones were confirmed by Sanger sequencing (BigDye 3.1 technology; Applied Biosystems) using OXA-48-pro-f/preOXA-48B primers (Table S2) (52).

To measure bacterial fitness, *E. coli* MG1655 $\Delta malF$ (MP14-23) was constructed as a competitor strain by transducing the kanamycin resistance marker from the Keio strain JW3993 with P1-vir into *E. coli* MG1655 as previously described (53, 54). The marker was then removed with the helper vector pCP20 (55). The competitor strain MP14-23 was then transformed with pUN- bla_{OXA-48} and the corresponding variants (Table S1). Transformants were selected on LB plates containing 25 mg/liter chloramphenicol.

For protein expression and purification, bla_{OXA-48} in the pDEST17 expression vector (Thermo Fisher Scientific) was mutagenized using a QuikChange II site-directed mutagenesis kit as described above. *E. coli* DH5 α was transformed with the DNA constructs, and clones were selected on LB agar containing 100 mg/liter ampicillin. The vectors were isolated using a plasmid maxi kit (Qiagen, Hilden, Germany) and transformed into *E. coli* BL21 AI (Thermo Fisher Scientific). Point mutations were verified by Sanger sequencing using T7 primers (Thermo Fisher Scientific) (Table S2).

Bacterial fitness: head-to-head competition. Strains were grown overnight in LB supplemented with chloramphenicol (25 mg/liter) at 37°C and 700 rpm on a plate shaker (Edmund Bühler). For each competition, we coinoculated $\sim 1 \times 10^7$ CFU/ml of each competitor in 1 ml LB broth, supplemented

either with chloramphenicol (25 mg/liter) and ceftazidime (0.06 mg/liter) or with chloramphenicol only. Then, 96-deep-well plates (VWR) were incubated at 37°C and 700 rpm for 8 h. Each competition was performed in three biological replicates. The initial and final CFU/ml for both competitors were determined by differential plating on tetracycline maltose agar (10 g/liter tryptone, 5 g/liter sodium chloride, 1 g/liter yeast extract, 15 g/liter agar, 10 g/liter maltose, supplemented with 1 ml 5% 2,3,5 tri-phenyl tetrazolium chloride). Relative fitness (w) was determined according to equation 1, where mal^+ and mal^- are, respectively, the mal^+ and $\Delta malF$ strain backgrounds carrying the different pUN vectors (Table S1).

$$w = \frac{\log_2 \frac{mal^+_{final}}{mal^+_{initial}}}{\log_2 \frac{mal^-_{final}}{mal^-_{initial}}} \quad (1)$$

The mal^+ pUN- bla_{OXA-48} strain (MP08-61) was competed against $\Delta malF$ strains carrying each of the pUN vectors encoding wild-type bla_{OXA-48} or single variants (Table S1). Additionally, the mal^+ pUN- bla_{OXA-48} -F72L (MP08-67) and mal^+ pUN- bla_{OXA-48} -L158P (MP08-63) strains were used as competitors, respectively, against strains $\Delta malF$ pUN- bla_{OXA-48} -F72L/G131S (MP14-32) and $\Delta malF$ pUN- bla_{OXA-48} -N146S/L158P (MP14-33), respectively. Data analysis and graphical illustrations were performed in R 4.0.2 (56).

Recombinant enzyme expression and purification. Overexpression of OXA-48 and the corresponding variants was done in terrific broth supplemented with 100 mg/liter ampicillin. *E. coli* BL21 AI carrying pDEST-17- bla_{OXA-48} and OXA-48 variants (Table S1) were grown at 37°C and 220 rpm to an optical density of 0.4 to 0.5. Protein expression was induced with 0.1% L-arabinose (Sigma-Aldrich). Expression took place for 16 h at 15°C and 220 rpm. Harvested cells were sonicated, and recombinant proteins were purified as described previously (17, 57). F156C and G160C were found to be insoluble. To increase their solubility, 5 mM β -mercaptoethanol was used during the sonication process.

Molecular mass verification. ESI-MS was performed on the purified enzymes as described previously (58). In short, a buffer exchange to 0.1% formic acid (Merck Millipore, Burlington, MA, USA) was performed using centrifugal molecular cutoff filters (Merck Millipore; 10,000 Da). The protein masses were determined using an Orbitrap Fusion Lumos device (Thermo Fisher Scientific). Injection was performed using an EASY-nano LC instrument (Thermo Fisher Scientific) with a 15-cm C_{18} EASY-spray column. Mass calculations were done using BioPharma Finder 3.0 protein deconvolution software (Thermo Fisher Scientific, Massachusetts, USA).

Steady-state enzyme kinetics. Catalytic efficiencies (k_{cat}/K_m) for the recombinantly expressed enzymes were determined under steady-state conditions for ampicillin ($\Delta\xi = -820 \text{ M}^{-1} \text{ cm}^{-1}$, 232 nm), piperacillin ($\Delta\xi = -820 \text{ M}^{-1} \text{ cm}^{-1}$, 235 nm), ceftazidime ($\Delta\xi = -9,000 \text{ M}^{-1} \text{ cm}^{-1}$, 260 nm), cefepime ($\Delta\xi = -10,000 \text{ M}^{-1} \text{ cm}^{-1}$, 260 nm), imipenem ($\Delta\xi = -9,000 \text{ M}^{-1} \text{ cm}^{-1}$, 300 nm), and meropenem ($\Delta\xi = -6,500 \text{ M}^{-1} \text{ cm}^{-1}$, 300 nm) by measuring the initial enzymatic reaction rate. The enzyme concentrations are summarized in Table S3. All determinations were performed at least in duplicates at a final assay volume of 100 μl . UV-transparent 96-well plates (Corning, Kennebunk, ME, USA) were used. All test results were obtained at 25°C and in 0.1 M phosphate buffer (pH 7.0) supplemented with 50 mM NaHCO_3 (Sigma-Aldrich). Calculations were performed using Prism 9.0 (GraphPad Software).

Thermostability. We determined the fluorescence-based protein thermostability for OXA-48 as described previously (17). In short, the proteins were diluted in 50 mM HEPES (VWR), pH 7.5 supplemented with 50 mM potassium sulfate (Honeywell, North Carolina, USA) to a final concentration of 0.2 mg/ml protein and 5 \times SYPRO orange (Sigma-Aldrich). A temperature gradient of 25 to 70°C (heating rate, 1°C per min) was applied using an MJ minicycler (Bio-Rad, Hercules, CA, USA). All experiments were performed in triplicates.

Molecular dynamics simulations. System setup was performed as described previously (59). In brief, acyl-enzyme of OXA-48 with covalently bound ceftazidime was originally built using the structure of OXA-48 with imipenem (PDB no. 5QB4) (60) and replacing imipenem with ceftazidime (PDB no. 6Q5F) (17), which ensured keeping the Ω -loop ordered (as found in the apoenzyme). For OXA-163, the same ceftazidime binding pose was combined with apoenzyme crystal structure (PDB no. 4S2L) (61). All OXA-48 variants were modeled using the mutagenesis tool in PyMOL, choosing the rotamer with the least steric clashes with surrounding atoms. Enzymes were solvated in a 10-Å cubic box of TIP3P water with net charge neutralized by replacing bulk water molecules with counterions. Parameters for nonstandard residues (carboxylated K73, ceftazidime acyl-enzyme) have been published previously (59).

All systems were initially briefly minimized (1,000 steps of steepest descent followed by 1,000 steps of conjugate gradient), heated from 50 K to 300 K in 20 ps, and then simulated for 120 ns in the NPT ensemble (saving a frame every 20 ps). Langevin dynamics were used with a collision frequency of 0.2 and a 2-fs time step; all bonds involving hydrogens were constrained using the SHAKE algorithm. Periodic boundary conditions in explicit solvent were applied in all simulations. Five independent simulations were run per enzyme variant (for a total of 600 ns per variant), and all calculations were done with the Amber18 program package (pmemd.cuda) (62) using the ff14SB force field (63) for the protein and TIP3P for water (64, 65). All analyses were done using CPPTRAJ from AmberTools (66). Root mean square fluctuation (RMSF) calculations were performed by first calculating an average structure from the MD simulation, aligning the trajectory against the average structure excluding four residues from both the N- and C-terminal ends as well as the loop residues of interest (G145-I164 for the Ω -loop and T213-I219 for the β 5- β 6-loop), and then calculating the RMSF for the corresponding loop main chain heavy atoms (CA, C, N, O). The first 20 ns were excluded from all analyses to allow time for system equilibration. PC analysis was performed on $C\alpha$ -atoms (excluding four residues from both the N- and C-terminal ends), using all trajectories of OXA-48 and variants together (5 independent simulations of 120 ns per variant).

Crystallization and structure determination. Crystals were grown in a 1- μl hanging drop containing 5 mg/ml enzyme and mixed 1:1 with reservoir solution containing 0.1 M Tris, pH 9.0 (Sigma-Aldrich), and 28 to

30% polyethylene glycol (PEG) mono ethylene ether 500 (Sigma-Aldrich) at 4°C. Crystals were harvested, cryo-protected by adding 15% ethylene glycol (Sigma-Aldrich) to the reservoir solution, and then frozen in liquid nitrogen.

Diffraction data were collected on BL14.1 BESSY II, Berlin, Germany, at 100 K, wavelength 0.9184 Å, and the diffraction images were indexed and integrated using XDS (67). AIMLESS was used for scaling (68). When scaling the final data set (Table S4), we aimed for high overall completeness and $CC_{1/2} > 0.5$ and a mean intensity above 1.0 in the outer resolution shell. The structure was solved by molecular replacement with chain A of PDB no. 5QB4 (60) and the program PHENIX 1.12 (69). Parts of the model were rebuilt using Coot (70). Figures were prepared using PyMOL 1.8 (Schrödinger, New York, NY, USA). Ligand and protein interactions were calculated using Protein Contacts Atlas (71).

Data availability. Atom coordinates and structure factors for the OXA-48 variant L67F are available in the protein data bank (PDB no. 7ASS). Underlying data are stored in an online repository at https://github.com/GAMMAtri/Cryptic_b-lactamase_evolution.

SUPPLEMENTAL MATERIAL

Supplemental material is available online only.

TABLE S1, DOCX file, 0.04 MB.

TABLE S2, DOCX file, 0.02 MB.

TABLE S3, DOCX file, 0.01 MB.

TABLE S4, DOCX file, 0.02 MB.

ACKNOWLEDGMENTS

We are very grateful to Linus Sandegren, Uppsala University, Sweden, and Francisco Dionísio, University of Lisbon, Portugal, for providing strains. We thank Karina Xavier (The Instituto Gulbenkian Ciência, Oeiras, Portugal) for providing the P1-vir phage. Provision of beam time at BL14.1 at Bessy II, Berlin, Germany, is highly valued.

Hanna-Kirsti S. Leiros was supported by the Norwegian Research Council (273332/2018). Bjarte A. Lund was supported by the Norwegian Research Council (262695 and 274858). Pål J. Johnsen was supported by Northern Norway Regional Health Authority, UiT The Arctic University of Norway (Project SFP1292-16), and JPI-EC-AMR (project 271176/H10). Viivi H. A. Hirvonen was supported by the UKRI Medical Research Council (MR/N0137941/1). Marc W. van der Kamp is a BBSRC David Phillips fellow and thanks the Biotechnology and Biological Sciences Research Council for funding (BB/M026280/1).

Simulations were performed using the computational facilities of the Advanced Computing Research Centre, University of Bristol. We also extend our thanks to François Pierre Alexandre Cléon, Vidar Sørum, Antal Martinecz, and Alexander Wessel for their help.

The publication charges for this article were funded by a grant from the publication fund of UiT The Arctic University of Norway.

We declare no competing interests.

C.F., P.J.J., Ø.S., and H.-K.S.L. worked out the conceptual framework. C.F. conducted the evolution. C.F. and J.A.G. performed microbiological testing. C.F., J.A.G., and K.H. constructed strains. C.F. purified enzymes and measured kinetics. C.F. and H.-K.S.L. solved the crystal structure. B.A.L. performed initial molecular dynamic simulations as a proof of principle. V.H.A.H. and M.W.V.D.K. designed, performed, and analyzed the molecular dynamic simulations. C.F. wrote the manuscript with contributions from all coauthors.

REFERENCES

- Bush K, Bradford PA. 2016. β -lactams and β -lactamase inhibitors: an overview. *Cold Spring Harb Perspect Med* 6:a025247. <https://doi.org/10.1101/cshperspect.a025247>.
- Bush K. 2018. Past and present perspectives on β -lactamases. *Antimicrob Agents Chemother* 62:e01076-18. <https://doi.org/10.1128/AAC.01076-18>.
- Bonomo RA. 2017. β -Lactamases: a focus on current challenges. *Cold Spring Harb Perspect Med* 7:a025239. <https://doi.org/10.1101/cshperspect.a025239>.
- Pitout JDD, Peirano G, Kock MM, Strydom KA, Matsumura Y. 2019. The global ascendency of OXA-48-type carbapenemases. *Clin Microbiol Rev* 33:e00102-19.
- Negri MC, Lipsitch M, Blazquez J, Levin BR, Baquero F. 2000. Concentration-dependent selection of small phenotypic differences in TEM β -lactamase-mediated antibiotic resistance. *Antimicrob Agents Chemother* 44:2485–2491. <https://doi.org/10.1128/aac.44.9.2485-2491.2000>.
- Baquero F, Negri MC, Morosini MI, Blazquez J. 1997. The antibiotic selective process: concentration-specific amplification of low-level resistant populations. *Ciba Found Symp* 207:93–105. discussion 105–11. <https://doi.org/10.1002/9780470515358.ch7>.
- Baquero F. 2001. Low-level antibacterial resistance: a gateway to clinical resistance. *Drug Resist Updat* 4:93–105. <https://doi.org/10.1054/drup.2001.0196>.
- Baquero F, Negri MC. 1997. Selective compartments for resistant microorganisms in antibiotic gradients. *Bioessays* 19:731–736. <https://doi.org/10.1002/bies.950190814>.
- Gullberg E, Cao S, Berg OG, Ilback C, Sandegren L, Hughes D, Andersson DI. 2011. Selection of resistant bacteria at very low antibiotic concentrations. *PLoS Pathog* 7:e1002158. <https://doi.org/10.1371/journal.ppat.1002158>.

10. Gullberg E, Albrecht LM, Karlsson C, Sandegren L, Andersson DI. 2014. Selection of a multidrug resistance plasmid by sublethal levels of antibiotics and heavy metals. *mBio* 5:e01918-14. <https://doi.org/10.1128/mBio.01918-14>.
11. Westhoff S, van Leeuwe TM, Qachach O, Zhang Z, van Wezel GP, Rozen DE. 2017. The evolution of no-cost resistance at sub-MIC concentrations of streptomycin in *Streptomyces coelicolor*. *ISME J* 11:1168–1178. <https://doi.org/10.1038/ismej.2016.194>.
12. Baquero F, Coque TM. 2014. Widening the spaces of selection: evolution along sublethal antimicrobial gradients. *mBio* 5:e02270. <https://doi.org/10.1128/mBio.02270-14>.
13. Bagge N, Hentzer M, Andersen JB, Ciofu O, Givskov M, Hoiby N. 2004. Dynamics and spatial distribution of β -lactamase expression in *Pseudomonas aeruginosa* biofilms. *Antimicrob Agents Chemother* 48:1168–1174. <https://doi.org/10.1128/aac.48.4.1168-1174.2004>.
14. Murray AK, Zhang L, Yin X, Zhang T, Buckling A, Snape J, Gaze WH. 2018. Novel insights into selection for antibiotic resistance in complex microbial communities. *mBio* 9:e00969-18. <https://doi.org/10.1128/mBio.00969-18>.
15. Docquier JD, Calderone V, De Luca F, Benvenuti M, Giuliani F, Bellucci L, Tafi A, Nordmann P, Botta M, Rossolini GM, Mangani S. 2009. Crystal structure of the OXA-48 β -lactamase reveals mechanistic diversity among class D carbapenemases. *Chem Biol* 16:540–547. <https://doi.org/10.1016/j.chembiol.2009.04.010>.
16. Poirel L, Heritier C, Tolun V, Nordmann P. 2004. Emergence of oxacillinase-mediated resistance to imipenem in *Klebsiella pneumoniae*. *Antimicrob Agents Chemother* 48:15–22. <https://doi.org/10.1128/aac.48.1.15-22.2004>.
17. Fröhlich C, Sørum V, Thomassen AM, Johnsen PJ, Leiros HS, Samuelsen Ø. 2019. OXA-48-mediated ceftazidime-avibactam resistance is associated with evolutionary trade-offs. *mSphere* 4:e00024-19. <https://doi.org/10.1128/mSphere.00024-19>.
18. Gomez S, Pasteran F, Faccone D, Bettiol M, Veliz O, De Belder D, Rapoport M, Gatti B, Petroni A, Corso A. 2013. Inpatient emergence of OXA-247: a novel carbapenemase found in a patient previously infected with OXA-163-producing *Klebsiella pneumoniae*. *Clin Microbiol Infect* 19:E233–E235. <https://doi.org/10.1111/1469-0691.12142>.
19. Poirel L, Castanheira M, Carrer A, Rodriguez CP, Jones RN, Smayevsky J, Nordmann P. 2011. OXA-163, an OXA-48-related class D β -lactamase with extended activity toward expanded-spectrum cephalosporins. *Antimicrob Agents Chemother* 55:2546–2551. <https://doi.org/10.1128/AAC.00022-11>.
20. Dortet L, Oueslati S, Jeannot K, Tande D, Naas T, Nordmann P. 2015. Genetic and biochemical characterization of OXA-405, an OXA-48-type extended-spectrum β -lactamase without significant carbapenemase activity. *Antimicrob Agents Chemother* 59:3823–3828. <https://doi.org/10.1128/AAC.05058-14>.
21. Mairi A, Pantel A, Sotto A, Lavigne JP, Touati A. 2018. OXA-48-like carbapenemases producing *Enterobacteriaceae* in different niches. *Eur J Clin Microbiol Infect Dis* 37:587–604. <https://doi.org/10.1007/s10096-017-3112-7>.
22. Naas T, Oueslati S, Bonnin RA, Dabos ML, Zavala A, Dortet L, Retaillieu P, Iorga BI. 2017. β -lactamase database (BLDB): structure and function. *J Enzyme Inhib Med Chem* 32:917–919. <https://doi.org/10.1080/14756366.2017.1344235>.
23. Tacao M, Silva I, Henriques I. 2017. Culture-independent methods reveal high diversity of OXA-48-like genes in water environments. *J Water Health* 15:519–525. <https://doi.org/10.2166/wh.2017.260>.
24. Preston KE, Hitchcock SA, Aziz AY, Tine JA. 2014. The complete nucleotide sequence of the multi-drug resistance-encoding IncL/M plasmid pACM1. *Plasmid* 76:54–65. <https://doi.org/10.1016/j.plasmid.2014.08.005>.
25. Thomas VL, McReynolds AC, Shoichet BK. 2010. Structural bases for stability-function tradeoffs in antibiotic resistance. *J Mol Biol* 396:47–59. <https://doi.org/10.1016/j.jmb.2009.11.005>.
26. Mehta SC, Rice K, Palzkill T. 2015. Natural variants of the KPC-2 carbapenemase have evolved increased catalytic efficiency for ceftazidime hydrolysis at the cost of enzyme stability. *PLoS Pathog* 11:e1004949. <https://doi.org/10.1371/journal.ppat.1004949>.
27. Baquero F, Negri MC, Morosini MI, Blazquez J. 1998. Selection of very small differences in bacterial evolution. *Int Microbiol* 1:295–300.
28. Baquero F, Negri MC, Morosini MI, Blazquez J. 1998. Antibiotic-selective environments. *Clin Infect Dis* 27 Suppl 1:S5–S11. <https://doi.org/10.1086/514916>.
29. Baier F, Hong N, Yang G, Pabis A, Miton CM, Barrozo A, Carr PD, Kamerlin SC, Jackson CJ, Tokuriki N. 2019. Cryptic genetic variation shapes the adaptive evolutionary potential of enzymes. *Elife* 8:e40789. <https://doi.org/10.7554/eLife.40789>.
30. Zheng J, Payne JL, Wagner A. 2019. Cryptic genetic variation accelerates evolution by opening access to diverse adaptive peaks. *Science* 365:347–353. <https://doi.org/10.1126/science.aax1837>.
31. Socha RD, Chen J, Tokuriki N. 2019. The molecular mechanisms underlying hidden phenotypic variation among metallo- β -lactamases. *J Mol Biol* 431:1172–1185. <https://doi.org/10.1016/j.jmb.2019.01.041>.
32. Oueslati S, Retaillieu P, Marchini L, Berthault C, Dortet L, Bonnin RA, Iorga BI, Naas T. 2020. Role of arginine 214 in the substrate specificity of OXA-48. *Antimicrob Agents Chemother* 64:e02329-19. <https://doi.org/10.1128/AAC.02329-19>.
33. Dabos L, Bogaerts P, Bonnin RA, Zavala A, Sacre P, Iorga BI, Huang DT, Glupczynski Y, Naas T. 2018. Genetic and biochemical characterization of OXA-519, a novel OXA-48-like β -lactamase. *Antimicrob Agents Chemother* 62:e00469-18. <https://doi.org/10.1128/AAC.00469-18>.
34. Lund BA, Thomassen AM, Carlsen TJO, Leiros HKS. 2017. Structure, activity and thermostability investigations of OXA-163, OXA-181 and OXA-245 using biochemical analysis, crystal structures and differential scanning calorimetry analysis. *Acta Crystallogr F Struct Biol Commun* 73:579–587. <https://doi.org/10.1107/S2053230X17013838>.
35. Dabos L, Zavala A, Bonnin RA, Beckstein O, Retaillieu P, Iorga BI, Naas T. 2020. Substrate specificity of OXA-48 after β 5- β 6 loop replacement. *ACS Infect Dis* 6:1032–1043. <https://doi.org/10.1021/acinfecdis.9b00452>.
36. De Luca F, Benvenuti M, Carboni F, Pozzi C, Rossolini GM, Mangani S, Docquier JD. 2011. Evolution to carbapenem-hydrolyzing activity in non-carbapenemase class D β -lactamase OXA-10 by rational protein design. *Proc Natl Acad Sci U S A* 108:18424–18429. <https://doi.org/10.1073/pnas.1110530108>.
37. Venditti C, Nisii C, Ballardini M, Meledandri M, Di Caro A. 2019. Identification of L169P mutation in the Ω loop of KPC-3 after a short course of ceftazidime/avibactam. *J Antimicrob Chemother* 74:2466–2467. <https://doi.org/10.1093/jac/dkz201>.
38. Stojanoski V, Chow DC, Hu L, Sankaran B, Gilbert HF, Prasad BV, Palzkill T. 2015. A triple mutant in the Ω -loop of TEM-1 β -lactamase changes the substrate profile via a large conformational change and an altered general base for catalysis. *J Biol Chem* 290:10382–10394. <https://doi.org/10.1074/jbc.M114.633438>.
39. Levitt PS, Papp-Wallace KM, Taracila MA, Hujer AM, Winkler ML, Smith KM, Xu Y, Harris ME, Bonomo RA. 2012. Exploring the role of a conserved class A residue in the Ω -loop of KPC-2 β -lactamase: a mechanism for ceftazidime hydrolysis. *J Biol Chem* 287:31783–31793. <https://doi.org/10.1074/jbc.M112.348540>.
40. Baurin S, Vercheval L, Bouillenne F, Falzone C, Brans A, Jacquamet L, Ferrer JL, Sauvage E, Dehareng D, Frere JM, Charlier P, Galleni M, Kerff F. 2009. Critical role of tryptophan 154 for the activity and stability of class D β -lactamases. *Biochemistry* 48:11252–11263. <https://doi.org/10.1021/bi901548c>.
41. Fournier D, Hocquet D, Dehecq B, Cholley P, Plesiat P. 2010. Detection of a new extended-spectrum oxacillinase in *Pseudomonas aeruginosa*. *J Antimicrob Chemother* 65:364–365. <https://doi.org/10.1093/jac/dkp438>.
42. Meziane-Cherif D, Bonnet R, Haouz A, Courvalin P. 2016. Structural insights into the loss of penicillinase and the gain of ceftazidimase activities by OXA-145 β -lactamase in *Pseudomonas aeruginosa*. *J Antimicrob Chemother* 71:395–402. <https://doi.org/10.1093/jac/dkv375>.
43. Yang G, Miton CM, Tokuriki N. 2020. A mechanistic view of enzyme evolution. *Protein Sci* 29:1724–1747. <https://doi.org/10.1002/pro.3901>.
44. de Visser JA, Rozen DE. 2006. Clonal interference and the periodic selection of new beneficial mutations in *Escherichia coli*. *Genetics* 172:2093–2100. <https://doi.org/10.1534/genetics.105.052373>.
45. Shields RK, Nguyen MH, Press EG, Chen L, Kreiswirth BN, Clancy CJ. 2017. In vitro selection of meropenem resistance among ceftazidime-avibactam-resistant, meropenem-susceptible *Klebsiella pneumoniae* isolates with variant KPC-3 carbapenemases. *Antimicrob Agents Chemother* 61:e00079-17. <https://doi.org/10.1128/AAC.00079-17>.
46. Shields RK, Chen L, Cheng S, Chavda KD, Press EG, Snyder A, Pandey R, Doi Y, Kreiswirth BN, Nguyen MH, Clancy CJ. 2017. Emergence of ceftazidime-avibactam resistance due to plasmid-borne bla_{KPC-3} mutations during treatment of carbapenem-resistant *Klebsiella pneumoniae* infections. *Antimicrob Agents Chemother* 61:e02097-16. <https://doi.org/10.1128/AAC.02097-16>.
47. Yurtsev EA, Chao HX, Datta MS, Artemova T, Gore J. 2013. Bacterial cheating drives the population dynamics of cooperative antibiotic resistance plasmids. *Mol Syst Biol* 9:683. <https://doi.org/10.1038/msb.2013.39>.

48. Ribeiro AR, Sures B, Schmidt TC. 2018. Cephalosporin antibiotics in the aquatic environment: a critical review of occurrence, fate, ecotoxicity and removal technologies. *Environ Pollut* 241:1153–1166. <https://doi.org/10.1016/j.envpol.2018.06.040>.
49. Watkinson AJ, Murby EJ, Kolpin DW, Costanzo SD. 2009. The occurrence of antibiotics in an urban watershed: from wastewater to drinking water. *Sci Total Environ* 407:2711–2723. <https://doi.org/10.1016/j.scitotenv.2008.11.059>.
50. Tacao M, Correia A, Henriques IS. 2015. Low prevalence of carbapenem-resistant bacteria in river water: resistance is mostly related to intrinsic mechanisms. *Microb Drug Resist* 21:497–506. <https://doi.org/10.1089/mdr.2015.0072>.
51. Jensen PR, Hammer K. 1998. Artificial promoters for metabolic optimization. *Biotechnol Bioeng* 58:191–195. [https://doi.org/10.1002/\(SICI\)1097-0290\(19980420\)58:2/3<191::AID-BIT11>3.0.CO;2-G](https://doi.org/10.1002/(SICI)1097-0290(19980420)58:2/3<191::AID-BIT11>3.0.CO;2-G).
52. Samuelsen Ø, Naseer U, Karah N, Lindemann PC, Kanestrom A, Leegaard TM, Sundsfjord A. 2013. Identification of *Enterobacteriaceae* isolates with OXA-48 and coproduction of OXA-181 and NDM-1 in Norway. *J Antimicrob Chemother* 68:1682–1685. <https://doi.org/10.1093/jac/dkt058>.
53. Thomason LC, Costantino N, Court DL. 2007. *E. coli* genome manipulation by P1 transduction. *Curr Protoc Mol Biol Chapter 1:Unit 1.17*. <https://doi.org/10.1002/0471142727.mb0117s79>.
54. Baba T, Mori H. 2008. The construction of systematic in-frame, single-gene knockout mutant collection in *Escherichia coli* K-12. *Methods Mol Biol* 416:171–181. https://doi.org/10.1007/978-1-59745-321-9_11.
55. Datsenko KA, Wanner BL. 2000. One-step inactivation of chromosomal genes in *Escherichia coli* K-12 using PCR products. *Proc Natl Acad Sci U S A* 97:6640–6645. <https://doi.org/10.1073/pnas.120163297>.
56. R Core Team. 2018. R: a language and environment for statistical computing. R Foundation for Statistical Computing, Vienna, Austria.
57. Lund BA, Christopheit T, Guttormsen Y, Bayer A, Leiros HK. 2016. Screening and design of inhibitor scaffolds for the antibiotic resistance oxacillinase-48 (OXA-48) through surface plasmon resonance screening. *J Med Chem* 59:5542–5554. <https://doi.org/10.1021/acs.jmedchem.6b00660>.
58. Fröhlich C, Sørum V, Huber S, Samuelsen O, Berglund F, Kristiansson E, Kotsakis SD, Marathe NP, Larsson DGJ, Leiros SH. 2020. Structural and biochemical characterization of the environmental MBLs MYO-1, ECV-1 and SHD-1. *J Antimicrob Chemother* 75:2554–2563. <https://doi.org/10.1093/jac/dkaa175>.
59. Hirvonen VHA, Mulholland AJ, Spencer J, van der Kamp MW. 2020. Small changes in hydration determine cephalosporinase activity of OXA-48 β -lactamases. *ACS Catal* 10:6188–6196. <https://doi.org/10.1021/acscatal.0c00596>.
60. Akhter S, Lund BA, Ismael A, Langer M, Isaksson J, Christopheit T, Leiros HS, Bayer A. 2018. A focused fragment library targeting the antibiotic resistance enzyme - Oxacillinase-48: synthesis, structural evaluation and inhibitor design. *Eur J Med Chem* 145:634–648. <https://doi.org/10.1016/j.ejmech.2017.12.085>.
61. Stojanoski V, Chow DC, Fryszczyn B, Hu L, Nordmann P, Poirel L, Sankaran B, Prasad BV, Palzkill T. 2015. Structural basis for different substrate profiles of two closely related class D β -lactamases and their inhibition by halogens. *Biochemistry* 54:3370–3380. <https://doi.org/10.1021/acs.biochem.5b00298>.
62. Rubenstein AB, Blacklock K, Nguyen H, Case DA, Khare SD. 2018. Systematic comparison of Amber and Rosetta energy functions for protein structure evaluation. *J Chem Theory Comput* 14:6015–6025. <https://doi.org/10.1021/acs.jctc.8b00303>.
63. Maier JA, Martinez C, Kasavajhala K, Wickstrom L, Hauser KE, Simmerling C. 2015. ff14SB: improving the accuracy of protein side chain and backbone parameters from ff99SB. *J Chem Theory Comput* 11:3696–3713. <https://doi.org/10.1021/acs.jctc.5b00255>.
64. Grand SL, Götz AW, Walker RC. 2013. SPFP: speed without compromise: a mixed precision model for GPU accelerated molecular dynamics simulations. *Computer Physics Communications* 184:374–380. <https://doi.org/10.1016/j.cpc.2012.09.022>.
65. Salomon-Ferrer R, Gotz AW, Poole D, Le Grand S, Walker RC. 2013. Routine microsecond molecular dynamics simulations with AMBER on GPUs. 2. Explicit solvent particle mesh Ewald. *J Chem Theory Comput* 9:3878–3888. <https://doi.org/10.1021/ct400314y>.
66. Roe DR, Cheatham TE III. 2013. PTRAJ and CPPTRAJ: software for processing and analysis of molecular dynamics trajectory data. *J Chem Theory Comput* 9:3084–3095. <https://doi.org/10.1021/ct400341p>.
67. Kabsch W. 2010. XDS. *Acta Crystallogr D Biol Crystallogr* 66:125–132. <https://doi.org/10.1107/S0907444909047337>.
68. Evans PR, Murshudov GN. 2013. How good are my data and what is the resolution? *Acta Crystallogr D Biol Crystallogr* 69:1204–1214. <https://doi.org/10.1107/S0907444913000061>.
69. Adams PD, Afonine PV, Bunkoczi G, Chen VB, Davis IW, Echols N, Headd JJ, Hung LW, Kapral GJ, Grosse-Kunstleve RW, McCoy AJ, Moriarty NW, Oeffner R, Read RJ, Richardson DC, Richardson JS, Terwilliger TC, Zwart PH. 2010. PHENIX: a comprehensive Python-based system for macromolecular structure solution. *Acta Crystallogr D Biol Crystallogr* 66:213–221. <https://doi.org/10.1107/S0907444909052925>.
70. Emsley P, Lohkamp B, Scott WG, Cowtan K. 2010. Features and development of Coot. *Acta Crystallogr D Biol Crystallogr* 66:486–501. <https://doi.org/10.1107/S0907444910007493>.
71. Kayikci M, Venkatakrishnan AJ, Scott-Brown J, Ravarani CNJ, Flock T, Babu MM. 2018. Visualization and analysis of non-covalent contacts using the Protein Contacts Atlas. *Nat Struct Mol Biol* 25:185–194. <https://doi.org/10.1038/s41594-017-0019-z>.

Table S1. Strains used and constructed in this study

<i>E. coli</i> Strain(s)	Comment	Source/ Reference
MP13-01/ MP08-01	K12 MG1655	Uppsala/Lisbon University
MP13-06 ^a	MP13-01 transformed with p50579417_3_OXA-48	(1)
MP13-34	MP13-06 evolved in MH broth, population 1: 50 generations	this study
MP13-35	MP13-06 evolved in MH broth, population 1: 100 generations	this study
MP13-36	MP13-06 evolved in MH broth, population 1: 150 generations	this study
MP13-37	MP13-06 evolved in MH broth, population 1: 200 generations	this study
MP13-38	MP13-06 evolved in MH broth, population 1: 250 generations	this study
MP13-39	MP13-06 evolved in MH broth, population 1: 300 generations	this study
MP13-40	MP13-06 evolved in MH broth, population 2: 50 generations	this study
MP13-41	MP13-06 evolved in MH broth, population 2:100 generations	this study
MP13-42	MP13-06 evolved in MH broth, population 2:150 generations	this study
MP13-43	MP13-06 evolved in MH broth, population 2: 200 generations	this study
MP13-44	MP13-06 evolved in MH broth, population 2: 250 generations	this study
MP13-45	MP13-06 evolved in MH broth, population 2: 300 generations	this study
MP13-46	MP13-06 evolved in MH broth, population 3: 50 generations	this study
MP13-47	MP13-06 evolved in MH broth, population 3: 100 generations	this study
MP13-48	MP13-06 evolved in MH broth, population 3: 150 generations	this study
MP13-49	MP13-06 evolved in MH broth, population 3: 200 generations	this study
MP13-50	MP13-06 evolved in MH broth, population 3: 250 generations	this study
MP13-51	MP13-06 evolved in MH broth, population 3: 300 generations	this study
MP13-52	MP13-06 evolved in ceftazidime, population 4: 50 generations	this study
MP13-53	MP13-06 evolved in ceftazidime, population 4: 100 generations	this study
MP13-54	MP13-06 evolved in ceftazidime, population 4: 150 generations	this study
MP13-55	MP13-06 evolved in ceftazidime, population 4: 200 generations	this study
MP13-56	MP13-06 evolved in ceftazidime, population 4: 250 generations	this study
MP13-57	MP13-06 evolved in ceftazidime, population 4: 300 generations	this study
MP13-58	MP13-06 evolved in ceftazidime, population 5: 50 generations	this study
MP13-59	MP13-06 evolved in ceftazidime, population 5: 100 generations	this study
MP13-60	MP13-06 evolved in ceftazidime, population 5: 150 generations	this study

MP13-61	MP13-06 evolved in ceftazidime, population 5: 200 generations	this study
MP13-62	MP13-06 evolved in ceftazidime, population 5: 250 generations	this study
MP13-63	MP13-06 evolved in ceftazidime, population 5: 300 generations	this study
MP13-64	MP13-06 evolved in ceftazidime, population 6: 50 generations	this study
MP13-65	MP13-06 evolved in ceftazidime, population 6: 100 generations	this study
MP13-66	MP13-06 evolved in ceftazidime, population 6: 150 generations	this study
MP13-67	MP13-06 evolved in ceftazidime, population 6: 200 generations	this study
MP13-68	MP13-06 evolved in ceftazidime, population 6: 250 generations	this study
MP13-69	MP13-06 evolved in ceftazidime, population 6: 300 generations	this study

For MIC measurements (high copy number vector):

MP13-04	TOP10, recipient strain for pCR-blunt II-TOPO	Invitrogen
MP13-11	MP13-04, transformed with pCR-blunt II- <i>bla</i> _{OXA-48}	(1)
MP13-21	MP13-04, transformed with pCR-blunt II- <i>bla</i> _{OXA-48} -L67F	this study
MP13-16	MP13-04, transformed with pCR-blunt II- <i>bla</i> _{OXA-48} -P68S	this study
MP13-14	MP13-04, transformed with pCR-blunt II- <i>bla</i> _{OXA-48} -F72L	this study
MP13-17	MP13-04, transformed with pCR-blunt II- <i>bla</i> _{OXA-48} -F156C	this study
MP13-18	MP13-04, transformed with pCR-blunt II- <i>bla</i> _{OXA-48} -F156V	this study
MP13-15	MP13-04, transformed with pCR-blunt II- <i>bla</i> _{OXA-48} -L158P	this study
MP13-19	MP13-04, transformed with pCR-blunt II- <i>bla</i> _{OXA-48} -G160C	this study
MP13-33	MP13-04, transformed with pCR-blunt II- <i>bla</i> _{OXA-48} -F72L/G131S	this study
MP13-20	MP13-04, transformed with pCR-blunt II- <i>bla</i> _{OXA-48} -N146S/L158P	this study

For dose-response measurements and head-to-head competitions (low copy number vector):

JW3393	K12 BW25113, $\Delta malF729::kan$	(2)
MP14-23	MG1655 $\Delta malF$ constructed based on MP08-01 (<i>mal</i> [*])	this study
MP08-61	MP08-01 with pUN- <i>bla</i> _{OXA-48}	this study
MP14-24	MP14-23 with pUN- <i>bla</i> _{OXA-48}	this study
MP14-29	MP14-23 with pUN- <i>bla</i> _{OXA-48} -L67F	this study
MP14-26	MP14-23 with pUN- <i>bla</i> _{OXA-48} -P68S	this study
MP14-27	MP14-23 with pUN- <i>bla</i> _{OXA-48} -F72L	this study
MP14-30	MP14-23 with pUN- <i>bla</i> _{OXA-48} -F156C	this study
MP14-31	MP14-23 with pUN- <i>bla</i> _{OXA-48} -F156V	this study
MP14-25	MP14-23 with pUN- <i>bla</i> _{OXA-48} -L158P	this study

MP14-28	MP14-23 with pUN- <i>bla</i> _{OXA-48} -G160C	this study
MP14-32	MP14-23 with pUN- <i>bla</i> _{OXA-48} -F72L/G131S	this study
MP08-67	MP08-01 with pUN- <i>bla</i> _{OXA-48} -F72L	this study
MP14-33	MP14-23 with pUN- <i>bla</i> _{OXA-48} -N146S/L158P	this study
MP08-63	MP08-01 with pUN- <i>bla</i> _{OXA-48} -L158P	this study

For protein expression and purification:

MP13-02	BL21 AI recipient for pDEST17 expression vector	Invitrogen
MP13-23	MP13-02, transformed with pDEST17- <i>bla</i> _{OXA-48}	(1)
MP13-24	MP13-02, transformed with pDEST17- <i>bla</i> _{OXA-48} -L67F	this study
MP13-25	MP13-02, transformed with pDEST17- <i>bla</i> _{OXA-48} -P68S	this study
MP13-26	MP13-02, transformed with pDEST17- <i>bla</i> _{OXA-48} -F72L	this study
MP13-27	MP13-02, transformed with pDEST17- <i>bla</i> _{OXA-48} -F156C	this study
MP13-28	MP13-02, transformed with pDEST17- <i>bla</i> _{OXA-48} -F156V	this study
MP13-29	MP13-02, transformed with pDEST17- <i>bla</i> _{OXA-48} -L158P	this study
MP13-30	MP13-02, transformed with pDEST17- <i>bla</i> _{OXA-48} -G160C	this study
MP13-31	MP13-02, transformed with pDEST17- <i>bla</i> _{OXA-48} -F72L/G131S	this study
MP13-32	MP13-02, transformed with pDEST17- <i>bla</i> _{OXA-48} -N146S/L158P	this study

^a previously named as MP101(1)

References

1. Fröhlich C, Sørnum V, Thomassen AM, Johnsen PJ, Leiros HS, Samuelsen Ø. 2019. OXA-48-Mediated Ceftazidime-Avibactam Resistance Is Associated with Evolutionary Trade-Offs. *mSphere* 4.
2. Baba T, Ara T, Hasegawa M, Takai Y, Okumura Y, Baba M, Datsenko KA, Tomita M, Wanner BL, Mori H. 2006. Construction of *Escherichia coli* K-12 in-frame, single-gene knockout mutants: the Keio collection. *Mol Syst Biol* 2:2006 0008.

Table S2. Primers used in the study

Name ^a		5'-sequence-3'	Reference
preOXA-48	FP (A)	TATATTGCATTAAGCAAGGG	(1)
	RP (B)	CACACAAATACGCGCTAACC	
M13	FP	GTAAAACGACGGCCAG	Thermo Fisher Scientific
	RP	CAGGAAACAGCTATGAC	
T7	FP	TAATACGACTCACTATAGGG	Thermo Fisher Scientific
	RP	GCTAGTTATTGCTCAGCGG	
F67L	FP	GGGCGAACCAAGCATTTCCTCCGCATCTACC	this study
	RP	GGTAGATGCGGGAAAAAATGCTTGGTTTCGCC	
P68S	FP	CGGGCGAACCAAGCATTTCCTCCGCATCTACC	this study
	RP	GGTAGATGCGGA TAAAAATGCTTGGTTTCGCC	
F72L	FP	GCATTTTACCCGCATCTACCTTGAATTCCTCAATAGCTTGATCG	this study
	RP	CGATCAAGCTATTGGGAATTTCAAGGTAGATGCGGGTAAAAATGC	
L158P	FP	GTAGACAGTTTCTGGCCCGACGGTGGTATTTCG	this study
	RP	CGAATACCACCGTCGGGCCAGAACTGTCTAC	
F156C	FP	GGGCAATGTAGACAGTTGTTGGCTCGACG	this study
	RP	CGTCGAGCCAACAACGTCTACATTGCC	
F156V	FP	GGGCAATGTAGACAGTGTCTGGCTCGACGG	this study
	RP	CCGTCGAGCCAGACACTGTCTACATTGCC	
G160C	FP	CAGTTTCTGGCTCGACTGTGGTATTTCGAATTTTCGG	this study
	RP	CCGAAATTCGAATACCACAGTCGAGCCAGAACTG	
G131S-out	FR	AGCGAGGCACGTATGAGCAAG	this study
	RP	AATTTGGCGGGCAAATTCCTG	
N146S-out	FP	GTGAGGACATTTTCGGCAATG	this study
	RP	TACCATAATCGAAAGCATGTAGC	
OXA-48-pro-f		TTGACACAGATATTTATGATATAATAACTGAGTAAGCTTAACATAAGGAGGA AAAACATATGCGTGTATTAGCCTTATCGG	(2)
cat-r		GTAGCACCAGGCGTTAAGG	this study
p15A46		TCGTATGGGCTGACTTCAG	this study

^aFP= forward primer, RP reverse primer

References

1. Samuelsen Ø, Naseer U, Karah N, Lindemann PC, Kanestrom A, Leegaard TM, Sundsfjord A. 2013. Identification of *Enterobacteriaceae* isolates with OXA-48 and coproduction of OXA-181 and NDM-1 in Norway. *J Antimicrob Chemother* 68:1682-5.
2. Jensen PR, Hammer K. 1998. Artificial promoters for metabolic optimization. *Biotechnol Bioeng* 58:191-5.

Table S3. Enzyme concentrations (nM) for steady-state kinetics

OXA-48 variants	Ampicillin	Piperacillin	Ceftazidime	Cefepime	Imipenem	Meropenem
wild-type	1	1	100	100	25	25
L67F	10	100	500	500	50	50
P68S	10	100	500	500	50	50
F72L	10	100	1000	1000	50	50
F156C	10	100	500	500	50	100
F156V	100	100	500	500	50	100
L158P	100	100	500	500	50	50
G160C	10	100	500	500	50	50
F72L/G131S	100	100	500	500	50	50
N146S/L158P	100	100	500	500	50	100

Table S4. X-ray data collection and refinement statistics for the OXA-48 variant L67F in complex with hydrolysed ceftazidime. Values in parenthesis are for the highest resolution shell.

	OXA-48:L67F
PDB no.	7ASS
Diffraction source	BL14.2, Bessy
Wavelength (Å), Temperature (°C)	0.9184, -173
Crystal-detector distance (mm)	174.9
Rotation range per image (°), total rotation range (°)	0.10, 190
Space group	P2 ₁ 2 ₁ 2 ₁
<i>a</i> , <i>b</i> , <i>c</i> (Å)	88.56, 108.48, 125.42
Resolution range (Å)	50.00-1.91 (1.94-1.91)
No. of unique reflections	94247 (4653)
Multiplicity	7.1 (7.3)
Completeness (%)	100 (99.9)
R _{merge} (%)	16.5 (187.0)
R _{pim} (%)	9.9 (111.0)
Mean $\langle I/\sigma(I) \rangle$	9.6 (1.1)
C 1/2	0.997 (0.583)
Overall <i>B</i> -factor from Wilson plot (Å ²)	14.4
Resolution range (Å)	23.56-1.91
Final R _{work} (%)	18.9
Final R _{free} (%)	22.98
Molecules in asymmetric unit	4
No. of non-H atoms (all protein chains)	8896
-Ions (Cl)	5
-Ligand (2 ceftazidime molecules)	76
-Water	797
R.m.s. deviations	
-Bonds (Å)	0.011
-Angles (°)	1.028
Average <i>B</i> -factors (Å ²)	30.3
- Protein chains A/B/C/D	31.1/26.9/29.4/30.9
-Ion (Cl)	46.9
-Ligand (2 ceftazidime molecules)	55.5
-Water	35.5
Ramachandran plot	
Most favored (%)	96.9
Allowed (%)	3.1

Appendix: Paper III

OXA-48 evolution is realised by very distinct trajectories leading to similar resistance levels

Christopher Fröhlich¹, Karol Buda², Trine J.W. Carlsen¹, Pål J. Johnsen³, Hanna-Kirsti S. Leiros¹, Nobuhiko Tokuriki²

¹ Department of Chemistry, UiT The Arctic University of Norway, Tromsø, Norway

² Michael Smith Laboratories, University of British Columbia, Canada

³ Department of Pharmacy, UiT The Arctic University of Norway, Tromsø, Norway

AUTHOR CONTRIBUTION

CF, NT conceived the study. CF performed directed evolution, selection, and all cloning. CF performed susceptibility testing. CF and TJWC expressed and purified enzymes. CF determined thermostabilities. KB and NT performed the statistical analysis. TJWC crystallised proteins and HKSL solved structures. HKSL and CF refined structures. CF and NT wrote the manuscript with input from all co-authors.

ABSTRACT

β -lactamases, such as OXA-48, are of major importance in the development of antimicrobial resistance. Yet, our ability to predict their evolution during antibiotic therapy is highly limited by two processes: antagonistic pleiotropy and epistasis. Here, we performed directed evolution on independent replicates to gradually adapt OXA-48 against increasing concentrations of the 3rd generation cephalosporin ceftazidime (CAZ). Over five rounds of evolution, we found completely distinct mutational set-ups allowing OXA-48, with acquisition of only four to five mutations, to increase CAZ resistance by up to 40-fold. Structural determination of one CAZ optimised OXA-48 mutant revealed a re-shaped and widened active site, likely allowing for better drug accommodation. The characterisation of adaptive landscapes, encompassing all mutational combinations, against multiple substrates demonstrated that initial mutations, marginally increasing CAZ resistance, caused strong

functional trade-offs against the penicillin piperacillin (PIP) and reduced the thermostability of OXA-48. However, the acquisition of subsequent mutations, further increasing CAZ resistance, did not exacerbate either trade-off, and thus resulted in an enzyme conferring resistance against PIP and CAZ. In-depth statistical analysis of the multidimensional landscapes showed that positive magnitude epistasis was a key player in driving the development of CAZ resistance and limiting the trade-off against PIP. Using a statistical model, we further exposed that pairwise and higher-order epistasis impairs the predictability of phenotypic outcomes. Our work demonstrates that OXA-48 can evolve through very distinct genetic trajectories leading to the similar phenotypic outcomes.

INTRODUCTION

The continuous evolution of antimicrobial degrading enzymes represents a major challenge for global human health^{1,2}. The plasticity of such enzymes allows them to adapt and expand their functional properties by, for example, enhancing the ability to degrade newer generations of antimicrobials^{3,4}. However, the expansion of functional properties is likely limited for many, if not most, enzymes and adaptation often causes functional trade-offs towards alternative drug(s), a phenomenon so-called 'collateral sensitivity' or 'antagonistic pleiotropy'⁴⁻¹¹. In theory, targeting these collateral effects could open the way for possible new treatment strategies to combat drug-resistant pathogens and overcome the development of resistance¹⁰. However, the utilisation of such strategies is restricted by our understanding of evolutionary dynamics and evolutionary limits of resistance enzymes.

One approach is to perform *in vitro* directed evolution to empirically test the evolutionary trajectories and dynamics of antimicrobial degrading enzymes. Several previous studies have demonstrated that directed evolution can identify the same spectrum of adaptive mutations that occurred in clinical settings^{9,12,13}. Moreover, adaptation towards new substrates often involves the accumulation of multiple mutations, and is driven by the non-additive interplay (epistasis) between multiple mutations. Thus, unveiling epistasis is also crucial for understanding the evolutionary dynamics of proteins. For example, some mutations become beneficial only after other mutation(s) are fixated due to positive epistasis, and by contrast, some initially beneficial mutations have shown to become inaccessible once other mutation(s) appear due to negative epistasis¹⁴⁻¹⁶. Such dynamics dictate the overall accessibility of evolutionary pathways and adaptive peaks within mutational landscapes¹⁶.

The evolutionary process of enzymes may be best depicted in genotype-phenotype landscapes, characterizing all possible combinations of mutations and visualising the accessibility of adaptive mutational paths to a phenotypic resistance maximum. Other studies investigated adaptive landscapes by showing the prevalence of epistasis, and limited accessible pathways to the phenotypic maxima during evolution of new enzymatic functions¹⁴⁻¹⁶. In particular, quantitative and statistical analyses of the genotype-phenotype landscapes,

coupled with biophysical and structural characterizations, have successfully exposed the molecular mechanisms underlying adaptive strategies¹⁷. Importantly, to understand the evolutionary dynamics of collateral effects, epistatic interactions between accumulating adaptive mutations need to be considered, as they may substantially reshape phenotypic landscapes, and thus the trade-off between native and new substrates. Consequently, systematic and statistical analyses on multi-dimensional genotype-phenotype landscapes are necessary to recapitulate the molecular basis underlying phenotypic pleiotropy and collateral effects of mutations.

Since first being reported in 2004, the Ambler class D β -lactamase OXA-48 has disseminated among various Gram-negative pathogens due to it being encoded on a successful epidemic plasmid and become one of the most relevant β -lactamases globally^{18,19}. While OXA-48 inherently possesses high hydrolysis activity against penicillins, such as piperacillin (PIP), its ability to catalyse 3rd generation cephalosporins including the clinically important ceftazidime (CAZ) is neglectable^{18,20}. However, variants such as OXA-163, OXA-247 and OXA-405 with a deletion in the β 5- β 6 loop have been recently identified, and exhibit increased hydrolytic activity against ceftazidime²¹⁻²³. In addition, we recently identified various single mutants of OXA-48 (e.g., L67F, P68A/S, F72L in the α 3 helix, and F156C/V, L158P, G160C in the Ω -loop), marginally elevating CAZ resistance in *Escherichia coli*^{24,25}. Interestingly, these natural and laboratory identified variants exhibited strong functional trade-offs against penicillins and carbapenems²⁴⁻²⁷. Those observations have poised many important questions regarding the evolution of OXA-48: *i)* To which extent can OXA-48 adapt to confer CAZ resistance? *ii)* How many mutations are required to fully adapt to CAZ? *iii)* Is there only one mutational pathway or multiple pathways to reach adaptive peaks? *iv)* How does CAZ and PIP resistance trade-off? *v)* How does epistasis shape the adaptive landscape? *vi)* What are the molecular and structural mechanisms for the adaptation?

Here, we performed directed evolution of OXA-48 combining in-depth mutational, microbiological, biophysical and structural characterizations to unveil the evolutionary potential, trend, and basis for the underlying development of CAZ resistance. First, we

conducted an iterative cycle of directed evolution using three independent replicates and investigated the genotypic and phenotypic changes underlying the evolutionary trajectories. Second, we constructed adaptive landscapes on a subset of mutations that are responsible for the increase in CAZ resistance and characterized the genotype-phenotype landscapes towards the alternative substrate PIP. First, we analysed how the acquisition of mutations acquired early during the evolution caused pleiotropy by determining their PIP resistance and the thermostability of purified single mutants. Second, we analysed how pleiotropic effects in multi-step mutants changed along the evolutionary trajectories. The multidimensionally characterised landscapes were further subjected to a statistical analysis, to elucidate how epistasis shapes the evolutionary dynamics of OXA-48, in terms of evolutionary potential to CAZ, and associated collateral sensitivity towards PIP. Finally, we characterized structural changes in a CAZ adapted variant, and unveiled the molecular basis underlying the adaptation.

RESULTS

Evolution of OXA-48: similar phenotypes but distinct mutational pathways

To investigate the evolutionary potential of OXA-48, we performed three independent replicates of directed evolution towards increasing concentrations of CAZ (Figure 1A), resulting in trajectories I, II and III (TI to TIII). Briefly, mutational libraries were generated using error-prone PCR, containing at least 5000 variants and on average 1 to 2 amino acid changes per gene. The libraries were subcloned into a low-copy number vector (p15A origin, ~10 copies per cell), transformed into *E. coli* E. cloni[®] 10G cells and selected on LB-agar with increasing concentrations of CAZ. Up to 10 colonies were selected from the plates with the highest concentration of CAZ, characterised by Sanger sequencing and by susceptibility testing. Clones exhibiting the highest CAZ resistance were isolated and served as a template for the next round of mutagenesis (Figure 1B). The level of resistance for each variant was determined by measuring dose-response curves and calculating the half maximal inhibitory concentration (IC_{50}).

While expression of wild-type OXA-48 (wtOXA-48) did not increase the IC_{50} towards CAZ, five rounds of directed evolution resulted in variants exhibiting CAZ IC_{50} values up to ~40-fold above the baseline resistance of the ancestral *E. coli* strain (Table 1). In all three trajectories resistance development increased similarly and plateaued within one to five rounds of directed evolution (Figure 1C), suggesting that the trajectories reached local maxima or evolutionary dead ends. To understand the genotypic variation causing the changes in CAZ resistance, we determined the sequence of intermediate variants obtained after every round of directed evolution and found that five to 10 mutations were accumulated within each trajectory. Unexpectedly, the mutations acquired were completely distinct between the three trajectories, neither the same mutation nor the same amino acid position was shared across the trajectories (Figure 1D). Yet, all mutations clustered around the active site and were often found in structural elements which have previously been described to modulate substrate specificity such as the α 3 helix, the Ω - and β 5- β 6 loops (Figure 1E)^{24,25,28,29}. To identify the mutations that contribute to the development of CAZ resistance, we selected a sub-set of

mutations either located closely around the active site and/or reported within naturally evolving variants (four out of five mutations for TI, six out of 10 for TII, and six out of eight for TIII), and generated variants with all possible mutational combinations for each trajectory. Corresponding to the sub-set selection of TI to TIII, this resulted in 3 adaptive landscapes (LI:16 variants, LII: 64 variants, LIII: 64 variants), which were characterized by determining their IC_{50} values (Figure S1A, IC_{50} values: Table S1 to S3). We found that only four out of the 16 tested mutations increased CAZ resistance significantly by 2- to 3-fold in the initial step of the evolution: only a single mutation from LI (F72L) and LIII (L158P), and two mutations from LII (Q124H and F156D). The other 12 mutations acted neutrally (<1.5-fold increase in IC_{50}) compared to wtOXA-48. Yet, the majority seemed to exhibit conditional positive effects, as the overall CAZ resistance in each landscape increased by up to 26- to 40-fold (Figure S1). However, some mutations from our selected sub-set were not required to reach these maxima. For example, while for LI all four mutations contributed to resistance development, only four out of six were needed to reach the maxima in the landscapes LII and LIII, which could indicate the presence of hitchhikers (Figure S1).

Table 1: Determined IC_{50} values towards ceftazidime for clones selected during the directed evolution experiment.

Selected clones ^{a,b}	IC_{50} (mg/L)		
	Trajectory I	Trajectory II	Trajectory III
Round 1	0.029	0.078	0.327
Round 2	0.121	0.317	0.235
Round 3	0.221	0.350	0.204
Round 4	0.461	0.143	0.330
Round 5	0.556	0.324	0.300

^a *E. coli* E. cloni[®] 10G ceftazidime IC_{50} = 0.012 mg/L

^b *E. coli* E. cloni[®] 10G + *bla*_{OXA-48} ceftazidime IC_{50} = 0.013 mg/L

Even though we identified variants harbouring multiple changes already after the first round of directed evolution (Figure 1D), the landscapes showed that CAZ resistance can be increased step-by-step, and thus the here identified variants with multiple changes are accessible by natural selection (Figure 1F). Next, we aimed to understand whether the sequential accumulation of mutations represent the most efficient trajectories (highest increase in CAZ with least mutational changes). We found that for all landscapes resistance developed through genotypes conferring lower resistance and that alternative trajectories were accessible, leading to same maxima. This suggests that evolution proceeded through variants with sub-optimal phenotypes (Figure 1E).

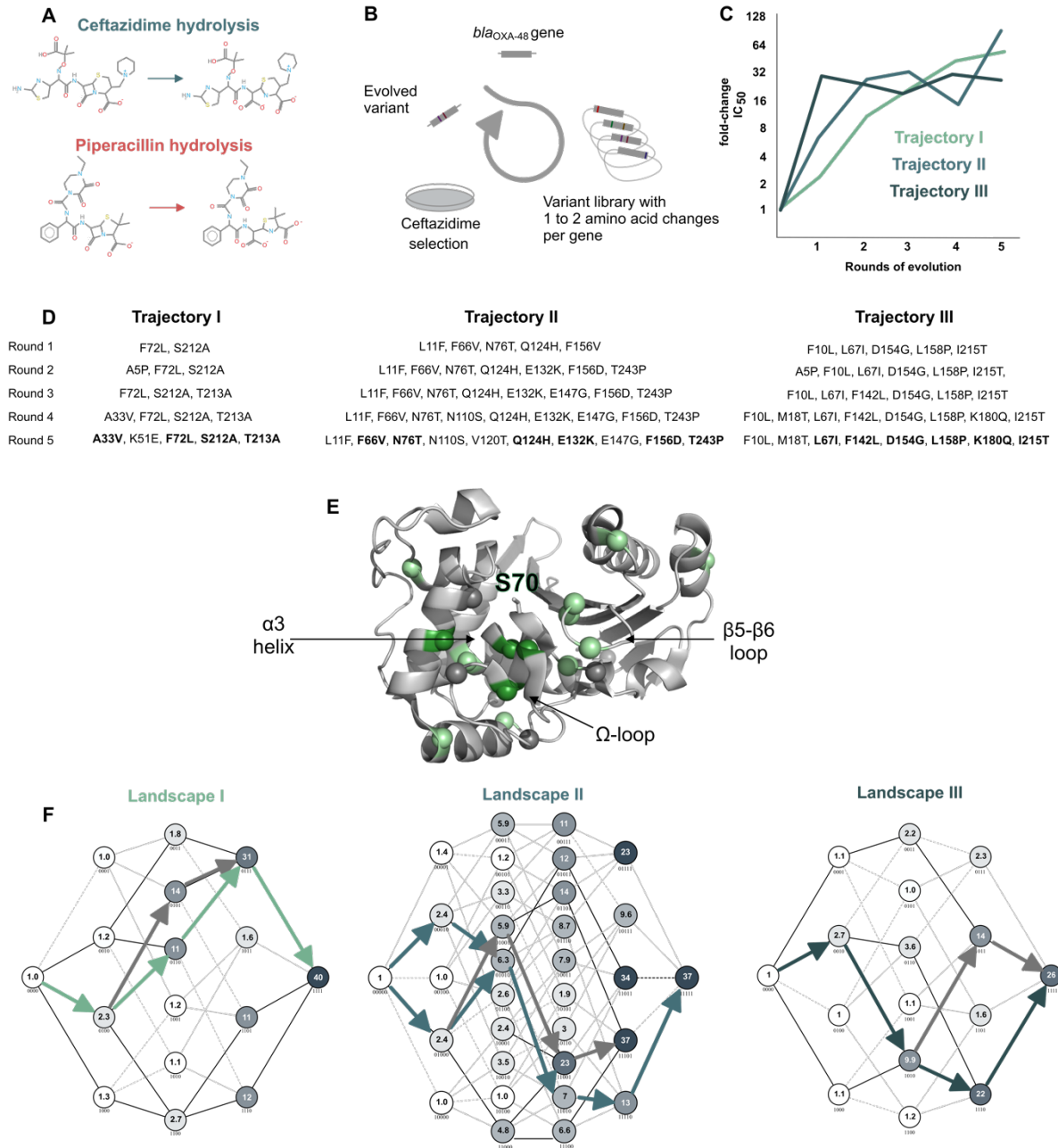


Figure 1: Evolution of OXA-48. A. Chemical structures of the 3rd generation cephalosporin ceftazidime and the penicillin piperacillin. B. Schematic overview of the experimental set-up. C. Fold-change in ceftazidime *IC*₅₀ for clones selected over different rounds of directed evolution for all three trajectories/replicates. D. OXA-48 mutants recovered after every round. Mutations shown in bold were selected to construct fitness landscapes. E. Structural overview on the location of initial mutations (green), functional mutations later acquired during the evolution (light green) and mutations not sampled and likely not functional (grey). F. Adaptive landscapes for CAZ resistance development in OXA-48 with only mutations contributing to

CAZ resistance. The full landscape including mutations acting neutrally throughout the landscape are shown in Figure S1. Each node represents a unique variant. The mutational combination for each node is shown as numerical code where '0' refers to the wtOXA-48 amino acid and '1' represents a specific mutation (that is for landscape I: A33V, F72L, S212A, T213; for landscape II: N76T, Q124H, E132K, F156D, T243P; for landscape III: L67I, F142L, L158P, I215T). For example, 1001 refers to the mutational combination of A33V/T213A within landscape I. The number within each node represents the ceftazidime IC_{50} fold-change of the mutational combination compared to wtOXA-48. The colored arrows show the stepwise increase in CAZ resistance depicts the development of CAZ resistance through the least mutational step and variants displaying the highest resistance.

Incompatibility of initial mutations causes distinct mutational pathways

TI to TIII exhibited very similar trends for both the number of adaptive mutations (four to five mutations) and the level of CAZ resistance (~26 to 40-fold). This is an uncommon observation compared to other directed evolution studies of enzymes with multiple replicates, which typically identified the same key mutations repeatedly in multiple trajectories^{30,31}. This indicates that extensive epistasis among mutations in different trajectories exists where adaptive mutations in one trajectory may restrict the effect of adaptive mutations from other trajectories. To test this, we probed the incompatibility between different adaptive mutations by adding the initial mutations F156D (LII) and L158P (LIII) onto the evolved CAZ-optimised variant of LI (LI-4: A33V/F72L/S212A/T213A). Indeed, while F156D and L158P increased CAZ resistance by ~2-fold compared to wtOXA-48 (Figure 1F) both mutations behaved neutrally in the LI-4 variant (Figure 2). This suggests that the three trajectories likely follow independent mutational pathways which are rather exclusive to each other, and reached distinct local maxima in the adaptive landscape.

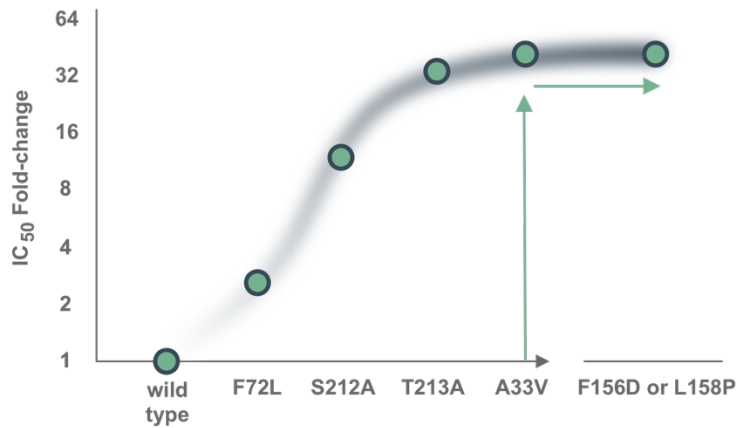


Figure 2: Development of the ceftazidime IC_{50} fold-change in the optimised variant L1-4 (F72L/S212A/T213A/A33V) after introduction of F156D and F158P. The stepwise acquisition of F72L, S212A, T213A, and A33V elevated the ceftazidime IC_{50} by 40-fold which was not further increased upon the acquisition of F156D and L158P.

CAZ adaption causes a strong but limited PIP trade-off

We sought to understand how the development of CAZ resistance affected resistance against PIP, a substrate which is efficiently hydrolysed by OXA-48, by obtaining IC_{50} data for all variants within all adaptive landscapes (Figure S2). In general, all three trajectories exhibited trade-offs between CAZ and PIP resistance. All four mutations (F72L, Q124H, F156D and L158P) initially increasing CAZ resistance in wtOXA-48 decreased PIP resistance. Moreover, for these mutants PIP resistance decreased by 8- to 96-fold which significantly exceeded their 2- to 3-fold improvement in CAZ resistance. Further, of all mutations not affecting CAZ resistance initially (compared to wtOXA-48), only two (N76T and S212A) decreased resistance to PIP (25 and >125-fold, respectively). Consequently, our data show that single mutants increasing CAZ resistance tend to exhibit strong trade-offs against PIP, where the initial loss in PIP resistance outweighs the initial gain in CAZ resistance. Such strong functional trade-offs are rather an exception during adaptive evolution, as most studied enzymes tend to exhibit weak trade-offs with high evolvability of new functions and without strongly compromising their native activity^{4,32-34}.

To further our understanding of how these trade-offs develop across the adaptive landscapes, especially with increasing CAZ resistance, we examined the correlation between changes in IC_{50} towards CAZ and PIP resistance for all combinatorial mutations (Figure 3A). Overall, the trajectories exhibit a rather unique IC_{50} trade-off trend between the “native” and “new” substrates; a convex relationship between CAZ and PIP. While the trajectories exhibited strong initial trade-offs, we found that PIP resistance did not reduce with increasing resistance towards CAZ. Indeed, PIP resistance was stably maintained 3- to 8-fold above the susceptibility of *E. coli* without OXA-48 expression (Figure 3A). Consequently, the trade-off over the evolutionary course was rather limited, where ~30- to 40-fold increased resistance against CAZ resulted in an overall PIP resistance reduction of also 30 to 40-fold. Thus, the evolved variants maintained bifunctionality, which conferred increased CAZ and PIP resistance in *E. coli*. Strikingly, the observation is consistent across the three trajectories, although they comprise distinct sets of mutations, suggesting that this evolutionary trend in OXA-48 may be universal regardless of the genetic solution.

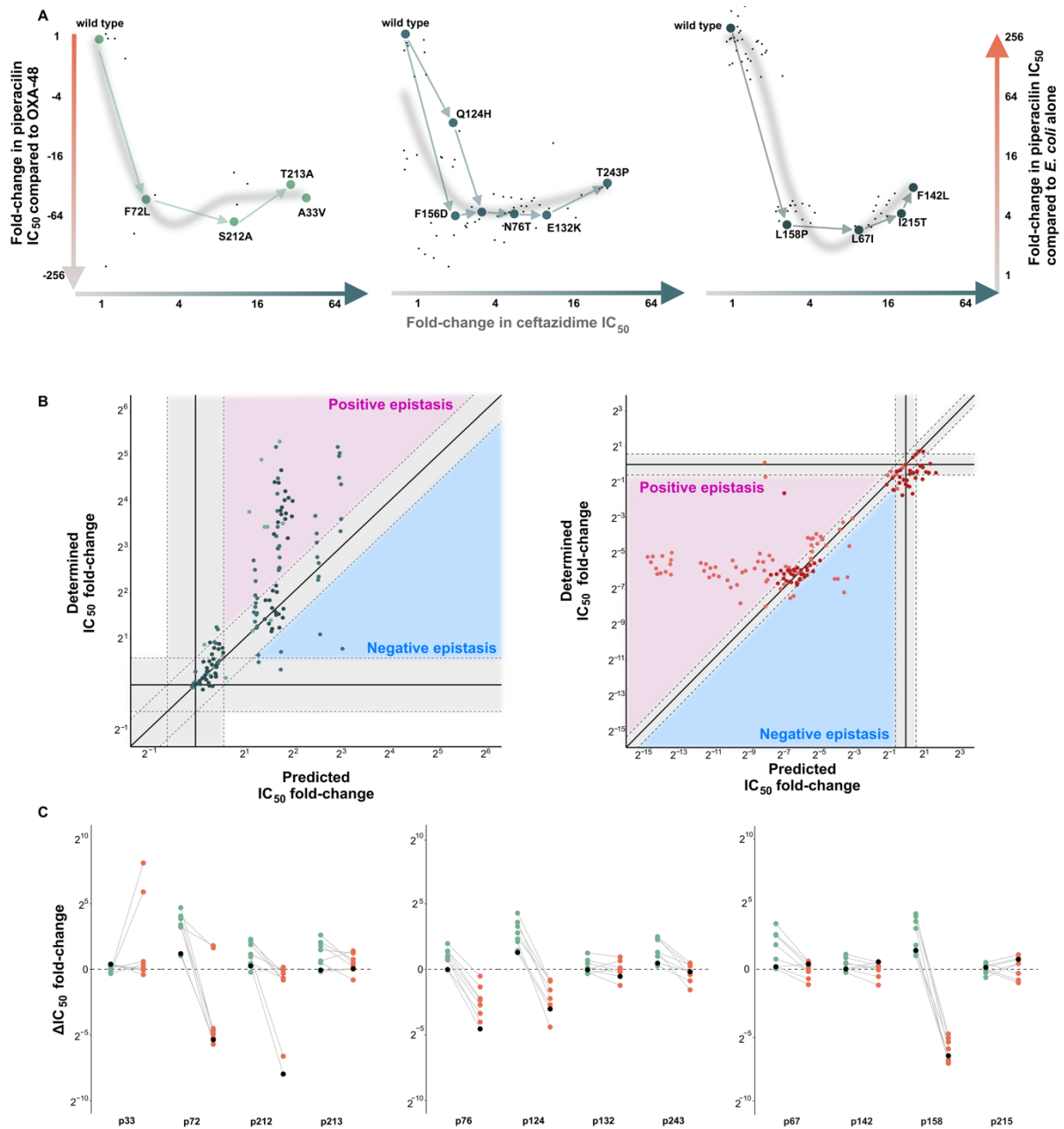


Figure 3: Trade-off and epistasis. A. Relationship between PIP resistance in *E. coli* E.cloni[®] 10G with (left axis) and without (right axis) OXA-48 versus CAZ IC_{50} fold-changes for all mutational combinations. Fold-changes were calculated compared to IC_{50} values obtained from *E. coli* E.cloni[®] 10G with and without wtOXA-48. The green arrows show the accumulation of mutations within each trajectory according to their appearance during directed evolution. The grey line represents the average trade-off. B. Determined versus predicted IC_{50} fold-changes for landscapes characterised towards CAZ (left, green dots) and PIP (right, orange dots). The colored dots represent the landscapes I (lightest), II (medium) and III

(darkest). The grey areas show non-significant fold-changes (<1.5-fold). While dots within the pink area show positive epistasis where the resistance is higher than expected, dots within the blue area demonstrate negative epistasis. C. The difference in IC_{50} fold-changes after the initial introduction of a mutation into wtOXA-48 (black dots) and the difference in IC_{50} fold-changes of the same mutation in different genetic background (double, triple mutants etc.). The phenotypic variation is shown for of each mutant position for ceftazidime (green) and piperacillin (orange).

Initial mutations cause a stability related trade-off

Generally, most of acquired mutations are destabilising and only a small fraction of mutations is thought to improve thermostability^{35,36}. This has consequences for the evolvability of new enzymatic functions, as enzymes need to be maintained above a stability threshold in order to possess functionality. To understand whether there is a correlation between the global enzymatic thermostability and CAZ and PIP resistance, all 16 single mutants from our adaptive landscapes were expressed, His-tag purified and their thermostability was determined (Table S4). Firstly, our investigations showed that 50% of all single mutations decreased the global thermostability by more than 0.5°C and were usually highly destabilising (up to ~8°C). In addition, 38% of all mutations were neutral or changed the thermostability only marginally (< 0.5°C). Only two out of 16 single variants were found to be stabilising, where the stabilising effect ranged from only 1 to 2°C. Secondly, we compared all single variants to wtOXA-48 and plotted their change in thermostability (ΔT_M) versus their IC_{50} fold-changes (Figure 4A). The above-mentioned initial variants increasing CAZ resistance such as F72L, Q124H, F156D and L158P were highly destabilising and decreased thermostability by ~6 to 8°C. Thus, initial mutations increasing CAZ resistance tend to lower the thermostability of OXA-48, which is in agreement with previous studies^{24,37}.

Next, we investigated how thermostability changes within variants exhibiting increased CAZ resistance. For LI, F72L improved CAZ resistance by 2-fold and decreased thermostability by 7°C compared to wtOXA-48. The stepwise acquisition of S212A, T213A

and A33V increased CAZ resistance gradually up to 40-fold (Figure 1F). Yet, the thermostability of these variants remained rather unchanged and after the initial introduction of F72L (Figure 4B). Thus, our data suggest that initial adaptive mutations may be destabilising, but that CAZ resistance within such variants can increase without further compromising thermostability.

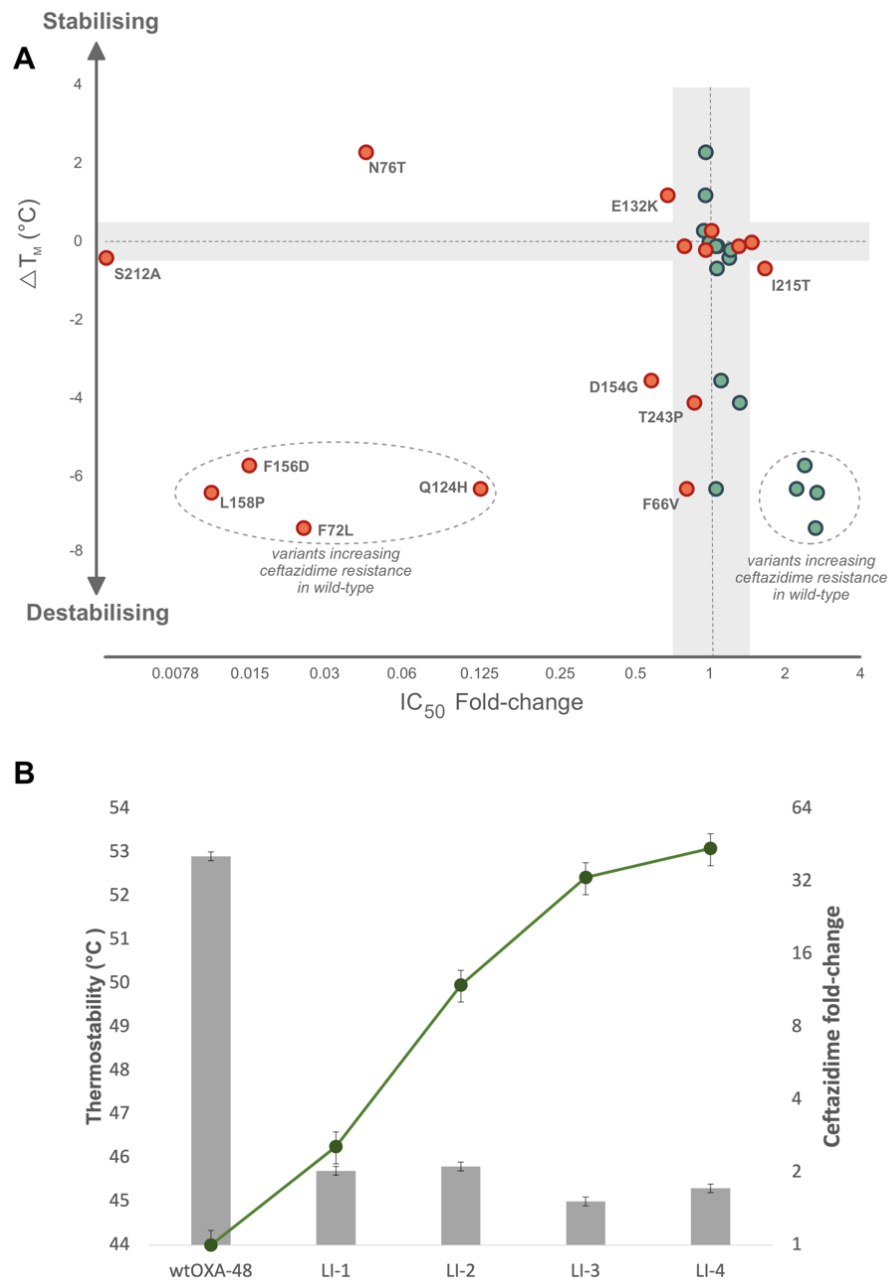


Figure 4: Relationship between thermostability *versus* IC₅₀ fold-change for CAZ. A. Thermostability of all selected single mutants *versus* the corresponding CAZ (green dots) and

PIP (orange dots) IC_{50} fold-changes was plotted. The grey areas indicate small susceptibility and thermostability changes of ± 1.5 -fold and $\pm 0.5^{\circ}\text{C}$. B. Thermostability of mutants (wtOXA-48: wild-type OXA-48, LI-1: F72L, LI-2: F72L/S212A, LI-3: F72L/S212A/T213A, LI-4: A33/F72L/S212A/T213A) from landscape I (bars) and their CAZ IC_{50} fold-change (dots). The displayed IC_{50} fold-changes are normalised to resistance conferred by wtOXA-48. Error bars represent the standard deviation from three replicates.

Positive magnitude epistasis drives both resistance and trade-off

The adaptive landscapes for CAZ and PIP suggested the prevalence of epistasis among adaptive mutations in OXA-48. As a result of epistasis, all landscapes exhibited highly rugged topology, where only a fraction (eight of 24 for LI, seven of 24 for LII and six of 24 for LIII) of all possible trajectories are accessible as gradual and stepwise increment to the closest local maximum (Figure 1F). We quantified the extent of epistasis underlying the landscapes of PIP and CAZ. In brief, epistasis was calculated based on the difference between determined and predicted IC_{50} fold-changes. The prediction was done based on a null model using only the mutational effects of single mutants and assuming that if combined their effect behaved additively.

Plotting the determined *versus* predicted CAZ IC_{50} fold-changes showed that generally determined CAZ resistance was higher than predicted, and, only in LII, some variants exhibited lower values (Figure 3B). For example, the evolved variants of LI to LIII with the highest CAZ resistance are predicted to increase CAZ resistance by only ~8-fold (or 2^3 on a \log_2 scale), however, their determined resistance is ~2-log steps higher (2^5 on a \log_2 scale) than expected. This suggests that positive epistasis between adaptive mutations is prevalent in the CAZ landscapes, where initial mutations recruit subsequent mutations, which behave neutrally in wtOXA-48, and render their functional effect positive (Figure 3B). To better understand the distribution of epistatic effects, we performed an analysis of all mutations and how they affected resistance phenotypes in all possible genetic backgrounds (Figure 3C). This disclosed that the majority of amino acids are affected by substantial epistasis where CAZ resistance varied by >2-fold change depending on the genetic composition. Among others, the amino acid positions 67, 72, 124 and 158 showed the highest variability, where depending on the genetic background, CAZ resistance varied up to ~11-fold, compared to wtOXA-48.

Similarly, the determined IC_{50} fold-changes for PIP resistance in LI and LII were higher than predicted. Indeed, some of the evolved variants in LI and LII are predicted to exhibit >300-fold reduced PIP resistance, compared to wtOXA-48. In fact, a reduction by more >300-fold would lead to no detectable PIP resistance in the *E. coli* background. However, we

observed that these variants still exhibited significant resistance levels against PIP, which were 4- to 16-fold higher than the *E. coli* background. This is likely caused by positive epistasis between deleterious mutations, where the combination of multiple negative mutations exhibits diminishing losses. On the contrary, the predicted values for LIII largely agreed with the determined susceptibilities. Also here, we investigated how phenotypic data scattered for each position (Figure 3C). Among others, the position 72, 124 and 156 displayed the highest variability in PIP resistance, depending on the genetic background. For position 158, all mutational combinations performed worse than wtOXA-48, demonstrating that the PIP trade-off was mainly determined by L158P. Furthermore, while the introduction of mutations such as F72L, N76T and S212A into wtOXA-48 caused a strong reduction in PIP resistance, in combination with other mutations of the landscapes, positive epistasis likely compensated for the initial trade-off.

Thus, epistatic effects between CAZ and PIP landscapes seem to be similar, where the effect of one mutation, in other genetic backgrounds than wtOXA-48, tend to generate higher variability (Figure 3C). Taken together, the convex relationship between OXA-48-mediated CAZ *versus* PIP resistance is mainly caused by positive epistasis. Our data further suggests that the fixation of initial adaptive mutations render the mutational effect of subsequently acquired mutations. This opens pathways to gradually increase CAZ resistance and at the same time “buffers” the deleterious effect of mutations leading to stabilised resistance levels of PIP.

Adaptive landscapes are shaped by pairwise and high-order epistasis

The characterization of LI to LIII towards two substrates provided material to study the predictability of evolutionary outcomes with limited phenotypic information. More specifically, we investigated how much phenotypic data is required to predict the resistance development of variants accumulating multiple genetic changes. This question is of high importance as recent development of high-throughput phenotyping of massive mutational libraries, using deep mutational scanning allows us to determine the effects of all possible single changes, some sets of pairwise and higher order mutational combinations, effectively³⁸. To that end, we developed a “feed-forward” model (see method description) where CAZ and PIP resistance of multi-step mutants was predicted using different orders of phenotypic information. In brief, we first used the abovementioned additive model, which reflects all single step mutants in wtOXA-48 and predicted resistance development of all double, triple mutants etc. We calculated epistatic coefficients for each genotype in each order. For example, we calculated how the acquisition of a third mutation would change resistance compared to the corresponding double mutant. Next, we stepwise informed the additive model with these coefficients of higher orders such as double and triple etc. mutants and determined the improvement in predictability for the residual landscape. The predictability was quantified for each order of the model as the mean average error (MAE) between the determined and predicted IC_{50} fold-changes (Table 2, see method description).

Table 2: Predictability of CAZ and PIP resistance based on the mean average error (MAE) between determined and predicted IC_{50} fold-changes and their standard deviation. Thus, the MAE represents the average fold-change between determined and predicted resistance of the residual landscapes. The standard deviation is a measure of how the residual MAEs scatter.

	CAZ resistance prediction based on MAE			PIP resistance prediction based on MAE		
	Landscape I	Landscape II	Landscape III	Landscape I	Landscape II	Landscape III
Order 1	2.9±2.5	1.9±1.7	1.7±1.8	23±14	9.2±6.5	1.8±1.7
Order 2	1.7±1.6	1.7±1.5	1.4±1.4	16±18	2.9±2.6	8.1±4.0
Order 3	1.9	1.9±2.1	2.1±1.9	1.87	2.8±2.4	10.8±6.9
Order 4	NA	1.8±1.7	2.9±2.9	NA	1.9±1.8	5.6±4.4
Order 5	NA	1.7	3.0	NA	4.2	6.5

NA, not applicable

Using only single mutational effects to predict the MAE (1st order), we found that CAZ and PIP resistance was on average underestimated by 2- to 3-fold and 2 to 22-fold, respectively. The inclusion of phenotypic data from all double mutants (2nd order) improved the predictability in TI and TII for both CAZ and PIP. For example, the 1st order model of LI for CAZ is estimated with an MAE of ~3-fold, which was improved to 1.7-fold when accounting for pair-wise interactions (2nd order). The inclusion of 3rd and higher orders improved the predictability further in LI for PIP, but only caused modest improvement in LI and LII for CAZ and LII for PIP. This suggests that the information of the pairwise interactions is necessary and largely sufficient to predict evolutionary outcomes on average caused by four to five mutations. In TIII, the 1st order prediction largely recapitulates all variants' resistance, however, the incorporation of the second step worsened the predictions, and the inclusion of the 3rd and higher steps reconciled the discrepancy, suggesting that higher-order epistasis is still prevalent among mutations, and the epistatic nature of the genotypes appears to be too unrobust to predict.

To understand how single values, contributing to MAEs for different orders, scatter, we also calculated their standard deviations. Compared to the MAE, the standard deviation was

high for all landscapes and orders, indicating that each order hosts phenotypes with much lower predictability, likely due to case-specific pairwise and higher order epistasis.

Re-shaping of the active site allows improved accommodation of CAZ

To understand how OXA-48 structurally adapted to increase CAZ resistance, the endpoint mutants for each landscape were purified and crystalised. We were able to obtain two individual crystals structures for our LI-4 variant with and without covalently bound CAZ within the active site (named from here on LI-4 and LI-4-CAZ). The structures were solved to 1.17 Å (LI-4, 1 chain, space group C2) and 2.66 Å (LI-4-CAZ, 4 chains, space group P6₁), respectively.

In our previous work, we showed that F72 is involved in aromatic stacking interactions with F156 and W157 in the Ω -loop, and that in F72L, a lack of this interaction caused an increased flexibility of the Ω -loop. In LI-4, the same mutation was identified in combination with A33V, S212A and T213A. To understand whether these mutations imposed structural changes within the active site, the structure of LI-4 without CAZ was superimposed onto the wtOXA-48 structure (PDB no. 4S2P³⁹). Superimposition resulted in an overall low root mean square deviation of 0.4 Å. However, we found that the Ω -loop was turned by 90°, increasing the structural space between the Ω - and β 5- β 6 loops (Figure 5A). In addition, this change caused the active site to reshape and many active site residues were found to be displaced (Figure 5B). For example, W157 stabilises the carboxylated lysine in wtOXA-48. In our LI-4 structure, this residue was displaced by 5.6 Å (C α -atom) and moved outwards of the active site. Similarly, the C α -atom of L158, a residue involved in carbapenem binding^{40,41}, was moved by 3 Å (Figure S3A). D154, which interacts electrostatically with R218 in wtOXA-48, was moved by 9 Å (C α -atom) and found to be 6 Å closer to the β 5- β 6 loop (Figure S3B).

Despite two amino acid changes in the β 5- β 6 loop (S212A and T213A), the shape of this loop was preserved in LI-4. In wtOXA-48, the Ω - and β 5- β 6 loops interact *via* a salt bridge mediated by D159 and R214. In our structure, the side chain of R214 was disordered since

no electron density could be detected, and thus it is not clear whether these loops interact through the same molecular mechanism.

Next, we investigated substrate binding in the LI-4-CAZ, compared to the wtOXA-48 structure, and our previously published structure on OXA-48:P68A with CAZ covalently bound in the active site(Figure 5C)²⁴. Similar to P68A, the Ω -loop in LI-4-CAZ was displaced upon CAZ binding and could therefore not be reconstructed. The oxyimino group of CAZ reached ~1 Å deeper into the active site of LI-4-CAZ, compared to P68A-CAZ, but the overall CAZ molecules was only subtle re-positioned, and thus underwent comparable interactions. For example, the amino acids at the positions T209, Y211 and R250 were involved in stabilising CAZ within the active site of LI-4-CAZ. However, in our P68A structure, both S212 and T213 were involved in H-bonds interactions with CAZ, which were not present in the structure of LI-4-CAZ due to the alanine at position 212 and 213. Further, the above-mentioned arginine at position 214 was also disordered in LI-4-CAZ. The position of R214, was also found to be affected in P68A-CAZ²⁴. The fact that, in both LI-4 and LI-4-CAZ, R214 was disordered indicates that the mutations acquired may change the interplay between the Ω - and β 5- β 6 loops. As a result, the new conformation of the Ω -loop (as found in LI-4) may allow the negatively charged oxyimino group to sink deeper into the active site (Figure S3A and B).

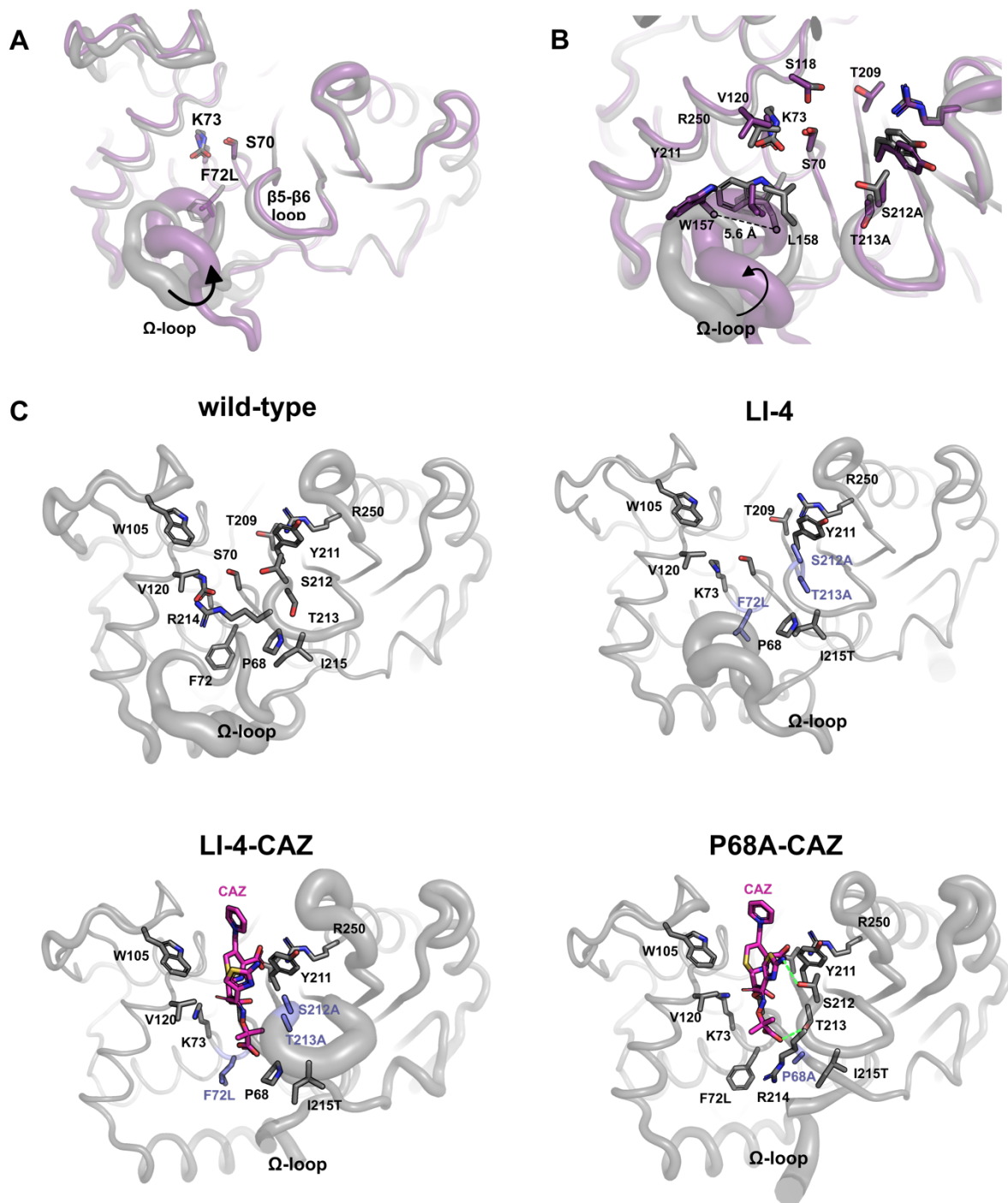


Figure 5: Structural overview of the adaptational process towards ceftazidime (CAZ) in OXA-48. A. Superimposition of wild-type OXA-48 (grey, 4S2P chain A) onto our LI-4 mutant (violet, A33V/F72L/S212A/T213A) without CAZ bound within the active site. The black arrow indicates the structural movement of the Ω -loop. B. The movement of the Ω -loop in LI-4 (violet) reshaped the active site compared to wild-type OXA-48 (grey, 4S2P chain A), where several active site residues were found to be displayed. Structural comparison between wild-type

OXA-48 (top left, 4S2P), LI-4 (top right), LI-4-CAZ (bottom left) and P68A-CAZ (bottom right). CAZ is shown in pink and amino acid changes in violet. For P68A-CAZ, H-bonds between S212/T213 and CAZ are shown in green.

DISCUSSION

Here, we investigated the evolution of the globally circulating β -lactamase OXA-48 towards the oxyimino cephalosporin CAZ and showed that the evolutionary process caused strong pleiotropic effects. Indeed, mutations initially acquired and responsible for increased CAZ resistance induced both strong functional (Figure 3A; ~3-fold gain in CAZ resistance *versus* ~100-fold loss in PIP resistance) and thermostability-related (Figure 4A; ~6 to 8°C decrease) trade-offs. This is in line with other studies showing that the evolution of oxyimino cephalosporin resistance, in various β -lactamases, is frequently related to strong functional and thermostability trade-offs^{4,32-34}. Strong functional trade-offs are thought to be rather an exception during evolution, as many enzymes have been described to initially improve new functions without significantly comprising their native activity^{4,42}. However, if they occur, they have been related to structural differences of the new substrate, such as significant changes in size and charge⁴. Consequently, the evolution of β -lactamases towards bulkier β -lactams, such as oxyimino cephalosporins, has been frequently reported to cause strong functional trade-offs towards other β -lactams^{31,43-46}. Studies on the molecular mechanisms of these trade-offs have shown that adaption to bulkier β -lactam substrates likely causes increased conformational freedom, resulting in non-productive binding modes for other β -lactams due to a reduction in their deacylation rate^{47,48}. It is likely that a similar mechanism underlies the PIP trade-off observed in our evolved variants. Previously conducted molecular dynamic simulations of F72L and L158P demonstrated increased flexibility of the Ω - and β 5- β 6 loops in OXA-48, which could in fact increase conformational freedom and lead to non-productive binding^{4,32-34}. Our data further indicate that initial mutations, which increase CAZ resistance, are mainly responsible for the strong functional trade-off, since PIP resistance was stably maintained at low levels and CAZ resistance increased during evolution. Taken together, initial mutations in OXA-48, responsible for increased resistance towards CAZ, confer an evolutionary trade-off towards PIP. However, this trade-off is limited during long-term evolution, likely due to positive epistasis, resulting in OXA-48 variants with the ability to confer resistance against both PIP and CAZ.

Previous structural investigations on OXA-48 showed that the carboxylated, and thus negatively charged oxyimino side chain of CAZ, reaches into the active site where it collides with amino acids from the Ω - and β 5- β 6-loop. Poor accommodation and structural clashes of CAZ have been described for other serine β -lactamases, such as the class A enzymes KPC, TEM and CTX-M, and are thought to be responsible for the relatively low catalytic activity against CAZ compared to other β -lactams³. Here, we used X-ray crystallography to study the structure of our CAZ optimised LI-4 variant and found that the active site around the Ω -loop was re-shaped. This adaptation broadened the structural space between the Ω - and β 5- β 6 loops and likely improves the accommodation of ceftazidime (Figure S3). Similar strategies have been observed for various other β -lactamases, such as OXA-163, TEM and CTX-M, where the expansion of the active site improved the accommodation of oxyimino cephalosporins and consequently the catalysis. Interestingly, in OXA-48 variants (e.g., OXA-163, OXA-232, OXA-247, and OXA-405) identified in clinical isolates, increased CAZ resistance is promoted by deletions and amino acid substitutions around the β 5- β 6 loop^{21-23,49}. On the contrary, the results from this and our previous work showed that CAZ resistance can also develop through sequential acquisition of point mutations, demonstrating that similar fitness optima can be reached through multiple distinct trajectories^{24,25}.

From a clinical microbiology point of view, the ability to predict resistance development and trade-offs could have profound implications on choice and success of antimicrobial treatment strategies. To test how epistasis impairs such predictability, we evolved different replicates of OXA-48 independently. Compared to previous studies, we were able to re-identify several initial mutations such as L158P, F72L and F156x, indicating that the selection of initial mutations is repeatable. However, mutations acquired early during the adaptive process might impose epistasis and direct evolutionary trajectories^{22,33}. By doing so, they may influence the effect of other beneficial mutations, preventing their fixation. This has likely happened during the natural evolution of TEM-1 and CTX-M-1 towards cefotaxime and CAZ, respectively, where distinct evolutionary starting points created a historical contingency shaping the

genetical composition during long-term evolution^{22,33}. Similarly, we found that selection for increased OXA-48 mediated CAZ resistance led to mutationally distinct trajectories, conferring similar levels of CAZ resistance. To probe the compatibility of our trajectories, we combined initial mutations from different trajectories responsible for increased CAZ resistance with the CAZ optimised variant LI-4 (Figure 2). Our data show that despite the selective advantage of F156D and L158P in wtOXA-48, they do not further improve resistance in the optimised variant. Thus, our data provides further support for the role of epistasis driving the divergence of evolutionary trajectories.

To further understand phenotypic predictability solely from the genotype, we investigated how epistatic effects impair our ability to predict antimicrobial resistance development. First, we found that the evolution of OXA-48 is driven by pairwise and higher-order epistasis which is in agreement with other studies^{14-16,50,51}. To understand predictability, we set up a “feed-forward” model to quantify how much phenotypic information is needed to predict CAZ and PIP resistance of different variants from our landscapes. Our data show that the inclusion of pair-wise interactions often improved predictability (Table 2), however, there was a substantial amount of higher order epistasis in most of the trajectories, which impaired a robust prediction of resistance phenotypes. To that end, while the average predictability improved with accounting for pairwise interactions, the variation of the predicted values remained high compared to the corresponding MAE, showing that the predictability of phenotypes is heterogeneous.

In conclusion, positive epistasis drives the divergent evolution of OXA-48 mediated CAZ resistance. In addition, this adaptational process comes with a strong, but limited functional trade-off against PIP, resulting in an enzyme with the ability to catalyse both drugs. The presence of epistasis and the fact that multiple distinct evolutionary trajectories were selectable impaired the predictability of both resistance and trade-off development.

MATERIALS AND METHODS

General material

LB agar, broth, chloramphenicol, ampicillin, CAZ, and PIP were purchased from Sigma-Aldrich (MO, USA). Primers (P) used for this study are shown in Table S5. All cloning enzymes were purchased from Thermo Fisher Scientific (MA, USA), if not stated otherwise. The *E. coli* E. cloni® 10G was obtained from Lucigen (WI, USA).

Cloning and vector construction

The construction of the low copy number vector pUN-*bla*_{OXA-48} was previously published²⁵. This vector was further modified (pUNE). First, the primers P9 and P10 were used to remove the NcoI cutting site within the chloramphenicol resistance gene. Second, using P3/P4 on the vector backbone and P1/P2 on the *bla*_{OXA-48} insert, a XhoI restriction site was inserted after the *bla*_{OXA-48} stop codon, and pre-existing NdeI restriction site was modified to NcoI by inserting a glycine residue the starting amino acid. PCR amplicons were digested using NcoI, XhoI, DpnI for 1 h at 37°C. Digestion mixtures were purified and ligated in a molar ratio of 1:3. Colonies were selected on 25 mg/L chloramphenicol LB agar plates and verified using Sanger sequencing. For susceptibility testing, variants of OXA-48 were re-constructed in the pUNE vector background using Goldengate cloning (construction of landscape) or sub-cloned as mentioned above using the corresponding primers (Table S5). In short, we performed whole vector amplification followed by digestions with LguI for 1 h 37°C. Ligations were performed using 10-20 ng of DNA, transformed into *E. coli* E. cloni® 10G cells and clones were grown on 25 mg/L chloramphenicol LB agar plates. For protein expression, OXA-48 variants were sub-cloned into a pDEST-17 expression vector without the leader sequence and with a 6-His-tag using P2/P37 and P35/P36. Amplicons were digested using NotI and XhoI, ligated as described above and transformed into *E. coli* E. cloni® 10G. Vectors were isolated using the Qiagen plasmid miniprep kit. pDEST-17 expression vectors were transformed into *E. coli* BL21 AI. Clones were selected on agar containing ampicillin 100 mg/L and verified using Sanger sequencing.

pUNE stock preparation for error prone PCR

From a 100 mL *E. coli* E.cloni[®] 10G culture carrying pUNE-*bla*_{OXA-48}, the vector was isolated using a Qiagen Midi kit (Qiagen, Hilde, Germany). 500 ng of the vector were digested with NcoI, XhoI and FastAP for 1 to 2 h at 37°C and agarose gel (0.7%) purified using the Zymoclean[®] kit (Zymo Research, CA, USA) to a final concentration of 10 to 20 ng/μL and stored at -20°C for ligation.

Directed evolution and library construction

Error-prone PCR was performed using 10 ng pUNE-4-*bla*_{OXA-48}, GoTag (Promega, Madison, WI, USA), 25 mM MgCl₂ (Promega), 10 μM P7/P8 and either 50 μM oxo-dGTP or 1 μM dPTP. PCR products were DpnI digested for 1 h and 37°C and 5 ng of each product were used for a second PCR, which was performed as described above, but without mutagenic nucleotides. The second PCR product was then digested using NcoI and XhoI for 1 h at 37°C and ligated in a 1:3 ratio with the digested and purified pUNE vector backbone. The ligation mix was electroporated into *E. coli* E.cloni[®] 10G cells, recovered in LB broth for 1 h at 37°C and plated on 25 mg/L chloramphenicol LB agar plates. Library sizes were determined by cell counts and mutation frequencies were determined using Sanger sequencing.

Selective plating and susceptibility measurements

E. coli E.cloni[®] 10G cultures harbouring either pUNE-4-*bla*_{OXA-48} or a library of OXA-48 were plated on LB agar plates containing increasing concentrations of CAZ and grown overnight at 37°C. Colonies grown on the highest concentrations were recovered and their genotype characterised by Sanger sequencing. Before determining their *IC*₅₀ values, the corresponding mutant alleles were sub-cloned into an isogenic vector backbone and transformed into *E. coli* E.cloni[®] 10G cells, to exclude mutational effects outside of the target gene. *IC*₅₀ values were determined as previously published²⁵.

Protein expression and purification

Cultures of *E. coli* BL21 AI harbouring pDEST17-*bla*_{OXA-48} and mutant alleles were grown in 10 to 50 mL LB broth supplemented with 100 mg/L ampicillin at 37°C. Protein expression was induced by adding L-arabinose (Sigma-Aldrich) to a final concentration of 0.2% when the cultures reached a OD₆₀₀ of 0.4. Cultures were expressed for 16 h at 15°C, centrifuged at 4°C

for 30 min and the cell pellets were stored at -20°C for purification. Despite using 0.2 mL HisPur® Ni-NTA spin columns (0.2 mL), protein purification was done as published previously^{24,52}.

Thermostability

Fluorescence-based thermostability was performed as previously published^{24,25}. However, compared to previous studies, the purified wtOXA-48 and the corresponding mutants still contained the 6-His tag and TEV cleaving site. In brief, the enzymes were diluted in 50 mM HEPES (VWR, PA, USA), pH 7.5 and 50 mM potassium sulfate (Honeywell, NC, USA) and mixed with 5xSYPRO orange (Sigma-Aldrich). The final enzyme concentration was 0.2 mg/mL. A temperature gradient of 25 to 70°C with a heating rate of 1°C per min was applied using an MJ minicycler (Bio-Rad, Hercules, CA, USA). All experiments were performed in triplicates.

Epistasis calculations and prediction model

Under the assumption of no epistasis in a trajectory, the functional contribution of each mutation would be equal in each genotype. Therefore, the predicted function for any genotype using the additive model can be computed by taking the product the functional contribution of each single point mutation present in the genotype. This was done to calculate the predicted resistance phenotypes for all genotypes in each trajectory.

To understand the contribution of epistasis and how epistasis impairs predictability, we set up a 'feed-forward' model. The term 'feed-forward' refers to the use of the previous order (e.g., pairwise interactions) to compute epistatic coefficients for the higher orders (triple, quadruple, etc.). For example, by using the additive model (contribution of only single mutations), we calculated the ratio between determined and predicted IC_{50} values (Figure S5). The resulting fold-changes presented epistatic coefficients which were then used to inform and compute all higher orders. The predicted function of a genotype in higher orders of the model was computed by multiplying all epistatic coefficients on all Hamiltonian paths to the genotype's node in a fitness landscape. The epistatic coefficients for the next higher order were computed by taking the ratio of the determined over predicted IC_{50} for each genotype.

To assess the predictability of a trajectory with a given 'order of the feed-forward model, the mean absolute error (MAE) was computed for all genotypes not explicitly defined by the epistatic coefficients:

$$\text{MAE} = \frac{\sum_{i=1}^n |\text{Predicted}_i - \text{Determined}_i|}{n}$$

For example, epistatic coefficients of the 2nd order (pairwise interactions) were used to predict resistance development of mutants with three or more mutations, as described above. To understand how close this prediction was to the determined IC_{50} values, the MAE and the standard deviation was calculated and provides an average value for this prediction.

Crystallography and structure determination

Crystallisation was performed in a 1- μ L hanging drop containing 10 mg/mL enzyme and mixed 1:1 with reservoir solution containing 0.1 M Tris, pH 9.0 (Sigma-Aldrich), and 28 to 30% polyethylene glycol (PEG) mono ethylene ether 500 (Sigma-Aldrich) at 4°C. Crystals were cryoprotected by using 15% ethylene glycol (Sigma-Aldrich) in addition to the reservoir solution, and subsequently frozen in liquid nitrogen. Diffraction data were collected on ID30B, ESRF, France, at 100 K, wavelength 0.9184 Å, and the diffraction images were indexed and integrated using XDS⁵³. For data scaling, AIMLESS was used⁵⁴ and an overall high completeness and $CC1/2 > 0.5$ and a mean intensity above 1.0 in the outer resolution shell was aimed for (Table S6). Molecular replacement was performed using chain A of PDB no. 6Q5F²⁴ and the program PHENIX 1.12⁵⁵. Parts of the model were rebuilt using Coot⁵⁶. Figures were prepared using PyMOL 1.8 (Schrödinger, New York, NY, USA). Ligand and protein interactions were calculated using the Protein Contacts Atlas⁵⁷.

REFERENCES

- 1 Cassini, A., Hogberg, L. D., Plachouras, D., Quattrocchi, A., Hoxha, A., Simonsen, G. S., Colomb-Cotinat, M., Kretzschmar, M. E., Devleeschauwer, B., Cecchini, M., Ouakrim, D. A., Oliveira, T. C., Struelens, M. J., Suetens, C. & Monnet, D. L. Attributable deaths and disability-adjusted life-years caused by infections with antibiotic-resistant bacteria in the EU and the European Economic Area in 2015: a population-level modelling analysis. *Lancet Infect Dis* **19**, 56-66, doi:10.1016/S1473-3099(18)30605-4 (2019).
- 2 Walsh, T. R. A one-health approach to antimicrobial resistance. *Nat Microbiol* **3**, 854-855, doi:10.1038/s41564-018-0208-5 (2018).
- 3 Palzkill, T. Structural and Mechanistic Basis for Extended-Spectrum Drug-Resistance Mutations in Altering the Specificity of TEM, CTX-M, and KPC β -lactamases. *Front Mol Biosci* **5**, 16, doi:10.3389/fmolb.2018.00016 (2018).
- 4 Khersonsky, O. & Tawfik, D. S. Enzyme promiscuity: a mechanistic and evolutionary perspective. *Annu Rev Biochem* **79**, 471-505, doi:10.1146/annurev-biochem-030409-143718 (2010).
- 5 Imamovic, L. & Sommer, M. O. A. Use of Collateral Sensitivity Networks to Design Drug Cycling Protocols That Avoid Resistance Development. *Science Translational Medicine* **5**, 204ra132-204ra132, doi:10.1126/scitranslmed.3006609 (2013).
- 6 Pal, C., Papp, B. & Lazar, V. Collateral sensitivity of antibiotic-resistant microbes. *Trends Microbiol* **23**, 401-407, doi:10.1016/j.tim.2015.02.009 (2015).
- 7 Podnecky, N. L., Fredheim, E. G. A., Kloos, J., Sorum, V., Primicerio, R., Roberts, A. P., Rozen, D. E., Samuelsen, O. & Johnsen, P. J. Conserved collateral antibiotic susceptibility networks in diverse clinical strains of *Escherichia coli*. *Nat Commun* **9**, 3673, doi:10.1038/s41467-018-06143-y (2018).
- 8 Munck, C., Gumpert, H. K., Wallin, A. I., Wang, H. H. & Sommer, M. O. Prediction of resistance development against drug combinations by collateral responses to component drugs. *Sci Transl Med* **6**, 262ra156, doi:10.1126/scitranslmed.3009940 (2014).
- 9 Rosenkilde, C. E. H., Munck, C., Porse, A., Linkevicius, M., Andersson, D. I. & Sommer, M. O. A. Collateral sensitivity constrains resistance evolution of the CTX-M-15 β -lactamase. *Nat Commun* **10**, 618, doi:10.1038/s41467-019-08529-y (2019).
- 10 Baym, M., Stone, L. K. & Kishony, R. Multidrug evolutionary strategies to reverse antibiotic resistance. *Science* **351**, aad3292, doi:10.1126/science.aad3292 (2016).
- 11 Tokuriki, N., Jackson, C. J., Afriat-Jurnou, L., Wyganowski, K. T., Tang, R. & Tawfik, D. S. Diminishing returns and tradeoffs constrain the laboratory optimization of an enzyme. *Nat Commun* **3**, 1257, doi:10.1038/ncomms2246 (2012).

- 12 Bontron, S., Poirel, L. & Nordmann, P. *In vitro* prediction of the evolution of GES-1 β -lactamase hydrolytic activity. *Antimicrob Agents Chemother* **59**, 1664-1670, doi:10.1128/AAC.04450-14 (2015).
- 13 Nyerges, A., Csorgo, B., Draskovits, G., Kintses, B., Szili, P., Ferenc, G., Revesz, T., Ari, E., Nagy, I., Balint, B., Vasarhelyi, B. M., Bihari, P., Szamel, M., Balogh, D., Papp, H., Kalapis, D., Papp, B. & Pal, C. Directed evolution of multiple genomic loci allows the prediction of antibiotic resistance. *Proc Natl Acad Sci U S A* **115**, E5726-E5735, doi:10.1073/pnas.1801646115 (2018).
- 14 Miton, C. M. & Tokuriki, N. How mutational epistasis impairs predictability in protein evolution and design. *Protein Sci* **25**, 1260-1272, doi:10.1002/pro.2876 (2016).
- 15 Domingo, J., Baeza-Centurion, P. & Lehner, B. The Causes and Consequences of Genetic Interactions (Epistasis). *Annu Rev Genomics Hum Genet* **20**, 433-460, doi:10.1146/annurev-genom-083118-014857 (2019).
- 16 Starr, T. N. & Thornton, J. W. Epistasis in protein evolution. *Protein Sci* **25**, 1204-1218, doi:10.1002/pro.2897 (2016).
- 17 Yang, G., Miton, C. M. & Tokuriki, N. A mechanistic view of enzyme evolution. *Protein Sci* **29**, 1724-1747, doi:10.1002/pro.3901 (2020).
- 18 Poirel, L., Heritier, C., Tolun, V. & Nordmann, P. Emergence of oxacillinase-mediated resistance to imipenem in *Klebsiella pneumoniae*. *Antimicrob Agents Chemother* **48**, 15-22, doi:10.1128/aac.48.1.15-22.2004 (2004).
- 19 Pitout, J. D. D., Peirano, G., Kock, M. M., Strydom, K. A. & Matsumura, Y. The Global Ascendency of OXA-48-Type Carbapenemases. *Clin Microbiol Rev* **33**, doi:10.1128/CMR.00102-19 (2019).
- 20 Docquier, J. D., Calderone, V., De Luca, F., Benvenuti, M., Giuliani, F., Bellucci, L., Tafi, A., Nordmann, P., Botta, M., Rossolini, G. M. & Mangani, S. Crystal structure of the OXA-48 β -lactamase reveals mechanistic diversity among class D carbapenemases. *Chem Biol* **16**, 540-547, doi:10.1016/j.chembiol.2009.04.010 (2009).
- 21 Dortet, L., Oueslati, S., Jeannot, K., Tande, D., Naas, T. & Nordmann, P. Genetic and biochemical characterization of OXA-405, an OXA-48-type extended-spectrum β -lactamase without significant carbapenemase activity. *Antimicrob Agents Chemother* **59**, 3823-3828, doi:10.1128/AAC.05058-14 (2015).
- 22 Gomez, S., Pasteran, F., Faccone, D., Bettioli, M., Veliz, O., De Belder, D., Rapoport, M., Gatti, B., Petroni, A. & Corso, A. Inpatient emergence of OXA-247: a novel carbapenemase found in a patient previously infected with OXA-163-producing *Klebsiella pneumoniae*. *Clin Microbiol Infect* **19**, E233-235, doi:10.1111/1469-0691.12142 (2013).
- 23 Poirel, L., Castanheira, M., Carrer, A., Rodriguez, C. P., Jones, R. N., Smayevsky, J. & Nordmann, P. OXA-163, an OXA-48-related class D β -lactamase with extended

- activity toward expanded-spectrum cephalosporins. *Antimicrob Agents Chemother* **55**, 2546-2551, doi:10.1128/AAC.00022-11 (2011).
- 24 Fröhlich, C., Sorum, V., Thomassen, A. M., Johnsen, P. J., Leiros, H. S. & Samuelsen, O. OXA-48-Mediated Ceftazidime-Avibactam Resistance Is Associated with Evolutionary Trade-Offs. *mSphere* **4**, doi:10.1128/mSphere.00024-19 (2019).
- 25 Fröhlich, C., Gama, J. A., Harms, K., Hirvonen, V. H. A., Lund, B. A., van der Kamp, M. W., Johnsen, P. J., Samuelsen, Ø. & Leiros, H.-K. S. Cryptic β -lactamase evolution is driven by low β -lactam concentrations. *bioRxiv*, 2020.2012.2001.404343, doi:10.1101/2020.12.01.404343 (2020).
- 26 Oueslati, S., Nordmann, P. & Poirel, L. Heterogeneous hydrolytic features for OXA-48-like β -lactamases. *J Antimicrob Chemother* **70**, 1059-1063, doi:10.1093/jac/dku524 (2015).
- 27 Yoon, E. J. & Jeong, S. H. Class D β -lactamases. *J Antimicrob Chemother*, doi:10.1093/jac/dkaa513 (2020).
- 28 De Luca, F., Benvenuti, M., Carboni, F., Pozzi, C., Rossolini, G. M., Mangani, S. & Docquier, J. D. Evolution to carbapenem-hydrolyzing activity in noncarbapenemase class D β -lactamase OXA-10 by rational protein design. *Proc Natl Acad Sci U S A* **108**, 18424-18429, doi:10.1073/pnas.1110530108 (2011).
- 29 Dabos, L., Zavala, A., Bonnin, R. A., Beckstein, O., Retailleau, P., Iorga, B. I. & Naas, T. Substrate Specificity of OXA-48 after β 5- β 6 Loop Replacement. *ACS Infect Dis* **6**, 1032-1043, doi:10.1021/acsinfecdis.9b00452 (2020).
- 30 Salverda, M. L., Dellus, E., Gorter, F. A., Debets, A. J., van der Oost, J., Hoekstra, R. F., Tawfik, D. S. & de Visser, J. A. Initial mutations direct alternative pathways of protein evolution. *PLoS Genet* **7**, e1001321, doi:10.1371/journal.pgen.1001321 (2011).
- 31 Novais, A., Comas, I., Baquero, F., Canton, R., Coque, T. M., Moya, A., Gonzalez-Candelas, F. & Galan, J. C. Evolutionary trajectories of β -lactamase CTX-M-1 cluster enzymes: predicting antibiotic resistance. *PLoS Pathog* **6**, e1000735, doi:10.1371/journal.ppat.1000735 (2010).
- 32 McLoughlin, S. Y. & Copley, S. D. A compromise required by gene sharing enables survival: Implications for evolution of new enzyme activities. *Proc Natl Acad Sci U S A* **105**, 13497-13502, doi:10.1073/pnas.0804804105 (2008).
- 33 Watts, K. T., Mijts, B. N., Lee, P. C., Manning, A. J. & Schmidt-Dannert, C. Discovery of a substrate selectivity switch in tyrosine ammonia-lyase, a member of the aromatic amino acid lyase family. *Chem Biol* **13**, 1317-1326, doi:10.1016/j.chembiol.2006.10.008 (2006).
- 34 Soskine, M. & Tawfik, D. S. Mutational effects and the evolution of new protein functions. *Nat Rev Genet* **11**, 572-582, doi:10.1038/nrg2808 (2010).

- 35 Tokuriki, N., Stricher, F., Serrano, L. & Tawfik, D. S. How protein stability and new functions trade off. *PLoS Comput Biol* **4**, e1000002, doi:10.1371/journal.pcbi.1000002 (2008).
- 36 Tokuriki, N. & Tawfik, D. S. Stability effects of mutations and protein evolvability. *Curr Opin Struct Biol* **19**, 596-604, doi:10.1016/j.sbi.2009.08.003 (2009).
- 37 Fröhlich, C., Gama, J. A., Harms, K., Hirvonen, V. H. A., Lund, B. A., van der Kamp, M. W., Johnsen, P. J., Samuelson, Ø. & Leiros, H. K. S. Cryptic β -lactamase evolution is driven by low β -lactam concentrations. *mSphere* **6**, doi:10.1128/mSphere.00108-21 (2021).
- 38 Chen, J. Z., Fowler, D. M. & Tokuriki, N. Comprehensive exploration of the translocation, stability and substrate recognition requirements in VIM-2 lactamase. *Elife* **9**, doi:10.7554/eLife.56707 (2020).
- 39 King, D. T., King, A. M., Lal, S. M., Wright, G. D. & Strynadka, N. C. Molecular Mechanism of Avibactam-Mediated β -Lactamase Inhibition. *ACS Infect Dis* **1**, 175-184, doi:10.1021/acsinfecdis.5b00007 (2015).
- 40 Smith, C. A., Stewart, N. K., Toth, M. & Vakulenko, S. B. Structural Insights into the Mechanism of Carbapenemase Activity of the OXA-48 β -Lactamase. *Antimicrob Agents Chemother* **63**, doi:10.1128/AAC.01202-19 (2019).
- 41 Akhtar, A., Pemberton, O. A. & Chen, Y. Structural Basis for Substrate Specificity and Carbapenemase Activity of OXA-48 Class D β -Lactamase. *ACS Infect Dis* **6**, 261-271, doi:10.1021/acsinfecdis.9b00304 (2020).
- 42 Kaltenbach, M., Emond, S., Hollfelder, F. & Tokuriki, N. Functional Trade-Offs in Promiscuous Enzymes Cannot Be Explained by Intrinsic Mutational Robustness of the Native Activity. *PLoS Genet* **12**, e1006305, doi:10.1371/journal.pgen.1006305 (2016).
- 43 Livermore, D. M., Warner, M., Jamrozny, D., Mushtaq, S., Nichols, W. W., Mustafa, N. & Woodford, N. *In vitro* selection of ceftazidime-avibactam resistance in *Enterobacteriaceae* with KPC-3 carbapenemase. *Antimicrob Agents Chemother* **59**, 5324-5330, doi:10.1128/AAC.00678-15 (2015).
- 44 Giddins, M. J., Macesic, N., Annavajhala, M. K., Stump, S., Khan, S., McConville, T. H., Mehta, M., Gomez-Simmonds, A. & Uhlemann, A. C. Successive Emergence of Ceftazidime-Avibactam Resistance through Distinct Genomic Adaptations in *bla*_{KPC-2}-Harboring *Klebsiella pneumoniae* Sequence Type 307 Isolates. *Antimicrob Agents Chemother* **62**, doi:10.1128/AAC.02101-17 (2018).
- 45 Shields, R. K., Nguyen, M. H., Press, E. G., Chen, L., Kreiswirth, B. N. & Clancy, C. J. Emergence of Ceftazidime-Avibactam Resistance and Restoration of Carbapenem Susceptibility in *Klebsiella pneumoniae* Carbapenemase-Producing *K pneumoniae*: A Case Report and Review of Literature. *Open Forum Infect Dis* **4**, ofx101, doi:10.1093/ofid/ofx101 (2017).

- 46 Haidar, G., Clancy, C. J., Shields, R. K., Hao, B., Cheng, S. & Nguyen, M. H. Mutations in *bla*_{KPC-3} That Confer Ceftazidime-Avibactam Resistance Encode Novel KPC-3 Variants That Function as Extended-Spectrum β -Lactamases. *Antimicrob Agents Chemother* **61**, doi:10.1128/AAC.02534-16 (2017).
- 47 Saves, I., Burlet-Schiltz, O., Maveyraud, L., Samama, J. P., Prome, J. C. & Masson, J. M. Mass spectral kinetic study of acylation and deacylation during the hydrolysis of penicillins and cefotaxime by β -lactamase TEM-1 and the G238S mutant. *Biochemistry* **34**, 11660-11667, doi:10.1021/bi00037a003 (1995).
- 48 Stojanoski, V., Hu, L., Sankaran, B., Wang, F., Tao, P., Prasad, B. V. V. & Palzkill, T. Mechanistic Basis of OXA-48-like β -Lactamases' Hydrolysis of Carbapenems. *ACS Infect Dis* **7**, 445-460, doi:10.1021/acsinfecdis.0c00798 (2021).
- 49 Oueslati, S., Retailleau, P., Marchini, L., Berthault, C., Dortet, L., Bonnin, R. A., Iorga, B. I. & Naas, T. Role of Arginine 214 in the Substrate Specificity of OXA-48. *Antimicrob Agents Chemother* **64**, doi:10.1128/AAC.02329-19 (2020).
- 50 Sailer, Z. R. & Harms, M. J. High-order epistasis shapes evolutionary trajectories. *PLoS Comput Biol* **13**, e1005541, doi:10.1371/journal.pcbi.1005541 (2017).
- 51 Yang, G., Anderson, D. W., Baier, F., Dohmen, E., Hong, N., Carr, P. D., Kamerlin, S. C. L., Jackson, C. J., Bornberg-Bauer, E. & Tokuriki, N. Higher-order epistasis shapes the fitness landscape of a xenobiotic-degrading enzyme. *Nat Chem Biol* **15**, 1120-1128, doi:10.1038/s41589-019-0386-3 (2019).
- 52 Lund, B. A., Christopeit, T., Guttormsen, Y., Bayer, A. & Leiros, H. K. Screening and Design of Inhibitor Scaffolds for the Antibiotic Resistance Oxacillinase-48 (OXA-48) through Surface Plasmon Resonance Screening. *J Med Chem* **59**, 5542-5554, doi:10.1021/acs.jmedchem.6b00660 (2016).
- 53 Kabsch, W. Xds. *Acta Crystallogr D Biol Crystallogr* **66**, 125-132, doi:10.1107/S0907444909047337 (2010).
- 54 Evans, P. R. & Murshudov, G. N. How good are my data and what is the resolution? *Acta Crystallographica Section D* **69**, 1204-1214, doi:doi:10.1107/S0907444913000061 (2013).
- 55 Adams, P. D., Afonine, P. V., Bunkoczi, G., Chen, V. B., Davis, I. W., Echols, N., Headd, J. J., Hung, L. W., Kapral, G. J., Grosse-Kunstleve, R. W., McCoy, A. J., Moriarty, N. W., Oeffner, R., Read, R. J., Richardson, D. C., Richardson, J. S., Terwilliger, T. C. & Zwart, P. H. PHENIX: a comprehensive Python-based system for macromolecular structure solution. *Acta Crystallogr D Biol Crystallogr* **66**, 213-221, doi:10.1107/S0907444909052925 (2010).
- 56 Emsley, P., Lohkamp, B., Scott, W. G. & Cowtan, K. Features and development of Coot. *Acta Crystallogr D Biol Crystallogr* **66**, 486-501, doi:10.1107/S0907444910007493 (2010).

- 57 Kayikci, M., Venkatakrishnan, A. J., Scott-Brown, J., Ravarani, C. N. J., Flock, T. & Babu, M. M. Visualization and analysis of non-covalent contacts using the Protein Contacts Atlas. *Nat Struct Mol Biol* **25**, 185-194, doi:10.1038/s41594-017-0019-z (2018).

SUPPLEMENTARY TABLES

Table S1. Overview of all IC_{50} values (mg/L) for landscape I: A33V, F72L, S212A and T213A

Number code ^a	Amino acids ^b	Number of mutations ^c	CAZ IC_{50} (mg/L)	SD for CAZ IC_{50} (mg/L)	PIP IC_{50} (mg/L)	SD for PIP IC_{50} (mg/L)
0000	AFST	0	0.013	0.002	20.842	7.725
0001	AFSA	1	0.012	0.001	21.407	8.483
0010	AFAT	1	0.015	0.002	0.082	0.012
0011	AFAA	2	0.023	0.005	0.216	0.019
0100	ALST	1	0.029	0.006	0.505	0.096
0101	ALSA	2	0.177	0.063	0.700	0.105
0110	ALAT	2	0.140	0.003	0.285	0.060
0111	ALAA	3	0.389	0.025	0.671	0.151
1000	VFST	1	0.017	0.004	20.289	1.583
1001	VFSA	2	0.015	0.001	20.432	1.550
1010	VFAT	2	0.014	0.000	22.443	2.699
1011	VFAA	3	0.020	0.003	12.835	3.995
1100	VLST	2	0.034	0.002	0.536	0.051
1101	VLSA	3	0.141	0.028	0.896	0.130
1110	VLAT	3	0.148	0.042	0.429	0.090
1111	VLAA	4	0.513	0.093	0.505	0.161

^a number code as displayed in the landscapes, '0' indicates the wild-type and '1' a mutation

^b amino acid code referring to the A33V, F72L, S212A and T213A

^c compared to wild-type OXA-48

CAZ: ceftazidime, PIP: piperacillin, SD: standard deviation

Table S2. Overview of all IC_{50} values (mg/L) for landscape II: F66V, N76T, Q124H, E132K, F156D and T243P

Number code ^a	Amino acids ^b	Number of mutations ^c	CAZ IC_{50} (mg/L)	SD for CAZ IC_{50} (mg/L)	PIP IC_{50} (mg/L)	SD for PIP IC_{50} (mg/L)
000000	FNQEFT	0	0.013	0.002	20.842	7.725
000001	FNQEFP	1	0.018	0.004	18.268	5.562
000010	FNQEDT	1	0.031	0.003	0.306	0.043
000011	FNQEDP	2	0.075	0.014	0.322	0.066
000100	FNQKFT	1	0.012	0.001	14.280	2.786
000101	FNQKFP	2	0.015	0.002	7.766	3.040
000110	FNQKDT	2	0.042	0.006	0.375	0.088
000111	FNQKDP	3	0.140	0.017	0.391	0.147
001000	FNHEFT	1	0.031	0.012	2.560	0.553
001001	FNHEFP	2	0.076	0.017	0.865	0.319
001010	FNHEDT	2	0.081	0.017	0.331	0.044
001011	FNHEDP	3	0.159	0.022	0.310	0.032
001100	FNHKFT	2	0.033	0.002	2.191	0.326
001101	FNHKFP	3	0.179	0.011	1.656	0.366
001110	FNHKDT	3	0.111	0.016	0.382	0.079
001111	FNHKDP	4	0.296	0.046	0.497	0.075
010000	FTQEFT	1	0.013	0.001	0.894	0.036
010001	FTQEFP	2	0.031	0.005	1.125	0.080
010010	FTQEDT	2	0.044	0.007	0.265	0.050
010011	FTQEDP	3	0.101	0.023	0.383	0.023
010100	FTQKFT	2	0.012	0.001	1.395	0.280
010101	FTQKFP	3	0.024	0.004	1.178	0.018
010110	FTQKDT	3	0.038	0.002	0.256	0.038
010111	FTQKDP	4	0.122	0.033	0.431	0.115
011000	FTHEFT	2	0.062	0.019	0.507	0.069
011001	FTHEFP	3	0.294	0.008	0.601	0.106
011010	FTHEDT	3	0.089	0.017	0.319	0.037
011011	FTHEDP	4	0.430	0.046	0.591	0.112
011100	FTHKFT	3	0.084	0.018	0.467	0.107
011101	FTHKFP	4	0.472	0.202	0.650	0.148
011110	FTHKDT	4	0.166	0.019	0.363	0.149
011111	FTHKDP	5	0.473	0.039	0.579	0.027
100000	VNQEFT	1	0.013	0.001	17.014	3.274
100001	VNQEFP	2	0.018	0.001	8.135	0.435
100010	VNQEDT	2	0.018	0.003	0.125	0.046
100011	VNQEDP	3	0.021	0.002	0.114	0.041
100100	VNQKFT	2	0.013	0.001	15.971	0.529

100101	VNQKFP	3	0.018	0.003	13.663	6.153
100110	VNQKDT	3	0.030	0.000	0.195	0.042
100111	VNQKDP	4	0.074	0.030	0.164	0.006
101000	VNHEFT	2	0.020	0.008	0.258	0.113
101001	VNHEFP	3	0.016	0.001	0.142	0.098
101010	VNHEDT	3	0.027	0.008	0.093	0.004
101011	VNHEDP	4	0.022	0.002	0.192	0.046
101100	VNHKFT	3	0.037	0.003	0.242	0.038
101101	VNHKFP	4	0.073	0.027	0.241	0.069
101110	VNHKDT	4	0.063	0.031	0.173	0.006
101111	VNHKDP	5	0.132	0.054	0.228	0.087
110000	VTQEFT	2	0.016	0.003	1.257	0.041
110001	VTQEFP	3	0.030	0.006	0.953	0.218
110010	VTQEDT	3	0.047	0.015	0.281	0.014
110011	VTQEDP	4	0.088	0.039	0.370	0.036
110100	VTQKFT	3	0.013	0.002	1.151	0.112
110101	VTQKFP	4	0.024	0.006	1.200	0.016
110110	VTQKDT	4	0.050	0.015	0.332	0.033
110111	VTQKDP	5	0.101	0.011	0.451	0.141
111000	VTHEFT	3	0.038	0.011	0.233	0.015
111001	VTHEFP	4	0.105	0.015	0.335	0.074
111010	VTHEDT	4	0.066	0.012	0.301	0.024
111011	VTHEDP	5	0.268	0.094	0.292	0.067
111100	VTHKFT	4	0.073	0.021	0.476	0.011
111101	VTHKFP	5	0.233	0.031	0.363	0.018
111110	VTHKDT	5	0.127	0.022	0.462	0.065
111111	VTHKDP	6	0.411	0.054	0.571	0.151

^a number code as displayed in the landscapes, '0' indicates the wild-type and '1' a mutation

^b amino acid code referring to the F66V, N76T, Q124H, E132K, F156D and T243P

^c compared to wild-type OXA-48

CAZ: ceftazidime, PIP: piperacillin, SD: standard deviation

Table S3. Overview of all IC_{50} values (mg/L) for landscape III: L67I, F142L, D154G,L158P,K180Q and I215T.

Number code ^a	Amino acids ^b	Number of mutations ^c	CAZ IC_{50} (mg/L)	SD for CAZ IC_{50} (mg/L)	PIP IC_{50} (mg/L)	SD for PIP IC_{50} (mg/L)
000000	LFDLKI	0	0.013	0.002	20.842	7.725
000001	LFDLKT	1	0.014	0.002	34.940	7.074
000010	LFDLQI	1	0.014	0.001	16.639	4.060
000011	LFDLQT	2	0.014	0.001	15.108	2.605
000100	LFDPKI	1	0.035	0.005	0.216	0.019
000101	LFDPKT	2	0.029	0.004	0.291	0.031
000110	LFDPQI	2	0.032	0.003	6.814	1.269
000111	LFDPQT	3	0.039	0.008	0.373	0.055
001000	LFGLKI	1	0.014	0.003	12.299	2.332
001001	LFGLKT	2	0.018	0.003	9.661	1.310
001010	LFGLQI	2	0.016	0.003	9.523	0.029
001011	LFGLQT	3	0.019	0.003	12.783	2.138
001100	LFGPKI	2	0.041	0.013	0.292	0.052
001101	LFGPKT	3	0.037	0.004	0.333	0.049
001110	LFGPQI	3	0.058	0.023	0.284	0.077
001111	LFGPQT	4	0.035	0.005	0.293	0.105
010000	LLDLKI	1	0.013	0.001	30.927	6.902
010001	LLDLKT	2	0.012	0.001	15.152	2.085
010010	LLDLQI	2	0.013	0.002	16.470	0.899
010011	LLDLQT	3	0.017	0.004	34.546	3.766
010100	LLDPKI	2	0.046	0.010	0.242	0.023
010101	LLDPKT	3	0.030	0.003	0.325	0.034
010110	LLDPQI	3	0.046	0.004	0.350	0.038
010111	LLDPQT	4	0.037	0.004	0.337	0.082
011000	LLGLKI	2	0.018	0.006	6.284	2.720
011001	LLGLKT	3	0.024	0.008	12.336	2.132
011010	LLGLQI	3	0.016	0.001	15.975	2.815
011011	LLGLQT	4	0.022	0.003	14.351	2.573
011100	LLGPKI	3	0.053	0.023	0.222	0.009
011101	LLGPKT	4	0.030	0.004	0.234	0.021
011110	LLGPQI	4	0.052	0.009	0.333	0.081
011111	LLGPQT	5	0.040	0.003	0.338	0.007
100000	IFDLKI	1	0.015	0.004	27.496	11.140
100001	IFDLKT	2	0.014	0.002	15.573	0.973
100010	IFDLQI	2	0.013	0.002	9.135	1.440
100011	IFDLQT	3	0.015	0.003	19.542	1.274
100100	IFDPKI	2	0.126	0.041	0.192	0.079

100101	IFDPKT	3	0.180	0.043	0.412	0.035
100110	IFDPQI	3	0.150	0.050	0.213	0.027
100111	IFDPQT	4	0.210	0.012	0.260	0.034
101000	IFGLKI	2	0.017	0.005	10.163	1.881
101001	IFGLKT	3	0.022	0.003	6.675	0.835
101010	IFGLQI	3	0.017	0.007	7.759	1.110
101011	IFGLQT	4	0.022	0.004	11.253	0.633
101100	IFGPKI	3	0.170	0.051	0.245	0.071
101101	IFGPKT	4	0.118	0.030	0.208	0.009
101110	IFGPQI	4	0.159	0.046	0.203	0.062
101111	IFGPQT	5	0.164	0.017	0.295	0.071
110000	ILD LKI	2	0.015	0.002	18.705	4.640
110001	ILD LKT	3	0.020	0.004	15.091	1.668
110010	ILD LQI	3	0.013	0.001	16.098	2.235
110011	ILD LQT	4	0.014	0.001	21.436	1.442
110100	ILD PKI	3	0.277	0.034	0.280	0.051
110101	ILD PKT	4	0.332	0.069	0.496	0.081
110110	ILD PQI	4	0.274	0.035	0.289	0.054
110111	ILD PQT	5	0.241	0.014	0.444	0.048
111000	ILGLKI	3	0.013	0.003	8.788	1.108
111001	ILGLKT	4	0.024	0.002	11.739	1.938
111010	ILGLQI	4	0.017	0.001	11.404	1.899
111011	ILGLQT	5	0.021	0.001	15.470	1.257
111100	ILGPKI	4	0.189	0.045	0.278	0.024
111101	ILGPKT	5	0.218	0.014	0.378	0.076
111110	ILGPQI	5	0.173	0.007	0.335	0.031
111111	ILGPQT	6	0.208	0.036	0.339	0.045

^a number code as displayed in the landscapes, '0' indicates the wild-type and '1' a mutation

^b amino acid code referring to the L67I, F142L, D154G, L158P, K180Q and I215T

^c compared to wild-type OXA-48

CAZ: ceftazidime, PIP: piperacillin, SD: standard deviation

Table S4: Thermostability of all selected single mutants compared to wtOXA-48.

OXA-48 mutants ^a	Average thermostability (°C) ^b	Standard deviation (°C)	Difference to wtOXA-48 (°C)
wild-type	52.9	0.1	0
A33V	52.7	0.1	-0.2
F66V	46.6	0.1	-6.3
L67I	52.9	0.1	-0.1
F72L	45.7	0.1	-7.3
N76T	55.3	0.1	2.3
Q124H	46.6	0.2	-6.3
E132K	54.1	0.3	1.2
F142L	52.9	0.1	0.0
F156D	47.3	0.1	-5.7
L158P	46.5	0.1	-6.4
D154G	49.4	0.1	-3.5
K180Q	52.8	0.1	-0.1
S212A	52.5	0.1	-0.4
T213A	53.3	0.1	0.3
I215T	52.3	0.2	-0.7
T243P	48.8	0.2	-4.1

^apurified enzyme, without the leader sequence but including 6-His-tag and the TEV-cleaving site

^bdetermined in triplicates

Table S5: Primers used in this study

No.	Name		5'-3'
1	NcoI-OXA	F	gcttccatgggacgtgtattagccttatcggc
2	XhoI-OXA	R	gcttctcgagctaggggaataatcttctgttgagc
3	pUN-NcoI	F	gctttcccatggatgttttctccttatgtaagcttactcag
4	pUN-XhoI	R	gcttctcgagaagtggtagcgcgtatttg
7	preOXaseqc	F	gattacgcgcagaccaaacg
8	postOXaseqc	R	cctattccctaaagggttattgagaatg
9	Removing NcoI in chloramphenicol, F		tttttgctcttctgccatcgtgaaaacggggg
10	Removing NcoI in chloramphenicol, R		tttttgctctcgggcaaatattatacgcaaggcg
15	F72L	F	tttttgctcttcgcatctaccctgaaaattccaatagctt
		R	tttttgctcttcgatcgggtaaaaatgctg
16	S212A	F	tttttgctcttcactggatacgcgactagaatcgaacctaagattgg
		R	tttttgctcttcccagt ttagcccgaataatagtcacc
17	T213A	F	tttttgctcttcactggatactcggcgagaatcgaacctaagattgg
		R	P16 reverse
18	S212A/T213A	F	ttttt gctcttcactggatacgcggcgagaatcgaacctaagattgg
		R	P16 reverse
20	L67I	F	ttttt gctctccaagcatttattcccgcactctaccttaa
		R	ttttt gctcttcgctt ggctcggcgttaag
21	D154G	F	ttttt gctcttcggcaatgtaggcagttctggctcgacgggtg
		R	ttttt gctcttctgcccgaatgtcctcattac
22	D154G/ L158P	F	ttttt gctcttcggcaatgtaggcagttctggccggacgggtg
		R	P21 reverse
23	L158P	F	ttttt gctcttcggcaatgtagacagttctggccggacgggtg
		R	P21 reverse
24	I215T	F	ttttt gctcttctcgactagaaccgaacctaagattggctg
		R	ttttt gctcttcgctcagatccagtttagc
25	A33V	F	ttttt gctcttcagttggaatgtcacttactgaacat
		R	ttttt gctctccaactttgtttcttgccattc
26	F142L	F	ttttt gctcttctacatgctctggattatggaatgaggacat
		R	ttttt gctcttctgtagcatctgctcatacg
27	F66V	F	ttttt gctcttcaaccaagcaggttaccgccatctacc
		R	ttttt gctcttctggctcggcgttaagatt
28	F156D	F	ttttt gctcttctgtagacagtgattggctcgacgggtg
		R	ttttt gctcttctctacattgcccgaatgctc
29	T243P	F	ttttt gctcttcgatatgccccgctcggatggttaggg
		R	ttttt gctcttcatatccatattcatcgcaaa

30	K180Q	F	tttttgctctctatcacaatcagttacacgtatcggag
		R	tttttgctctctgatacagcttcttaaaaa
35	pDest17 vector- NotI	F	tttttgcgccgcttcgaggtgatggtgatggtgatggtacgacata
36	pDest17 vector- XhoI	R	tttttctcgagtgattcgaggctgctaacaagccccg
		F	tttttgcgccgcagagaacctgtatttcagggaaggaatggcaagaaaacaaa
37	NotI-TEV-OXA-48		agttgg
		R	P2 reverse
		F	tttttgctctcaaaattcccaccagcttgatcgccctcgattt
38	N76T	R	tttttgctctcattttaaaggtagatgcggg
		F	tttttgctctccctgttatcatgaattgcccgcaaattgg
39	Q124H	R	tttttgctctcacaggcacaactgaatattt
		F	tttttgctctcaaattggcaaagcacgtatgagcaagatgct
40	E132K	R	tttttgctctcatttggcgggcaaattcttg
		F	P40 forward
47	Q124H/E132K	R	tttttgctctcatttggcgggcaaattcatg

F: forward, R: reverse

Table S6: X-ray data collection and refinement statistics

	LI-4	LI-4-CAZ
Beamline	ID30B, ESRF	ID30B, ESRF
Wavelength (Å)	0.9763	0.9763
Resolution range (Å)	24.95-1.17 (1.19-1.17)	24.39-2.66 (2.78-2.66)
Space group	C2	P 6 ₁
Unit cell: a,b,c (Å)	94.40, 42.54, 64.30	202.15, 202.15, 55.70
α, β, γ (°)	90, 106.88, 90	90, 90, 120
Total reflections	356104 (16085)	230393 (28723)
Unique reflections	82172 (4063)	37514 (4578)
Multiplicity	4.3 (4.0)	6.1 (6.3)
Completeness (%)	99.7 (99.9)	99.2 (100.0)
Mean I/sigma(I)	8.7 (1.1)	9.1 (1.0)
Overall B-factor from Wilson plot (Å ²)	12.7	73.12
R _{merge}	0.067 (0.798)	0.108 (1.555)
R _{measured}	0.086 (1.244)	0.129 (1.846)
R _{pim}	0.041 (0.615)	0.052 (0.761)
CC _{1/2}	0.996 (0.521)	0.997 (0.367)
Resolution range (Å)	24.95-1.17	24.39 - 2.66
Reflections used in refinement	82157 (8180)	37109 (3390)
Reflections used for R-free	1248 (113)	1809 (181)
Final R _{work}	0.1647 (0.3070)	0.2028 (0.3291)
Final R _{free}	0.1871 (0.2873)	0.2722 (0.3682)
No. of non-hydrogen atoms	2557	7669
-macromolecules	2183	7472
-ligands	22	113
-solvent	352	84 (2xCl ⁻ and 3xCAZ)
R.m.s. deviations		
-bonds (Å)	0.009	0.009
-angles (°)	1.16	1.09
Ramachandran plot		
-Favoured (%)	98.75	92.52
-Allowed (%)	1.25	7.03
Average B-factor (Å ²)	23.67	96.35
-macromolecules (Å ²)	21.77	96.57
-ligands (Å ²)	27.91	94.36
-solvent (Å ²)	35.18	78.99
Number of TLS groups	1	21

Statistics for the highest-resolution shell are shown in parentheses.

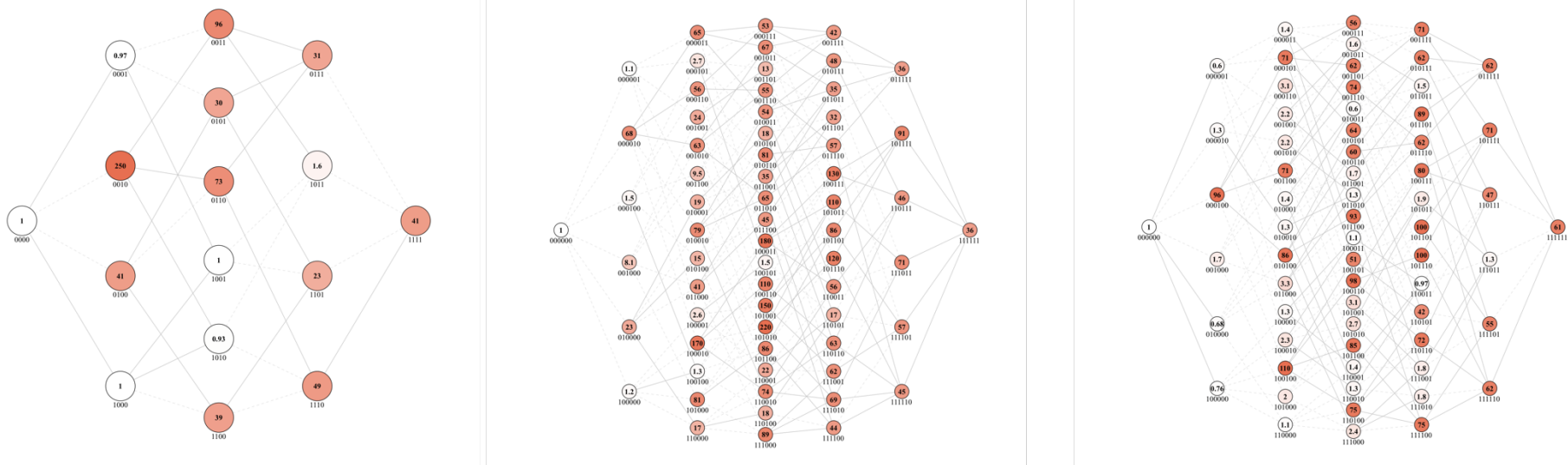


Figure S2: Landscapes I, II and III (from left to right) for all mutational combinations characterised towards PIP. Each node represents a unique variant. The mutational combination for each node is shown as numerical code where '0' refers to the wtOXA-48 amino acid and '1' represents a specific mutation (that is for landscape I: A33V, F72L, S212A, T213; for landscape II: F66V, N76T, Q124H, E132K, F156D, T243P; for landscape III: L67I, F142L, D154G, L158P, K180Q, I215T). For example, '1010' refers to the mutational combination of A33V/S212A within landscape I. The number within each node shows the reversed ($1/x$) IC_{50} fold-change, compared to wild-type OXA-48. Thus, the number in each node represents the loss in piperacillin resistance. For example, the genotype '0010' (S212A) in landscape I exhibits an IC_{50} 250-fold lower than wild-type OXA-48.

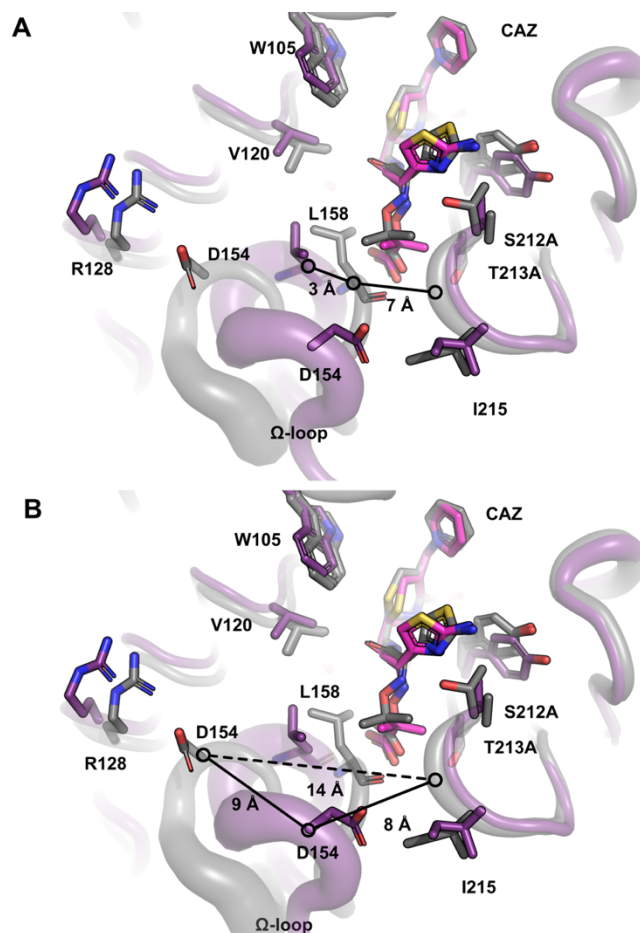


Figure S3: Structural re-arrangement of the OXA-48 active site and ceftazidime (CAZ) positioning. The of LI-4 without CAZ (purple) was superimposed onto wild-type structure of OXA-48 (grey, 4S2P). In addition, the position of CAZ in LI-4 -CAZ (pink) and in the previously published structure of OXA-48: P68A (grey) to demonstrate the distance between CAZ and the Ω -loop. A. The molecular distance of L158 in the Ω -loop if the wild-type and mutant structure compared the backbone of R214 on the β 5- β 6 loop was calculated. B. Similarly, the movement of D154 in the Ω -loop towards the backbone of R214 on the β 5- β 6 loop was calculated.

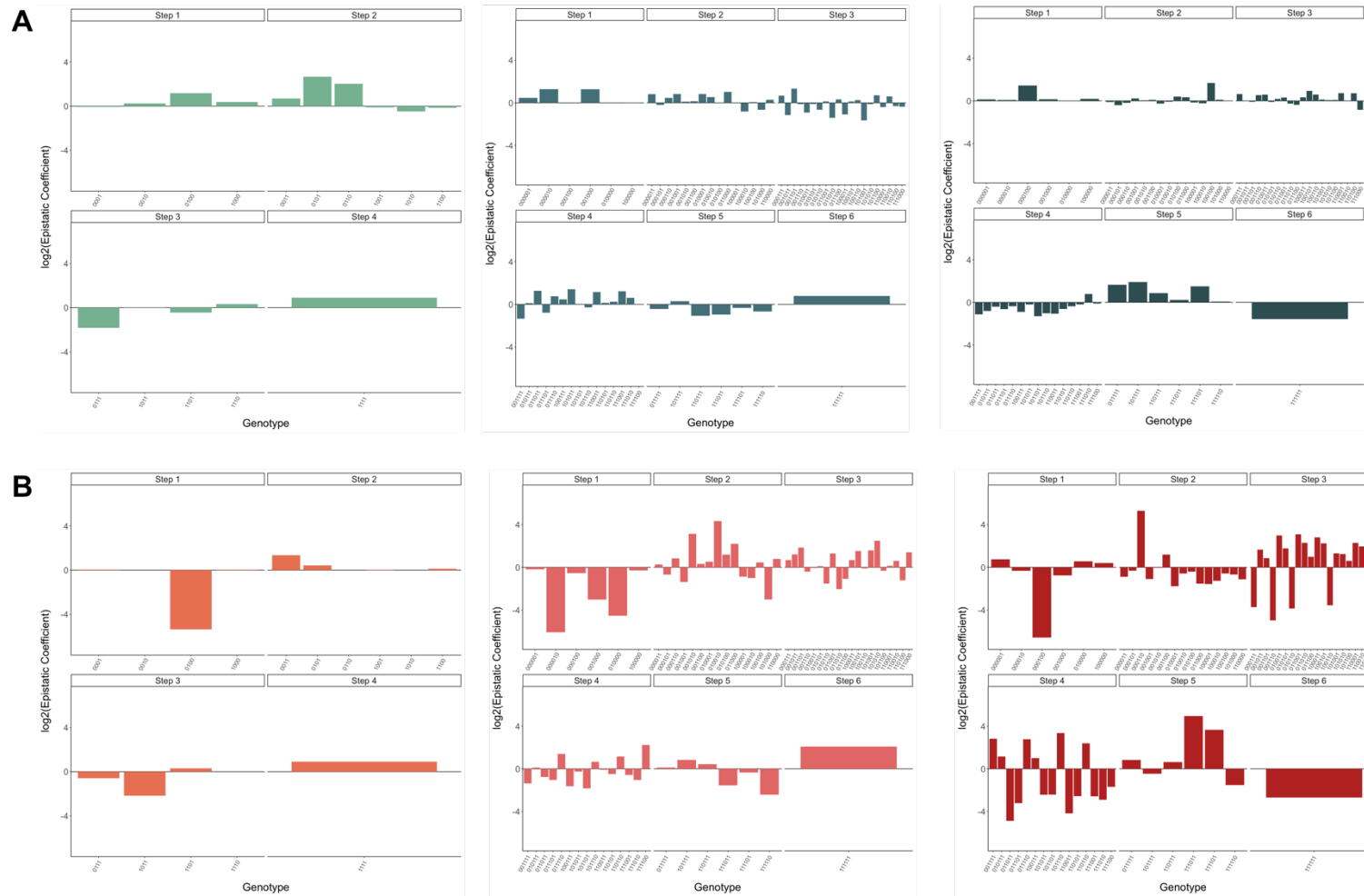


Figure S5: Epistatic contributions calculated based on the feed-forward model. A. Epistatic coefficients for landscape I to III (left to right) characterised towards ceftazidime. B. Epistatic coefficients for landscape I to III (left to right) characterised towards piperacillin.

Appendix: Review

